

Inhibiting and Characterising Biofilms Formed by Gram- negative Uropathogenic Bacteria

A thesis submitted to The University of Manchester for the degree of
Doctor of Philosophy (PhD)
in the Faculty of Medical and Human Sciences

2013

Nishal Govindji

School of Medicine

Table of Contents		Page
Table of Contents		2
List of Figures		10
List of Tables		21
List of Abbreviations		25
Abstract		26
Declaration and Copyright Statement		28
Publications and Presentations		30
Dedication		31
Acknowledgements		32
1. Introduction		34
1. 1. The bacterial biofilm		35
1. 2. Biofilm formation and structure		39
1. 2. 1. Stages of biofilm formation		39
1. 2. 1. 1. Stage 1a: Surface conditioning		39
1. 2. 1. 2. Stage 1b: Cell – surface interaction and attachment		39
1. 2. 1. 3. Stage 2: Cell accumulation and microcolony formation		41
1. 2. 1. 4. Stage 3: Extracellular polymeric substance production		41
1. 2. 1. 5. Stage 4: Biofilm maturation		42
1. 2. 1. 6. Stage 5: Detachment		42
1. 3. Quorum sensing and microbial biofilms		44
1. 4. Epidemiology of catheter-associated urinary tract infections		46
1. 4. 1. Urethral catheters		47
1. 4. 2. Uses and duration of catheterisation		50

1. 5.	Gram-negative organisms involved in UTI infection	50
1. 6.	The pathogenesis of catheter-associated urinary tract infections	52
1. 6. 1.	Eradication of infection	52
1. 7.	Mechanisms of biofilm-associated antimicrobial resistance	54
1. 7. 1.	The exopolymeric matrix	55
1. 7. 2.	Persister cells	57
1. 7. 3.	Horizontal gene transfer	55
1. 7. 4.	Evasion of host defences	55
1. 8.	Novel approaches to inhibit biofilm formation	56
1. 8. 1.	Limiting initial adhesion and interaction of bacterial cells	58
1. 8. 2.	Limiting communication: quorum sensing inhibitors	59
1. 8. 3.	Reactivating metabolic activity	60
1. 8. 4.	Developing anti-adhesive surfaces: urinary catheter surfaces which reduce bacterial colonisation	61
1. 8. 4. 1.	The use of antimicrobials as catheter coatings	62
1. 8. 4. 1. 1.	Silver as an antimicrobial coating	62
1. 8. 4. 1. 2.	Antibiotics as catheter coatings	63
1. 8. 4. 1. 3.	Nitric oxide as a catheter coating	64
1. 8. 4. 1. 4.	Antimicrobial peptides as catheter coatings	64
1. 9.	Novel antimicrobial compounds used in this study	65
1. 9. 1.	Polyamines as biocides	65
1. 9. 2.	Quaternary ammonium compounds and biguanides as biocides	66
1. 9. 2. 1.	Antimicrobial resistance to quaternary ammonium compounds	67
1. 10.	The aims of this research	69
1. 10. 1.	Aim 1: Identify a novel antimicrobial cationic compound	69
1. 10. 2.	Aim 2: Analyse the response of bacteria when treated with a novel antimicrobial cationic compound	70
2.	Materials and Methods	71
2. 1.	Bacterial strains, media and growth conditions	72
2. 2.	Biofilm flow through system	73
2. 3.	Preparation of bacteria for western blot to detect the presence of OprF in <i>P. aeruginosa</i>	75
2. 3. 1.	Planktonic growth	75

2. 3. 2.	Biofilm and planktonic growth	75
2. 3. 3.	Preparation of proteins of <i>P. aeruginosa</i>	75
2. 4.	SDS-PAGE and western blot	76
2. 5.	Preparation of antimicrobial agents	78
2. 5. 1.	Polyamines	79
2. 5. 1. 1.	Buffered polyamines	79
2. 6.	Quaternisation of polyamines	79
2. 7.	Quaternary ammonium compounds	80
2. 7. 1.	Determination of the molecular weights for the quaternary ammonium compounds	81
2. 8.	Monitoring of pH	81
2. 9.	Determination of the minimum inhibitory concentration (MIC) of antimicrobial agents under study	82
2. 10.	Microtitre plate biofilm formation assay	82
2. 11.	Glass chamber slide biofilm formation assay	83
2. 12.	Viable cell counts	83
2. 13.	Pre-coating polystyrene microtitre plates and glass with Byotrol™	84
2. 14.	MBEC (Minimum Biofilm Eradication Concentration) assay	84
2. 15.	Bright field microscopy	85
2. 16.	Non-contact mode atomic force microscopy (AFM)	86
2. 17.	Preparation of <i>E. coli</i> K12 grown to mid-exponential phase for two dimensional gel electrophoresis and transcriptomic analysis	86
2. 18.	Preparation of bacteria grown for 24 hours for two dimensional gel electrophoresis	87
2. 18. 1.	Biofilm and planktonic growth control	87
2. 18. 2.	Biofilm and planktonic growth in sub-MIC Byotrol™	88
2. 19.	Preparation of whole cell protein extracts for two dimensional gel electrophoresis	88
2. 20.	Determination of total protein concentration	89
2. 21.	Two dimensional gel electrophoresis (2DGE)	90
2. 21. 1.	Active rehydration	90
2. 21. 2.	Iso-electric focussing (1st dimension separation of proteins)	92
2. 21. 3.	Equilibration	93
2. 21. 4.	SDS-Polyacrylamide Gel Electrophoresis (SDS-PAGE) (2nd dimension separation of proteins)	93

2. 21. 5.	Silver staining of gels	93
2. 21. 6.	Interpretation of two-dimensional gels and analysis of differentially expressed proteins	94
2. 21. 7.	Protein identification by LC-MS/MS analysis	94
2. 21. 7. 1.	Digestion	95
2. 21. 7. 2.	LC MS/MS	95
2. 21. 7. 3.	Data analysis of proteins	95
2. 22.	Preparation of RNA for transcriptomics	95
2. 22. 1.	Quality control and preparation of transcripts	96
2. 22. 2.	Data analysis of transcripts	97
2. 22. 2. 1.	Expression analysis: Data normalisation	97
2. 22. 2. 2.	Generation of summary data and KEGG maps in MG-RAST	99
2. 22. 2. 3.	Analysis of unmapped reads	98
3.	An analysis of the effect that natural polyamines have on biofilm formation	99
3. 1.	Polyamine interaction with porins	100
3. 2.	Optimisation of bacterial growth on a microtitre plate	102
3. 2. 1.	Optimisation of bacterial growth on different microtitre plate surfaces	102
3. 2. 2.	Optimisation of the minimum growth time which allows for biofilm visualisation after staining	102
3. 3.	The effect of polyamines and pH on bacterial growth	105
3. 3. 1.	The effect of pH alone on bacterial growth	108
3. 3. 2.	The effect of quaternised polyamines on biofilm formation on microtitre plates	109
3. 3. 3.	The effect of buffered spermine on biofilm formation and planktonic growth on microtitre plates	116
3. 4.	Western blot analysis of OprF	119
3. 5.	Discussion	120
4.	The effect of quaternary ammonium compounds on biofilm growth	122

4. 1.	Quaternary ammonium compounds as biocides	123
4. 1. 1.	QACs: mode of action	123
4. 2.	The susceptibility of bacterial growth to polyquaterniums	124
4. 3.	The susceptibility of bacteria to Polyquaternium-6 (PQ-6)	145
4. 4.	The susceptibility of bacteria to the proprietary antimicrobial Byotrol™ and its individual components: PHMB, BAC and DDQ	153
4. 4. 1.	Pre-coating a surface with Byotrol™	159
4. 4. 1. 2.	Atomic force microscopy of a glass surface pre-coated with Byotrol™	162
4. 4. 2.	Eradication of an established biofilm with Byotrol™: MBEC assay system	164
4. 5.	Discussion	167
4. 5. 1.	The difference between <i>E. coli</i> , <i>K. pneumoniae</i> and <i>P. aeruginosa</i>	167
4. 5. 2.	The effect of molecular weight on inhibition of bacterial growth	167
4. 5. 3.	Validation of MIC and minimum biofilm inhibitory concentrations	169
4. 5. 4.	The effect of Byotrol™ on bacterial growth	169
5.	Proteomic analysis of <i>E. coli</i> K12 in response to Byotrol™	171
5. 1.	Proteomic analysis of <i>E. coli</i> K12	172
5. 1. 2.	Two-dimensional gel electrophoresis (2DGE)	172
5. 1. 2. 1.	Isoelectric focussing: the separation of proteins in the first dimension	172
5. 1. 2. 2.	SDS PAGE: the separation of proteins in the second dimension	172
5. 1. 2. 3.	Visualisation of resolved proteins	173
5. 2.	Optimisation of 2DGE	174
5. 2. 1.	Optimisation to reduce horizontal protein streaking and increased protein resolution in 2DGE	176
5. 2. 2.	Optimisation of IPG strip pH range	178
5. 3.	Proteomic comparison of planktonic and biofilm cells grown for 24 hours (growth controls)	177

5. 4.	Proteomic comparison of planktonic cells grown with and without Byotrol™ (growth control) for 24 hours.	184
5. 5.	Proteomic comparison of planktonic and biofilm cells treated with sub-MIC Byotrol™ for 24 hours	191
5. 6.	Proteomic comparison of planktonic cells grown to mid-exponential phase (5 hours), with and without Byotrol™	196
5. 7.	Discussion	204
5. 7. 1.	Landmark protein: phosphoglycerate kinase	205
5. 7. 2.	Tryptophanase and indole production	205
5. 7. 3.	D-ribose periplasmic binding protein	206
5. 7. 4.	Serine hydroxymethyltransferase	207
5. 7. 5.	Lactaldehyde dehydrogenase	207
5. 7. 6.	Dihydrolipoyl dehydrogenase	208
5. 7. 7.	Glucose-1-phosphatase	208
5. 7. 8.	Conclusion	208
6.	Transcriptomic analysis of <i>E. coli</i> K12 in response to Byotrol™	210
6. 1.	An introduction to RNA-seq	211
6. 1. 1.	Principles of RNA-Seq	212
6. 2.	Global gene expression of <i>E. coli</i> K12 when treated and challenged with Byotrol™	213
6. 3.	Genes differentially expressed in response to Byotrol™	217
6. 4.	Classification of differentially expressed genes according to function	221
6. 5.	Genes differentially expressed in <i>E. coli</i> K12 cells treated with Byotrol™ compared to the growth control	225
6. 6.	Genes differentially expressed in <i>E. coli</i> K12 cells challenged with Byotrol™ compared to cells treated with Byotrol™	226
6. 6. 1.	Genes up-regulated in <i>E. coli</i> K12 cells challenged with Byotrol™ compared to cells treated with Byotrol™	226
6. 6. 2.	Genes down-regulated in <i>E. coli</i> K12 cells challenged with Byotrol™ compared to cells treated with Byotrol™	229
6. 7.	Genes differentially expressed in <i>E. coli</i> K12 cells challenged with Byotrol™ compared to the growth control	231

6. 7. 1.	Genes up-regulated in <i>E. coli</i> K12 cells challenged with Byotrol™ compared to the growth control	233
6. 7. 2.	Genes down-regulated in <i>E. coli</i> K12 cells challenged with Byotrol™ compared to the growth control	233
6. 8.	Unmapped reads	236
6. 9.	Discussion	238
6. 9. 1.	Genes up-regulated in response to Byotrol™	238
6. 9. 1. 1.	Up-regulation of genes associated with transcriptional regulation and DNA binding	238
6. 9. 1. 2.	Up-regulation of genes involved in protein synthesis	238
6. 9. 1. 3.	Up-regulation of genes specific to stress response	239
6. 9. 1. 4.	Up-regulation of genes involved in quorum sensing	240
6. 9. 1. 5.	Up-regulation of pili and curli fimbriae genes	241
6. 9. 2.	Genes down-regulated in response to Byotrol™	241
6. 9. 2. 1.	Down-regulation of genes involved in flagellar synthesis	241
6. 9. 2. 2.	Down-regulation of genes involved in central metabolism	242
6. 9. 2. 3.	Down-regulation of genes involved in iron transfer	242
6. 9. 2. 4.	Down-regulation of specific stress response genes	243
6. 9. 3.	Correlation of gene expression with protein expression	244
6. 9. 3. 1.	D-ribose periplasmic binding protein	244
6. 9. 3. 2.	Tryptophanase and indole production	244
6. 9. 4.	Genes both up and down-regulated under the same condition	245
6. 9. 5.	Induction of biofilm-related genes under stress	245
6. 9. 6.	Greater differential expression of genes in cells challenged with Byotrol™ compared to cells treated with Byotrol™	246
6. 9. 7.	Unmapped reads	246
7.	General Discussion and Future Work	248
7. 1.	The search for a novel cationic antimicrobial	250
7. 2.	The effects of Byotrol™ on the biological pathways of <i>E. coli</i>	252
7. 3.	Proposals for use of Byotrol™ as a novel catheter coating	254
7. 4.	Conclusion	255
	References	256

Appendices on disc

Appendix A: Raw data for Chapter 2. Materials and Methods

Appendix B: Raw data for Chapter 3. An analysis on the effect that natural polyamines have on biofilm formation

Appendix C: Raw data for Chapter 4. The effect of quaternary ammonium compounds on biofilm growth

Appendix D: Raw data for Chapter 5. Proteomic analysis of *E. coli* K12 in response to Byotrol™

Appendix E: Raw data for Chapter 6. Transcriptomic analysis of the *E. coli* K12 in response to Byotrol™

Appendix E. 1: MSDS PHMB

Final word count: 65, 014.

List of Figures

Figure 1. 1. The stages of biofilm formation under flow conditions.	43
Figure 1. 2. Diagram demonstrating the function of the <i>lsr</i> operon in the transport of autoinducer-2 (AI-2) (pentagons). AI-2 is synthesised intracellularly by LuxS and accumulates extracellularly. LsrB binds AI-2 in the periplasm and internalised by LsrBCDA. LsrK phosphorylates AI-2 which induces the expression of the <i>lsr</i> operon by repressing LsrR, the repressor of the <i>lsr</i> operon (adapted from (Xavier & Bassler, 2005)).	46
Figure 1. 3. Foley catheter insertion in females and males.	48
Figure 1. 4. The lifecycle of a catheter. Stages of a catheter's lifetime at which interventions for reduction or prevention of infection can be applied (Meddings & Saint, 2011).	49
Figure 1. 5. Intervening at the stages of biofilm formation. Stages of biofilm formation at which novel approaches to biofilm inhibition can be applied (Bordi & de Bentzmann, 2011).	57
Figure 2. 1. Schematic representation of the biofilm flow through model.	73
Figure 2. 2. An 8 hour growth curve of <i>E. coli</i> K12 grown under 3 conditions: <i>E. coli</i> K12 was grown without Byotrol™ (growth control); treated with sub-MIC Byotrol™ and grown for 5 hours without Byotrol™ then challenged for 2 hours with 4 times MIC Byotrol™. Error bars indicate the standard deviation.	87
Figure 3. 1. The synthesis of the polyamines spermine, spermidine and putrescine used in this study. Ornithine decarboxylation resulting in the biosynthesis of putrescine, spermidine and spermine.	101
Figure 3. 2. The synthesis of the polyamine cadaverine used in this study. L-Lysine decarboxylation resulting in the biosynthesis of cadaverine.	101
Figure 3. 3. Optimisation of bacterial growth on different microtitre plate surfaces. <i>E. coli</i> K12 and the clinical isolates of <i>K. pneumoniae</i> and <i>P. aeruginosa</i> were grown for 18 hours at 37°C, on 3 different microtitre plates: non-tissue culture treated, tissue culture treated and a non-tissue culture treated plate treated with poly-D-lysine. The results are expressed as the mean of nine	

replicate wells involving 3 biological replicates for each strain. Error bars indicate the standard error of the mean.	103
Figure 3. 4. Minimum growth time required for biofilm formation which can be visualised by crystal violet staining. <i>E. coli</i> K12 and the clinical isolates of <i>K. pneumoniae</i> and <i>P. aeruginosa</i> were grown for 4, 6, 8 and 18 hours at 37°C to determine the optimal growth time which allows for sufficient biofilm to be visualised by crystal violet staining. The results are expressed as the mean of nine replicate wells involving 3 biological replicates for each strain. Error bars indicate the standard error of the mean.	104
Figure 3. 5. The microtitre plate biofilm formation assay to determine the biofilm inhibitory concentration of the polyamines spermine, spermidine, cadaverine and putrescine against <i>E. coli</i> K12 biofilm formation grown for 18 hours at 37°C. The results are expressed as the mean of nine replicate wells involving 3 biological replicates for each strain. Error bars indicate the standard error of the mean.	106
Figure 3. 6. The glass chamber slide assay to determine the biofilm inhibitory concentration of the polyamines spermine, spermidine, cadaverine and putrescine against <i>E. coli</i> K12 biofilms grown for 18 hours at 37°C. The results are expressed as the mean of nine replicate wells involving 3 biological replicates for each strain. Error bars indicate the standard error of the mean.	107
Figure 3. 7. The effect of increasing concentrations of sodium hydroxide (NaOH) on <i>E. coli</i> K12 biofilm growth. The bars indicate the average biofilm growth, the black line indicates the pH. The results are expressed as the mean of 3 replicate wells involving 3 biological replicates for each strain. Error bars indicate the standard error of the mean.	108
Figure 3. 8. The reaction scheme demonstrating the quaternisation of spermine. The six hydrogen atoms of the four primary amines of spermine reacted with methyl iodide to produce hydrogen iodide. The methyl groups replace each of the hydrogen atoms associated with the nitrogen atoms to form quaternary ammonium groups. This reaction completes the quaternisation of spermine.	110

- Figure 3. 9.** Characterisation of quaternised spermine. **a)** ^1H NMR (D_2O) spectrum of a stationary sample of quaternised spermine. Capital letters from A-D correspond to the groups which are circled on the structure of quaternised spermine (part b); **b)** structure of quaternised spermine showing the number of hydrogen atoms associated with each carbon atom (e.g. 9 H) below the structure and capital letters from A-D which identify the groups which correspond to the peaks on the NMR spectrum..... 111
- Figure 3. 10.** Characterisation of quaternised spermidine. **a)** ^1H NMR (D_2O) spectrum of a stationary sample of quaternised spermidine. Capital letters from A-D correspond to the groups which are circled on the structure of quaternised spermidine (part b); **b)** structure of quaternised spermidine showing the number of hydrogen atoms associated with each carbon atom (e.g. 9 H) below the structure and capital letters from A-D which identify the groups which correspond to the peaks on the NMR spectrum..... 112
- Figure 3. 11.** Characterisation of quaternised cadaverine. **a)** ^1H NMR (D_2O) spectrum of a stationary sample of quaternised cadaverine. Capital letters from A-D correspond to the groups which are circled on the structure of quaternised cadaverine (part b); **b)** structure of quaternised cadaverine showing the number of hydrogen atoms associated with each carbon atom (e.g. 9 H) below the structure and capital letters from A-D which identify the groups which correspond to the peaks on the NMR spectrum..... 113
- Figure 3. 12.** Characterisation of quaternised putrescine. **a)** ^1H NMR (D_2O) spectrum of a stationary sample of quaternised putrescine. Capital letters from A-D correspond to the groups which are circled on the structure of quaternised putrescine (part b); **b)** structure of quaternised putrescine showing the number of hydrogen atoms associated with each carbon atom (e.g. 9 H) below the structure and capital letters from A-D which identify the groups which correspond to the peaks on the NMR spectrum..... 114
- Figure 3. 13.** The MIC assay to determine the effect of spermine with the pH adjusted to 7, against *E. coli* K12, and clinical isolates of *K. pneumoniae* and *P. aeruginosa* biofilm formation grown for 18 hours at 37°C and analysed by the microtitre plate biofilm formation assay. The results are expressed as the mean of 16 replicate wells involving two biological replicates for each strain. Error bars indicate the standard error of the mean. 117

Figure 3. 14. The microtitre plate biofilm formation assay to determine the effect of spermine with the pH adjusted to 7, against <i>E. coli</i> K12, and clinical isolates of <i>K. pneumoniae</i> and <i>P. aeruginosa</i> biofilm cells grown for 18 hours at 37°C and analysed by the MIC assay. The results are expressed as the mean of 16 replicate wells involving two biological replicates for each strain. Error bars indicate the standard error of the mean.	118
Figure 3. 15. Western blot analysis of OprF from <i>P. aeruginosa</i> probed with monoclonal antibody MA7-3. Lane 1: Biofilm grown for 18 hours on glass slides, static; Lane 2: Planktonic growth after 18 hours shaking. Both samples contained the same concentration of protein as determined by the Bradford assay. This western blot is a representation of a minimum of 3 biological replicates.....	119
Figure 4. 1 a. Polyquaternium compounds used in this study.....	125
Figure 4. 2 b. Polyquaternium compounds used in this study (continued).....	126
Figure 4. 3. The dose response of Polyquaternium-4 against the planktonic cells of <i>E. coli</i> K12 and clinical isolates of <i>E. coli</i> , <i>K. pneumoniae</i> and <i>P. aeruginosa</i> , grown for 18 hours.	131
Figure 4. 4. The dose response of Polyquaternium-4 against the biofilm cells of <i>E. coli</i> K12 and clinical isolates of <i>E. coli</i> , <i>K. pneumoniae</i> and <i>P. aeruginosa</i> , grown for 18 hours.	132
Figure 4. 5. The dose response of Polyquaternium-6 (12 kDa) against the planktonic cells of <i>E. coli</i> K12 and clinical isolates of <i>E. coli</i> , <i>K. pneumoniae</i> and <i>P. aeruginosa</i> , grown for 18 hours.	133
Figure 4. 6. The dose response of Polyquaternium-6 (12 kDa) against the biofilm cells of <i>E. coli</i> K12 and clinical isolates of <i>E. coli</i> , <i>K. pneumoniae</i> and <i>P. aeruginosa</i> , grown for 18 hours.	134
Figure 4. 7. The dose response of Polyquaternium-7 against the planktonic cells of <i>E. coli</i> K12 and clinical isolates of <i>E. coli</i> , <i>K. pneumoniae</i> and <i>P. aeruginosa</i> , grown for 18 hours.	135
Figure 4. 8. The dose response of Polyquaternium-7 against the biofilm cells of <i>E. coli</i> K12 and clinical isolates of <i>E. coli</i> , <i>K. pneumoniae</i> and <i>P. aeruginosa</i> , grown for 18 hours.	136

Figure 4. 9. The dose response of Polyquaternium-10 against the planktonic cells of <i>E. coli</i> K12 and clinical isolates of <i>E. coli</i> , <i>K. pneumoniae</i> and <i>P. aeruginosa</i> , grown for 18 hours.	137
Figure 4. 10. The dose response of Polyquaternium-10 against the biofilm cells of <i>E. coli</i> K12 and clinical isolates of <i>E. coli</i> , <i>K. pneumoniae</i> and <i>P. aeruginosa</i> , grown for 18 hours.	138
Figure 4. 11. The dose response of Polyquaternium-28 against the planktonic cells of <i>E. coli</i> K12 and clinical isolates of <i>E. coli</i> , <i>K. pneumoniae</i> and <i>P. aeruginosa</i> , grown for 18 hours.	139
Figure 4. 12. The dose response of Polyquaternium-28 against the biofilm cells of <i>E. coli</i> K12 and clinical isolates of <i>E. coli</i> , <i>K. pneumoniae</i> and <i>P. aeruginosa</i> , grown for 18 hours.	140
Figure 4. 13. The dose response of Polyquaternium-37 against the planktonic cells of <i>E. coli</i> K12 and clinical isolates of <i>E. coli</i> , <i>K. pneumoniae</i> and <i>P. aeruginosa</i> , grown for 18 hours.	141
Figure 4. 14. The dose response of Polyquaternium-37 against the planktonic cells of <i>E. coli</i> K12 and clinical isolates of <i>E. coli</i> , <i>K. pneumoniae</i> and <i>P. aeruginosa</i> , grown for 18 hours.	142
Figure 4. 15. The dose response of Byotrol™ against the planktonic cells of <i>E. coli</i> K12 and clinical isolates of <i>E. coli</i> , <i>K. pneumoniae</i> and <i>P. aeruginosa</i> , grown for 18 hours.	143
Figure 4. 16. The dose response of Byotrol™ against the biofilm cells of <i>E. coli</i> K12 and clinical isolates of <i>E. coli</i> , <i>K. pneumoniae</i> and <i>P. aeruginosa</i> , grown for 18 hours.	144
Figure 4. 17. The dose response of Polyquaternium-6 (38 kDa) against the planktonic cells of <i>E. coli</i> K12 and clinical isolates of <i>E. coli</i> , <i>K. pneumoniae</i> and <i>P. aeruginosa</i> , grown for 18 hours.	147
Figure 4. 18. The dose response of Polyquaternium-6 (38 kDa) against the biofilm cells of <i>E. coli</i> K12 and clinical isolates of <i>E. coli</i> , <i>K. pneumoniae</i> and <i>P. aeruginosa</i> , grown for 18 hours.	148

Figure 4. 19. The dose response of Polyquaternium-6 (400 kDa) against the planktonic cells of <i>E. coli</i> K12 and clinical isolates of <i>E. coli</i> , <i>K. pneumoniae</i> and <i>P. aeruginosa</i> , grown for 18 hours.	149
Figure 4. 20. The dose response of Polyquaternium-6 (400 kDa) against the biofilm cells of <i>E. coli</i> K12 and clinical isolates of <i>E. coli</i> , <i>K. pneumoniae</i> and <i>P. aeruginosa</i> , grown for 18 hours.	150
Figure 4. 21. Viable cell counts determining the activity of increasing concentrations of Polyquaternium-6 (12 kDa) against the planktonic cells of <i>E. coli</i> K12 and the clinical isolates of <i>E. coli</i> , <i>K. pneumoniae</i> and <i>P. aeruginosa</i> grown for 18 hours. Growth is presented as the colony forming units/mL (CFU/mL) from an average of a minimum of 3 biological replicates. Error bars indicate the standard deviation.	151
Figure 4. 22. Bright field microscopy of biofilms treated with Polyquaternium-6 (12 kDa) Bright field microscopy images (100x magnification) showing the effects of increasing concentrations of Polyquaternium-6 on the biofilm formation of <i>E. coli</i> K12 and the clinical isolates of <i>E. coli</i> , <i>K. pneumoniae</i> and <i>P. aeruginosa</i> grown for 18 hours and stained with crystal violet.	152
Figure 4. 23. The individual constituents of Byotrol™: BAC, DDQ and PHMB.....	153
Figure 4. 24. Viable cell counts determining the activity of increasing concentrations of Byotrol™ against the planktonic cells of <i>E. coli</i> K12 and the clinical isolates of <i>E. coli</i> , <i>K. pneumoniae</i> and <i>P. aeruginosa</i> grown for 18 hours. Growth is presented as the colony forming units/mL (CFU/mL) from an average of a minimum of 3 biological replicates. Error bars indicate the standard deviation.....	157
Figure 4. 25. Bright field microscopy of biofilms treated with Byotrol™. Bright field microscopy images (100x magnification) showing the effects of increasing concentrations of Byotrol™ on the biofilm formation of <i>E. coli</i> K12 and the clinical isolates of <i>E. coli</i> , <i>K. pneumoniae</i> and <i>P. aeruginosa</i> grown for 18 hours and stained with crystal violet.	158
Figure 4. 26. The effects of a Byotrol™ coated glass surface on biofilm development.	160

Figure 4. 27. The effects of a Byotrol™ coated polystyrene surface on biofilm development.	161
Figure 4. 28. The coating potential of Byotrol™: a) atomic force microscopy images of a glass surface coated with 5 µg/mL and 1 mg/mL Byotrol™ for 18 hours; b) a scratch was made across the surface to indicate the depth of the coatings. The film depth was determined by measuring the distance across the scratches in 3 distinct areas.	163
Figure 4. 29. Eradication of an 18 hour biofilm: Minimum biofilm eradication concentration (MBEC) determining the activity of increasing concentrations of Byotrol™ on a biofilm grown on polystyrene pegs for 18 hours and treated with Byotrol™ for 18 hours under static conditions at 37°C. Bacterial cells were allowed to recover in fresh media for 18 hours. The extent of biofilm formation was determined by crystal violet staining and solubilised. The absorbance values of the solubilised stain displayed represent the mean of over 24 experiments, involving a minimum of 3 biological replicates for each strain. Error bars indicate the standard error of the mean.	165
Figure 4. 30. P-MIC for planktonic cells shed from a biofilm: The activity of increasing concentrations of Byotrol™ on a biofilm grown on polystyrene pegs for 18 hours and treated with Byotrol™ for 18 hours under static conditions at 37°C. The growth of planktonic cells shed from the biofilm grown on the pegs was determined by reading the absorbance. The absorbance values represent the mean of over 24 experiments, involving minimum of 3 biological replicates for each strain. Error bars indicate the standard error of the mean.	166
Figure 4. 31. The folding effect of polyquaterniums as the polymer chain length increases and the molecular weight increases. The positive charges are closer together when a polymer folds, and this reduces its antimicrobial effect, as the positive charge is sequestered by the counter-ion.....	168
Figure 5. 1. Diagram outlining the growth conditions for <i>E. coli</i> K12 cells from which proteins were extracted for analysis.	174
Figure 5. 2. Optimisation of the DTT concentration used for protein extraction. 200 µg of protein extracted from planktonic cells grown for 24 hours using an	

extraction buffer with a range of DTT concentrations were resolved on 17 cm, pH 3-10 IPG strips. Arrows indicates the furthest distance to which the proteins are resolved.....	175
Figure 5. 3. 2DGE optimisation of DTT concentration.	176
Figure 5. 4. 2DGE of proteins using 17 cm, pH 3-10 IPG strips. 200 µg of protein extracted from planktonic cells grown for 24 hours, resolved by isoelectric focussing and then on a 10% SDS-PAGE gel. Proteins were visualised by silver staining. Each gel represents a separate biological replicate.....	177
Figure 5. 5. Replicate gels displaying resolved proteins extracted from planktonic and biofilm cells of <i>E. coli</i> K12 demonstrate reproducibility.....	178
Figure 5. 6. Identification of differentially expressed proteins extracted from the growth controls of the planktonic and biofilm phenotypes of <i>E. coli</i> K12: a) proteins extracted from planktonic cells grown for 24 hours (growth control); b) proteins extracted from biofilm cells grown for 24 hours (growth control). Numbered white arrows indicate proteins which are differentially expressed. Proteins in the white circle (a) are landmark proteins.	179
Figure 5. 7. The enlarged detail of tryptophanase up-regulated in the biofilm phenotype when compared to the planktonic phenotype of <i>E. coli</i> K12: a) tryptophanase extracted from planktonic cells grown for 24 hours; b) tryptophanase extracted from biofilm cells grown for 24 hours. Differentially expressed proteins are indicated with numbered arrows...	182
Figure 5. 8. The enlarged detail of D-ribose periplasmic binding protein down-regulated in the biofilm phenotype when compared to the planktonic phenotype of <i>E. coli</i> K12: a) D-ribose periplasmic binding protein extracted from planktonic cells grown for 24 hours; b) D-ribose periplasmic binding protein extracted from biofilm cells grown for 24 hours. Differentially expressed proteins are indicated with numbered arrows.	182
Figure 5. 9. Replicate gels displaying resolved proteins extracted from planktonic cells of <i>E. coli</i> K12 grown a) without Byotrol™ (growth control) and b) with sub-MIC Byotrol™ 24 hours. All proteins were separated using iso-electric	

focussing in the first dimension and 10% SDS-PAGE in the second dimension and visualised by silver staining.	184
Figure 5. 10. Identification of differentially expressed proteins extracted from planktonic cells grown for 24 hours a) without Byotrol™ (growth control) and b) treated with Byotrol™. Numbered white arrows indicate differentially expressed proteins. Proteins in the white circle (a) are landmark proteins.	186
Figure 5. 11. The enlarged detail of up-regulated proteins identified in the planktonic phenotype of <i>E. coli</i> K12 grown for 24 hours when a) treated with Byotrol™, compared to b) <i>E. coli</i> K12 planktonic cells grown without Byotrol™ (growth control). Numbered white arrows indicate proteins which are differentially expressed.....	189
Figure 5. 12. The enlarged detail of down-regulated proteins identified in the planktonic phenotype of <i>E. coli</i> K12 cells grown for 24 hours a) without Byotrol™ (growth control) and b) treated with Byotrol™. Numbered white arrows indicate proteins which are differentially expressed.	189
Figure 5. 13. Replicate gels displaying resolved proteins extracted from a) planktonic and b) biofilm cells of <i>E. coli</i> K12 treated with sub-MIC Byotrol™ for 24 hours. All proteins were separated using iso-electric focussing in the first dimension, 10% SDS-PAGE in the second dimension and visualised by silver staining.	191
Figure 5. 14. Identification of differentially expressed proteins extracted from a) planktonic and b) biofilm cells treated with sub-MIC Byotrol™ for 24 hours. Numbered white arrows indicate proteins which are differentially expressed. Proteins in the white circle (a) are landmark proteins.	193
Figure 5. 15. The enlarged detail of lactaldehyde dehydrogenase up-regulated in a) planktonic cells of <i>E. coli</i> K12 when compared to b) biofilm cells treated with sub-MIC Byotrol™ for 24 hours. Numbered white arrows indicate differentially expressed proteins.	194
Figure 5. 16. Replicate gels displaying resolved proteins extracted from the planktonic phenotype of <i>E. coli</i> K12 grown under 3 conditions: a) growth to mid-log phase (5 hours); b) growth treated with sub-MIC Byotrol™ (0.6 µg/mL) for 5 hours; c) growth for 5 hours, challenged for 2 hours with 4 times MIC	

Byotrol™ (10.5 µg/mL). All proteins were separated using iso-electric focussing in the first dimension, 10% SDS-PAGE in the second dimension and visualised by silver staining.....	197
Figure 5. 18. The enlarged detail of differentially expressed proteins of the planktonic phenotype of <i>E. coli</i> K12 grown a) to mid-exponential phase (5 hours) without Byotrol™; b) to mid-exponential phase (5 hours) with sub-MIC Byotrol™; c) to mid-exponential phase (5 hours) without Byotrol™ and challenged for 2 hours with 4 times MIC (10.5 µg/mL) Byotrol™. Numbered white arrows indicate differentially expressed proteins.	200
Figure 5. 19. The enlarged detail of differentially expressed proteins of the planktonic phenotype of <i>E. coli</i> K12 grown a) to mid-exponential phase (5 hours) without Byotrol™; b) to mid-exponential phase (5 hours) with sub-MIC Byotrol™; c) to mid-exponential phase (5 hours) without Byotrol™ and challenged for 2 hours with 4 times MIC (10.5 µg/mL) Byotrol™. Numbered white arrows indicate differentially expressed proteins.	200
Figure 5. 20. Indole as a global regulator of cellular functions in <i>E. coli</i>	209
Figure 6. 1. Illustration of the terms used to describe the principles of RNA-Seq. The number of reads is related to the sequencing depth. Each read is mapped to a reference genome and the number of genes that map to a gene is referred to as the gene count. The gene count is related to the length of the gene.	212
Figure 6. 2. Breakdown of <i>E. coli</i> K12 growth control sequences into 5 distinct categories.....	214
Figure 6. 3. Analysis flowchart with detailed breakdown of sequences of <i>E. coli</i> K12 growth control.	214
Figure 6. 4. Analysis flowchart with detailed breakdown of sequences of <i>E. coli</i> K12 treated with sub-MIC Byotrol™ (treated).	215
Figure 6. 5. Breakdown of sequences of <i>E. coli</i> K12 cells treated with sub-MIC Byotrol™, into 5 distinct categories (treated).	215
Figure 6. 7. Analysis flowchart with detailed breakdown of sequences of <i>E. coli</i> K12 grown to mid-exponential phase and challenged with 4 times MIC Byotrol™ 2 hours (challenge).	216

Figure 6. 6. Breakdown of <i>E. coli</i> K12 cells grown to mid-exponential phase and challenged with 4 times MIC Byotrol™ 2 hours, into 5 distinct categories (challenge).....	216
Figure 6. 8. Total number of differentially expressed genes (fold change of ≤ 2 and ≥ 2) in the three different growth conditions: growth control, cells treated with Byotrol™ (treated) and cells challenged with Byotrol™ for 2 hours after 5 hours of growth (challenge).	217
Figure 6. 9. Venn diagram demonstrating the distribution of highly differentially expressed genes (fold change of ≤ 5 and ≥ 5) when compared across the different growth conditions (growth control, <i>E. coli</i> K12 cells treated with sub-MIC Byotrol™ and <i>E. coli</i> K12 cells challenged with 4 times MIC Byotrol™).....	218
Figure 6. 10. Proportion of up and down regulated genes as a total of the genes differentially expressed (fold change of ≤ 5 and ≥ 5) under the three different growth conditions	221
Figure 6. 11. Number of genes up and down-regulated when compared to the different growth conditions, catergorised according to gene function.....	225
Figure 6. 12. Components of flagella and the genes involved in the synthesis of flagella apparatus. Genes highlighted within a box are those that are differentially expressed in the current study (Image adapted from California, 2012). ...	230
Figure 6. 13. Identification of unmapped reads in <i>E. coli</i> K12 growth control cells. ...	238

List of Tables

Table 1. 1. Microorganisms associated with the colonisation of different medical devices.....	38
Table 1. 2. Catheters and comments on their uses.	47
Table 1. 3. Summary of efflux determinants relevant to the compounds and organisms used in the current study (Poole, 2005a).	67
Table 2. 1. Reagents for growth medium.	72
Table 2. 2. Buffers and reagents for the biofilm flow through system.....	74
Table 2. 3. Reagents and buffers for SDS-PAGE and western blot analysis.	77
Table 2. 4. Quaternary ammonium compounds used in this study.	80
Table 2. 5. Summary of columns used for size exclusion chromatography (SEC). Molecular weight (Mw) range based on polyethylene oxide calibration. ...	81
Table 2. 6. Components of rehydration buffer.	88
Table 2. 7. Reagents and buffers for two-dimensional gel electrophoresis.....	90
Table 2. 8. IEF program used for first dimension separation of proteins using a 17 cm IPG strip. Step 1 ensures salts are removed and are not carried through into the separation steps. Steps 2-7 mediate the electrophoretic mobility of proteins along the pH gradient on the strip. The focussing of proteins occurs during step 8. Step 9 is important for holding the proteins in their positions to minimise diffusion from their iso-electric point.	92
Table 3. 1. The minimum biofilm inhibitory concentration of quaternised polyamines on <i>E. coli</i> K12, and clinical isolates of <i>K. pneumoniae</i> and <i>P. aeruginosa</i> biofilm formation grown for 18 hours at 37°C, analysed by the microtitre plate assay. The results are expressed as mM and mg/mL concentrations.	115
Table 4. 1. Nomenclature of polyquaternium compounds used in this study.	124
Table 4. 3. The minimum inhibitory concentration (MIC) of polyquaternium (PQ) compounds and Byotrol™ for the planktonic growth of <i>E. coli</i> K12 and the clinical isolates of <i>E. coli</i> , <i>K. pneumoniae</i> and <i>P. aeruginosa</i>	129

Table 4. 4. The minimum biofilm inhibitory concentration of polyquaternium (PQ) compounds and Byotrol™ for the biofilm growth of <i>E. coli</i> K12 and the clinical isolates of <i>E. coli</i> , <i>K. pneumoniae</i> and <i>P. aeruginosa</i>	130
Table 4. 5. The minimum inhibitory concentration of increasing molecular weights of Polyquaternium-6 (PQ-6) compounds for the planktonic growth of <i>E. coli</i> K12 and the clinical isolates of <i>E. coli</i> , <i>K. pneumoniae</i> and <i>P. aeruginosa</i>	146
Table 4. 6. The minimum biofilm inhibitory concentration of increasing molecular weights of Polyquaternium-6 (PQ-6) compounds for the planktonic growth of <i>E. coli</i> K12 and the clinical isolates of <i>E. coli</i> , <i>K. pneumoniae</i> and <i>P. aeruginosa</i>	146
Table 4. 7. Minimum inhibitory concentrations (MICs) of Byotrol™ and its constituents, PHMB, DDQ and BAC against <i>E. coli</i> K12 and the clinical isolates of <i>E. coli</i> , <i>K. pneumoniae</i> and <i>P. aeruginosa</i>	155
Table 4. 8. Minimum biofilm inhibitory concentrations of Byotrol™ and its constituents, PHMB, DDQ and BAC against <i>E. coli</i> K12 and the clinical isolates of <i>E. coli</i> , <i>K. pneumoniae</i> and <i>P. aeruginosa</i>	155
Table 5. 1. The identification of differentially expressed proteins by mass spectrometry.	181
Table 5. 2. Statistical analysis of differentially expressed proteins extracted from the planktonic and biofilm phenotypes of <i>E. coli</i> K12 grown for 24 hours. Protein labels correspond to numbering in Figure 5. 7 and Figure 5. 8. The fold induction and repression of proteins in the biofilm phenotype is calculated by using the integrated density values of proteins differentially expressed in the biofilm growth control in relation to the planktonic growth control. <i>t</i> -values were calculated using the unpaired two-tailed <i>t</i> -test. A <i>t</i> -value of <0.05 is considered statistically significant.....	183
Table 5. 3. Identification of differentially expressed proteins by mass spectrometry..	188
Table 5. 4. The statistical analysis of differentially expressed proteins extracted from the planktonic phenotypes of <i>E. coli</i> K12 grown with and without Byotrol™ for 24 hours.	190

Table 5. 5. The identification of differentially expressed proteins by mass spectrometry.	194
Table 5. 6. The statistical analysis of differentially expressed proteins extracted from the planktonic and biofilm phenotypes of <i>E. coli</i> K12 treated with sub-MIC Byotrol™ for 24 hours.....	195
Table 5. 7. Identification of differentially expressed proteins by mass spectrometry. Proteins were identified from 2DGE analysis of the planktonic phenotype of <i>E. coli</i> K12 grown to mid-exponential phase (5 hours) under 3 growth conditions. The protein label corresponds to numbering on the gels in Figure 5. 18 and Figure 5. 19. The protein name and accession number were taken from a search on the UniProt <i>E. coli</i> K12 database. The number of matched peptides were derived from the number of peptides which accurately match the protein sequence, a number >2 is considered to be fully identified.	199
Table 5. 8. The statistical analysis of differentially expressed proteins extracted from the planktonic phenotype of <i>E. coli</i> K12 grown for 5 hours. Protein labels correspond to numbering in Figure 5. 18 and Figure 5. 19. The fold induction and repression of proteins in the biofilm phenotype were calculated by using the integrated density values of proteins differentially expressed under the two conditions. <i>t</i> -values were calculated using the unpaired two-tailed <i>t</i> -test. A <i>t</i> -value of <0.05 is considered statistically significant.	202
Table 5. 9. Comparison of protein expression changes between the different growth conditions and phenotypes of <i>E. coli</i> K12: ↑ indicates the up-regulation of the protein in relation to the growth control; ↓ indicates the down-regulation of the protein in relation to the growth control; – indicates no difference in expression in relation to the growth control.....	203
Table 6. 1. Classification of genes up-regulated in response to Byotrol™ according to their function.	223
Table 6. 2. Classification of genes down-regulated in response to Byotrol™ according to their gene function.....	224

Table 6. 3. Genes in <i>E. coli</i> K12 that were differentially expressed in response to treatment with Byotrol™ compared to the growth control. Genes with a fold change ≥ 5 and ≤ 5 are displayed.	226
Table 6. 4. Genes in <i>E. coli</i> K12 up-regulated in response to challenge with Byotrol™ compared to treatment with Byotrol™. Genes with a fold change ≥ 5 are displayed.....	227
Table 6. 6. Genes in <i>E. coli</i> K12 that were up-regulated in response to challenge with Byotrol™ compared to the growth control. Genes with a fold change greater 5 compared to untreated cells are displayed.....	231
Table 6. 7. Genes in <i>E. coli</i> K12 that were down-regulated in response to challenge with Byotrol™ compared to the growth control. Genes with a fold change greater 5 compared to untreated cells are displayed.....	234
Table 6. 8. Genes up-regulated in one growth condition and down-regulated in another.	235
Table 6. 9. Genomes and sequences identified by BLAST to which unmapped reads align and the range of hits (reads) to the genome or sequence.....	237

List of Abbreviations

%	percent	mA	milliampere
<	less than	MBEC	minimum bacterial eradication concentration
>	greater than	Mg²⁺	magnesium ion
°C	degrees Celcius	mg/mL	milligram per millilitre
µg/mL	micrograms per microlitre	MIC	minimum inhibitory concentration
µm	micrometre	mL	millilitre
µm²	micrometre squared	mm	millimetre
2DGE	two-dimensional gel electrophoresis	mM	millimolar
4QS	4-quinolones	Mw	molecular weight
AFM	atomic force microscopy	NaOH	sodium hydroxide
Ag	silver	nL	nanolitre
AHL	N-acyl homoserine lactone	nm	nanometre
ATP	adenosine triphosphate	NMR	nuclear magnetic resonance
approx./‘~’	approximately	NO	nitric oxide
BAC	benzalkonium chloride	OD	optical density
bp	base pair	OMIC	Organic Materials Innovation Centre
CA	California state	Omp	outer membrane protein
Ca²⁺	calcium ion	OR	Oregon state
cat. no.	catalogue number	PBS	phosphate buffered saline
CAUTI	catheter associated urinary tract infection	PFTE	polytetrafluoroethylene
CFU/mL	colony forming units per millilitre	PHMB	polyhexamethylene biguanide
CIC	clean intermittent catheter	pI	isoelectric point
CLSI	Clinical and Laboratory Standards Institute	PICC	peripherally inserted central catheter
cm	centimetre	PQ	polyquaternium
CMFT	Central Manchester Foundation Trust	PQS	Pseudomonas quinolone signal
CVC	central venous line	PVC	polyvinyl chloride
D₂O	deuterium oxide	QAC	quaternary ammonium compound
Da	dalton	QS	quorum sensing
DPD	dihydroxy-pentanedione	r. p. m.	revolutions per minute
DTT	dithiothreitol	RNA	ribonucleic acid
DNA	deoxyribonucleic acid	SDS	sodium dodecyl sulphate
eDNA	extracellular DNA	PAGE	polyacrylamide gel electrophoresis
EPEC	enteropathogenic <i>E. coli</i>	SEC	size exclusion chromatography
EPS	extrapolymeric substance	SICC	subclavian inserted central catheter
FDA	Food and Drug Administration	TEMED	tetramethylethylenediamine
H⁺	hydrogen ion	THF	tetrahydrofuran
GPC	gas permeation chromatography	UPEC	uropathogenic <i>E. coli</i>
IgG	immunoglobulin G	UTI	urinary tract infection
IPG	immobilised pH gradient	UV	ultra violet
JICC	jugular inserted central catheter	V	volts
kDa	kilodalton	v/v	volume to volume
KEGG	Kyoto Encyclopedia of Genes and Genomes	w/v	mass to volume
LB	lysogeny broth or Luria-Bertani	wt %	weight percent
M	molar	x g	times gravity

THE UNIVERSITY OF MANCHESTER

ABSTRACT OF THESIS submitted by Nishal Govindji for the degree of Doctor of Philosophy (Ph. D.) and entitled Inhibiting Biofilms Formed by Gram-negative Uropathogenic Bacteria

June 2013

Urinary catheters are indispensable in healthcare and, with an ageing population, their use will continue to increase. However, they are commonly associated with colonisation and urinary tract infections (UTIs) caused by the attachment of bacteria to the catheter surface. Application of a novel cationic compound as a catheter coating may have a significant impact on the costs associated with treatment of UTIs and reduce the need for catheter replacement, as well as decreasing the number of UTI associated morbidity and mortality. Cationic compounds in particular are known to interact with the negatively charged outer membrane of bacteria, therefore have a broad spectrum of activity. The purpose of this study was to source and evaluate a novel cationic antimicrobial for use as a potential coating to impede biofilm formation on urinary catheters, and to investigate the cellular response to the selected lead compound.

This research has demonstrated that the antimicrobial activity of commercially available Byotrol™ was superior to that of polyamines and quaternary ammonium compounds that were screened. Using high-throughput antimicrobial assays, such as the minimum inhibitory concentration and microtitre plate biofilm forming assays, the inhibitory concentrations of Byotrol™ were found to range from 3 µg/mL to 15 µg/mL for planktonic cultures, and 3 µg/mL to 20 µg/mL for the biofilm growth of uropathogenic bacteria. Furthermore, the minimum biofilm eradication concentration assay demonstrated that 200-1000 µg/mL Byotrol™ was able to eradicate an established biofilm. Byotrol™ may also have significant potential as a device coating, as pre-coating data on glass slides and microtitre plates with the compound inhibited bacterial growth on the surface at concentrations of 400 µg/mL for *E. coli*, and 1000 µg/mL *K. pneumoniae*. Atomic force microscopy validated the expectation that higher concentrations of Byotrol™ coated a surface more evenly than lower concentrations. Using two-dimensional gel electrophoresis, the metabolic protein tryptophanase was seen to be significantly over-expressed when *E. coli* K12 was treated with sub-inhibitory concentrations of Byotrol™. A transcriptomic approach using RNA-Seq

demonstrated that a majority of the differentially expressed genes were identified in cells that were challenged with 4 times the minimum inhibitory concentration of Byotrol™. Genes associated with protein synthesis and stress response were significantly up-regulated. Interestingly, the global gene regulators AI-2 and indole were significantly up-regulated, which may have an influence on the expression of genes related to motility, biofilm formation and acid-resistance. Genes associated with chemotaxis and motility, acid-resistance and iron transport were significantly down-regulated, particularly in cells challenged with Byotrol™.

Byotrol™ displayed antimicrobial activity both in suspension and as a coating. Identification of differentially expressed genes and proteins, when the bacteria were treated and challenged with Byotrol™, has, for the first time, revealed the bacterial cell's response to this biocide. The findings may enable the development of strategies to prevent or better manage catheter associated urinary tract infection (CAUTI).

Declaration

No portion of the work referred to in the thesis has been submitted in support of an application for another degree or qualification of this or any other university or other institute of learning.

Copyright Statement

- i.** The author of this thesis (including any appendices and/or schedules to this thesis) owns certain copyright or related rights in it (the “Copyright”) and she has given The University of Manchester certain rights to use such Copyright, including for administrative purposes.
- ii.** Copies of this thesis, either in full or in extracts and whether in hard or electronic copy, may be made only in accordance with the Copyright, Designs and Patents Act 1988 (as amended) and regulations issued under it or, where appropriate, in accordance with licensing agreements which the University has from time to time. This page must form part of any such copies made.
- iii.** The ownership of certain Copyright, patents, designs, trade marks and other intellectual property (the “Intellectual Property”) and any reproductions of copyright works in the thesis, for examples graphs and tables (“Reproductions”), which may be described in this thesis, may not be owned by the author and may be owned by third parties. Such Intellectual Property and Reproductions cannot and must not be made available for use without the prior written permission of the owner(s) of the relevant Intellectual Property and/or Reproductions.
- iv.** Further information of the conditions under which disclosure, publication and commercialisation of this thesis, the Copyright and any Intellectual Property Rights and/or Reproductions described in it may take place is available in the University IP Policy (see <http://campus.manchester.ac.uk/medialibrary/policies/intellectual-property.pdf>), in any relevant Thesis restriction declarations deposited in the University Library, The University Library’s regulations (see <http://www.manchester.ac.uk/library/aboutus/regulations>) and in The University’s policy on presentation of Theses.

Publications

Govindji, N., Wills, P., Upton, M., Tirelli, N. & Webb, M. (2013). The anti-biofilm effects of Byotrol™. *Journal of Applied Microbiology*, 114 (5) 1285-93.

Presentations

Prize winner at PRISM Conference, Liverpool, 2011

Prize winner for oral presentation at Postgraduate Researchers in Science and Medicine Conference, Liverpool.

Poster presentation at SGM Spring Conference, Dublin, 2012.

Poster presentation at Age UK Grantholders Conference, Nottingham, 2011.

Oral presentation at PRISM Conference, Liverpool, 2011.

Poster presentation at North West Microbiology Conference, Manchester, 2011.

Poster presentation at Biofilms4 International Conference, Winchester, 2010.

Poster presentation at Age UK Grantholders Conference, Nottingham, 2010.

Poster presentation at Vitae/PRISM Conference, Lancaster, 2010.

Poster presentation at Age UK Grantholders Conference, Birmingham, 2009.

This thesis is dedicated to my parents.

The unconditional love that you have both poured into my life has brought me to where I am today. You taught me how to live through my education with good character and to believe in myself. This thesis, my greatest academic achievement to date, is a testament to everything you have brought me up to be.

Thank you for your guidance, support, encouragement, sacrifice and love.

I offer this work at the Lotus Feet of Bhagawan.

Acknowledgements

I offer my gratitude to Dr. Michelle Webb for her day-to-day support, and my co-supervisor Prof. Nicola Tirelli for his guidance early on during this project. I thank them both sincerely for giving me the opportunity to fulfil my ambition of achieving a Ph. D.

I owe so much of my progress on this career path to my co-supervisor, Dr. Mat Upton. From the moment I finished my undergraduate degree, Mat has taken me under his wing. Although he will modestly say that he was simply doing his job, words can not express how invaluable and reassuring it has been, knowing that I have had him there for support and guidance. Above all, Mat has been an example to me of how to be a genuine and kind person in the workplace, of how to fulfil one's duties with conscientiousness and integrity, and most importantly, how to be a responsible, caring and thoughtful leader. I'll never forget these lessons as I progress on my journey as a Scientist and I hope to be a better person for it.

I also thank Rowan Orme, an amazing person, who, simply out of the goodness of his heart, has carried me through some of the most testing and difficult times during this research. He has built my confidence as a researcher and encouraged me to continue to the next stage just when it seemed that all hope was lost! I thank you, Rowan, from the bottom of my heart for supporting me and mentoring me.

Thank you to John Moat, a trustworthy, extremely generous and selfless friend from Mat Upton's group. From the days of my Masters, John has always been there to watch my back, and has been the person I have been able to call upon and turn to when in need of absolutely anything! Thank you so much John, it's so much more appreciated than words can describe.

I also wish to thank Pete Wills for his guidance with a lot of the Chemistry in this thesis. His patience towards me has been invaluable, especially during very laborious times, as well as the more stressful times. You're a brilliant Chemist and I wish you the greatest success. I extend the thanks to my other Chemistry buddies, the members of Prof. Tirelli's group, especially Chris Cadman for his help with the quaternisation of polyamines.

I thank Age UK, the funding body for this research. I hope that this work adds to the knowledge and understanding needed to bring us closer to making life in old age a more comfortable one.

My heartfelt thanks go to my friends and colleagues in the lab, especially to the knowledgeable post-docs! There have also been many important people who have made my journey less isolated and my life more balanced and enjoyable... my friends from life outside the lab and those where I spent most of my life, in the lab!

Finally, a special thank you to my family; my parents and my sister Reena. I am eternally grateful for all you have sacrificed during the years leading up to fulfilling this ambition, knowing how much it will benefit my future. That leads me to Neel...your understanding and consideration during the most stressful and crucial time of this journey has been amazing. I truly am blessed to have you all in my life.

Chapter 1

Introduction

Indwelling urinary catheters are commonly used in the nosocomial environment and as with many medical devices, are susceptible to colonisation by bacteria. Complications arise when bacteria attach to the surface of the device and develop into biofilms, leading to infection. Once a biofilm has formed, it is notoriously difficult to treat; therefore the catheter needs to be replaced. In the hectic health care setting, catheter replacement often does not happen as frequently as is required to avoid infection, which may contribute to catheter associated urinary tract infections (CAUTIs). CAUTIs are one of the most common nosocomial infections. Moreover, every catheter that is replaced is an additional expense to the health service, and the procedure is a discomfort to the patient.

This project endeavored to identify inhibitors of biofilms formed by Gram-negative uropathogenic bacteria. As a mature biofilm is difficult to eradicate, the efforts of this research were focused on inhibiting the initial growth, attachment and proliferation of bacterial cells. This was achieved by screening cationic compounds, which are known to have the potential to be antimicrobial in nature. The inhibitor most successful at reducing planktonic and biofilm growth was then evaluated further using proteomic and transcriptomic analyses. Proteomics and transcriptomics are often used to evaluate the expression of proteins and genes when cells are under the stress of treatment. These are also useful tools to analyse the metabolic pathways involved in biofilm formation in relation to the planktonic phenotype.

Genes and proteins are up-regulated or over-expressed if they are essential for the growth and survival of bacteria when in the presence of sub-inhibitory concentrations of the novel inhibitor. Knowledge of how bacteria respond to a biocide is important in understanding how they may adapt and survive under stress conditions.

1.1 The bacterial biofilm

As long ago as 1683, Antonie van Leeuwenhoek, out of curiosity, scraped a pungent deposit off his teeth and used his home-made microscope to examine what it was. This was the first microscopic visualisation of bacteria and the discovery of the biofilm (Costerton, 2007a).

A biofilm is a multilayer community of bacterial cells embedded in a hydrated extracellular polymeric substance, enabling the colonisation of a living or inert surface, or phase boundary. This subsequently contributes to the virulence of the organisms within the biofilm matrix and is the main cause of antimicrobial resistance (Flemming *et al.*, 2000; Sadvovskaya *et al.*, 2005). The biofilm is the preferred way for bacteria to live and therefore is their natural state of existence (Jefferson, 2004).

However, since the research by Robert Koch, for which he won a Nobel Prize in 1905, microbiologists have concentrated their efforts on understanding bacteria in pure culture, in the free-living planktonic form. Thankfully, the study of biofilms was taken up again many decades later in the 1930s and 40s by ZoBell and Anderson whose research focussed on biofilm formation from sea water, on glass surfaces (Zobell & Anderson, 1936; Zobell, 1943). Inspired by the research of ZoBell and Anderson, the now highly reputable Canadian scientist J. William Costerton and his team of researchers began their quest to further the understanding of the biofilm phenotype and its prevalence and importance in many different environments.

It has since been deduced that microbial biofilms form in a myriad of environments and are ubiquitous in nature (Costerton *et al.*, 1995; Macfarlane & Macfarlane, 2006). In fact, over 99% of microorganisms on Earth live as a biofilm (Vu *et al.*, 2009). Much of the early research on biofilms was done in natural aquatic environments ranging from the fresh alpine streams in the Bugaboo Mountains of Southern British Columbia to the deep waters of the oceans (Costerton *et al.*, 1987; Trachoo, 2003; Zobell & Anderson, 1936).

From this extensive research, it was determined that biofilms can grow well in any environment which have an adequate nutrient supply (Costerton & Lewandowski, 1995) including most abiotic surfaces and all natural ecosystems (Costerton, 2007a). For example, biofilms can be found on all plants and vegetation that support the growth of polymicrobial biofilms that grow both as commensal and pathogenic communities on plant roots, tissues, phloem and xylem, seeds, stems and leaves, and the surrounding soil and rhizosphere (Danhorn & Fuqua, 2007).

Microbial biofilms also form as commensal communities on biotic surfaces in a diverse number of sites of the healthy human body, each with different and challenging

environments. The relatively dry environment of the skin, for example, is host to a wide range of bacterial and fungal biofilms; the human vagina has its own ecosystem of bacteria and yeasts that change at different stages of the menstrual cycle, and at different stages of a female's life (Costerton, 2007b). The early colonisation of the intestinal mucosa has been the topic of research for decades (MacFarlane & Macfarlane, 2003; Macfarlane & Dillon, 2007). Biofilms in the intestine are dynamic populations that competitively occupy binding sites on intestinal endothelial cells that would otherwise be targets for pathogenic adhesins. In the intestines, the natural flora of bacterial biofilms also play important roles in digestion and metabolism. Natural biofilms often consist of multiple species of microorganisms, but in some cases can also exist as single species (Mah & O'Toole, 2001).

Much research has been dedicated to understanding biofilm formation and the pathogenesis of disease. One of the most common biofilms that we encounter day-to-day is formed on the tooth surface, known as dental plaque, predominantly caused by *Acinomyces* and *Streptococcus* spp. Growth of a biofilm on the tooth can lead to dental caries and gingivitis (Stenudd *et al.*, 2001). In immunocompromised hosts such as those with cystic fibrosis, biofilm formation of the mucosal surface of the lungs has also been studied in great depth (Sriramulu *et al.*, 2005). Delayed wound healing is often a predisposing factor for biofilm formation often caused by *Pseudomonas* spp. (Guo & Dipietro, 2010).

Biofilm formation on any abiotic surface is also a great concern that expands to, and encompasses, all manner of industries and disciplines. These include engineering, ecology, industrial aquatic environments, the food processing and beverage industries, metal industries, water and oil piping industries and medicine as biofilm formation can cause surface biocorrosion, pipe blockage, contamination and infection (Costerton, 2007b; Trachoo, 2003; Van & Michiels, 2005). However, there has never been a more important implication of biofilm formation on abiotic surfaces, than the bacterial colonisation of medical biomaterials. It is this that is of great importance and which needs to be understood in greater depth. Medical devices such as artificial heart valves, prosthetic devices, surgically implanted devices, contact lenses, wound drainage tubes, dressings, intrauterine contraception devices, sutures, intravenous catheters and urinary catheters are frequently colonised with biofilms, and can cause chronic infection and even mortality (Costerton *et al.*, 1987). Table 1. 1 highlights the range of

microorganisms that are associated with different indwelling medical devices. Each of these devices has their own challenging environments, which the bacteria associated with colonisation have adapted to in order to survive. This therefore presents great challenges in our efforts to eradicate bacterial growth and control infection.

Table 1. 1. Microorganisms associated with the colonisation of different medical devices.

(Donlan, 2001b; Donlan & Costerton, 2002; Mermel *et al.*, 2001; Mulla & Revdiwala; Revdiwala *et al.*, 2011).

Medical Device	Microorganisms
Prosthetic heart valves	Coagulase-negative staphylococci, enterococci, Gram-negative coccobacilli, <i>S. aureus</i> , streptococci
Central venous catheters	<i>C. albicans</i> , coagulase-negative staphylococci, <i>E. faecalis</i> , <i>K. pneumonia</i> , <i>P. aeruginosa</i> , <i>S. aureus</i>
Contact lenses	<i>Candida</i> spp., <i>E. coli</i> , <i>Fusarium</i> spp. <i>P. aeruginosa</i> , <i>Proteus</i> spp., <i>S. aureus</i> , <i>S. epidermidis</i> , <i>Serratia</i> spp.
Intrauterine devices	<i>C. albicans</i> , <i>Corynebacterium</i> spp., enterococci, Group B Streptococci, <i>Micrococcus</i> spp., <i>S. aureus</i> , <i>S. epidermidis</i>
Urinary catheters	<i>E. aerogenes</i> , <i>E. coli</i> , <i>E. faecalis</i> , <i>K. pneumonia</i> , <i>P. aeruginosa</i> , <i>P. mirabilis</i> , <i>P. vulgaris</i> , <i>S. epidermidis</i>

1. 2. Biofilm formation and structure

In any natural environment, it is less common that a single species biofilm will form. A biofilm is more likely to consist of a range of species, thereby making natural biofilms a unique and complex environment (Sutherland, 2001).

1. 2. 1. Stages of biofilm formation

A biofilm is in a constant state of change and adaptation and biofilm formation is a complex multi-step process that occurs as a combination of two separate factors: genetic and physico-chemical (Wimpenny *et al.*, 2000). Although the intricacies of biofilm formation may differ from species to species and strain to strain, and may vary depending on the environment in which the biofilm is formed, the fundamental stages of biofilm formation are, on the whole, universal. Figure 1.1 shows the stages of biofilm formation under flow conditions.

1. 2. 1. 1. *Stage 1a: Surface conditioning*

In order for bacteria to attach to a surface, a conditioning layer is required prior to the initial attachment stage (Busscher *et al.*, 2000). This is the first true stage of biofilm formation. The conditioning layer in a urinary catheter is formed of organic compounds, which include proteins, electrolytes, surface active compounds and cholesterol (Schneider, 1996).

1. 2. 1. 2. *Stage 1b: Cell – surface interaction and attachment*

The next stage of biofilm formation is cell – surface interaction; the stage of initial attachment, which occurs rapidly (Hussain *et al.*, 1997). The interaction of primary colonisers to a surface can occur in two ways: passively, due to Brownian motion, gravity, diffusion or the flow of liquid or air, all involving interaction forces (Brown & Smith, 2003) or actively, due to positioning mechanisms such as flagella motility and surface appendages (de Kievit & Iglewski, 2003).

Attachment involving interaction forces, or electrostatic forces, charge interactions and hydrophobicity, result in reversible adherence of bacteria to a surface by a single pole

(Brown & Smith, 2003) (Figure 1. 1; stage 1). The duration of this type of attachment depends greatly on the strength of the force. Irreversible attachment is a much more stable state which occurs when the long axis of the bacterial cell body is positioned parallel to the surface, and adherence proteins and extracellular proteins are expressed or secreted to cement the bacteria to the surface (Brown & Smith, 2003; Toutain *et al.*, 2004) (Figure 1. 1; stage 1 and stage 2).

The degree to which uropathogenic organisms cause infection depends largely on their virulence factors. The capsule, siderophores, lipopolysaccharide, cytotoxic necrotising factor, proteases and surface adhesins such as the flagella, curli and pili are all important virulence factors, some of which play a vital role in biofilm formation (Hatt & Rather, 2008; Johnson, 1991; Lejeune, 2003).

Flagella motility enables 3 forms of movement: gliding, darting and twitching, all of which are important mechanisms for the positioning of microorganisms. The flagella motility of *Pseudomonas aeruginosa* bring the organism in close contact with the surface, and their type IV pili enable attachment to the surface due to twitching motility, whereby cells are propelled across a surface, increasing their opportunity for attachment (de Kievit & Iglewski, 2003; O'Toole & Kolter, 1998). Twitching motility is also a feature of *Escherichia coli* (Brown & Smith, 2003) which enable them to attach to surfaces with their fimbriae (Stoodley *et al.*, 2000).

All surface adhesins are important virulence factors of *E. coli* (Hatt & Rather, 2008; Johnson, 1991). Although the surface components expressed on laboratory strains of *E. coli* can differ to clinical pathogenic strains of *E. coli* and possibly differ even more on commensal strains (Reisner *et al.*, 2006), the one adhesin that is common to all strains of *E. coli* are the type 1 fimbriae and these are significant in attachment to the surface for biofilm formation (Johnson *et al.*, 2006; Van & Michiels, 2005). In fact, the type 1 fimbriae are conserved among most species of the *Enterobacteriaceae*, including *Klebsiella pneumoniae* which requires the type 1 fimbriae for attachment and colonisation of the cells in the bladder (Kil *et al.*, 1997).

1. 2. 1. 3. Stage 2: Cell accumulation and microcolony formation

The second stage is cell accumulation which involves cell-cell co-adhesion (Figure 1. 1; stage 2). A multi-layer of bacterial cells form microcolonies as mid-late colonisers adhere to primary colonisers. This occurs over a period of a few hours (Busscher *et al.*, 2000).

1. 2. 1. 4. Stage 3: Extracellular polymeric substance production

After initial attachment and adhesion, the cells rapidly develop into multicellular, multilayered colonies which embed themselves into the extracellular matrix that they secrete (Sutherland, 2001) (Figure 1. 1; stage 3). This matrix is an extracellular polymeric substance (EPS), which consists of polysaccharides, proteins, nucleic acids, lipids, multivalent cations and inorganic particles (Mayer *et al.*, 1999). The EPS is essential to the structure and function of a biofilm, so much so that the EPS forms approximately 50-90% of the total biofilm mass (Donlan, 2002). The EPS matrix allows for further cell - cell interactions (Toutain *et al.*, 2004) providing protection for the bacteria, as well as cementing them to the surface they are attached to, and concentrating nutrients and communication molecules (Davies, 2000). In Gram-negative bacteria, the EPS is anionic due to negatively charged compounds present such as uronic acids and pyruvate. Divalent cations within the biofilm, such as magnesium and calcium, are therefore able to enhance the binding force of the biofilm rendering it more stable (Vu *et al.*, 2009).

One of the most important components of the EPS is extracellular DNA (eDNA) (Flemming *et al.*, 2007; Whitchurch *et al.*, 2002). eDNA is thought to come from lysed cells, however, instead of being carriers of genetic information as is the known function of genomic DNA, eDNA forms part of the structure of a biofilm (Bockelmann *et al.*, 2006). In one study, eDNA is a prerequisite for *P. aeruginosa* alginate production, without which, this species is not able to establish a biofilm (Whitchurch *et al.*, 2002), highlighting that eDNA is an important structural component of the EPS.

Different species within a biofilm will produce differing amounts of EPS. Furthermore, it may be that bacteria of the same species in different environments produce different amounts of EPS depending on the stress conditions encountered. The level of EPS production is different depending on the physiological state of the biofilm and the

availability and balance of carbon and other limiting nutrients - the greater the amount of carbon, the greater the EPS synthesis (Sutherland, 2001). Taking all this into consideration, the bacterial biofilm when viewed at any one time, under any set of conditions or isolated from any environment, will differ considerably and will certainly not be uniform (Mayer *et al.*, 1999; Sutherland, 2001).

As well as varying degrees of EPS synthesis, different species and strains of bacteria may produce different types of polysaccharides which form part of the EPS. For example, much study has been done on the properties, structure and function of *P. aeruginosa*, which in some environments over-produces a very mucoid exopolysaccharide called alginate. The degree to which alginate is expressed varies and is often not present in biofilms formed *in vitro*, however, wherever alginate is produced by *P. aeruginosa*, the thickness of the biofilm is enhanced, and the resistance of the bacterial cells to host factors and antibiotics increases (Jefferson & Pier, 2003).

1. 2. 1. 5. Stage 4: Biofilm maturation

In the fourth stage of biofilm formation, the biofilm grows and matures (Figure 1. 1, stage 4). It forms a complex architecture of channels and pores where the bacteria can move within the EPS (of which more is produced). The biofilm at its more mature stage of life consists of voids, whereby nutrients can freely move into the matrix and waste products are removed (Costerton *et al.*, 1994). In *P. aeruginosa* biofilms, for example, at around 6 days of biofilm growth, a thick mushroom-like structure develops. This distinct structure contains important water filled channels that enable the transport of nutrients and oxygen into the biofilm matrix, and the flow of waste products out (de Kievit & Iglewski, 2003; Jefferson & Pier, 2003).

1. 2. 1. 6. Stage 5: Detachment

Detachment of portions of the biofilm (Figure 1. 1; stage 5) occurs when cells separate due to physical mechanisms such as shear forces, which can cause sloughing and erosion, or direct contact with the biofilm resulting in abrasion. Chemical factors may stimulate detachment, for example substrate changes, nutrient changes and changes in the EPS. It is also suggested that some strains detach due to biological factors. Examples of programmed cell release have been described in *P. aeruginosa* (de Kievit

& Iglewski, 2003), where quorum sensing molecules which are involved in cell-cell communication, can build up to activate cell-density-dependent genes which are expressed to synthesise proteins that encourage detachment. The release of enzymes and compounds that enhance detachment by inducing the dispersement of cells and the degradation of the EPS can also result in detachment (Davies, 2000; Moore *et al.*, 2000). Detachment is integral to biofilm life as detached cells can reattach to the surface downstream of the parent biofilm, and form a new biofilm (Figure 1. 1; stage 5).

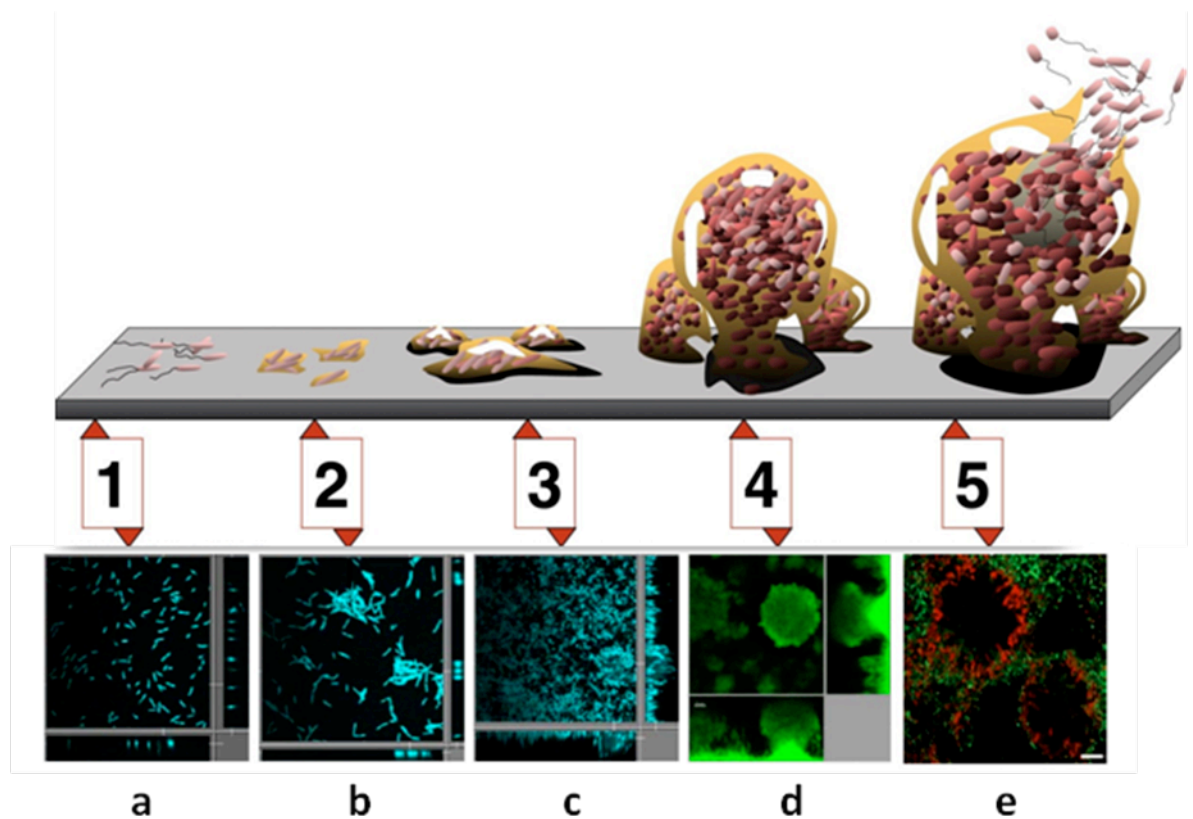


Figure 1. 1. The stages of biofilm formation under flow conditions.

1. Stage 1, cell-surface interaction, initial reversible attachment and irreversible attachment; **2.** stage 2, cell accumulation and formation of microcolonies; **3.** stage 3, secretion of extracellular matrix; **4.** stage 4, biofilm maturation; **5.** stage 5, detachment and dispersion (Monroe, 2007). *P. aeruginosa* microscope images. **a-c.** DAPI stained cells; **d.** chromosomal green fluorescent stained cells; **e.** LIVE/DEAD BacLight Kit (Boles *et al.*, 2005; Bordi & de Bentzmann, 2011).

1. 3. Quorum sensing and microbial biofilms

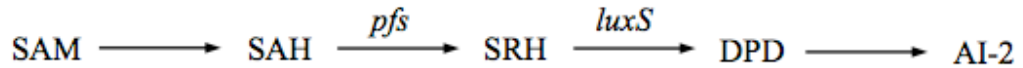
Cell-cell signalling, or quorum sensing, is the intercellular mechanism of communication that communities of bacterial cells utilise to behave in a collective manner for advantageous gains. There is a great deal of evidence to show that quorum sensing has a significant role in biofilm formation, including biofilm maturation, immune evasion, antibiotic tolerance and virulence factor production (Brown & Smith, 2003; Williams & Camara, 2009).

The quorum sensing system has two components: a transcriptional activator and an autoinducer, which is a signalling molecule that acts to up- or down-regulate gene expression upon the basis of cell density, so that each bacterial cell can alter the expression of certain genes in accordance with the development of the biofilm (Brown & Smith, 2003; Jefferson & Pier, 2003). Cell-cell signalling plays an extremely vital role in the physiological state of cells during biofilm formation (Prigent-Combaret *et al.*, 1999). Signal diffusion within the biofilm is dependent on the permeability of the biofilm matrix and the degree of hydrophobicity within the matrix. The understanding is that a dense biofilm matrix would concentrate the signalling molecule and a hydrophilic signalling molecule would diffuse away from a highly hydrophobic matrix (Brown & Smith, 2003).

Gram-negative bacteria produce *N*-acyl homoserine lactones (AHLs) which are signal molecules produced by the LuxI family of autoinducers (Williams, 2007). The LuxR family are response regulators. When AHL is bound, the configuration of LuxR is altered, which triggers the activation of transcription (Rasmussen *et al.*, 2005). *P. aeruginosa* has LuxI and LuxR homologues called Las (LasI-LasR) and Rhl (RhlI-RhlR) that control virulence factors such as proteases, pyocyanin, elastase and surfactants such as rhamnolipids (Pesci *et al.*, 1997; Van Gennip *et al.*, 2009). In order to produce diverse virulence factors, in addition to the AHL pathway, *P. aeruginosa* has a second pathway called 4-quinolones (4QS), one of the most important of which is the *Pseudomonas* quinolone signal (PQS) (Lesic *et al.*, 2007).

There is also another autoinducer called autoinducer-2 (AI-2), which mediates quorum sensing in both Gram-positive and Gram-negative bacteria, and as such, in most cases, is referred to as the ‘universal autoinducer’ (Schauder *et al.*, 2001). As this autoinducer

is present in a broad spectrum of bacterial species, it is implicated in interspecies communication. AI-2 is a metabolic product of 4,5-dihydroxy-2,3-pentanedione (DPD) (Tavender *et al.*, 2008), as outlined in the pathway:



S-adenosylmethione (SAM) is converted to S-adenosylhomocysteine (SAH). The enzyme Pfs catalyses SAH to S-ribosylhomocysteine. The *luxS* gene encodes LuxS which acts on DPD to produce AI-2 and homocysteine (Brito *et al.*, 2013).

The LuxS protein is responsible for the synthesis of AI-2, which accumulates extracellularly and then sensed and internalised by the *lsr* operon in the bacterial cell. The regulatory network for the uptake of AI-2 in *E. coli* is the LsrABCD transporter complex (Li *et al.*, 2007). The *lsrB* gene encodes the periplasmic AI-2 binding protein LsrB, *lsrC* and *lsrD* encode the channel proteins LsrC and LsrD, *lsrA* encodes the ATPase protein, LsrA, which provides the energy for the internalisation of AI-2 (Xavier & Bassler, 2005). LsrK phosphorylates AI-2 and the phosphorylated AI-2 in turn represses LsrR expression, thereby inducing the transcription of the *lsr* operon (Brito *et al.*, 2013). The *lsr* operon and its role in AI-2 transport are shown in Figure 1. 2.

In addition to biofilm formation, there are other advantages for bacterial cells that utilise the AI-2 system of quorum sensing. These include enabling them to migrate to a more nutrient rich environment, encouraging sporulation, plus all of the benefits that bacterial cells enjoy within the shelter and protection of the EPS matrix, as described earlier (Section 1. 2. 1. 4), which are only to be had in a biofilm community and not when cells are in the planktonic state (de Kievit & Iglewski, 2003).

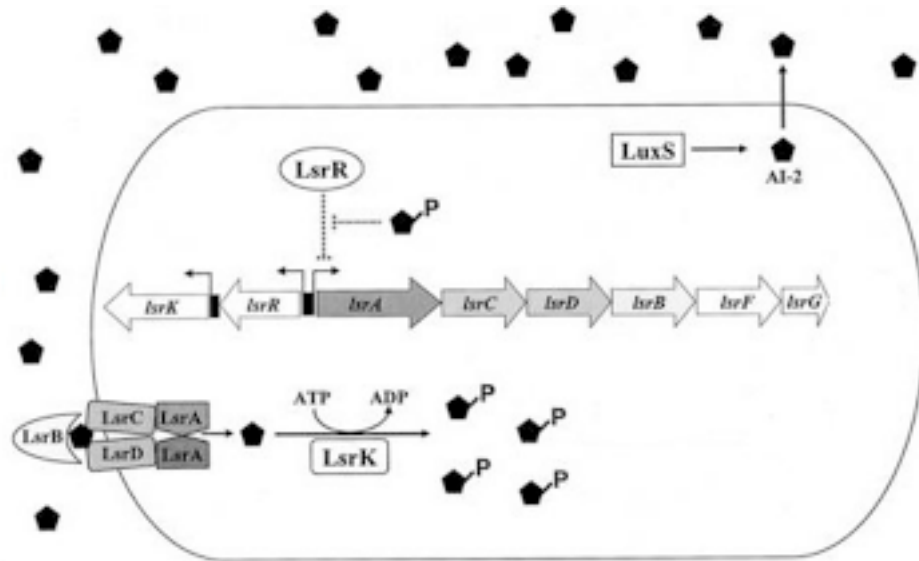


Figure 1. 2. Diagram demonstrating the function of the *lsr* operon in the transport of autoinducer-2 (AI-2) (pentagons). AI-2 is synthesised intracellularly by LuxS and accumulates extracellularly. LsrB binds AI-2 in the periplasm and internalised by LsrBCDA. LsrK phosphorylates AI-2 which induces the expression of the *lsr* operon by repressing LsrR, the repressor of the *lsr* operon (adapted from (Xavier & Bassler, 2005)).

1. 4. Epidemiology of catheter-associated urinary tract infections

Catheters are used in a variety of clinical situations for administering a range of therapeutic treatments and for fluid exchange from the body (Revell, 2003). The different catheters used are displayed in Table 1. 2.

Table 1. 2. Catheters and comments on their uses.

Catheter Type	Comments
Coude tip (Foley)	Most commonly used urinary catheter ¹ . Can be used transiently or long-term. Implicated in 80% of urinary tract infections ² .
Tunnelled CVC (PICC)	Long-term use for introduction of chemotherapeutic agents and for haemodialysis patients ³ . Surgically inserted ³ .
Non-tunnelled CVC (PICC, SICC, JICC)	Most commonly used CVC, therefore it accounts for 90% of catheter related septicaemia ⁴ . Surgically inserted into the chest or neck to administer blood, nutrients, medication or fluids directly into the subclavian artery.
Peripheral catheter (PICC)	Catheter inserted into the vein in the arm. Short-term use for the administration of intravenous antibiotics and chemotherapy. Rarely associated with bloodstream infection ⁴ .

¹(Jacobsen *et al.*, 2008); ²(Kunin, 2009); (Meares, 1991) ³(Allon, 2003); ⁴(Mermel *et al.*, 2001). Note: CVC, central venous catheter; PICC, peripherally inserted central catheter; SICC, subclavian inserted central *catheter*; JICC, jugular inserted central catheter.

1 4. 1. Urethral catheters

In clinical practice, 15-25% of patients have a urethral catheter during their hospital stay (Hooton *et al.*, 2010); therefore this catheter is of particular interest to this study. There are a number of indwelling urinary catheters and the choice of catheter and duration of catheterisation depends on the patient and the purpose. The Foley catheter is an indwelling, self-retaining, closed drainage urethral catheter which was invented by Fredrick E. B. Foley in the 1930s (Lawrence & Turner, 2005). Foley designed this

catheter with a balloon tip that is inflated in the bladder to hold the catheter in place (Figure 1. 3) (Jacobsen *et al.*, 2008).

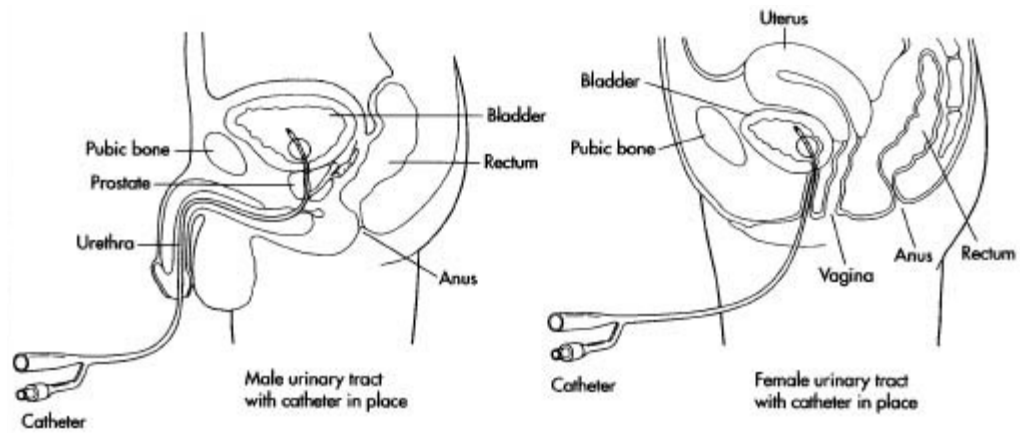


Figure 1. 3. Foley catheter insertion in females and males.

The Foley catheter is the most common catheter used for long term hospitalised patients and the elderly in long-term community health care with bladder dysfunctions and incontinence (Getliffe & Newton, 2006; Ramakrishnan & Mold, 2005).

The formation of biofilms on urethral catheters and the subsequent clinical presentation depend on five main factors: the duration of catheterisation; the host immune status and their susceptibility to infection; the type of catheter and therefore the surface of the catheter; the quality of catheter care and the strains of bacteria involved (Wong and Hooton, 2005). The lifecycle of a catheter is presented in Figure 1. 4 and shows the possible stages of a catheter's life which can be targeted to prevent or reduce catheter infection (Meddings & Saint, 2011).

In general, if catheterisation is minimised (Figure 1. 4, stage 1) and sterile techniques are used at stages 1, 3 and 4 of Figure 1. 4, the incidence of a catheter associated urinary tract infection (CAUTI) is reduced (Allepuz-Palau *et al.*, 2004; Cornia *et al.*, 2003; Thornton & Andriole, 1970; Topal *et al.*, 2005).

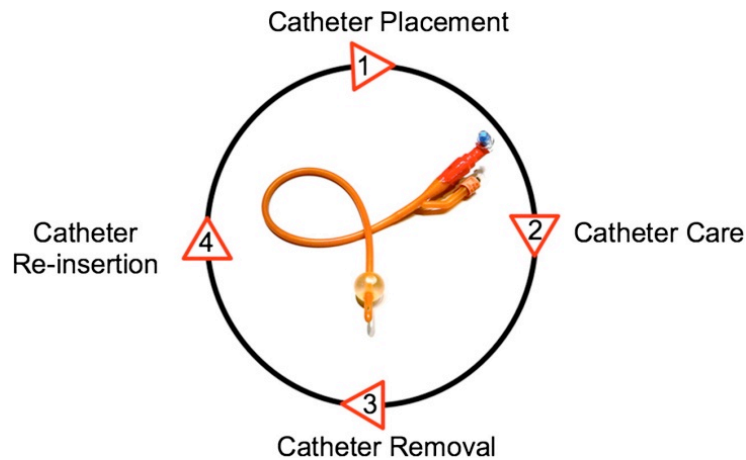


Figure 1. 4. The lifecycle of a catheter. Stages of a catheter's lifetime at which interventions for reduction or prevention of infection can be applied (Meddings & Saint, 2011).

The over-use and unnecessary use of catheterisation is of great concern due to the risk of CAUTI, so much so, that research and interventions to reduce the use of urinary catheters is very much current, and the recommendation is always to re-evaluate the need for catheterisation in the first instance (Andreessen *et al.*, 2012; Fakih *et al.*, 2010; Hooton *et al.*, 2010; Knoll *et al.*, 2011; van den Broek *et al.*, 2011). The busy nature of the clinical situation results in clinical staff prolonging the duration of catheterisation beyond that which is recommended and necessary (Meddings & Saint, 2011). The risk of developing a CAUTI increases by 5-10% for each day a catheter is inserted (Costerton, 2007b; Hatt & Rather, 2008). 80% of UTIs are caused by urinary catheters (Kunin, 2009; Meares, 1991) and as such are associated with a higher incidence of infection compared to other catheters (Ramakrishnan and Mold, 2005) contributing to an increase in hospital costs (Saint, 2000; Tambyah *et al.*, 2002). The estimated cost of urinary catheterisation and catheter related complication in the U.K. is approximately £40 million each year (Rawlinson & Clark, 2004). Although over-use of catheterisation is a great problem in the nosocomial environment (Fakih *et al.*, 2010), there is still not a suitable alternative in the cases where catheterisation is the correct option for the patient (Meddings & Saint, 2011).

1. 4. 2. Uses and duration of catheterisation

Stickler suggested that short term catheterisation or intermittent catheterisation with a clean intermittent catheter (CIC) (up to 7 days) does not pose a great risk, with 10-50% of catheterised patients developing infections (Stickler, 1996). Short-term catheters and CIC are used during urological surgery, relief of urinary tract obstruction, for women whilst they are giving birth, and to accurately measure urine output in critically ill patients. It is long-term catheters that pose a greater risk of infection. Long-term catheterisation (7 days or more) is commonly used for patients who have severe incontinence when other treatment types have failed; with patients who have a spinal cord injury who therefore have neurogenic bladder with urinary retention; incontinent patients with intractable skin breakdown and patients with a urinary obstruction which is untreatable or cannot be rectified immediately with surgery. It is suggested that all patients that have been catheterised for greater than 28 days will experience a CAUTI at some point during this period of catheterisation (Cravens & Zweig, 2000; Stickler, 1996).

1. 5. Gram-negative organisms involved in UTI infection

Not only is the most common nosocomial infection the urinary tract infection (UTI) but a catheter associated UTI (CAUTI) is one of the most prevalent bacterial infections of hospitals (Hatt & Rather, 2008; Jacobsen *et al.*, 2008; Johnson *et al.*, 2006; Trautner & Darouiche, 2004).

The most common Gram-negative bacteria implicated in UTIs are *E. coli*, *P. aeruginosa*, *K. pneumoniae*, *Enterobacter* and *Proteus mirabilis*. UTIs are also caused by *Candida albicans*, coagulase-negative staphylococci and enterococci (Donlan, 2001a; Emori & Gaynes, 1993). *E. coli* cause 70-95% of all UTI infections (Anderson *et al.*, 2003).

E. coli are facultatively anaerobic, Gram-negative bacilli that are a part of the *Enterobacteriaceae* family (Barrow & Feltham, 2003). These bacteria are amongst the first genera of bacteria to colonise the gastrointestinal tract of humans, hours after birth (Van & Michiels, 2005), and are the predominant facultative organism in the colon that form part of the commensal enteric microflora (Hudault *et al.*, 2001; Yan & Polk, 2004). As well as the commensal strains, there are five pathogenic groups of *E. coli* that

are found in the enteric tract of the human host, and can cause debilitating and life-threatening diarrhoea. These are classified according to the serotype, namely: enteropathogenic *E. coli* (EPEC), enterohaemorrhagic *E. coli*, enterotoxigenic *E. coli*, enteroinvasive *E. coli* and enteroaggregative *E. coli* (Trabulsi *et al.*, 1996). As well as enteropathogenic *E. coli*, there are extraintestinal *E. coli*, the main sub-group of which are uropathogenic *E. coli* (UPEC) (Kuhnert *et al.*, 2000). A number of these strains form biofilms that cause chronic UTIs and CAUTIs (Wiles *et al.*, 2008).

P. aeruginosa in most conditions grows as an aerobic, motile, Gram-negative bacterium (Barrow & Feltham, 2003). It is a saprophyte that is ubiquitous in soil and water environments but is an opportunistic pathogen that is commonly found to colonise the anaerobic mucous membrane of the cystic fibrosis lungs, as well as the moist environment of the urinary tract and the indwelling catheter (Pitt, 2007).

K. pneumoniae is a capsulate, non-motile, Gram-negative bacilli, commonly isolated from human faeces and water. In humans it colonises mucosal surfaces and is found as a saprophyte of the nasopharynx. In hospitals, the prevalence of *K. pneumoniae* is much more apparent, with carrier rates increasing with increasing length of stay (Podschun & Ullmann, 1998). It is a common cause of urinary tract infection, especially in patients with a spinal cord injury who are catheterised long term (Greenwood, 2007b; Kil *et al.*, 1997).

Proteus mirabilis is another Gram-negative bacillus implicated in catheter biofilm formation and is a highly motile organism, enabling *Proteus* to characteristically swarm over the surface of solid media when grown in the laboratory. *Proteus* is often isolated from hospitalised patients who have undergone surgery or catheterisation, and septicaemia due to *Proteus* is a complication of urinary tract infection. *P. mirabilis* and *K. pneumoniae* are both urease-producers and this creates alkaline conditions in the urine which can lead to the formation of calculi in the urinary tract (Greenwood, 2007a). The ability to produce urease enables 98% of *P. mirabilis*, 63.6% of *K. pneumoniae* and 32.6% of *P. aeruginosa* isolates to form unique crystalline biofilms, which in some cases can encrust the surface of long-term indwelling catheters, blocking the catheter so that it is no longer fit for purpose (Gorman & Jones, 2003; Hatt & Rather, 2008).

1. 6. The pathogenesis of catheter-associated urinary tract infections

There is evidence to demonstrate that the UPEC that colonise a catheter, are the same as the strains that originate in the intestine of the host and are found in the faecal flora, and therefore must originate from the same source (Agarwal *et al.*, 2012). The most common routes of urinary tract infection mainly involve faecal flora ascending to the bladder and kidneys via the urethra. The bacteria that colonise the distal urethra attach to the external surface of the catheter or the lumen of the catheter, as it is inserted into the bladder (Hooton, 2000; Jacobsen *et al.*, 2008).

Often, patients are catheterised out of convenience and alternatives to catheterisation are not sufficiently explored. Once a patient is catheterised, healthcare professionals may forget to monitor the patient regularly, which can lead to catheters remaining inserted for longer than is recommended (Saint *et al.*, 2000). The key to minimising a CAUTI is to first avoid the unnecessary use of catheterisation. If a patient meets the requirements for catheterisation, then the second, and most important consideration to avoid infection is to ensure that guidelines for aseptic insertion of the catheter is followed in order to maintain a sterile closed system. Finally, subsequent care and monitoring of the catheter should be maintained (Cohen & Dawe, 2009). In general, it has long been known that the lumen of a catheter is colonised when a sterile closed drainage system is not maintained (Geng *et al.*, 2012; Kunin & McCormac, 1966).

Another common route of infection is incomplete voiding of the bladder, whereby bacteria from the urinary meatus migrate to the bladder and proliferate using the urine as a nutrient source. They can then colonise the catheter (Hashmi *et al.*, 2003).

1. 6. 1. Eradication of infection

Common microbiological practice has evolved to suggest that the most effective way to eradicate infection is by the administration of systemic antibiotics, and these remain as the main forms of therapy for the treatment and prevention of infections. The choice of an antimicrobial for systemic infections is determined by the minimum inhibitory concentration (MIC) for each antibiotic against each specific bacterial strain. However, standard susceptibility tests are against planktonic bacterial cells and do not necessarily

correlate to the susceptibility to antibiotics by the same strains of bacteria when they are in a biofilm (Cerca *et al.*, 2005).

In most cases, UTIs in healthy patients are asymptomatic and do not require treatment (Tambyah, 2004), however, complications with UTIs, CAUTIs and kidney infections include prostatitis, cystitis, pyelonephritis haematuria and sepsis. Sepsis can cause death but the incidence is less than 1% in catheterised patients (Wang, 2002). There are also problems and complications associated with the increase in multi-drug resistant uropathogenic organisms, not to mention the increase in costs to hospitals and health care providers in managing UTIs and CAUTIs (Johnson *et al.*, 2006).

E. coli infections are routinely treated with ampicillin, co-amoxiclav, trimethoprim/sulfamethoxazole, nalidixic acid, tetracycline and fluoroquinolones (Kariuki *et al.*, 2007). Of these, *E. coli* has developed the greatest resistance to trimethoprim/sulfamethoxazole, ampicillin and tetracycline (Dromigny *et al.*, 2005).

P. aeruginosa infections are often treated with aminoglycosides, ciprofloxacin, piperacillin or ceftazidime (Zelenitsky *et al.*, 2003), however, multi-drug resistant strains can be resistant to a whole host of antibiotics including piperacillin, cefoperazone, ceftazidime, aztreonam, imipenem, cefepime, cefpirome, ofloxacin, ciprofloxacin, minocycline, and aminoglycosides (Hsueh *et al.*, 1998).

Klebsiella spp. are notoriously naturally multi-drug resistant and have the ability to acquire resistance readily (Anderl *et al.*, 2000). They produce β -lactamases and carbapenemases, as such, *Klebsiella* spp. which have these resistance conferring enzymes are unable to be treated with ampicillin and other broad-spectrum penicillins, cephalosporins, monobactams, carbapenems, fluoroquinolones and aminoglycosides (Munoz-Price *et al.*, 2010). Commonly, *K. pneumoniae* infection is treated with β -lactamase stable cephalosporins, fluoroquinolones, aminoglycosides, co-amoxiclav, trimethoprim and nitrofurantoin (Pallett & Hand, 2010). Polymyxins remain the most effective antibiotic against even the most resistant *Klebsiella* spp (Zavascki *et al.*, 2007). Resistance and sensitivity profiles of *Klebsiella* to drugs used are monitored carefully (Anderl *et al.*, 2000; Munoz-Price *et al.*, 2010).

Most strains of *P. mirabilis* are not β -lactamase producers and are therefore, on the whole, sensitive to benzylpenicillin, ampicillin and other β -lactam antibiotics, as well as aminoglycosides and cephalosporins, colistin, ciprofloxacin, rifampicin, naldixic acid and nitrofurantoin (O'Hara *et al.*, 2000). There is resistance mounting to ampicillin, tetracycline, erythromycin, chloramphenicol and generally to aminoglycosides and cephalosporins such as cefotaxime, which are now considerably less effective than they once were against *P. mirabilis* (Jombo *et al.*, 2012).

In general, there is growing resistance of uropathogenic organisms to trimethoprim and sulfamethizole, two of the most frequently prescribed antibiotics for urinary tract infection (Bjerrum *et al.*, 1999). The prevention and treatment of any systemic infection or UTI is imperative but even with increasing resistance of planktonic bacterial cells, treatment options are still available. Biofilms, as opposed to planktonic cells that cause CAUTIs, present clinicians and microbiologists with an entirely different set of challenges. These will be discussed further in the following sections.

1. 7. Mechanisms of biofilm-associated antimicrobial resistance

Biofilms are intrinsically more resistant to antimicrobials than their planktonic counterparts (Zhang *et al.*, 2011). An established biofilm can cause systemic infection in the host when the lumen of the indwelling catheter is subjected to the flow of urine at dynamic rates, which increases the opportunity for the upper layers of the biofilm to be detached from the extracellular polysaccharide and sent into the urinary tract and potentially into the circulation, often in large concentrations (Ryder, 2005). Although systemic antimicrobials can be administered to eradicate the infection in the host, the biofilm on a catheter surface is significantly more tenacious so until it is removed, will continue to grow, slough, and re-offend, causing another systemic infection. There are some well researched mechanisms of antimicrobial resistance that are mainly attributed to phenotypic factors of biofilms, thereby conferring innate antimicrobial resistance. These are the potential lack of antibiotic penetration, antimicrobial modification by enzymes, efflux mechanisms and repair systems, slow growth or no growth of the cells within a biofilm, the varied microenvironment in terms of oxygen concentration and other chemical gradients, all contribute to the resistance of cells to antibiotics and the host immune system (Brown & Smith, 2003).

1. 7. 1. The exopolymeric matrix

The EPS, the most notable feature of the biofilm, as well as its role in providing structure to the biofilm, also confers protection to the bacterial cells within the biofilm. The EPS has the ability to act as a barrier to antimicrobials and host immune cells (Bordi & de Bentzmann, 2011). *Klebsiella* spp. are well known multi-drug resistant organisms and also have many mechanisms that protect them from the action of drugs and the host immune response, such as the complex polysaccharide capsule and long chain lipopolysaccharide that protects the bacteria from serum complement activity (Merino *et al.*, 1992).

However, there is evidence to suggest that some antimicrobials do penetrate the biofilm, for instance, fluoroquinolones readily diffuse through the *K. pneumoniae* and *P. aeruginosa* biofilm (Anderl *et al.*, 2000; Vraný *et al.*, 1997) and tetracycline can rapidly diffuse in the *E. coli* biofilm (Stone *et al.*, 2002).

For the most part, the EPS delays penetration of antimicrobials (Mah & O'Toole, 2001). It may also be that the targets for conventional antibiotics against planktonic cells are not found to be the same when these cells are in a biofilm, which is a new and interesting concept for exploration (Costerton, 2007a; Mah & O'Toole, 2001). Due to evidence suggesting that the EPS is not completely impenetrable to antimicrobials, there must be other mechanisms, which add to the antimicrobial resistance of biofilms.

1. 7. 2. Persister cells

Persister cells are one of the most troublesome sub-population of cells in a biofilm. This is because these cells, which are in the depths of a biofilm, are often slow growing as a stress response survival mechanism which is induced by nutrient limitation and it is known that slow growing cells have antimicrobial tolerance (Costerton *et al.*, 1999). Persister cells in general are in a low metabolic physiological state, which also reduces the expression of genes encoding metabolic proteins, but enhances the expression of toxin genes that have a role in ensuring that metabolic processes are repressed (Shah *et al.*, 2006). There are also genes that are specifically expressed in persister cells, for example the *hip* locus in *P. aeruginosa* and *E. coli*, and the *sulA* and *relA* gene in *E. coli* that repress cell division and DNA synthesis (Black *et al.*, 1991; Piddock & Walters, 1992). Persister cells greatly contribute to the overall antimicrobial resistance of

biofilms (Dawson *et al.*, 2011; Keren *et al.*, 2004) and are the main cause of re-infection (Lewis, 2001).

1. 7. 3. Horizontal gene transfer

There are multi-drug resistant bacteria, such as *E. coli*, that confer their resistance to mobile genetic elements such as plasmids, gene cassettes and transposons (Saenz *et al.*, 2004). Due to the close proximity of cells within a biofilm, and the function of the EPS to concentrate not only communication molecules and nutrients, but also eDNA, there is active gene transfer between cells that encourage cross-resistance of cells within a biofilm (Madsen *et al.*, 2012). Conjugation and transformation both occur more often in a biofilm community rather than when cells are in the planktonic state (Sorensen *et al.*, 2005).

1. 7. 4. Evasion of host defences

The biofilm mode of growth offers a range of mechanisms to evade the host immune system. Phagocytes have reduced activity in ingesting cells that are in clumps of biofilm (Leid *et al.*, 2002). Leukocytes are not able to penetrate the biofilm matrix, as is the case for IgG, depending on the amount of EPS (Zhu *et al.*, 2001). Although biofilms do trigger cytokines and the release of macrophages, these probably do more harm to the host than the biofilm. Oxidative burst releases oxygen species, which are also not effective, as they are deactivated in the outer layers of the biofilm faster than they can diffuse into the depths of the biofilm. So overall, the host defences are disarmed in the face of a mature biofilm (Hassett *et al.*, 1999).

1. 8. Novel approaches to inhibit biofilm formation

Biofilm formation on urinary catheters has long been a recognised problem since the first latex Foley catheter resulted in a catheter-associated urinary tract infection. CAUTIs are implicated in the highest rate of nosocomial infection and are a huge expense to health care institutions (Tambyah *et al.*, 2002). This is because uropathogenic biofilms that cause CAUTIs are notoriously stubborn against our attempts to eradicate them. Systemically administered antibiotics alone are not ideal for

the eradication of a catheter biofilm, and once a biofilm has formed on a catheter, the catheter will most certainly have to be removed (Stamm & Hooton, 1993). This is discomfoting for the patient and is also expensive for the health service (Polonio *et al.*, 2001; Saint, 2000). The hope therefore lies with preventing a biofilm from forming in the first place (Donlan, 2001b).

The relentless rise in the incidence of antibiotic resistance in bacterial pathogens, as well as the relatively low rate of discovery and development of new, clinically useful antibiotics, has refocused attention on the potential of new antimicrobial and anti-biofilm therapies. Efforts have been made to intervene during the key stages of biofilm development and to inhibit genes and proteins that are unique and specific to the biofilm phenotype.

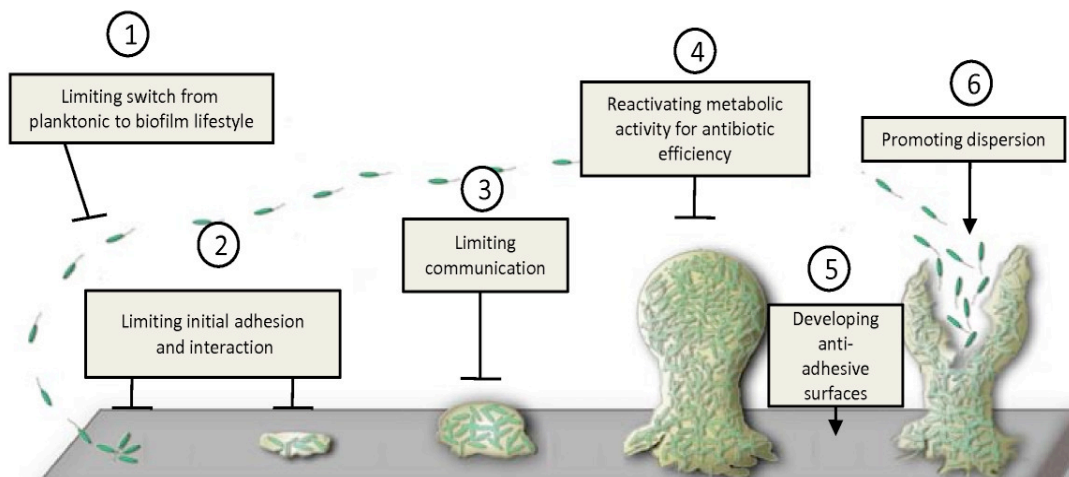


Figure 1. 5. Intervening at the stages of biofilm formation. Stages of biofilm formation at which novel approaches to biofilm inhibition can be applied (Bordi & de Bentzmann, 2011).

Although Figure 1. 5 describes 6 key stages at which to intervene and inhibit the progression of biofilm formation, steps 1, 2 and 5 concentrate on preventing initial attachment and the early stages of biofilm formation. It is therefore evident that preventing these early stages is far more attractive and within our reach to achieve success. The later stages of biofilm formation become increasingly complicated, especially as we are still learning about the intricate behaviours of bacteria within a

mature biofilm. The following sections will illustrate the nature of some of the interventions used to inhibit the uropathogenic bacteria *E. coli*, *P. aeruginosa* and *K. pneumoniae* from forming a biofilm, as these bacteria are of interest to this study.

1. 8. 1. Limiting initial adhesion and interaction of bacterial cells

Stage 2 of Figure 1. 5 suggests that as adhesion of bacterial cells to a surface is one of the most crucial stages of biofilm formation, this is a stage for intervention by novel anti-adhesive measures. Lactobacilli, a commensal organism of the vagina, produce antimicrobial biosurfactants, which have been evaluated for their use as an antimicrobial against uropathogenic bacteria (Velraeds *et al.*, 1996; Velraeds *et al.*, 1997). However, in general, lactobacilli are inhibitory to uropathogenic bacteria in an additional way; they are able to adhere to human uroepithelial cells both as whole cells and non-viable cell wall fragments that results in the competitive exclusion of uropathogenic bacteria. There may be some use in harnessing these natural mechanisms that our commensal bacteria utilise against pathogenic bacteria, as an antimicrobial therapy (Velraeds *et al.*, 1996).

Before a bacterium is able to attach to a surface, flagella synthesis and pili are important in getting the bacterial cell as close to a surface as possible without the bacterial cell itself being under the stress of electrostatic repulsion forces of the surface (Jenkins *et al.*, 2004). Inhibition of flagella synthesis is an attractive option to inhibit bacterial attachment. FleQ is thought to be the ‘master switch’ for flagella synthesis of all flagella (apart from FliA), therefore inhibition of the *fleQ* gene could go a long way in inhibiting the complex but tightly regulated synthesis of flagella (Dasgupta *et al.*, 2003; Tart *et al.*, 2006). *FliC* is an important gene in the synthesis of flagella. One of the most recent attempts to inhibit FliC is by Dong and co-workers, who found that inhibition of FliC in *P. aeruginosa* by salicylic acid has been shown to reduce motility. This may have an impact on the ability of this bacteria to form biofilms (Dong *et al.*, 2012).

Mannosides, which target FimH, have been used as a therapeutic agent against UPEC organisms. FimH, at the top of type 1 pili bind to mannosylated receptors on uroepithelial cells and are consequently able to form intracellular bacterial communities within the cells of the bladder. These bacteria are able to evade most exogenous bacterial defences. Mannosides have been tested in murine models and have

demonstrated an ability to bind to FimH, thereby inhibiting attachment (Kostakioti *et al.*, 2012; Wellens *et al.*, 2008).

There are also antimicrobial surfaces that kill bacteria upon contact. These will be discussed in Section 1.8.4.1.

1.8.2. Limiting communication: quorum sensing inhibitors

Inhibiting quorum sensing (QS) in bacteria appears to be an attractive option in the battle to combat antimicrobial resistance in biofilms (Kohler *et al.*, 2010) (Stage 3 of Figure 1.5). This is because QS is the main system of regulating virulence factors and contributes to biofilm maturation (Williams & Camara, 2009).

Inhibiting the various pathways involved in coding for the autoinducers is where most research has focussed (Ni *et al.*, 2009). There appear to be four main modes of quorum sensing inhibitors: i) analogs of autoinducers that interfere with natural autoinducer function; ii) antimicrobials that target quorum sensing, iii) furanone derivatives and iv) enzymes which inactivate autoinducers by degradation (Janssens *et al.*, 2008; Nalca *et al.*, 2006; Ni *et al.*, 2009).

Analogues of autoinducers include the first set of inhibitors of the PQS pathway in *P. aeruginosa* that is a halogenated anthranilic acid analog. This represses MvfR-dependant gene expression. MvfR is a key transcriptional regulator that is essential for the full pathogenicity of *P. aeruginosa* (Lesic *et al.*, 2007; Xiao *et al.*, 2006). There are also antimicrobials that target quorum sensing such as azithromycin, a macrolide antibiotic that is a successful inhibitor of quorum sensing and alginate production in *P. aeruginosa* (Hoffmann *et al.*, 2007; Nalca *et al.*, 2006; Skindersoe *et al.*, 2008), as are ciprofloxacin and ceftazidime (Skindersoe *et al.*, 2008). Furanone derivatives are also well studied quorum sensing inhibitors. They act by blocking AI-2 signalling and as AI-2 is known to be active in many species of bacteria, it may be regarded as a broad-spectrum quorum sensing inhibitor (Ren *et al.*, 2004b). More recently, garlic extracts have been tested as quorum sensing inhibitors in the first human randomised control clinical trial of a quorum sensing inhibitor of *P. aeruginosa* in cystic fibrosis sufferers (Bjarnsholt *et al.*, 2005; Rasmussen *et al.*, 2005; Smyth *et al.*, 2010). This trial did not show significant results but did have an effect with the improvement of lung function

(Smyth *et al.*, 2010). Bjarnsholt and co-workers have demonstrated that garlic extracts decrease quorum sensing making bacteria more sensitive to tobramycin (Bjarnsholt *et al.*, 2005).

There are many advantages to targeting QS pathways: first, by inhibiting QS the bacteria are still viable, which will enable the host defence system to have time to build a robust immune response without the need to use antibiotics. Second, the target is quite specific, so the host flora, which is beneficial to the host, is not eliminated and third, as the bacteria are not necessarily killed, there is a lower chance of the QS inhibitors causing selective pressure and enhancing antimicrobial resistance (Rasmussen *et al.*, 2005).

There are some disadvantages: the target will unlikely be broad spectrum as there are a variety of QS molecules; if a biofilm has formed, then QS may not be active and therefore the target is not valid; QS is quite complex and is not just relevant for biofilm formation. There may be down-stream consequences to inhibiting the pathways and products of QS. The study by Kohler (2010), highlights one important caveat which suggests that inhibiting the resistance of bacteria that utilise QS, can encourage the prevalence of bacteria that are not reliant on the same form of resistance (Brackman *et al.*, 2011; Kohler *et al.*, 2010). In another study it has been suggested that quorum sensing inhibitors increase the resistance of bacteria to conventional antibiotics (Brackman *et al.*, 2011).

1. 8. 3. Reactivating metabolic activity

Stage 4 of Figure 1. 5 suggests that reactivating the metabolic activity of cells may help with eradicating a biofilm. Cells that are in the depths of the biofilm matrix are often in an inactive or slow growing state, however, if the top layers of a biofilm are removed by shear force, for example, then fresh nutrients can be supplied to the dormant cells. This will stimulate their growth in the exponential state, which is where bacteria are most metabolically active, making them more sensitive to antimicrobials that target actively growing cells. Biofilm disruption may also result in the dilution of cell signals, thereby reducing the signal molecules that encourage bacteria to be inactive and therefore less susceptible to antimicrobials (Fux *et al.*, 2003).

1. 8. 4. Developing anti-adhesive surfaces: urinary catheter surfaces which reduce bacterial colonisation

Strategies to inhibit the structure and function of biofilms often present varied challenges due to the complex nature of biofilms and diversity of biofilm phenotypes across species. For this reason, efforts to reduce colonisation have been attempted, before the structure of a mature biofilm develops and becomes complex. These attempts include using materials that reduce bacterial attachment as suggested in Stage 5 of Figure 1. 5. Surface topography and surface properties are an important factor in biofilm formation. The smoother the surface, the less surface area available for the attachment of a bacterial cell, in addition to this, a smooth surface will expose the bacteria to shear forces that can help in removing a biofilm (Donlan, 2002). Surface hydrophobicity or hydrophilicity can also be of great importance to how attractive a surface is to a bacterial cell for initial attachment (Boks *et al.*, 2008), and research suggests that hydrophobic surfaces are more favourable to a bacterial cell for attachment (Absolom, 1988; Doyle, 2000).

Catheters are made from a large variety of materials. Urinary catheters were originally made from natural latex rubber due to its relative low cost and great flexibility. However, it also had a high incidence of toxicity, caused increased latex hypersensitivity in patients, low biocompatibility, blockage of the catheter lumen due to encrustation and a high level of bacterial colonisation (Lawrence & Turner, 2005; Ramakrishnan & Mold, 2005). As a result of these problems other catheter materials were sought such as silicone, polytetrafluoroethylene (PTFE or Teflon[®]), polyvinylchloride (PVC) and polyurethane. Silicone catheters overcome some of the problems associated with encrustation and catheter blocking but the surface still encourages bacterial adhesion and biofilm formation (Ryder, 2005). Bacterial adherence to silicone is much higher than to polyurethane or Teflon[®] (Lopezlopez *et al.*, 1991). The hydrogel-coated catheter has shown the most promise in reducing biofilm formation (Bologna *et al.*, 1999). Hydrogels are polymers that have been used to form thin layers on latex and silicone that increase the lubricity and smoothness of a catheter surface thereby reducing bacterial adhesion (Jones *et al.*, 2004). Hydrogels have been used as ideal candidates for antimicrobial impregnation (Ahearn *et al.*, 2000).

1. 8. 4. 1. The use of antimicrobials as catheter coatings

A relatively recent approach to overcome CAUTI is the development of antimicrobial catheter coatings, and with the incorporation of biofilm inhibitors that target genes or proteins that are instrumental in biofilm formation, this novel catheter surface could prove to be the most advantageous combination in preventing biofilm formation, or at least prolonging the life of the catheter (Wood, 2009). There are important criteria for an ideal antimicrobial to be incorporated into a biomaterial. It should be broad spectrum, its activity should last for the lifetime of the device without reduction by the substances flowing over it, it should not select for drug-resistant organisms and it should be active against all organisms that it is likely to interact with, and at a concentration that is bactericidal, as the application of sub-inhibitory levels of inhibitor can induce resistance or select for resistance in the bacteria (Stickler, 2000). Although all of these criteria are difficult to meet, there are some valid attempts that have been made, which will be discussed below.

1. 8. 4. 1. 1. Silver as an antimicrobial coating

Silver (Ag) and silver containing compounds are long standing antimicrobials (Burrell, 2003). The use of silver nitrate in wound management was first approved by the United States Food and Drug Administration (FDA) in the 1920s. However, during the golden age of antibiotic discovery, the use of silver diminished and antibiotic treatment of bacterial infections became standard practise (Demling, 2001). Silver once again became useful in the management of wounds but this time silver nitrate was combined with sulfadiazine, in a commercially available cream marketed as ‘Silvazine’. This had a greater spectrum of antimicrobial activity than either alone (Fox, 1968; George *et al.*, 1997). Although different silver species have differing levels of antimicrobial activity, overall, silver is synergistic with existing antibiotics, in that the susceptibility of bacterial cells, including those in biofilms, to conventional antibiotics such as nitrofurazone, is increased in the presence of silver (Johnson *et al.*, 1999; Kostenko *et al.*, 2010; McDonnell & Russell, 1999; Saint *et al.*, 1998).

Silver is now commonly used in a number of commercially available products in the cosmetic and domestic setting (Silver *et al.*, 2006). The use of silver in the medical setting is also increasing, with large companies such as Johnson and Johnson, and Smith & Nephew, UK, who market wound dressings impregnated with silver, that are

commercially available (Atiyeh *et al.*, 2007; Lee *et al.*, 2005; Silver *et al.*, 2006). Hydrogel-coated latex catheters impregnated with silver containing compounds on both the outer surface and lumen of the catheter has shown some effectiveness, however, only in the short-term (Bologna *et al.*, 1999; Verleyen *et al.*, 1999). From studies such as these, and the success of silver impregnated wound dressings, there was a lot of interest in silver as a urinary catheter coating; however there is conflicting evidence in the literature as to the efficacy of silver in the clinical environment. More recent large scale clinical trials with catheters coated with hydrogels and/or silver did not show significant inhibitory activity compared to non-coated silicone catheters (Johnson *et al.*, 2006; Srinivasan *et al.*, 2006; Thibon *et al.*, 2000).

Moreover, the main challenge of the urinary catheter is the hugely mixed population of resistant microorganisms that form a biofilm and cause infection, including bacteria, which display heavy metal resistance (Woods *et al.*, 2009). Silver resistant *E. coli* display active efflux of Ag^+ and have also been found to have mutations in the outer membrane porins, both important mechanisms conferring silver resistance that are thought to be chromosomally encoded (Franke *et al.*, 2001; Li *et al.*, 1997). Silver resistant *P. aeruginosa* has been isolated from burn patients who have been treated with silver coated wound dressings (Modak & Fox, 1981). Furthermore, silver is also known to be cytotoxic after long-term use (Ahamed *et al.*, 2010; Atiyeh *et al.*, 2007).

1. 8. 4. 1. 2. Antibiotics as catheter coatings

Minocycline and rifampin have been tested alone and in combination as an antimicrobial coating of catheters, including urethral catheters, however, the combination of the two antibiotics showed good inhibitory activity against Gram-positive and Gram-negative bacteria, as well as *C. albicans* for up to two weeks (Hanna *et al.*, 2006; Maki & Tambyah, 2001; Raad *et al.*, 1998).

Gentamycin, an aminoglycoside, has been studied as a coating incorporated into polyethylene-co-vinylacetate and polyethylene oxide, and when released slowly, showed antimicrobial activity for 5-7 days against Gram-positive and Gram-negative bacteria (Cho *et al.*, 2003). The same group developed catheters of the same material but coated with the fluoroquinolone antibiotic norfloxacin. This antibiotic was released continuously for up to 10-30 days with antimicrobial activity against *E. coli*, *K.*

pneumoniae, and *P. vulgaris* (Park *et al.*, 2003). As gentamycin is commonly used to treat UTI, Dave and co-workers have recently developed a novel polycaprolactone biocatalytic polymer coating impregnated with gentamycin sulphate, which showed inhibitory activity against *E. coli*, *P. aeruginosa* and *S. auerus* (Dave *et al.*, 2011).

Nitrofurazone, a broad-spectrum antibiotic against organisms that cause CAUTI, when compared to a silver hydrogel coated catheter, showed greater efficacy (Johnson *et al.*, 1999; Maki & Tambyah, 2001; Regev-Shoshani *et al.*, 2011). Although antibiotics have shown short term efficacy against bacteria, there is the risk of bacteria developing resistance to the antimicrobials used, especially if these antibiotics are leached from the catheter coating at sub-inhibitory concentrations (Tambyah, 2004).

1. 8. 4. 1. 3. Nitric oxide as a catheter coating

There have been many attempts to study nitric oxide (NO) as a coating of medical devices (Deupree & Schoenfisch, 2009; Hetrick *et al.*, 2009; Privett *et al.*, 2010). Recently, catheters impregnated with gaseous NO were found to not only be antimicrobial, but due to its slow release, created a zone of inhibition around the catheter thereby killing planktonic as well as biofilm cells (Regev-Shoshani *et al.*, 2010). Although it is suggested in the literature that bacteria have mechanisms to counter the toxicity of NO (Husain *et al.*, 2008), this is thought to deplete after some time, making cells more susceptible to NO, especially at high concentrations (Poole, 2005b). The research by Regav-Shoshani and co-workers showed that a catheter coated with NO demonstrated inhibitory activity for up to 14 days (Regev-Shoshani *et al.*, 2010). Mostly, research has been directed towards the delivery systems to release NO, so more work will be required to investigate the safety, efficacy and cost-effectiveness of NO *in vivo* (Schairer *et al.*, 2012).

1. 8. 4. 1. 4. Antimicrobial peptides as catheter coatings

Natural antimicrobial peptides are the focus of many research groups, with thousands of peptides having been discovered against all manner of species. In fact, in 2009 it was reported by Wang and co-workers that as many as 944 antibacterial peptides have been isolated (Wang *et al.*, 2009a), a number which is undoubtedly increasing year by year. Natural antimicrobial peptides have some key characteristics in common: i) they are

mostly cationic; ii) they are short in length and small in size and molecular weight and iii) they have amphipathic properties as part of their structures. These 3 things alone enable peptides to interact closely with the anionic bacterial membrane, their main target for growth inhibition (van 't Hof *et al.*, 2001). Covalently attaching peptides to biomaterials has been the focus of research for some years now. This has been attempted on different surfaces, including contact lenses (Haynie *et al.*, 1995; Willcox *et al.*, 2008).

Although microbial resistance to peptides is relatively low due to the mode of action of antimicrobial peptides, there are some resistance mechanisms that have evolved. Gram-negative bacteria have modified the lipid A component of their outer membrane that reduces the negative charge, thereby reducing the interaction between the anionic membrane and the cationic peptides (Nizet, 2006). Another mechanism is to bind and inactivate the peptide. Schmidtchen and co-workers found that this has been achieved by bacteria, including *P. aeruginosa*, that secrete proteases. These proteases release dermatan sulphate that can subsequently bind to and inactivate the antimicrobial peptide, human α -defensin (Schmidtchen *et al.*, 2001). As well as proteolytic degradation of the peptides, the other main disadvantage is the potentially high cost as well as the potential for humans to develop allergies to the peptides (Bradshaw, 2003).

1. 9. Novel antimicrobial compounds used in this study

In this study, natural polyamines, quaternary ammonium compounds, including polyquaternium compounds, and polybiguanides have been evaluated for their efficacy against planktonic cells and the early stages of biofilm growth.

1. 9. 1. Polyamines as biocides

Polyamines, which are natural biogenic polycationic compounds, are known to interact with porins (Iyer & Delcour, 1997). Porins may be involved in biofilm formation (Barrios *et al.*, 2006; Orme *et al.*, 2006) therefore polyamines may be potential inhibitors of biofilm formation.

Previous studies have demonstrated that polyamines interact with porins, specifically OmpC and OmpF, inducing and prolonging their incidence of closure (Iyer & Delcour, 1997). OmpC and OmpF, like other porins, are predominantly open and are responsible for the permeability of the cell membrane to nutrients and hydrophilic compounds (Samartzidou & Delcour, 1999). The polyamines spermine, spermidine, cadaverine and putrescine are of interest to this study due to their interaction with the porins and proteins in the polyanionic bacterial outer membrane, particularly as OmpA was shown to be important in the development of a biofilm (Barrios *et al.*, 2006; Orme *et al.*, 2006).

1. 9. 2. Quaternary ammonium compounds and biguanides as biocides

A range of compounds that have antimicrobial activity have been used successfully as disinfectants and antiseptics. The most common of these include biguanides, such as polyhexamethylene biguanide (PHMB) and quaternary ammonium compounds (QACs) (McDonnell & Russell, 1999) (also known as quaternary ammonium salts or quats). QACs are cationic compounds, which although diverse in their structures, all have a positively charged nitrogen atom covalently bonded to four alkyl groups (NR_4^+) in common. This offers the compound stability in terms of its charge, regardless of the pH of the solution. QACs and PHMB are commercially available and routinely used as the active ingredient in many antimicrobial and sanitising products, in swimming pools and as environmental biocides, due to their wide spectrum of activity against bacteria, yeasts, viruses and fungi (Kim *et al.*, 2011; Nohr & Macdonald, 1994). Novel to this study is the determination of polyquaternium compounds as antimicrobials. Apart from Polyquaternium-1 (Polyquad[®], Alcon Laboratories Inc. USA), which is used as a novel preservative in contact lens solutions (Codling *et al.*, 2003b; Rolando *et al.*, 2011) and Polyquaternium-6 (Polydiallyldimethylammonium chloride or Poly-DADMAC) (BIOGUARD[™] Nimbus[®] Technology, Quick-Med Technologies Inc. USA), most other polyquaterniums have not been studied for their antimicrobial potential, especially against clinical isolates.

The mode of action of QACs and PHMB, although not exactly the same, have much in common, in that they increase the permeability of the outer membrane by binding to the polyanionic lipopolysaccharides (LPS) which decorate the outer portion of the outer membrane. They are antimicrobial due to their ability to disorganise and destabilise the LPS and permeabilise the outer membrane (Vaara, 1992; Wilkinson & Gilbert, 1987).

1. 9. 2. 1. *Antimicrobial resistance to quaternary ammonium compounds*

Quaternary ammonium compounds (QACs) have been used in the domestic and food industries as disinfectants for some time due to their broad spectrum of activity, however, when bacteria are exposed to sub-inhibitory doses of biocides such as QACs, resistance can emerge. It is well documented that *P. aeruginosa* are intrinsically one of the least sensitive strains of bacteria to biocides such as PHMB and the QAC benzalkonium chloride (BAC) (Gilbert & Moore, 2005; Langsrud *et al.*, 2003). This is likely to be due to their alginate biofilm, however, they are also known to have multidrug efflux pumps which are the main mechanism conferring QAC resistance to not only *P. aeruginosa*, but bacteria in general (Poole, 2005a). Gram-positive bacteria have been well reported to accommodate QAC efflux pumps, of which many are plasmid encoded. *S. aureus* in particular have a whole host of *qac* genes. The efflux systems in Gram-negative bacteria, which generally give rise to QAC resistance, are also multidrug efflux transporters. In relation to *E. coli* and *K. pneumoniae*, *P. aeruginosa* has the most efflux encoding *qac* genes, which may explain its increased resistance to QACs. The most common efflux determinants that give rise to QAC resistance in the organisms relevant to this study are outlined in Table 1. 3.

Table 1. 3. Summary of efflux determinants relevant to the compounds and organisms used in the current study (Poole, 2005a).

Note: QAC: quaternary ammonium compound; BAC: benzalkonium chloride

Efflux determinant	Biocide	Organisms
QacE	QAC	<i>K. pneumoniae</i> , <i>P. aeruginosa</i> ¹
QacEΔ1	QAC	<i>K. pneumoniae</i> , <i>P. aeruginosa</i> ¹
QacG	QAC	<i>P. aeruginosa</i> ²
PmpM	BAC	<i>P. aeruginosa</i> ³
YhiUV-TolC	BAC	<i>E. coli</i> ⁴

¹(Kazama *et al.*, 1998); ²(Laraki *et al.*, 1999); ³(He *et al.*, 2004); ⁴(Nishino & Yamaguchi, 2001).

Unlike the Gram-positive *qac* genes, Gram-negative *qac* genes are chromosomally encoded. However, the most common efflux determinant in *E. coli*, *K. pneumoniae* and

P. aeruginosa are *qacE* and *qacEΔ1* (Poole, 2005a). These genes are encoded on mobile integron elements, the same genetic elements that encode for antibiotic resistance (Hardwick *et al.*, 2008) in particular, class 1 integrons (Gillings *et al.*, 2009a; Gillings *et al.*, 2009b; Hardwick *et al.*, 2008).

Despite the *qacE* and *qacEΔ1* genes encoding for resistance to QACs, one particular study by Kucken (2000), noted that there was not a significant difference in QAC resistance in bacteria that did or did not possess these genes. Therefore, this suggests that the *qacE* and *qacEΔ1* genes are not the most essential factor to determining bacterial susceptibility to QACs (Kucken *et al.*, 2000).

QACs are still attractive alternatives to conventional antimicrobials due to their broad spectrum of activity and use in a variety of settings. In the 50 or more years that QACs have been used as antimicrobials, only a few resistance mechanisms threaten their antimicrobial activity. A PubMed search for ‘quaternary ammonium compound resistance’ revealed just 74 hits. In comparison to a similar search for ‘silver resistance’, which revealed over 1500 hits. In addition to this, when trying to determine the range of quaternary ammonium compounds being investigated as antimicrobials, there are 14852 PubMed hits and only 8070 hits for ‘silver antimicrobial’. This is an indication that QAC resistance is not of great concern and is certainly an attractive alternative to silver, another widely used biocide in the clinical setting. With approaches to change the presentation of QACs, for example as a coating, there is every hope that QACs will continue to be the most commonly used and effective antimicrobials, especially at concentrations that are fully biocidal.

1. 10. The aims of this research

The literature review detailed in the introduction shows that biofilm formation on any medical device is a great problem in the nosocomial environment. The urinary catheter is one of the most commonly used medical devices, frequently required to treat urinary incontinence in older patients and patients with long term bladder dysfunctions. Systemic and chronic infections are a result of biofilm formation on the surface of urinary catheters (Costerton *et al.*, 1999). It has long been evident that an established, mature biofilm is notoriously difficult to eradicate, therefore the most effective method to impede biofilm development is to avoid or reduce the initial adhesion of bacteria to the catheter surface. The nonspecific attachment of bacteria onto any surface is a key determinant in subsequent biofilm formation, therefore, many approaches have been adopted to prevent bacterial attachment to surfaces of medical devices (Banerjee *et al.*, 2011; Knetsch, 2011). Cationic compounds represent a suitable antimicrobial as they define a structurally diverse class of antimicrobials with a broad spectrum of activity (Banerjee *et al.*, 2011).

To prevent biofilm formation, it would be desirable for future generations of materials to move towards incorporating novel inhibitors of functions vital to biofilm attachment and integrity. Anti-biofilm coatings containing novel cationic compounds may be efficacious and have a significant impact in the clinical setting, particularly on the costs associated with device replacement and in reducing patient morbidity and mortality. Observing antimicrobial activity in isolation is informative, but a deeper understanding of the effect of a biocide on cells may give additional benefit.

The aims of this project are to (1) identify a novel antimicrobial cationic compound and (2) understand the response of the bacteria at gene and protein level, when treated and challenged with the antimicrobial cationic compound. The objectives set in order to achieve these aims are described in the next two sections:

1. 10. 1. Aim 1: Identify a novel antimicrobial cationic compound

Natural polyamines and quaternary ammonium compounds will be screened for their antimicrobial action against the planktonic and biofilm phenotypes of Gram-negative uropathogenic bacteria. Strains tested will be the laboratory strain *E. coli* K12 and

clinical isolates of *E. coli*, *K. pneumoniae* and *P. aeruginosa* which were isolated from urinary tract infections, as these are the organisms most commonly identified in a CAUTI. The screening of antimicrobial cationic compounds will be achieved by first gaining an understanding of how effective the compounds are against planktonic growth using the minimum inhibitory concentration (MIC) assay and viable cell counts; and second, using microscopy and the high throughput method of the microtitre plate biofilm formation assay, to observe the effectiveness of the compounds on early stages of biofilm formation. The compound with the most potent inhibitory action against all of the bacterial species used in the study will be assessed further for their effectiveness as a surface coating, and against established biofilms.

1.10.2. Aim 2: Analyse the response of bacteria when treated with a novel antimicrobial cationic compound

The compound with the most potent antimicrobial activity will be used above and below the MIC to reveal the effect that it is having on protein and gene expression of *E. coli*, the organism most commonly isolated from CAUTI.

Two-dimensional gel electrophoresis (2DGE) has been successful in identifying over-expressed proteins in the biofilm phenotype as potential targets of biofilm inhibition (Orme *et al.*, 2006). A proteomic approach using 2DGE will therefore be used in the current study to identify proteins that are differentially expressed between the biofilm and planktonic phenotypes when treated and challenged with the inhibitory compound identified in comparison to control (untreated) samples. Planktonic cells will also be treated with the inhibitory compound at sub-inhibitory concentrations and challenged at 4 times the MIC. This will give the transcription profile of bacteria grown continuously with the compound at low concentrations, and when grown for a short period at high concentrations. A transcriptomic analysis of the cell's gene expression levels under these different conditions will be performed using RNA-Seq.

Chapter 2

Materials and Methods

2. 1. Bacterial strains, media and growth conditions

E. coli K12 sub-strain MG1655/XL1-blue, a well characterised laboratory strain with a K12 phage (Stratagene), and clinical isolates of *E. coli*, *K. pneumoniae* and *P. aeruginosa* obtained from urinary tract infections were used in this study, and were kindly supplied by the Central Manchester Foundation Trust (CMFT) (Clinical Sciences Building 2, Manchester, U.K.). Clinical isolates were identified by Vitek[®] 2 (BioMérieux, Inc.) by the staff at the CMFT. Stocks were stored at -80°C in 80% glycerol (Fisher Scientific Ltd.). Stock bacteria were cultured for 18 hours on Luria-Bertani, or more correctly, lysogeny broth (LB) agar plates (Table 2. 1) every two weeks. The working culture plates were stored at 4°C. Overnight cultures were prepared by inoculating 10 mL LB broth, in a 50 mL Falcon tube, with several colonies from the working culture plates, which were incubated for 18 hours with shaking at 200 r. p. m. All cultures and assays were incubated in an aerobic atmosphere at 37°C unless otherwise stated.

Table 2. 1. Reagents for growth medium.

LB broth	10 g tryptone ¹ 5 g yeast extract ¹ 10 g NaCl ² made up to 1 L with distilled water
LB agar	10 g tryptone ¹ 5 g yeast extract ¹ 10 g NaCl ² 15 g agar ³ made up to 1 L with distilled water

Suppliers*: ¹Becton, Dickenson Ltd.; ² Fisher Scientific Ltd.; ³ Melford Laboratories Ltd.

*All suppliers used throughout this thesis are based in the United Kingdom (U.K.), unless otherwise stated.

2.2. Biofilm flow through system

The biofilm forming phenotype of the bacteria used in this study was essential for the assays assessing biofilm growth. This was achieved by growing bacteria under the flow of media, which enhances the signalling molecules required for quorum sensing and up-regulating the expression of biofilm genes (Purevdorj *et al.*, 2002; Stoodley *et al.*, 1999). The biofilm flow through system was developed by S. Sandiford, as outlined in her Ph. D. thesis (Sandiford, 2010). A schematic diagram of the model is shown in Figure 2. 1. 10 titanium balls (4 mm diameter) were placed in a plastic housing (5 mL pipette tip) and attached to the top of a Duran bottle, which would collect effluent. The plastic housing containing the balls was then connected by clear PVC tubing (0.5 mm diameter) to a supply of LB broth. The system was autoclaved and sterile LB broth was delivered through the tubing and over the balls to moisten and condition the surface using a peristaltic pump (Watson Marlow Peristaltic Pump P-3, Pharmacia Fine Chemicals). The balls were inoculated by injecting through the plastic housing with 3 mL of an overnight culture of organism grown in LB broth using a sterile needle and syringe. The cells were left to adhere at 37°C for 5-10 minutes, after which time LB broth was delivered at a rate of 2 mL/minute by means of a peristaltic pump for 30 minutes. The balls were washed with sterile water at the same flow rate to remove any planktonic growth, after which media delivery was continued for a further 2-3 days to produce the maximum biofilm yield.

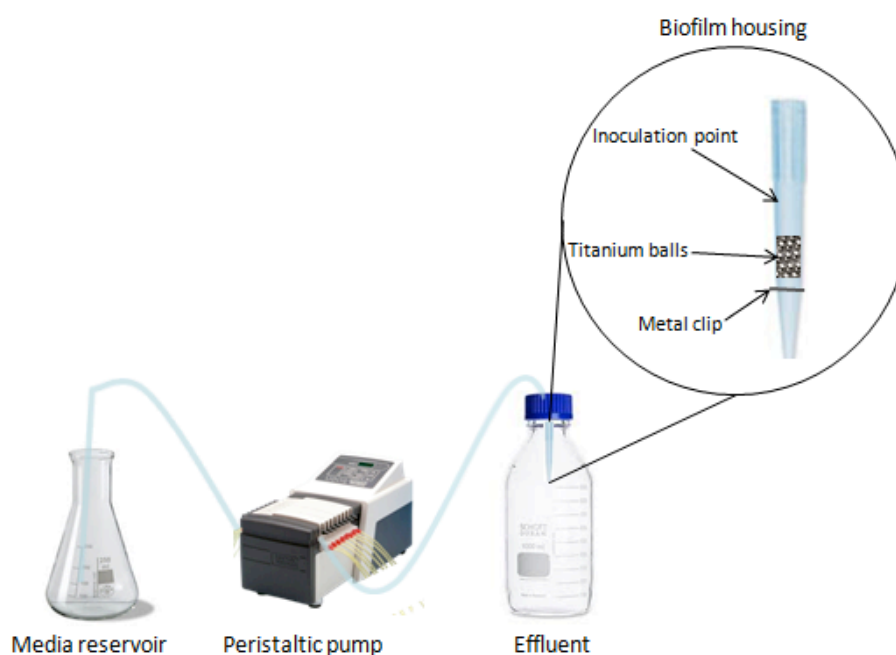


Figure 2. 1. Schematic representation of the biofilm flow through model.

Bacterial cells were removed by carefully collecting the titanium balls and washing the housing with 10 mL sterile water, collecting the cells into a sterile tube. Biofilm cells were centrifuged at maximum speed (3500 x g) (Sorvall® Legend RT, Kendro Laboratory Products, Germany) for 20 minutes at 4°C. The supernatant was decanted and the pellet was re-suspended and washed with 4 mL of Solution A (Table 2. 2) and centrifuged at 3500 x g for another 20 minutes at 4°C. This was repeated one more time. Cells were re-suspended in 500 µL of protein extraction buffer (Table 2. 2) and stored at -80°C until required.

Table 2. 2. Buffers and reagents for the biofilm flow through system.

Protein extraction buffer	5 M Urea ¹
	2 M Thiourea ²
	0.25% (w/v) CHAPS ²
	0.25% (v/v) Triton-X-100 ²
	10% (v/v) Propan-2-ol ³
	12.5% (v/v) Butanol ³
	5% (v/v) Glycerol ³
	1 mM Sodium metavanadate ²
	Complete Mini EDTA-free Protease Inhibitor Cocktail tablet ⁴
Solution A	50 mM Tris-HCl (pH 7.5) ³
	150 mM NaCl ³
	Complete Mini EDTA-free Protease Inhibitor Cocktail tablet ⁴

Suppliers: ¹National Diagnostics; ²Sigma-Aldrich Company Ltd.; ³Fisher Scientific Ltd.; ⁴Roche Applied Science.

2. 3. Preparation of bacteria for western blot to detect the presence of OprF in *P. aeruginosa*

2. 3. 1. Planktonic growth

Five *P. aeruginosa* colonies were taken from growth on an LB agar plate and used to inoculate 20 mL of LB broth and incubated for 18 hours aerobically at 200 r. p. m. at 37°C.

2. 3. 2. Biofilm and planktonic growth

Glass slides (Thermo Scientific) were placed in a plastic container and seeded with a 1/100 dilution of an overnight culture in LB broth and incubated at 37°C for 4-6 hours without agitation, on the basis that bacterial cells need a conditioning layer to promote adhesion to a surface (Kokare *et al.*, 2009). The layer of media components allowed for the initial attachment of bacteria to the glass surface. After the initial incubation period, the planktonic growth was decanted carefully into a separate sterile tube for further purification and analysis, and the glass slides were carefully washed by submerging the slides in sterile PBS and gently rocking for 2 minutes, the PBS was decanted. This was repeated two more times. The glass slides were transferred to a fresh container and submerged in fresh LB broth. The slides were incubated for a further 18 hours at 37°C, without shaking.

Planktonic cells were decanted into a sterile tube and glass slides were washed in 3 volumes of PBS as described previously. The remaining attached biofilm cells were removed by scraping the biofilm off the glass slides into a sterile petri dish and washing the slides by pipetting 2 mL volumes of a protein extraction buffer (Table 2. 2). Biofilm cells collected in Solution A were carefully transferred to a 50 mL tube, and the final volume of the biofilm suspension was made to 20 mL with protein extraction buffer.

2. 3. 3. Preparation of proteins of *P. aeruginosa*

Cell suspensions in protein extraction buffer were thawed rapidly by running cold water over the tubes. Cells were centrifuged at maximum speed (13200 x g) (Mini Spin, Eppendorf, Germany) for 15 minutes. The supernatant containing solubilised protein

was transferred to a clean Eppendorf tube, and the insoluble material in the pellet was discarded.

Proteins were precipitated by adding 3 volumes of 10% (v/v) ice cold trifluoroacetic acid (Sigma-Aldrich Company Ltd.) in 10% (v/v) acetone (Fisher Scientific Ltd.) to the solubilised protein and left at -20°C for 30 minutes. After this period, precipitated protein was harvested by centrifugation at 13200 x g for 15 minutes and the supernatant discarded. The protein pellet was washed with 300 µL of 10% (v/v) ice cold ethanol and harvested by centrifugation at 13200 x g for 15 minutes. The supernatant was carefully removed with a pipette and discarded. The pellet was left to air dry, and 200 µL of protein extraction buffer (Table 2. 2) was used to solubilise the protein with the aid of vortexing and repeated pipetting.

2. 4. SDS-PAGE and western blot

The reagents and buffers for SDS-PAGE and western blot analysis are outlined in Table 2. 3.

Table 2. 3. Reagents and buffers for SDS-PAGE and western blot analysis.

SDS loading buffer	120 mM Tris (pH 6.8) ¹ 20% (v/v) Glycerol ¹ 4% (w/v) SDS ¹ 0.1% (w/v) bromophenol blue ² 8% (v/v) β -mercaptoethanol ²
Resolving gel (12%)	3.35 mL distilled water 2.5 mL 1.5 M Tris-HCl (pH 8.8) ¹ 100 μ L 10% (w/v) SDS ¹ 4 mL 30% Acylamide bis-acrylamide (29:1) ³ 100 μ L 10% (w/v) Ammonium persulphate ⁴ 10 μ L TEMED ⁵
Stacking gel (4%)	3.05 mL distilled water 1.25 mL 5 M Tris-HCl (pH 6.8) ¹ 50 μ L 10% (w/v) SDS ¹ 650 μ L 30% Acylamide bis-acrylamide (29:1) ³ 50 μ L 10% (w/v) Ammonium persulphate ⁴ 10 μ L TEMED ⁵
TBS-T buffer	100 mM Tris ¹ 150 mM NaCl ¹ 0.05% (v/v) Tween-20 ²
Blocking buffer	TBS-T buffer 5% (w/v) Dried skimmed milk powder ⁶
Transfer buffer	25 mM Tris ¹ 150 mM Glycine ¹ 20% Methanol ¹

Suppliers: ¹Fisher Scientific Ltd.; ²Sigma-Aldrich Company Ltd. ³Bio-Rad Laboratories, Inc.; ⁴BDH, AnalaR; ⁵Fluka; ⁶Marvel.

20 μL biofilm and planktonic protein sample were each heated to 100°C for 5 minutes with 5 μL sodium dodecyl sulfate (SDS) loading buffer (total volume 25 μL) before loading in a 1.5 mm thick 12% polyacrylamide gel containing SDS (Table 2. 3). 10 μL of Precision Protein Duel Colour marker (Bio-Rad Laboratories, Inc.) was also loaded into the gel as a molecular weight marker. The samples were separated by electrophoresis by applying 120 V for 40 minutes or until the samples and marker were 1 cm from the bottom of the gel. The gel with the resolved proteins was incubated in transfer buffer and placed on a gentle rocker for 10 minutes. The proteins were transferred to a nitrocellulose membrane (HybondTM-ECL, 0.44 μm , AmershamTM) using a Semi-Dry blotting apparatus (Bio-Rad Trans-Blot[®] Semi-dry transfer cell) at 15 V for 1 hour. The filters and membrane were moistened in transfer buffer (Table 2. 3). After transfer the membrane was washed briefly in TBS-T (Table 2. 3) before being incubated in blocking buffer for 20–30 minutes with gentle rocking, at room temperature. For immunodetection, the membrane was incubated with the primary antibody, anti-OprF monoclonal antibody MA7-3 (kindly provided by Prof. Hancock, University of British Columbia, Canada (Rawling *et al.*, 1995), which was diluted 1/5000 in blocking buffer, overnight at 4°C with gentle rocking. The membrane was washed 4 times with TBS-T for 5 minutes each and incubated in a 1/2000 dilution of secondary antibody (polyclonal goat anti-mouse IG/HRP, Dako, Denmark) in blocking buffer for 1.5 hours at room temperature, with gentle rocking. Proteins were detected by incubating the membrane in the reagents of the ECL PlusTM western blotting detection kit (AmershamTM) for 1 minute at room temperature. The membrane was immediately transferred to a chemiluminescence film (Amersham HyperfilmTM ECL, GE Healthcare) in the dark and developed by incubating in 1:5 fixer solution (GBX Fixer/Replenisher, Kodak[®] processing chemicals for autoradiography films, Sigma-Aldrich Company Ltd.), washing in clean water and incubating in 1:5 developer solution (GBX Developer/Replenisher, Kodak[®] processing chemicals for autoradiography films, Sigma-Aldrich Company Ltd.), until bands were able to be visualised.

2. 5. Preparation of antimicrobial agents

All antimicrobials were prepared in sterile distilled water with the pH adjusted to 7 with 0.1 M sodium hydroxide (Fisher Scientific Ltd.). Fresh stock solutions were made every 2 weeks, and dilutions were freshly prepared from the stocks, for each assay,

immediately before dispensing into the wells. Concentrations were made at 2 times the final concentration required for the assay, according to the CLSI guidelines (CLSI, 2009).

2. 5. 1. Polyamines

Spermine (cat. no.: S1141), spermidine (cat. no.: S2626), cadaverine (cat. no.: D22606) and putrescine (cat. no.: D1,320-8) were used in this study. All polyamines were supplied by Sigma-Aldrich Company Ltd. A 100 mM stock of each polyamine was dissolved in Tris-HCl (Fisher Scientific Ltd.) (pH 7.0). Stocks were stored at -20°C. 500 mM stocks of spermine were prepared in the same way to test inhibition at higher concentration ranges for this polyamine.

2. 5. 1. 1. Buffered polyamines

50 mM stocks of each polyamine were prepared by diluting the 100 mM stocks in sterile phosphate buffered saline (PBS) (Sigma-Aldrich Company Ltd.), (pH 6.5 with concentrated hydrochloric acid). Stocks were stored at -20°C.

2. 6. Quaternisation of polyamines

The quaternisation reactions were carried out in parallel for each polyamine, in a Carousel 6 Parallel Reactor. 0.5 g of each polyamine was introduced in each reactor used, together with 1.5 times excess of potassium carbonate (Sigma-Aldrich Company Ltd.), compared to that required for the neutralisation of the amine groups present on each polyamine. 20 mL of methanol (Fisher Scientific Ltd.) was added to the reactor. Methyl iodide (Sigma-Aldrich Company Ltd.) was added gently with a pipette under nitrogen, in 3 times molar excess in relation to what was required for the quaternisation of the amines. The reaction was stirred at room temperature for 30 minutes, and then brought to 60°C overnight. Each solution was added drop-wise to 4 pre-weighed tubes for each polyamine, each containing 25 mL tetrahydrofuran (THF) (Sigma-Aldrich Company Ltd.). A precipitate was formed. This precipitate was centrifuged at 3500 x g for 5 minutes. The supernatant was decanted and the precipitate was re-suspended in fresh THF. This was repeated two more times. The final precipitate was dissolved in 20

mL water and freeze-dried. The tubes containing the final product were re-weighed to ensure any excess water had evaporated during freeze-drying. The products were characterised through ¹H-NMR (D₂O). 100 mM stocks of freeze-dried preparations of polyamines were prepared by dissolving in sterile distilled water. Stocks were stored at -80°C.

2. 7. Quaternary ammonium compounds

The quaternary ammonium compounds used in this study are listed in Table 2. 4. 20 mM stocks of each quaternary ammonium compound were prepared in sterile distilled water.

Table 2. 4. Quaternary ammonium compounds used in this study.

Quaternary ammonium compound	Tradename
Polyquaternium-4 (PQ-4) ¹	Cellquat [®] LS-50
Polyquaternium-6 (PQ-6) ²	
Polyquaternium-7 (PQ-7) ²	
Polyquaternium-10 (PQ-10) ²	
Polyquaternium-28 (PQ-28) ²	
Polyquaternium-37 (PQ-37) ³	
Byotrol [™] 4	G32 formulation
PHMB* (20 wt% in water) ⁵	Vantocil
DDQ (40 wt% in water) ⁶	Bardac 2240
BAC (50 wt% in water) ⁷	Acticide BAC 50M

Suppliers: ¹AkzoNobel; ²A & E Connock (Perfumery & Cosmetics) Ltd.; ³Cognis GmbH (Germany); ⁴Byotrol[™] Technology Ltd.; ⁵Arch Chemicals; ⁶ Lonza; ⁷ Thor.

*PHMB is a polymeric biguanide and is not classified as a quaternary ammonium compound (QAC), but as it is a component of Byotrol[™], it was tested alongside the other QACs.

2. 7. 1. Determination of the molecular weights for the quaternary ammonium compounds

Size exclusion chromatography (SEC) was carried out using the columns from TSK-GEL Filtration Columns (Supelco). Two different SEC systems were used: a low molecular weight and high molecular weight system. The particular columns used in these systems are shown in Table 2. 5. This procedure was kindly performed by the staff at the Organic Materials Innovation Centre (OMIC), University of Manchester.

Table 2. 5. Summary of columns used for size exclusion chromatography (SEC). Molecular weight (Mw) range based on polyethylene oxide calibration.

System	Columns	Mw range (Da)
Low molecular weight	G2000PW	<2000
	G3000PW	<50,000
High molecular weight	G4000PW	2000-300,000
	G5000PW	4000-1000,000

All SEC systems used a Gilson 132 refractive index detector, with at a flow rate of 0.5 mL/minute of a citric acid 0.1 M buffer at 25°C, calibrated using polyethylene oxide standards.

2. 8. Monitoring of pH

The pH of each concentration of inhibitor and controls were taken after the incubation time using pH indicator strips (Precision Laboratories, Inc.). Two readings for each concentration and each control on every plate were taken and an average was determined.

2. 9. Determination of the minimum inhibitory concentration (MIC) of antimicrobial agents under study

The minimum inhibitory concentration (MIC) of the antimicrobials was determined using standard methods (CLSI, 2009). Briefly, a stock concentration of antimicrobial was prepared in sterile distilled water with the pH adjusted to 7. This was used to prepare a range of dilutions in sterile distilled water, at double the final concentration required. 100 μ L of each concentration was dispensed into 8 replicate wells of a flat bottomed non-tissue culture treated polystyrene 96 well microtitre plate (cat. no.: 655161, Greiner Bio-one Ltd.) with a sterile lid (cat. no.: 656161, Greiner Bio-one Ltd.). 100 μ L of a 1:50 dilution of overnight cultures of bacteria were prepared in LB broth and dispensed into each well containing concentrations of the antimicrobial. Eight technical replicates were prepared on each plate for each concentration tested. A minimum of 3 biological replicates were performed for each experiment.

Positive growth controls were prepared by inoculating eight wells with 100 μ L 1:50 dilutions of bacteria and 100 μ L of sterile distilled water in which the antimicrobial was prepared. Negative controls were prepared in a further eight wells by dispensing 100 μ L of LB broth and 100 μ L sterile distilled water. The microtitre plates were incubated under aerobic, static conditions for 18 hours at 37°C.

After the incubation period, the optical density (OD) at 595 nm (OD_{595}) of planktonic growth was measured to quantify the MIC using a spectrophotometer (BMG Labtech FLUstar OPTIMA). The average OD from the eight negative control wells were subtracted from the OD of all test wells. The MIC is determined as the lowest concentration of antimicrobial that completely inhibits visual bacterial growth, or an OD_{595} of <0.05 (Ho *et al.*, 2011).

2. 10. Microtitre plate biofilm formation assay

After determining the MIC (Section 2. 9) excess media and any planktonic cells were decanted from the microtitre plate and each well was washed once with 200 μ L sterile phosphate buffered saline (PBS). The plate was left in an inverted position to air dry overnight at room temperature. Each well was stained with 150 μ L of 0.4% (w/v) crystal violet (Sigma-Aldrich Company Ltd.) at room temperature for 10 minutes and

washed with running tap water until the excess stain was removed and the running water appeared colourless. The plate was inverted and left to dry overnight at room temperature. The biofilm density was quantified by solubilising the crystal violet stain with 200 μL 99.5% ethanol (Fisher Scientific Ltd.) and measuring the OD_{595} of solubilised crystal violet in each well using a spectrophotometer plate reader (BMG Labtech FLUstar OPTIMA). The average OD from the eight negative control wells were subtracted from the OD of all test wells. A minimum of 3 biological replicates were performed for each experiment.

2. 11. Glass chamber slide biofilm formation assay

Antimicrobial concentrations and inoculum were prepared as described in Section 2. 9. Wells of a glass chamber slide (Lab-Tek™ Chamber slide™, Nunc) were filled with 150 μL of antimicrobial agent and 150 μL of a 1:50 dilution of inoculum. One well was used for each concentration, with one well on each slide prepared as a negative control and one well on each slide prepared as a growth control. The slides were incubated for 18 hours, after which they were inverted to decant the solutions in the wells. Each well was washed in 1 mL sterile PBS and slides were left in an inverted position to dry at room temperature overnight. Each well was stained with 250 μL 0.4% crystal violet for 10 minutes, and washed in running water until the water ran clear. The slides were left in an inverted position to dry at room temperature, overnight. The biofilm density was determined by solubilising the crystal violet in 300 μL ethanol, 200 μL of solubilised crystal violet was transferred to wells of a microtitre plate and the OD_{595} was determined using a spectrophotometer plate reader (BMG Labtech FLUstar OPTIMA). The quantification of biofilm density was determined as described in Section 2. 10.

2. 12. Viable cell counts

The Miles and Misra method (Miles *et al.*, 1938) was used to determine the viability of planktonic cells in the form of colony forming units per mL (CFU/mL). Briefly, a 1:10 dilution series from 10^{-1} to 10^{-7} from each concentration tested was prepared in sterile PBS. 20 μL of each dilution was dropped, in triplicate, onto LB agar plates and incubated overnight at 37°C. The countable dilution used was the dilution that produced

no more than thirty colonies per 20 μL drop of sample dispensed. Finally, the total viable cell counts are expressed as CFU/mL by using the following formula:

$$\frac{\text{Viable cell count} \times \text{dilution factor}}{\text{Volume dispensed (mL)}}$$

2. 13. Pre-coating polystyrene microtitre plates and glass with Byotrol™

Wells of a microtitre plate were filled with 200 μL Byotrol™ and wells of an 8 chamber glass slide (Lab-Tek™ Chamber slide™, Nunc) were filled with 300 μL Byotrol™ at increasing concentrations and incubated for 18 hours at 37°C. A larger volume of Byotrol™ was required to cover the surface of the wells on a glass chamber slide. After incubation, excess Byotrol™ was decanted and the microtitre plates and glass chamber slides were re-incubated for a further 18 hours at 37°C to allow for evaporation of water. A 1:100 dilution of overnight cultures of bacteria were prepared in LB broth, and a volume the same as that of Byotrol™ was dispensed to each well containing concentrations of the pre-coated antimicrobial and incubated for 8 hours at 37°C. Eight technical replicates were prepared on a microtitre plate, and 4-11 biological replicates were performed. On each glass chamber slide one technical replicate was prepared, and a minimum of 4 biological replicates were performed. After the incubation period, the wells of the microtitre plate were washed with PBS, stained and the stain was solubilised as for the microtitre plate biofilm formation assay. Wells of the glass chamber slide were washed with 1 mL PBS, stained with 250 μL crystal violet and the stain was solubilised with 300 μL ethanol. 200 μL solubilised stain from each well on the glass chamber slide was transferred to a fresh well of a microtitre plate and OD measurements were read as for the microtitre plate biofilm formation assay.

2. 14. MBEC (Minimum Biofilm Eradication Concentration) assay

200 μL of a 1:100 dilution of an overnight culture was dispensed into wells of a microtitre plate. A lid with protruding pegs (Transferable Solid Phase Screening System, Nunc) was placed into the wells and incubated under static conditions for 18 hours at 37°C. The pegs were transferred to a microtitre plate containing 200 μL sterile PBS and shaken to remove any non-adhered bacterial cells. The pegs were then placed in a microtitre plate containing a concentration range of each antimicrobial which was

prepared in the same manner as described for the MIC assay and microtitre plate biofilm production assay. The plates were incubated under static conditions for 18 hours. The pegs were then placed in 200 μ L PBS and shaken briefly to remove non-adhered cells before being immediately placed in 200 μ L fresh sterile media and incubated for a further 18 hours at 37°C to allow for re-growth of viable bacterial cells on the pegs. After incubation, the lid with protruding pegs was removed and the OD₅₉₅ of the plates containing any planktonic growth were read. The pegs were washed in 200 μ L PBS and allowed to dry overnight at room temperature before placing the pegs in 200 μ L 0.4% crystal violet for 15 minutes. The pegs were washed in running water and left to air dry overnight at room temperature. The biofilm density was quantified by solubilising the crystal violet stain with 200 μ L 99.5% ethanol and measuring the OD₅₉₅ of solubilised crystal violet using a spectrophotometer plate reader (BMG Labtech FLUstar OPTIMA). The average OD from the eight negative control wells were subtracted from the average OD from the eight technical replicates of each concentration in the test wells.

2. 15. Bright field microscopy

8 well glass chamber slides were used to analyse biofilms by bright field microscopy. Each well had 150 μ L of a solution of antimicrobial agent and 150 μ L of a 1:50 dilution of inoculum prepared from an overnight culture as described previously (Section 2. 9). One well on each slide contained a positive growth control prepared with 150 μ L inoculum and 150 μ L water, and one well was prepared as a negative control with 150 μ L media and 150 μ L water. After incubation for 18 hours at 37°C under static conditions, the wells were washed with 1 mL PBS and immediately stained with 0.4% crystal violet for 10 minutes. Excess stain was washed with running water and the slide was left to dry in an inverted position overnight. The chambers were removed and microscopy images were collected on an Olympus BX51 upright microscope using a 100x/1.30 UPlanFlu objective. Images were captured using a Coolsnap HQ camera (Photometrics) through MetaVue Software (Molecular Devices). Images were then processed and analysed using ImageJ (<http://rsb.info.nih.gov/ij>).

2. 16. Non-contact mode atomic force microscopy (AFM)

Wells of a glass chamber slide were pre-coated with 300 μL Byotrol™ at increasing concentrations, overnight at 37°C. After incubation, excess Byotrol™ was decanted and the slides were re-incubated for a further 18 hours at 37°C to allow for evaporation of water.

The glass slides with pre-coated Byotrol™ were secured to a metal disc using double sided tape and installed on the AFM scanner. An area of 20 μm^2 was scanned. Calibration of the AFM scanner was kindly performed prior to each experiment by Peter Wills (Ph. D. student, OMIC, University of Manchester).

Images were acquired in non-contact mode, whereby a cantilever attached to a sharp tip does not touch the coated surface. The cantilever is oscillated at a point which is greater than its resonance frequency; when the cantilever comes into contact with the van der Waals forces that extend above the coated glass surface, there is a decrease in the resonance frequency. To maintain a constant resonance frequency, the tip is adjusted appropriately and by measuring this adjustment in surface distance, the surface topography can be obtained.

2. 17. Preparation of *E. coli* K12 grown to mid-exponential phase for two dimensional gel electrophoresis and transcriptomic analysis

Proteins and RNA were extracted from a 1:100 dilution of an overnight culture of *E. coli* K12 grown to mid-exponential phase (approx. 5 hours) in a shaking incubator at 200 r. p. m, 37°C. The time at which to harvest cells growing at mid-exponential phase was determined by preparing an 8 hour growth curve (Figure 2. 2). Two-dimensional gel electrophoresis was performed with proteins extracted from the mid-exponential phase of growth in order to make a direct comparison to the transcriptomics results. Cells harvested at the mid-exponential phase are most viable as there are plenty of nutrients available and due to high metabolic activity, RNA yields are optimal (Qiagen, 2005).

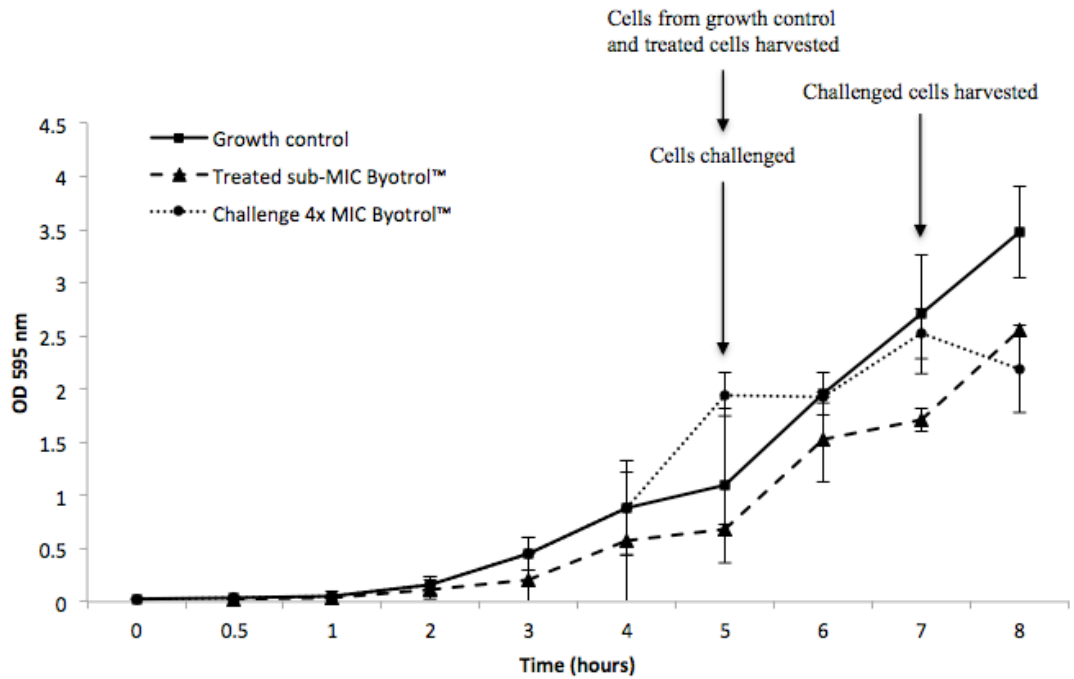


Figure 2. 2. An 8 hour growth curve of *E. coli* K12 grown under 3 conditions: *E. coli* K12 was grown without Byotrol™ (growth control); treated with sub-MIC Byotrol™ and grown for 5 hours without Byotrol™ then challenged for 2 hours with 4 times MIC Byotrol™. Error bars indicate the standard deviation.

Protein and RNA were extracted from a planktonic growth control; planktonic growth with sub-MIC Byotrol™ (0.6 µg/mL), which is 20% of the MIC; and planktonic growth challenged with 4 times the MIC Byotrol™ (10.5 µg/mL) for a further two hours. Cell growth was monitored by measuring the OD₅₉₅ at 1 hour intervals.

2. 18. Preparation of bacteria grown for 24 hours for two dimensional gel electrophoresis

Proteins were extracted at the stationary phase of growth (16-24 hours), as this was the phase of growth used for the microtitre plate assays to determine the MIC.

2. 18. 1. Biofilm and planktonic growth control

1 g of glass wool (Sigma-Aldrich Company Ltd.) was weighed as a single piece and placed into 50 mL of LB broth in a 250 mL conical flask, which was then autoclaved. A 1:100 dilution of an overnight culture of *E. coli* K12 was used to inoculate the 50 mL LB broth and incubated in a shaking incubator at 200 r. p. m. for 24 hours at 37°C to

ensure sufficient biofilm mass was obtained for subsequent analyses. The planktonic cells were decanted equally into Falcon tubes and biofilm cells were washed by immersing the glass wool in 20 mL sterile PBS and vortexing briefly. The glass wool was then immersed in a fresh 20 mL volume of PBS and sonicated (VibraCell™ Sonics®, Sonics & Materials Inc.) for 30 seconds, 3 times with 30 second intervals to remove biofilm cells from the glass wool. The biofilm cell suspension in PBS was kept on ice before whole cell extraction.

2. 18. 2. Biofilm and planktonic growth in sub-MIC Byotrol™

The biofilm and planktonic cells were grown as described in Section 2. 17 but in the presence of 0.6 µg/mL Byotrol™.

2. 19. Preparation of whole cell protein extracts for two dimensional gel electrophoresis

Planktonic and biofilm cells were harvested by separating the bacterial culture equally into 50 mL tubes and centrifuging at 3500 x g for 20 minutes at 4°C. The pellets containing whole cells were washed 3 times by re-suspending and centrifuging in 10 mL PBS at 3500 x g for 10 minutes at 4°C to remove excess media components.

The final pellets were re-suspended in 1 mL rehydration buffer and pooled. The suspension was left for 10 minutes at room temperature and sonicated on ice for 30 seconds 3 times, with 30 second intervals to limit frothing and overheating.

Table 2. 6. Components of rehydration buffer.

Rehydration buffer	2% (w/v) CHAPS ¹
	0.05% (w/v) DTT ²
	1 mM Sodium metavanadate ¹
	0.25% (v/v) Triton-X-100 ¹
	Made up in 9 M Urea ³

Suppliers: ¹Sigma-Aldrich Company Ltd.; ²Melford Laboratories Ltd.; ³National Diagnostics.

Proteins were precipitated by adding ice cold acetone and ice cold trifluoroacetic acid to the solubilised protein in an 8:1:1 ratio, respectively. The proteins were precipitated overnight at -20°C . After this period, precipitated protein was harvested by centrifugation at $3500 \times g$ for 20 minutes at 4°C , and the supernatant discarded. The protein pellet was washed 3 times by re-suspending and centrifuging the pellet with 1 mL of 80% ice cold ethanol at $13200 \times g$ for 1 minute. The supernatant was carefully removed with a pipette and discarded. The pellet was left to air dry until no more acetone was present. The pellet was dissolved in 1 mL rehydration buffer at room temperature with vortexing and pipetting every 10 minutes for 1 hour.

Proteins were harvested by centrifugation at $13200 \times g$ for 15 minutes. The supernatant containing protein was carefully transferred to a fresh, clean Eppendorf tube. The pellet containing cell debris was discarded.

2. 20. Determination of total protein concentration

To quantify the total protein concentration extracted from the bacterial cells, the Bradford Assay was used (Bradford, 1976). A standard curve (see Appendix A) was prepared using dilutions of rehydration buffer in bovine serum albumin (BSA) (BSA protein assay standard II, Bio-Rad Laboratories, Inc.). Concentrations of BSA prepared were 0.0 mg/mL (rehydration buffer alone) 0.2 mg/mL, 0.5 mg/mL, 0.8 mg/mL, 1.2 mg/mL and 1.5 mg/mL (BSA alone). 10 μL of each standard and test samples were dispensed in triplicate into wells of a microtitre plate, to which 200 μL Bradford Reagent (Sigma-Aldrich Company Ltd.) was added. The plate was shaken gently to mix the contents of the wells. Plates were incubated at room temperature for 15 minutes. OD_{595} measurements of the standards and samples were taken using a spectrophotometer (BMG Labtech FLUstar OPTIMA). A calibration curve was plotted from the standards, from which original protein extract concentration was adjusted to 200 μg concentrations by diluting in rehydration buffer. Protein extracts were stored at -80°C in 250 μL aliquots until required, when they were thawed on ice to prevent protein degradation.

2. 21. Two dimensional gel electrophoresis (2DGE)

Reagents and buffers for 2DGE are outlined in Table 2. 7.

2. 21. 1. Active rehydration

Rehydration was performed by transferring 250 μ L protein extract containing 1% (v/v) carrier ampholyte (Bio-Lyte[®] 3-10 buffer 100x, Bio-Rad Laboratories, Inc.) evenly into one lane of an iso-electric focussing tray, leaving 1 cm at each end where the electrodes are present. The IPG strip was allowed to reach room temperature and the backing strip was carefully removed. The acidic end of the strip was aligned with the anode when being placed gel side down on the protein solution, taking care to ensure all bubbles were removed. Active rehydration was performed by applying a 50 V potential difference across the strip for 18 hours. During this time the strip was overlaid with mineral oil (Bio-Rad Laboratories, Inc.) to prevent the strip from drying and to ensure the protein sample did not evaporate.

Table 2. 7. Reagents and buffers for two-dimensional gel electrophoresis.

IPG equilibration base buffer	6 M Urea ¹ 2% (w/v) SDS ² 50 mM Tris-HCl (pH 8.8) ² 20% (v/v) Glycerol ²
Reducing equilibration buffer	2% (w/v) DTT ³ to IPG equilibration base buffer
Alkylating equilibration buffer	2.5% (w/v) Iodoacetamide ⁴ to IPG equilibration base buffer
SDS running buffer	27 mM Tris-HCl pH 8.5 ² 190 mM Glycine ² 0.1% (w/v) SDS ² made up to 1 L with distilled water

Suppliers: ¹National Diagnostics; ²Fisher Scientific Ltd.; ³Melford Laboratories Ltd.; ⁴Sigma-Aldrich Company Ltd.; ⁵Bio-Rad Laboratories, Inc.; ⁶BDH, AnalaR; ⁷Fluka.

Table 2. 7. Continued.

Resolving gel (10%)	20.25 mL distilled water 12.5 mL 1.5 M Tris-HCl (pH 8.8) ² 500 μ L 10% (w/v) SDS ² 16.5 mL 30% Acylamide bis-acrylamide (29:1) ⁵ 250 μ L 10% (w/v) Ammonium persulphate ⁶ 25 μ L TEMED ⁷
Overlay agarose	1% (w/v) agarose ² in SDS running buffer A few crystals of bromophenol blue ⁴
Gel fixing solution	500 mL ethanol ² 100 mL acetic acid ² made up to 1 L with distilled water
Developing solution: Silver Stain Plus [™] kit	Silver Complex Solution ⁵ Reduction Moderator Solution ⁵ Image Development Reagent ⁵ Development Accelerator Reagent ⁵
Silver stain stop buffer/Storage solution	5% (v/v) acetic acid ² in distilled water

Suppliers: ¹National Diagnostics; ²Fisher Scientific Ltd.; ³Melford Laboratories Ltd.; ⁴Sigma-Aldrich Company Ltd.; ⁵Bio-Rad Laboratories, Inc.; ⁶BDH, AnalaR; ⁷Fluka.

2. 21. 2. Iso-electric focussing (1st dimension separation of proteins)

The first dimension separation enables the proteins to migrate through the gel in response to the voltage applied until they reach their isoelectric point (*pI*). Each protein will carry a charge at different pH. The *pI* of a protein is the pH at which the protein has a net neutral charge, whereby the protein carries an equal number of positive and negative charges. Since the proteins have no net charge, they are not affected by the voltage applied when they reach their *pI* and will cease to migrate.

After 18 hours of rehydration under active conditions, electrode wicks (Bio-Rad Laboratories, Inc.) were dampened with 10 μ L of ultra-pure deionised water (Sigma-Aldrich Company Ltd.). These were carefully placed between the electrodes and the strip to prevent the strip from burning under the increasing voltage being applied during the first dimension separation. For the 17 cm strip with a pH range of 3-10 and 5-8, the IEF program outlined in Table 2. 8 was used. After IEF, the oil can be carefully drained from the strips and the strips can be placed in storage trays, gel side up, and frozen at -20°C until required for the second dimension separation (Section 2. 21. 4).

Table 2. 8. IEF program used for first dimension separation of proteins using a 17 cm IPG strip. Step 1 ensures salts are removed and are not carried through into the separation steps. Steps 2-7 mediate the electrophoretic mobility of proteins along the pH gradient on the strip. The focussing of proteins occurs during step 8. Step 9 is important for holding the proteins in their positions to minimise diffusion from their iso-electric point.

Step	Voltage	Volt-Hours	Time (hours)	Ramp
1	500		2	Rapid
2	750		1	Linear
3	1000		1	Linear
4	1500		1	Linear
5	2000		1	Linear
6	2750		1	Linear
7	3750		1	Linear
8	5000	55000		Rapid
9	500		Hold	Rapid

2. 21. 3. Equilibration

Frozen strips were allowed to thaw for 15 minutes at room temperature before briefly being washed in SDS running buffer (Table 2. 7). The proteins were then reduced by equilibration in 2% w/v DTT (Table 2. 7) for 20 minutes followed by alkylation in 2.5% w/v iodoacetamide (Table 2. 7) for 20 minutes, each on an orbital shaker at room temperature. The strip was again equilibrated in SDS running buffer for 5 minutes.

2. 21. 4. SDS-Polyacrylamide Gel Electrophoresis (SDS-PAGE) (2nd dimension separation of proteins)

The second dimension separation is used to resolve proteins according to their molecular weight. A 10% resolving gel was prepared (Table 2. 7). 5 μ L Precision Protein Duel Colour marker was loaded onto an electrode wick and placed on the top left of the gel as a molecular weight marker. The IPG strip was placed on top of the gel with the acidic (+) end on the left and the basic (-) end on the right, and overlaid with 1% agarose prepared in SDS running buffer which contained a few crystals of bromophenol blue to visualise the migration of the proteins. Crystals of bromophenol blue were obtained by inserting the end of a pipette tip into the container of bromophenol blue to a depth of approximately 1 mm and transferring the attached grains to the overlay agarose solution. Prior to each use, the overlay agarose was heated in a microwave until the agarose had dissolved and was allowed to cool to touch before applying to the IPG strip.

The protein samples were separated by applying a current of 40-90 mA for 4-6 hours or until the samples and marker were 1 cm from the bottom of the gel. The gels were kept cool by circulating cold water through the heat exchanger in the core of the apparatus. Once complete, the gel was removed and incubated in gel fixing solution (Table 2. 7) with gentle agitation overnight.

2. 21. 5. Silver staining of gels

Gels were washed thoroughly in distilled water for at least an hour, with a change of water every 30 minutes. The Bio-Rad Silver Stain Plus protocol was followed, with reagents from the Bio-Rad Silver Stain Plus Kit prepared freshly at room temperature in low light conditions. 100 mL of the mixture of reagents were added to each gel and

allowed to develop in low light conditions on an orbital shaker until protein spots became visible. A 5% (v/v) acetic acid solution was used to stop the silver stain development reaction, and gels were stored in this solution until further analysis.

2. 21. 6. Interpretation of two-dimensional gels and analysis of differentially expressed proteins

For each growth condition and cell phenotype, protein extraction and separation was performed a minimum of 3 times from at least 3 biological replicates. Analysis to determine differentially expressed proteins was performed by eye. Images of gels were taken on the FluorChem™ 5500 imager using the AlphaEase FC (FluorChem™ 5500) software. The intensity of differentially expressed proteins was determined by measuring an area within the protein spot using the Spot Denso Analysis Tool. The area for each spot was kept consistent. This generated an Integrated Density Value which was used to determine the fold difference in protein expression between the same proteins extracted from cells grown under different conditions and in different phenotypes. The unpaired two-tailed student's *t*-test was used to assess the statistical significance of differentially expressed proteins. This tests the null hypothesis: that there is no statistical significance between the two groups. A value of <0.05 is considered to be statistically significant, i.e. the null hypothesis is rejected. The *t*-test was performed using Microsoft Excel's statistics function; however the formulation on which this is based is expressed below:

$$t = \frac{X_T - X_C}{\sqrt{\frac{\text{var}_T}{n_T} + \frac{\text{var}_C}{n_C}}}$$

X = mean; T and C = the two groups being compared; n = sample size.

2. 21. 7. Protein identification by LC-MS/MS analysis

Protein identification by liquid chromatography mass spectrometry/mass spectrometry (LC-MS/MS) was performed by the Biological Mass Spectrometry Core Research Facility, University of Manchester.

2. 21. 7. 1. Digestion

Samples for MS/MS analysis were prepared by excising and dehydrating protein spots in acetonitrile followed by vacuum centrifugation. Dried gel pieces were reduced with 10 mM DTT and alkylated with 55 mM iodoacetamide. Gel pieces were then washed alternately with 25 mM ammonium bicarbonate followed by acetonitrile. This was repeated, and the gel pieces dried by vacuum centrifugation. These proteins were proteolysed at 37°C for 18 hours with 5 µL trypsin (12.5 ng/µL) in 45 µL ammonium bicarbonate (25 mM).

2. 21. 7. 2. LC MS/MS

Digested samples were analysed by LC-MS/MS using an UltiMate[®] 3000 Rapid Separation LC (RSLC, Dionex Corporation, Sunnyvale, CA) coupled to a LTQ Velos Pro (Thermo Fisher Scientific, Waltham, MA) mass spectrometer.

Peptide mixtures were loaded onto a 75 mm x 250 µm i.d. 1.7 µm BEH C18, analytical column (Waters). For separation and elution, a gradient from 92% buffer A (0.1% (v/v) formic acid in water) and 8% buffer B (0.1% (v/v) formic acid in acetonitrile) to 33% buffer B was used, over 44 minutes at 300 nL/minute. Peptides were eluted directly into the MS/MS for analysis. Calibration of the MS/MS was performed externally using phosphoglucose tryptic digests as a standard for both stages.

2. 21. 7. 3. Data analysis of proteins

Data produced were searched using Mascot (Matrix Science), against the Uniprot database (version 3. 6. 2) with taxonomy of *E. coli* K12 selected. Data were validated using Scaffold (Proteome Software, Portland, OR).

2. 22. Preparation of RNA for transcriptomics

E. coli K12 was grown as described in Section 2. 17. In order to ensure that the cell concentration was within the parameters set by the protocol, trial growth curves were prepared and colony counts using the Miles and Misra method (as described in Section 2. 12) were performed every hour for 8 hours. Mid-exponential growth of *E. coli* K12

was determined to have a cell count of 1×10^6 CFU/mL. As this concentration of cells was high for the assay, the cells were diluted 1:4 in LB media before continuing with the steps outlined in the protocol. The RNA for each growth condition was divided into 10 technical replicates to ensure sufficient RNA was yielded. The RNA of *E. coli* K12 was extracted using the Qiagen RNeasy[®] Protect Bacteria Mini Kit (Qiagen) as directed by the RNAprotect[®] Bacteria Reagent Handbook, Protocol 1 and 7 (Qiagen, 2005). Each RNA sample was treated with DNase twice with the Qiagen RNase free on column DNase kit according to the instructions in Appendix B of the RNAprotect[®] Bacteria Reagent Handbook (Qiagen, 2005), to ensure sufficient DNase digestion. Elution for each of the samples was performed with 30 μ L RNase free water. This was carried out twice for each column and eluates were pooled. The RNA concentrations were determined using the NanoDrop spectrophotometer (NanoDrop Technologies, Inc.) according to the manufacturer's instructions.

The integrity of the RNA was determined first by visualisation on a 2% agarose gel (E-Gel[®] SizeSelect[™] 2% Agarose, Invitrogen[™]). 20 μ L 1:2 dilution total RNA in RNase free water (Qiagen) was loaded into the 2% agarose. A lane on the gel was loaded with 20 μ L 1:2 dilution DNA ladder (HyperLadder[™] 100 bp, formerly HyperLadder[™] IV, Bionline) in water. A voltage was applied by placing the E-gels[®] in the supplied Power Base (Invitrogen[™]). RNA bands were visualised under U.V. light and images were taken on the FluorChem[™] 5500 imager using the AlphaEase FC (FluorChem[™] 5500) software. RNA samples, for which the 16S and 23S rRNA bands were not distinctly observed, were discarded. Good quality RNA visualised on the agarose gel were diluted to 1-2 ng in RNase-free water for further validation of RNA integrity by the Genomic Technologies Core Facility, University of Manchester using the Agilent 2100 Bioanalyzer (Agilent Technologies) and Agilent RNA 6000 Pico Kit. The electropherogram determined the integrity of the samples. In all cases the samples were of a high quality, ready for further processing and analysis.

2.22.1. Quality control and preparation of transcripts

Staff at the Centre for Genomic Research, University of Liverpool, carried out this work. Ribosomal RNA depletion was performed on 5 μ g of total RNA using the Epicentre Ribo-Zero[™] rRNA Removal Kit (Meta-Bacteria) (Epicentre Biotechnologies, USA). The library preparation of the depleted RNA was carried out using the Epicentre

ScriptSeq v2 kit (Epicentre Biotechnologies, USA) using 40-50 ng of material and 10 cycles of PCR. For each sample, the whole of the PCR product was multiplexed and each sample was pooled and loaded on a single lane of a HiSeq Sequencing Platform (Illumina Inc. USA). Raw data were provided in the form of FASTQ files.

2. 22. 2. Data analysis of transcripts

The RNA-seq results from the Illumina system were output in FASTQ format. To calculate gene expression levels, RNA-seq analysis was performed using the commercially available CLC Genomics Workbench 6 platform and the CLC Main Workbench version 6.8.2 (<http://www.clcbio.com/genomics/>).

The individual trimmed sequence reads in the FASTQ files were mapped to the *E. coli* K12 sub-strain MG1655 reference genome (Accession number NC_000913). The RNA-seq analysis was carried out for sequence reads obtained from the growth control *E. coli* K12 (Growth control), *E. coli* K12 treated with sub-MIC Byotrol™ (Treated) and *E. coli* K12 challenged with 4 times MIC Byotrol™ (Challenge) separately using default parameters. Only the forward (R1) reads were used as this provided sufficient data which were not any further enhanced by the reverse (R2) reads.

2. 22. 2. 1. Expression analysis: Data normalisation

A gene is considered to be differentially expressed if a change in read counts between genes of different experimental samples is statistically significant (Fang *et al.*, 2012). The differential expression between the three growth conditions was derived by first normalising data within a sample using reads per kilobase per million mapped reads (RPKM) values (Mortazavi *et al.*, 2008).

$$\text{RPKM} = \frac{\text{number of reads of the transcript}}{\text{total reads}} \times \frac{\text{transcript length}}{1000}$$

This method of normalisation accounts for differences in transcript length as well as library size, within a sample.

Secondly, data was normalised based on the total number of reads, which takes into account differences in library size for each sample, and the proportion of counts that make up the total sum of counts in a sample. This was done using Kal's Z-test (Kal *et al.*, 1999).

As these data were analysed for relative abundance, the methods of normalisation took into account the ratio of the number of reads in relation to the total number of transcripts. The same methods were used across all of the samples.

The threshold for the fold change in expression based on these parameters was set as an expression value of ≤ 5 for down-regulated genes and ≥ 5 for up-regulated genes. The statistical significance of any differences in expression was determined by *p*-values of < 0.001 and False Discovery Rate (FDR) *p*-values of < 0.05 , which were calculated by the CLC genomics software.

2. 22. 2. 2. Generation of summary data and KEGG maps in MG-RAST

A breakdown of the sequence data or 'summary data' shown in Section 6. 2 and KEGG (Kyoto Encyclopedia of Genes and Genomes) maps of transcripts that were uniquely expressed under the different growth conditions, shown in Appendix D.10, were generated using the Metagenomics-RAST (MG-RAST) analysis server (<http://metagenomics.anl.gov/>). All genes were annotated against GenBank and the M5NR protein database. The MG-RAST project database for this current study is available for public access: (<http://metagenomics.anl.gov/linkin.cgi?project=3132>).

2. 22. 2. 3. Analysis of unmapped reads

NCBI BLAST (<http://blast.ncbi.nlm.nih.gov/Blast.cgi>) was used to align the unmapped reads to the nucleotide collection (nr) database for prokaryotes. BLAST results were filtered to eliminate matches with an E-value of less than $10e^{-6}$ (Strong *et al.*, 2013). Results from the BLAST search are presented in Appendix D. 11.

Chapter 3

An analysis of the effect that natural polyamines have on biofilm formation

3. 1. Polyamine interaction with porins

Porins such as the outer membrane protein A (OmpA) are involved in biofilm formation (Barrios *et al.*, 2006; Orme *et al.*, 2006), polyamines are known to interact with porins (Iyer *et al.*, 2000), therefore polyamines were investigated as potential inhibitors of biofilm formation in this chapter.

Polyamines are natural biogenic polycationic compounds. The polyamines spermine, spermidine and putrescine are produced during the decarboxylation stages of the L-ornithine pathway (Figure 3. 1) and the polyamine cadaverine is a product of the lysine degradation pathway (Figure 3. 2) (Iyer & Delcour, 1997). With the exception of spermine, which is associated only with eukaryotes, the other 3 polyamines are endogenous to both eukaryotes and prokaryotes (Iyer & Delcour, 1997; la Vega & Delcour, 1996).

Previous studies have investigated the interaction of polyamines with outer membrane proteins on single cells in a planktonic bacterial culture (Katsu *et al.*, 2002; Wortham *et al.*, 2007). There have also been studies that have used electrophysiological techniques such as patch clamp on giant cells or spheroplasts to investigate the effect of the polyamine cadaverine on porin function (Ingham *et al.*, 1990; la Vega & Delcour, 1996). These studies demonstrated that cadaverine interacts with porins, specifically OmpC and OmpF, inducing and prolonging their incidence of closure (Iyer & Delcour, 1997). OmpC and OmpF, like other porins, are predominantly open and are responsible for the permeability of the cell membrane to nutrients and hydrophilic compounds (Samartzidou & Delcour, 1999).

Spermine, spermidine, cadaverine and putrescine are of interest to this study due to their interaction with the porins and proteins in the polyanionic bacterial outer membrane, particularly as OmpA was shown to be important in the development of a biofilm (Barrios *et al.*, 2006; Orme *et al.*, 2006).

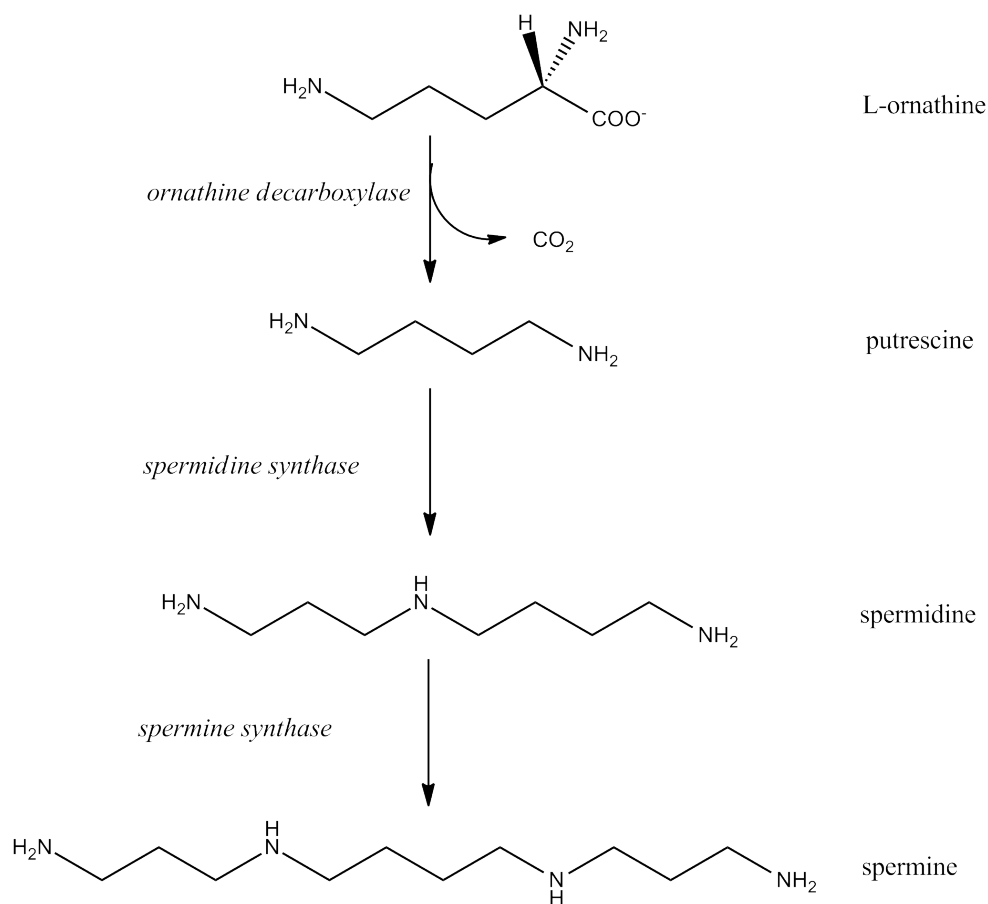


Figure 3. 1. The synthesis of the polyamines spermine, spermidine and putrescine used in this study. Ornithine decarboxylation resulting in the biosynthesis of putrescine, spermidine and spermine.

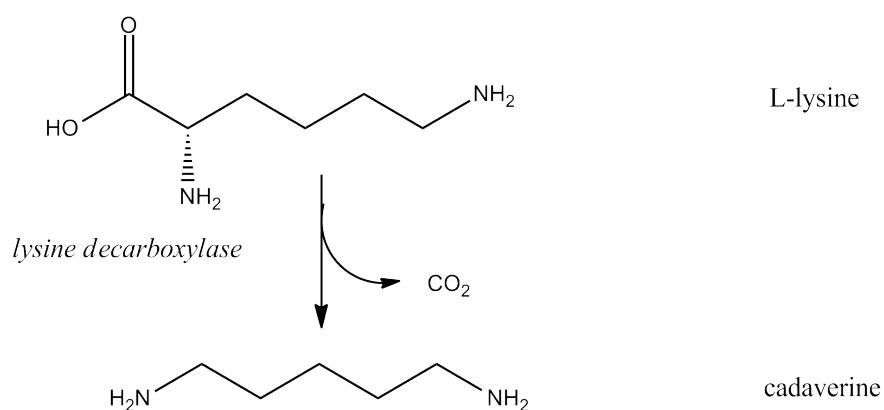


Figure 3. 2. The synthesis of the polyamine cadaverine used in this study. L-Lysine decarboxylation resulting in the biosynthesis of cadaverine.

3. 2. Optimisation of bacterial growth on a microtitre plate

The microtitre plate biofilm formation assay is the preferred method for the high-throughput analysis of biofilm formation and inhibition as it enables a high number of technical replicates for each concentration of potential inhibitors at a single time point for each bacterial strain. Bacterial growth on the surface of a microtitre plate varies from plate to plate and bacterial strain to bacterial strain, therefore, in order to measure the antimicrobial effect of the compounds used in this study, it was necessary to ensure that the conditions allow for sufficient biofilm formation. This can be determined by measuring the optical density (OD) after solubilising a biofilm that was stained with crystal violet. For this reason, the behaviour of each bacterial strain used in this study was optimised for biofilm formation.

3. 2. 1. Optimisation of bacterial growth on different microtitre plate surfaces

Bacteria do not readily attach to all surfaces; attachment is dependant on hydrophobic interactions, charge and surface roughness (Deighton *et al.*, 2001; Li & Logan, 2004). Therefore, the surface on which the bacteria are expected to adhere has to be taken into consideration. Bacteria were grown on 3 different microtitre plate surfaces: a non-tissue culture treated plate, a tissue-culture treated plate and a non-tissue culture plate treated with poly-D-lysine (Figure 3. 3). Poly-D-lysine, due to its net positive charge, is used in mammalian cell culture to promote cell binding to the plate surface (Harrison *et al.*, 2010). Bacterial adherence to a non-tissue culture treated plate was greater than on a tissue culture treated plate. A non-tissue culture treated plate, which was coated with poly-D-lysine did not promote biofilm formation (Figure 3. 3).

3. 2. 2. Optimisation of the minimum growth time which allows for biofilm visualisation after staining

The time taken for bacteria to adhere to the surface with sufficient density to be visualised by crystal violet staining was also optimised. *E. coli* K12 and the clinical isolates of *K. pneumoniae* and *P. aeruginosa* were grown on microtitre plates for 4, 6, 8 and 18 hours, then washed and stained with crystal violet. The stain was solubilised and the OD₅₉₅ was obtained to determine the time taken to achieve sufficient biofilm growth.

The results in Figure 3. 4 demonstrate that as time increased, biofilm formation increased. This was observed for all of the bacteria, with *P. aeruginosa* forming the most biofilm, followed by *E. coli* K12 and then *K. pneumoniae*. As 18 hours enabled sufficient biofilm development, this was the time point used for the microtitre plate biofilm formation assays in this study.

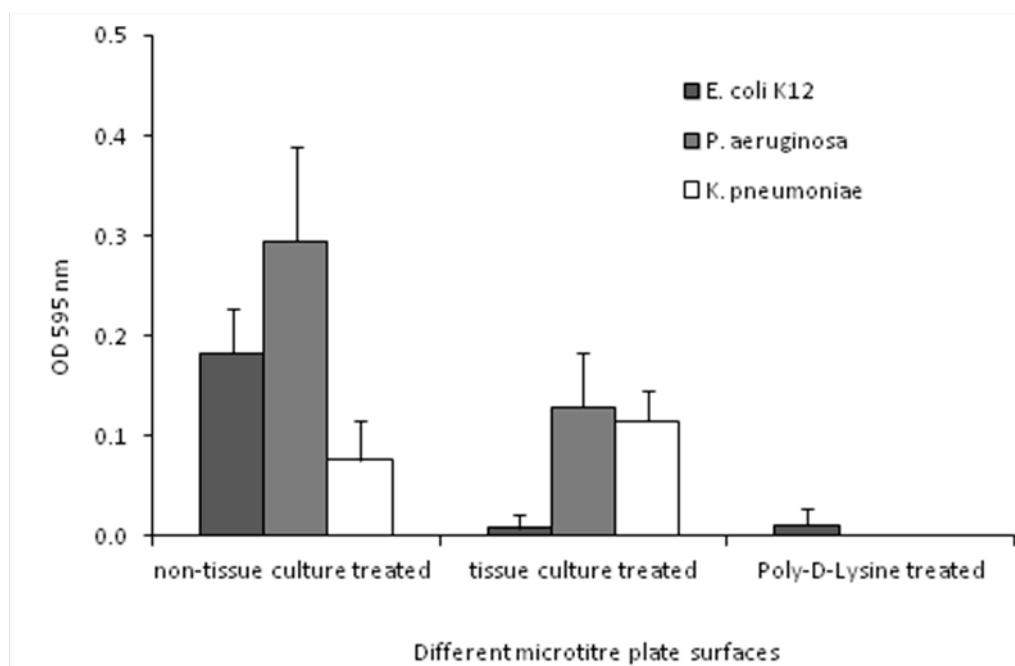


Figure 3. 3. Optimisation of bacterial growth on different microtitre plate surfaces. *E. coli* K12 and the clinical isolates of *K. pneumoniae* and *P. aeruginosa* were grown for 18 hours at 37°C, on 3 different microtitre plates: non-tissue culture treated, tissue culture treated and a non-tissue culture treated plate treated with poly-D-lysine. The results are expressed as the mean of nine replicate wells involving 3 biological replicates for each strain. Error bars indicate the standard error of the mean.

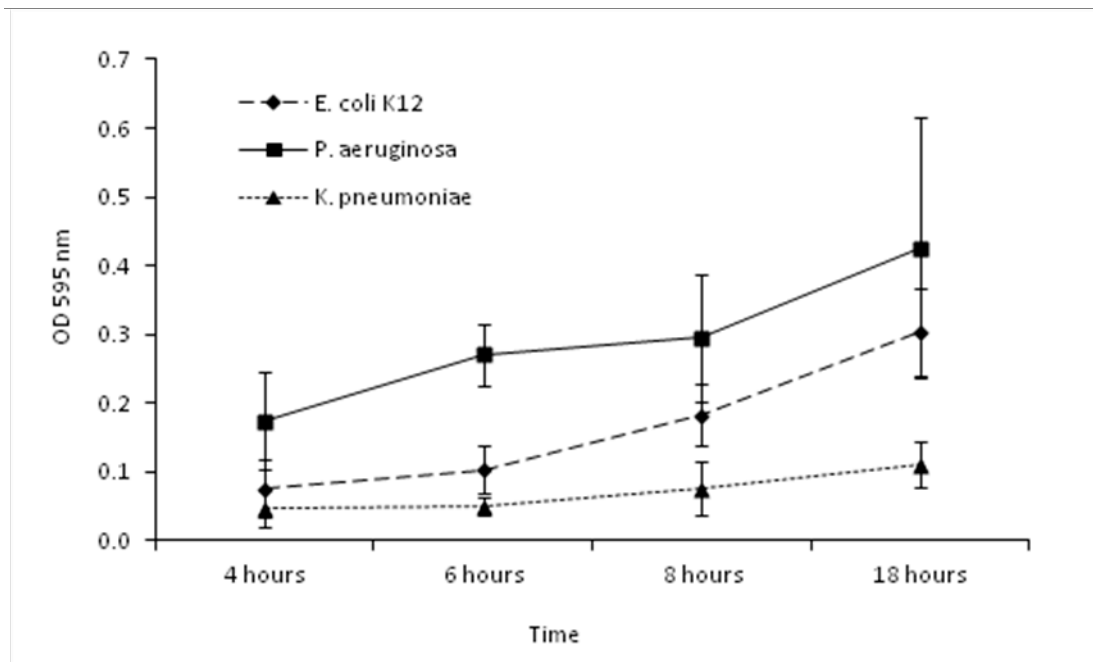


Figure 3. 4. Minimum growth time required for biofilm formation which can be visualised by crystal violet staining. *E. coli* K12 and the clinical isolates of *K. pneumoniae* and *P. aeruginosa* were grown for 4, 6, 8 and 18 hours at 37°C to determine the optimal growth time which allows for sufficient biofilm to be visualised by crystal violet staining. The results are expressed as the mean of nine replicate wells involving 3 biological replicates for each strain. Error bars indicate the standard error of the mean.

3. 3. The effect of polyamines and pH on bacterial growth

E. coli K12 biofilms were grown on microtitre plates for 18 hours at 37°C in the presence of each of the polyamines to assess their effect on biofilm growth (Figure 3. 5). At 10 mM spermine, spermidine and cadaverine, growth was reduced to ~30% of the growth control. At 10 mM putrescine, growth was reduced to ~70% of that of the control.

The glass chamber slide assay was compared to the microtitre plate biofilm formation assay (Figure 3. 6). The glass chamber slide assay was useful for the visualisation of bacteria by microscopy and therefore it was necessary to ensure that bacterial growth and inhibition showed the same trend as on the microtitre plate surface. The trend in growth and inhibition of biofilms did not differ between the two different surfaces (Figure 3. 6). The results of the glass chamber slide assay demonstrated a decrease in biofilm formation to ~40% of the growth control when treated with 1 mM spermine and at concentrations greater than this there was no visible growth. At 10 mM, growth was reduced to ~25% and ~10% by spermidine and cadaverine, respectively. Putrescine appeared to be less potent at these concentrations; it reduced growth to ~70% at 10 mM. It was also clear from the results in Figure 3. 5 and Figure 3. 6 that there was a correlation between an increase in pH as the concentrations of polyamines increase above 1 mM. For this reason it was difficult to determine if a decrease in biofilm formation was a consequence of the inhibitory effects of increasing pH or the inhibitory effects of the polyamine. In order to elucidate any actual inhibitory activity of polyamines, a series of experiments were performed, which are described in the rest of this chapter.

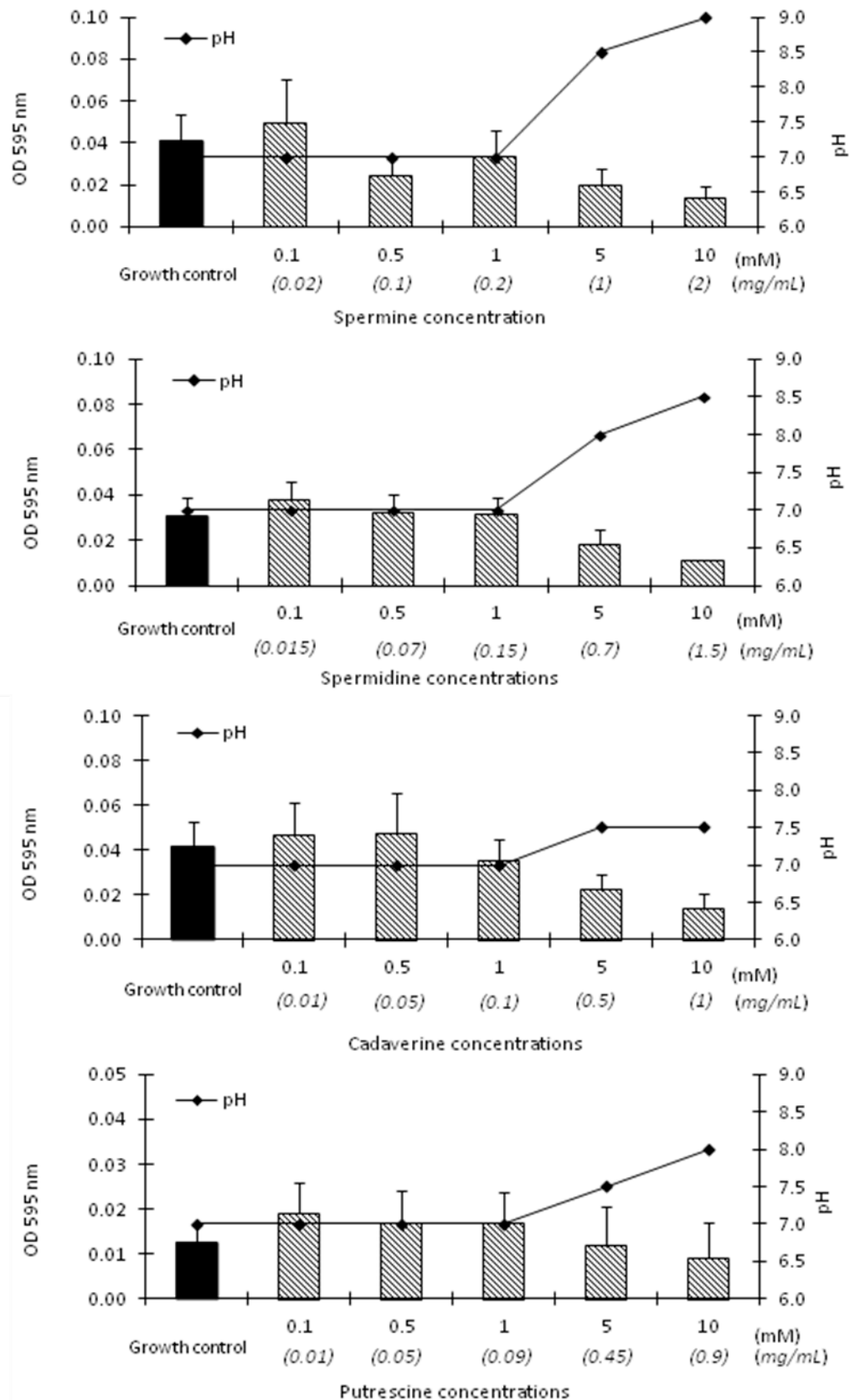


Figure 3. 5. The microtitre plate biofilm formation assay to determine the biofilm inhibitory concentration of the polyamines spermine, spermidine, cadaverine and putrescine against *E. coli* K12 biofilm formation grown for 18 hours at 37°C. The results are expressed as the mean of nine replicate wells involving 3 biological replicates for each strain. Error bars indicate the standard error of the mean.

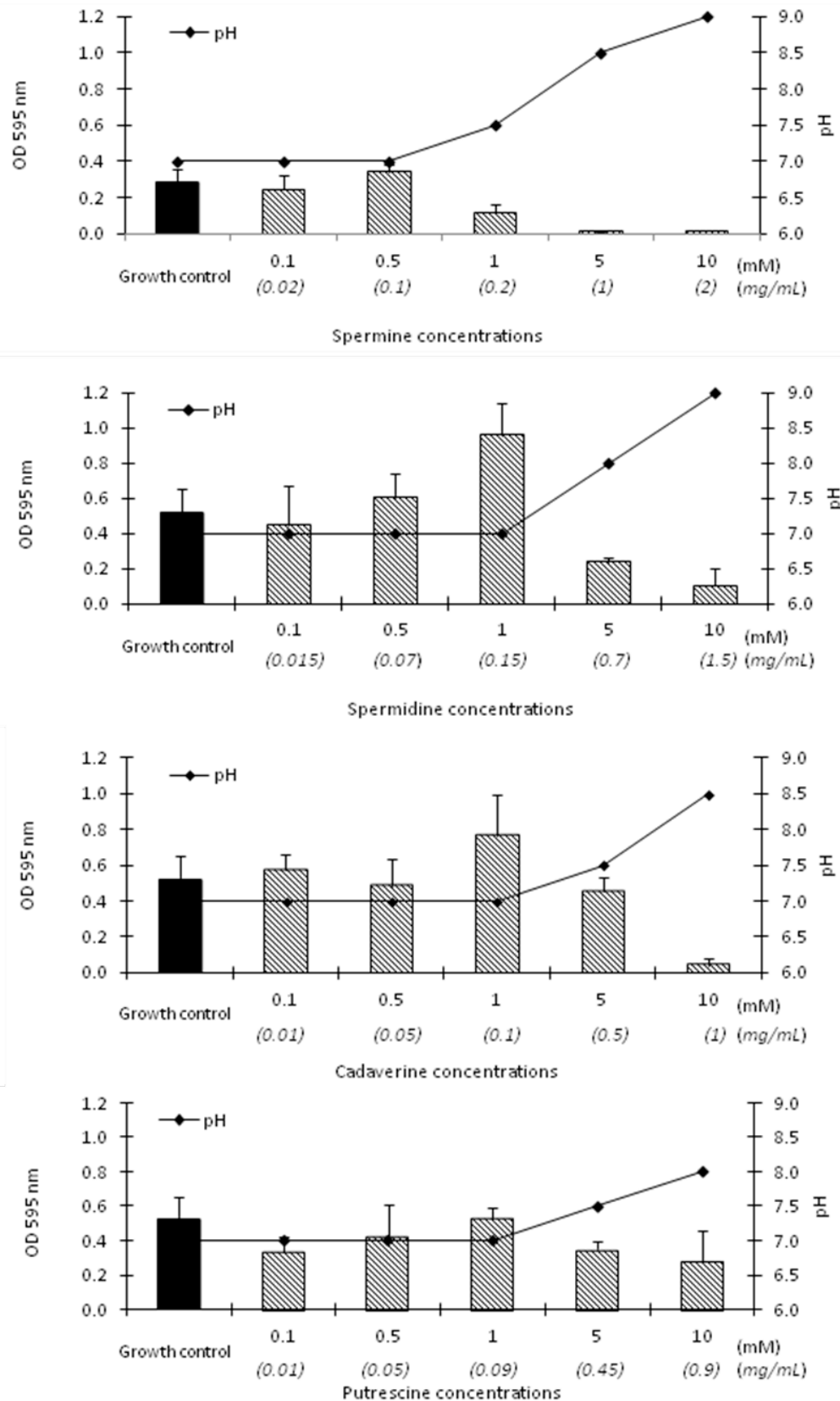


Figure 3. 6. The glass chamber slide assay to determine the biofilm inhibitory concentration of the polyamines spermine, spermidine, cadaverine and putrescine against *E. coli* K12 biofilms grown for 18 hours at 37°C. The results are expressed as the mean of nine replicate wells involving 3 biological replicates for each strain. Error bars indicate the standard error of the mean.

3.3.1. The effect of pH alone on bacterial growth

To determine if the inhibition of bacterial growth was due to a pH effect or to an increase in polyamine concentration, an assay was performed with increasing concentrations of sodium hydroxide (NaOH). *E. coli* K12 was grown in the presence of increasing concentrations of NaOH. The pH was recorded for the growth control and for each concentration of NaOH (Figure 3. 7).

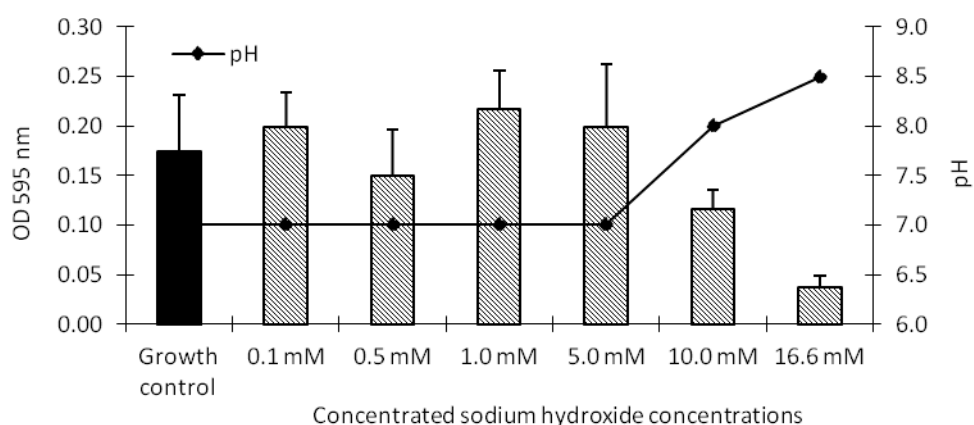


Figure 3. 7. The effect of increasing concentrations of sodium hydroxide (NaOH) on *E. coli* K12 biofilm growth. The bars indicate the average biofilm growth, the black line indicates the pH. The results are expressed as the mean of 3 replicate wells involving 3 biological replicates for each strain. Error bars indicate the standard error of the mean.

Figure 3. 7 demonstrate that the growth of *E. coli* K12 was reduced to ~70% at 10 mM NaOH where the pH was 8, and ~20% at 16.6 mM NaOH where the pH was 8.5. At pH 8.5, *E. coli* K12 growth was reduced to ~10% with spermine, ~25-50% with spermidine and ~10-30% with cadaverine (Figure 3. 6). This suggests that there may be some inhibitory effect imposed by the polyamines and inhibition was not solely down to the effect of an increase in pH. To test this further, polyamines were quaternised and buffered to eliminate the effect of increasing pH on biofilm growth.

3.3.2. The effect of quaternised polyamines on biofilm formation on microtitre plates

As primary amines, polyamines act as weak bases, therefore, in a solution of pH <10, the polyamines are able to accept hydrogen ions from their solution and increase their positive charge. This decrease in H⁺ ions of the solution increases the pH of the solution. A quaternary amine, also known as a quaternary ammonium ion, has a stable charge independent of the pH of their solution. The polyamines used in this study were quaternised to stabilise the pH. As an example of the stages involved in quaternisation, the quaternisation of spermine is detailed in Figure 3. 8. The same reaction was performed for each of the polyamines used in this study whereby NH₂ and NH groups were replaced with methyl groups.

To ensure that the polyamines had been fully quaternised, characterisation of the quaternised polyamine was performed using ¹H NMR, the spectra of which are displayed in Figure 3. 9 to Figure 3. 13. Each peak on the NMR spectra relates to a hydrogen atom present in the quaternised polyamine. The number of hydrogen atoms represented by the peak is detailed at the base of the peak. In the spectra, the quaternised groups are represented by the peaks labelled 'A' (and also 'C' for spermine and spermidine). When the spectra were compared to the structure of each quaternised polyamine, it confirmed that the polyamines were successfully quaternised.

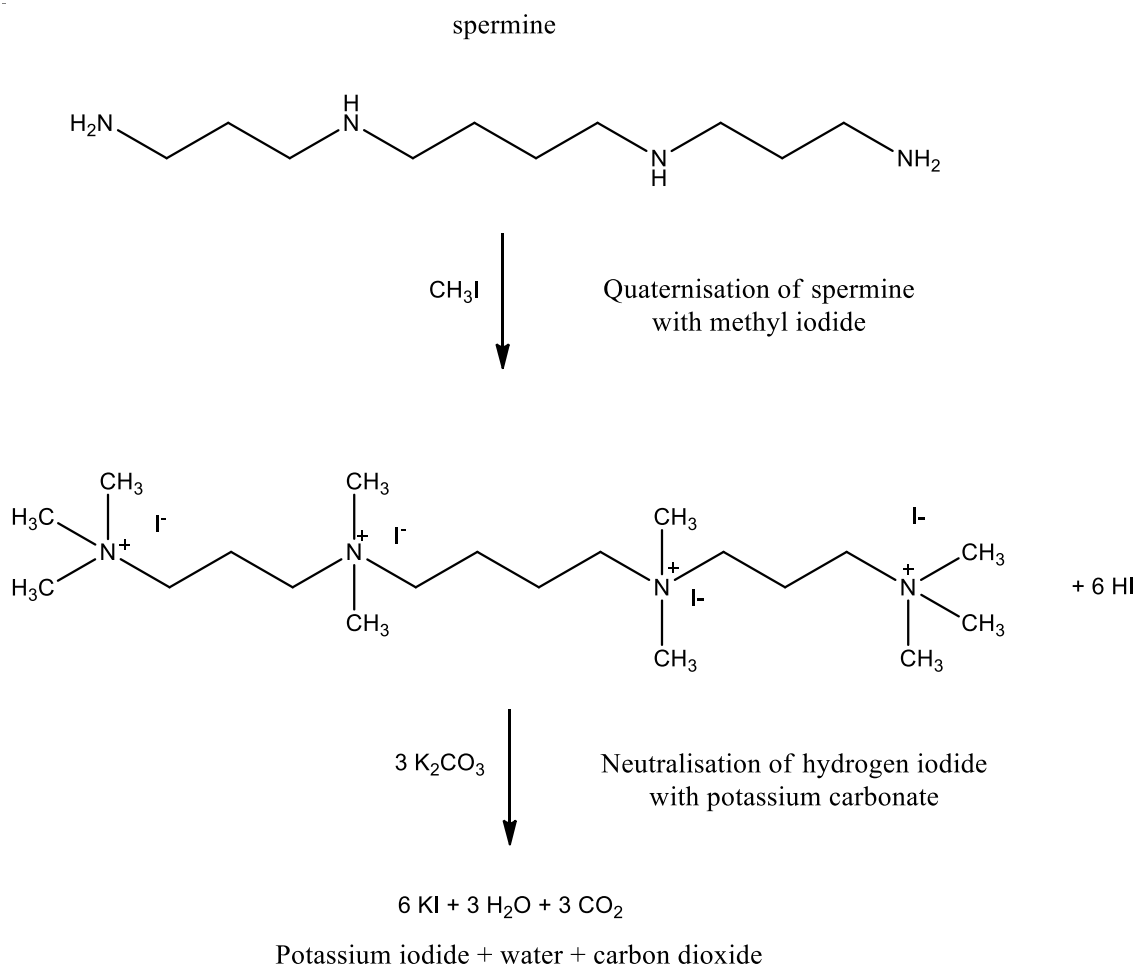


Figure 3. 8. The reaction scheme demonstrating the quaternisation of spermine. The six hydrogen atoms of the four primary amines of spermine reacted with methyl iodide to produce hydrogen iodide. The methyl groups replace each of the hydrogen atoms associated with the nitrogen atoms to form quaternary ammonium groups. This reaction completes the quaternisation of spermine.

Spermine

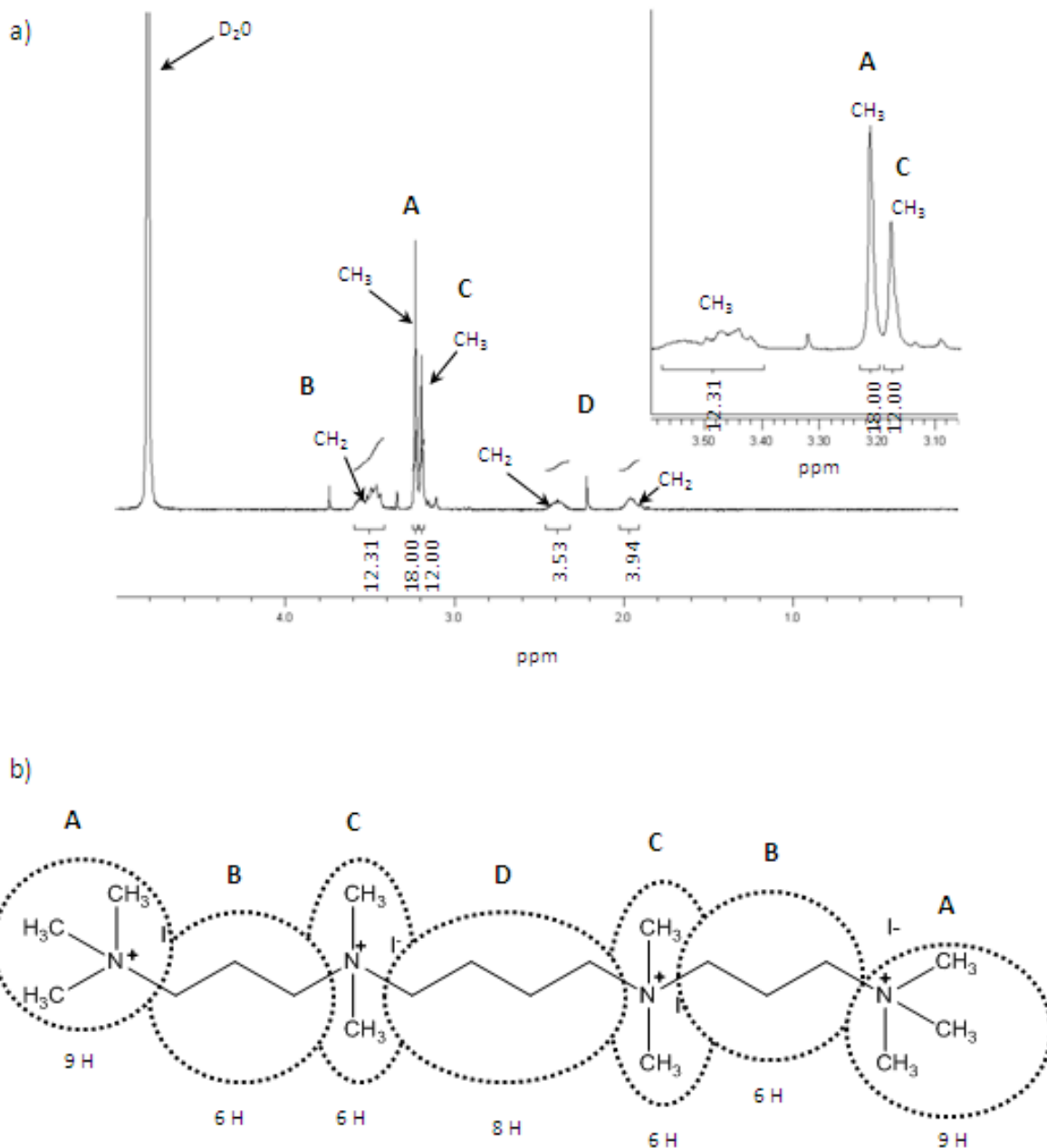


Figure 3. 9. Characterisation of quaternised spermine. **a)** ^1H NMR (D_2O) spectrum of a stationary sample of quaternised spermine. Capital letters from A-D correspond to the groups which are circled on the structure of quaternised spermine (part b); **b)** structure of quaternised spermine showing the number of hydrogen atoms associated with each carbon atom (e.g. 9 H) below the structure and capital letters from A-D which identify the groups which correspond to the peaks on the NMR spectrum.

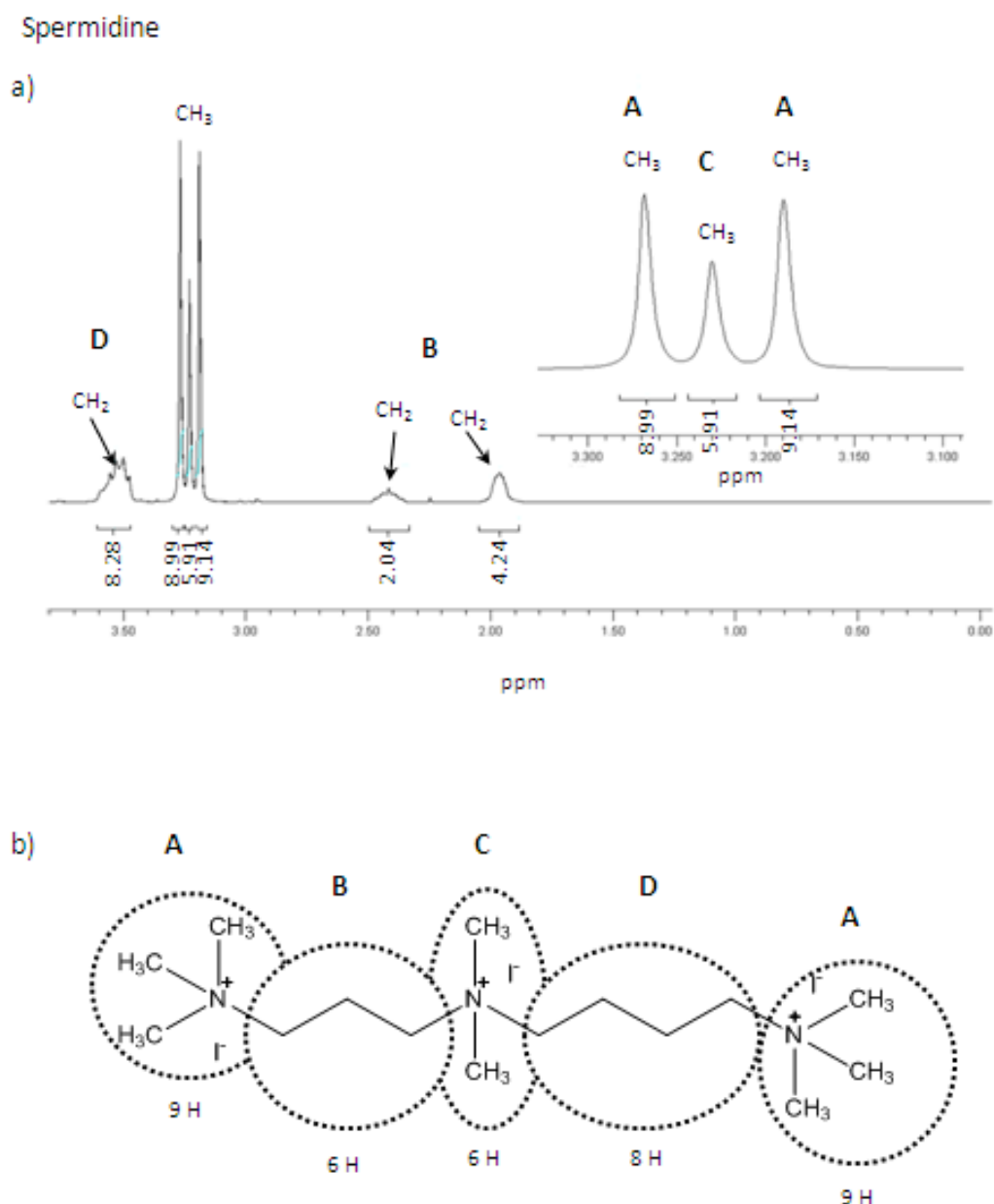


Figure 3. 10. Characterisation of quaternised spermidine. **a)** ^1H NMR (D_2O) spectrum of a stationary sample of quaternised spermidine. Capital letters from A-D correspond to the groups which are circled on the structure of quaternised spermidine (part b); **b)** structure of quaternised spermidine showing the number of hydrogen atoms associated with each carbon atom (e.g. 9 H) below the structure and capital letters from A-D which identify the groups which correspond to the peaks on the NMR spectrum.

Cadaverine

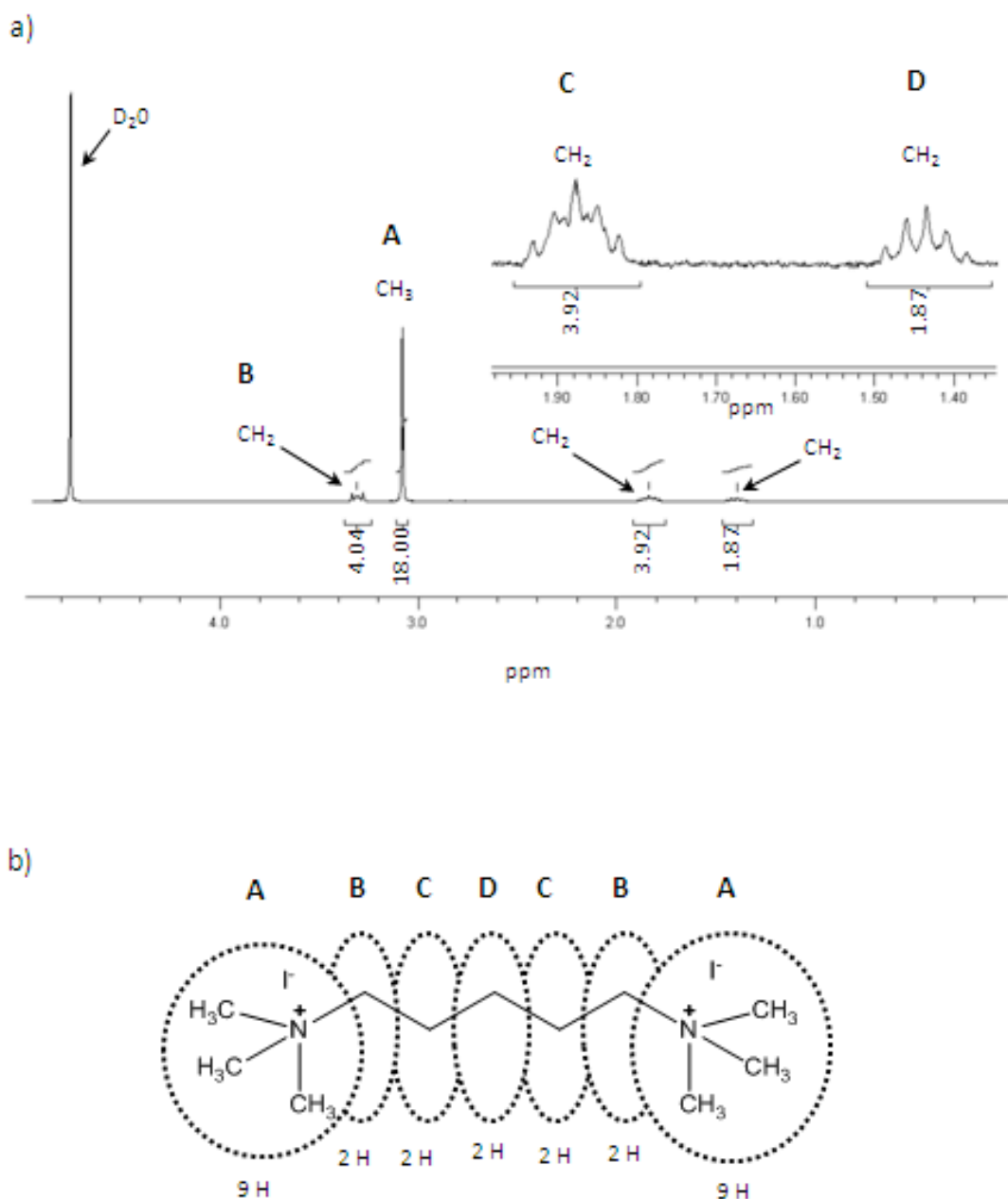


Figure 3. 11. Characterisation of quaternised cadaverine. **a)** ^1H NMR (D_2O) spectrum of a stationary sample of quaternised cadaverine. Capital letters from A-D correspond to the groups which are circled on the structure of quaternised cadaverine (part b); **b)** structure of quaternised cadaverine showing the number of hydrogen atoms associated with each carbon atom (e.g. 9 H) below the structure and capital letters from A-D which identify the groups which correspond to the peaks on the NMR spectrum.

Putrescine

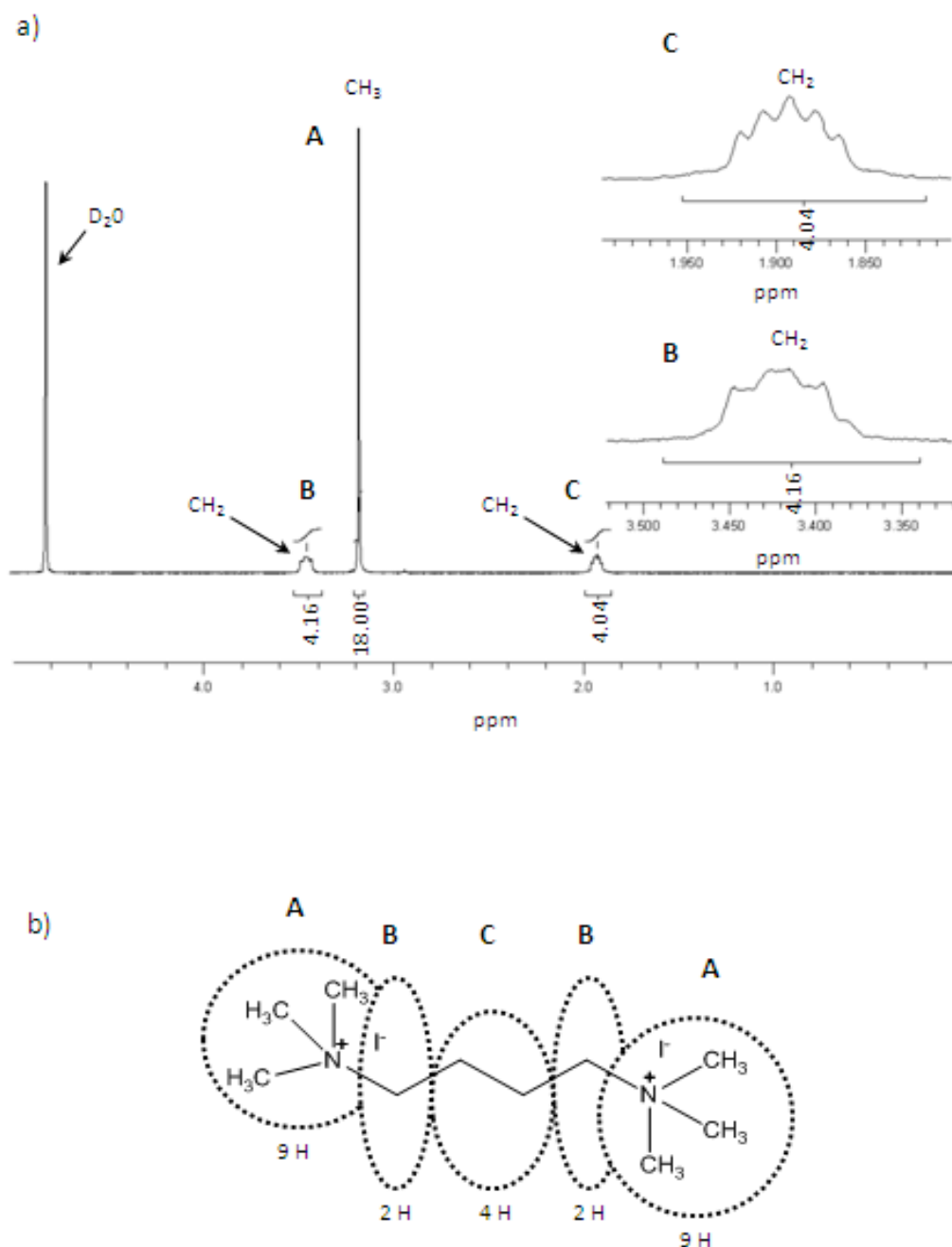


Figure 3. 12. Characterisation of quaternised putrescine. **a)** ^1H NMR (D_2O) spectrum of a stationary sample of quaternised putrescine. Capital letters from A-D correspond to the groups which are circled on the structure of quaternised putrescine (part b); **b)** structure of quaternised putrescine showing the number of hydrogen atoms associated with each carbon atom (e.g. 9 H) below the structure and capital letters from A-D which identify the groups which correspond to the peaks on the NMR spectrum.

The quaternised polyamines were tested to elucidate their potential inhibitory activity against biofilm growth. When quaternised, the pH remained constant at 7. The minimum biofilm inhibitory results, displayed in Table 3. 1 demonstrate that none of the quaternised polyamines inhibited the biofilm growth of any of the isolates tested.

Table 3. 1. The minimum biofilm inhibitory concentration of quaternised polyamines on *E. coli* K12, and clinical isolates of *K. pneumoniae* and *P. aeruginosa* biofilm formation grown for 18 hours at 37°C, analysed by the microtitre plate assay. The results are expressed as mM and mg/mL concentrations.

	Minimum biofilm inhibitory concentration		
	<i>E. coli</i> K12	<i>K. pneumoniae</i> clinical isolate	<i>P. aeruginosa</i> clinical isolate
Quaternised spermine	>10 mM >2 mg/mL	>10 mM >2 mg/mL	>10 mM >2 mg/mL
Quaternised spermidine	>10 mM >1.5 mg/mL	>10 mM >1.5 mg/mL	>10 mM >1.5 mg/mL
Quaternised cadaverine	>10 mM >1 mg/mL	>10 mM >1 mg/mL	>10 mM >1 mg/mL
Quaternised putrescine	>10 mM >0.9 mg/mL	>10 mM >0.9 mg/mL	>10 mM >0.9 mg/mL

3.3.3. The effect of buffered spermine on biofilm formation and planktonic growth on microtitre plates

Alongside testing the effect of quaternised polyamines on biofilm growth, polyamines were buffered in PBS. *E. coli* K12, and clinical isolates of *K. pneumoniae* and *P. aeruginosa* were grown on microtitre plates for 18 hours in the presence of buffered spermine with the pH adjusted to 7 to assess inhibition of biofilm growth (Figure 3. 13) and planktonic growth (Figure 3. 14) without the influence of an increase in pH. A higher concentration range of 0.1 mM to 200 mM spermine was used to determine the effects that concentrations greater than 10 mM had on bacterial growth, as this was the highest concentration tested previously.

Spermine started to inhibit biofilm growth at 80 mM. At this concentration biofilm growth was reduced to ~60% of the growth control for *E. coli* K12, ~90% for *K. pneumoniae* and ~60% for *P. aeruginosa* (Figure 3. 13). Planktonic growth was assessed to determine if spermine was able to reach the outer membrane proteins of cells that were not protected by the biofilm matrix. Planktonic growth was reduced to ~60-65% for both *E. coli* K12 and *P. aeruginosa* at 80 mM spermine. 80 mM and 100 mM spermine did not inhibit planktonic growth of *K. pneumoniae*; however 200 mM spermine reduced planktonic growth to ~40% (Figure 3. 14).

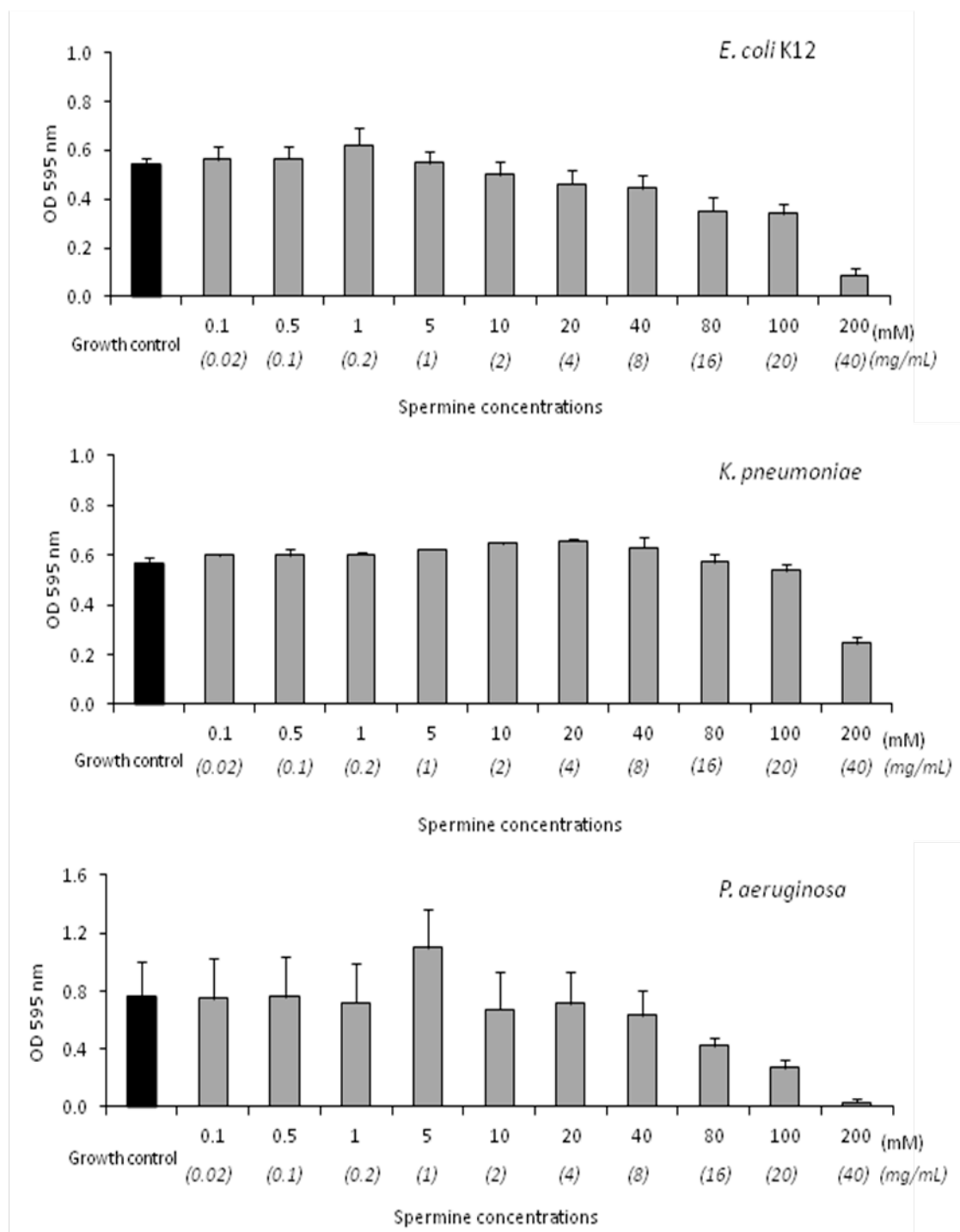


Figure 3. 13. The MIC assay to determine the effect of spermine with the pH adjusted to 7, against *E. coli* K12, and clinical isolates of *K. pneumoniae* and *P. aeruginosa* biofilm formation grown for 18 hours at 37°C and analysed by the microtitre plate biofilm formation assay. The results are expressed as the mean of 16 replicate wells involving two biological replicates for each strain. Error bars indicate the standard error of the mean.

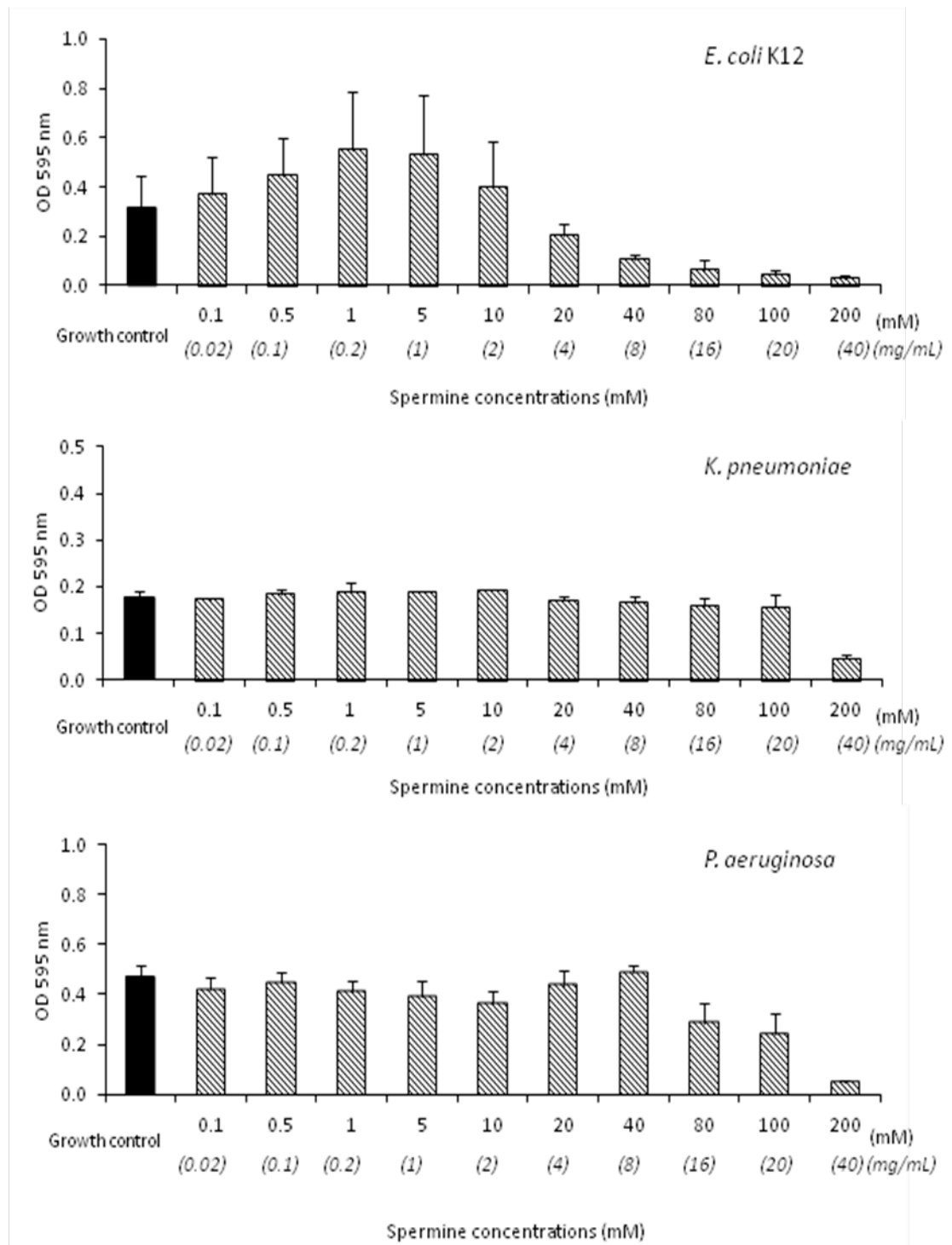


Figure 3. 14. The microtitre plate biofilm formation assay to determine the effect of spermine with the pH adjusted to 7, against *E. coli* K12, and clinical isolates of *K. pneumoniae* and *P. aeruginosa* biofilm cells grown for 18 hours at 37°C and analysed by the MIC assay. The results are expressed as the mean of 16 replicate wells involving two biological replicates for each strain. Error bars indicate the standard error of the mean.

3. 4. Western blot analysis of OprF

A previous study showed that OmpA is over-expressed in *E. coli* biofilms (Orme *et al.*, 2006). It was hypothesised that outer membrane protein F (OprF), an OmpA homologue in *P. aeruginosa*, would also be over-expressed in the biofilm phenotype. Alongside the assays to determine the antimicrobial activity of the polyamines, western blot analysis was performed to determine if OprF, a ~34 kDa protein, is over-expressed in the biofilm phenotype compared to the planktonic phenotype. This assay would therefore validate OmpA and its homologue, OprF, as potential targets for the inhibition of *P. aeruginosa* biofilm formation. In this experiment OprF expression in planktonic bacteria was compared to that in the biofilm phenotype. The western blot displayed in Figure 3. 15 showed that there was not a change in OprF protein expression between the biofilm and planktonic phenotypes suggesting that it may not be a suitable target for biofilm inhibition.

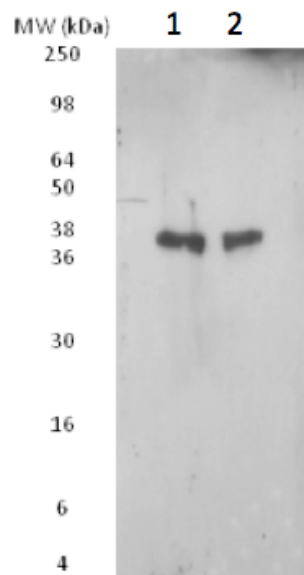


Figure 3. 15. Western blot analysis of OprF from *P. aeruginosa* probed with monoclonal antibody MA7-3. **Lane 1:** Biofilm grown for 18 hours on glass slides, static; **Lane 2:** Planktonic growth after 18 hours shaking. Both samples contained the same concentration of protein as determined by the Bradford assay. This western blot is a representation of a minimum of 3 biological replicates.

3. 5. Discussion

The work in this chapter was designed to determine if polyamines inhibit biofilm formation. Polyamines are known to interact with porins, and previous studies have demonstrated the importance of porins in biofilm formation (Barrios *et al.*, 2006; Orme *et al.*, 2006). Furthermore, a literature search did not reveal any previous studies on the interaction of extracellular polyamine on a population of cells in a biofilm, therefore to examine the effect of exogenous polyamine on biofilm growth is novel.

Polyamines at increasing concentrations have an increasing pH (Figure 3. 5 and Figure 3. 6). The experiments conducted with the polyamines not sufficiently buffered suggested that inhibition of biofilm formation occurred due to treatment with polyamines, particularly spermine. This effect was, however, most likely due to the non-specific action of a high pH environment. The polyamines were buffered with PBS to keep the pH constant at 7, after which, biofilm inhibition was not observed (Figure 3. 13). Alongside these experiments, the polyamines were quaternised to stabilise the pH and remove any inhibitory effect caused by an increase in pH. Biofilm inhibition was not seen with the quaternised polyamines against *E. coli* K12 and the clinical isolates of *K. pneumoniae* and *P. aeruginosa*. This further demonstrated that the inhibition observed with the polyamine solutions that were not buffered was mainly due to an increase in pH. Overall, this study did not result in complete bacterial inhibition with concentrations of up to 10 mM polyamine with the quaternised and buffered polyamines.

Polyamines are essential to all living cells. Due to their polycationic nature they are known to bind and stabilise negatively charged macromolecules, such as DNA and RNA and molecules involved in translation; they are therefore associated with cell growth (Schuber, 1989; Wortham *et al.*, 2007). Polyamines are also important in protecting DNA from free radicals by inactivating them thereby reducing oxidative stress. *P. mirabilis* mutants deficient in the polyamine putrescine have reduced growth and swarming (Wortham *et al.*, 2007). Polyamines are also essential for protecting the bacterial cell, for instance, when the bacterial cell is in an acidic environment, cadaverine synthesis is up-regulated as cadaverine neutralises external pH. Cadaverine therefore protects the cell from acidic conditions (Samartzidou & Delcour, 1999).

Studies have shown that extracellular polyamine may have a less potent effect on membrane protein function than endogenous periplasmic polyamine (Iyer & Delcour, 1997). Spermine is found at concentrations of approximately $\sim 10 \mu\text{M}$ - $30 \mu\text{M}$ in the eukaryotic cell. In the bacterial cell, spermidine concentrations can range from 0.05 mM - 10 mM , and up to 50 mM of cadaverine and putrescine (Iyer & Delcour, 1997). They are possibly present at considerably higher concentrations in the periplasmic space close to the cell envelope, between the inner and outer membranes, as this is where the enzymes required for their synthesis, and transporters required for their export, are present (Iyer & Delcour, 1997). The bacteria utilise this endogenous polyamine for growth and protection (Samartzidou & Delcour, 1999; Schuber, 1989; Wortham *et al.*, 2007). This may be the reason that concentrations lower than 10 mM for all the extracellular polyamines that were used in the assays of this study, did not inhibit biofilm growth (Figure 3. 13). For this reason, the effect of spermine on planktonic and biofilm growth was determined by increasing the concentration range up to 200 mM (Figure 3. 13 and Figure 3. 14). These higher concentrations are likely to be toxic to the epithelial cells of the urinary tract if used as a catheter coating; however it demonstrated that inhibition of bacterial growth by using a higher concentration range was more successful. An inhibitory effect was seen with spermine at 80 mM reducing *E. coli* K12 and *P. aeruginosa* biofilm growth to $\sim 60\%$ of the growth control. *K. pneumoniae* biofilm formation was not reduced to the same degree as the other bacteria at 80 mM and 200 mM spermine was required to reduce growth to $\sim 40\%$ (Figure 3. 13).

Although this study revealed that polyamines are not useful inhibitors of porin function and did not prevent biofilm formation by uropathogenic bacteria, it did allow for the optimisation of experimental conditions for the potential inhibitors that are described in Chapter 4.

Chapter 4

The effect of quaternary ammonium compounds on biofilm formation

The work described in this chapter appears in the publication:

Govindji, N., Wills, P., Upton, M., Tirelli, N. & Webb, M. (2013). The anti-biofilm effects of Byotrol™. *Journal of Applied Microbiology*, 114 (5) 1285-93.

4. 1. Quaternary ammonium compounds as biocides

Quaternary ammonium compounds (QACs) (also known as quaternary ammonium salts or quats), are polyatomic cations with varying and diverse structures that have a common chemical motif of a positively charged nitrogen atom covalently bonded to four alkyl groups (NR_4^+). The covalent bonding of the carbons to the nitrogen group means that they do not dissociate in acid-base reactions, and therefore offer the QAC a stable permanent positive ionic charge independent of the pH of the solution in which they may be (Walker, 2007). QACs are commercially available and routinely used as the active ingredient in many antimicrobial and sanitising products due to their wide spectrum of activity against bacteria, yeasts, viruses and fungi (Nohr & Macdonald, 1994).

4. 1. 1. QACs: mode of action

The QACs used in this study are membrane active surfactants with a broad spectrum activity. Cationically charged biocides adsorb to the cell envelope by ionic interactions with anionic membrane proteins, the lipopolysaccharides and the negatively charged phosphate head of the phospholipid bilayer of the outer membrane, they then permeabilise the outer membrane allowing diffusion to the cytoplasmic membrane (Ahlstrom, 1995; Gilbert, 1985; Ikeda *et al.*, 1984; Wortham *et al.*, 2007).

At high concentrations of QAC, the outer and cytoplasmic membranes are completely perturbed and the cell content is released (Ikeda *et al.*, 1984). This mode of action is similar to the action of most cationic detergents and is therefore relatively non-specific (Denyer, 1995). At MIC levels, the mode of action has more specific consequences: the antimicrobial integrates into the membrane and alters the phase-transition temperature. At physiological temperatures, the bacterial membrane is in a fluid phase, however with the interaction of QACs the membrane develops a liquid-crystalline structure and this results in a loss of physiological and osmoregulatory functions (Gilbert & Moore, 2005).

4.2. The susceptibility of bacterial growth to polyquaterniums

A group of QACs have been designated the term polyquaterniums (PQs) by the International Nomenclature for Cosmetic Ingredients (INCI). Polyquaterniums are polycationic polymers that have a QAC as an active part of their structure. They are commonly used in the cosmetic and domestic cleaning industry as stabilising agents and solution thickeners (Jachowicz *et al.*, 2008; Ribeiro *et al.*, 2004), however, some also have known antimicrobial properties. PQ-1, for example, is known to have antimicrobial and antifungal properties and is used as a sanitiser in contact lens solutions (Codling *et al.*, 2003a; Codling *et al.*, 2003b; Jones *et al.*, 2002).

A range of different PQs were tested against the uropathogenic organisms previously described. The details of each polyquaternium (PQ) are outlined in Table 4. 1. The commercial names of the compounds, as designated by the INCI, will be used throughout. The numbering of PQs is based on the order in which these PQs appear in the INCI's registry.

Table 4. 1. Nomenclature of polyquaternium compounds used in this study.

Commercial (INCI) name	Chemical name
Polyquaternium-4 (PQ-4)	Cellulose, 2-hydroxyethyl ether, polymer with <i>N,N</i> -dimethyl- <i>N</i> -2-propen-1-yl-2-propen-1-aminium chloride, graft (1:1)
Polyquaternium-6 (PQ-6)	Poly(diallyldimethyl ammonium) chloride
Polyquaternium-7 (PQ-7)	Poly(acrylamide- <i>co</i> -diallyldimethylammonium chloride)
Polyquaternium-10 (PQ-10)	Hydroxyethyl cellulose ethoxylate, quaternised
Polyquaternium-28 (PQ-28)	Poly(vinylpyrrolidone- <i>co</i> -methacrylamidopropyl trimethylammonium chloride)
Polyquaternium-37 (PQ-37)	Poly(2-dimethylamino)ethyl methacrylate methyl chloride

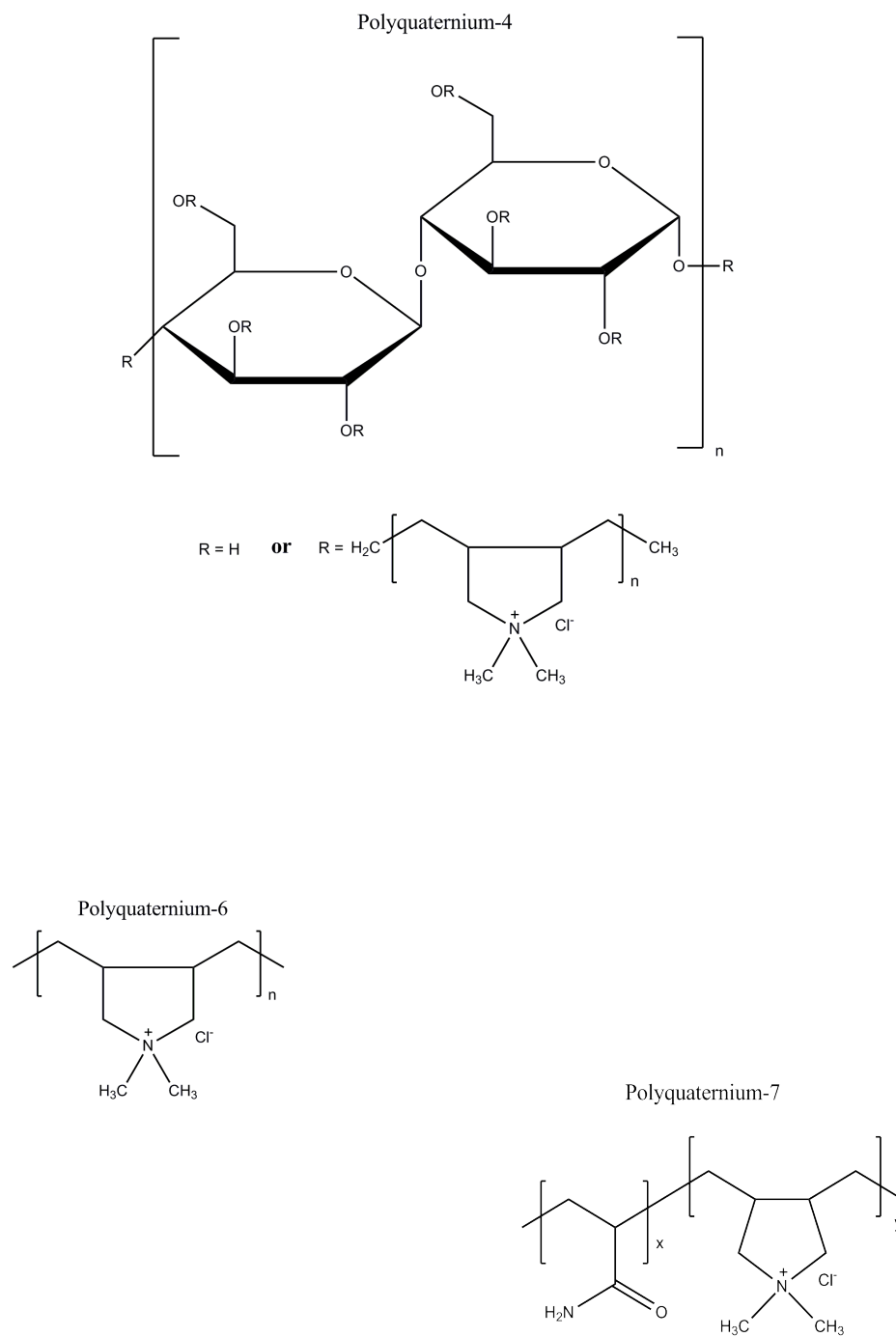


Figure 4. 1 a. Polyquaternium compounds used in this study.

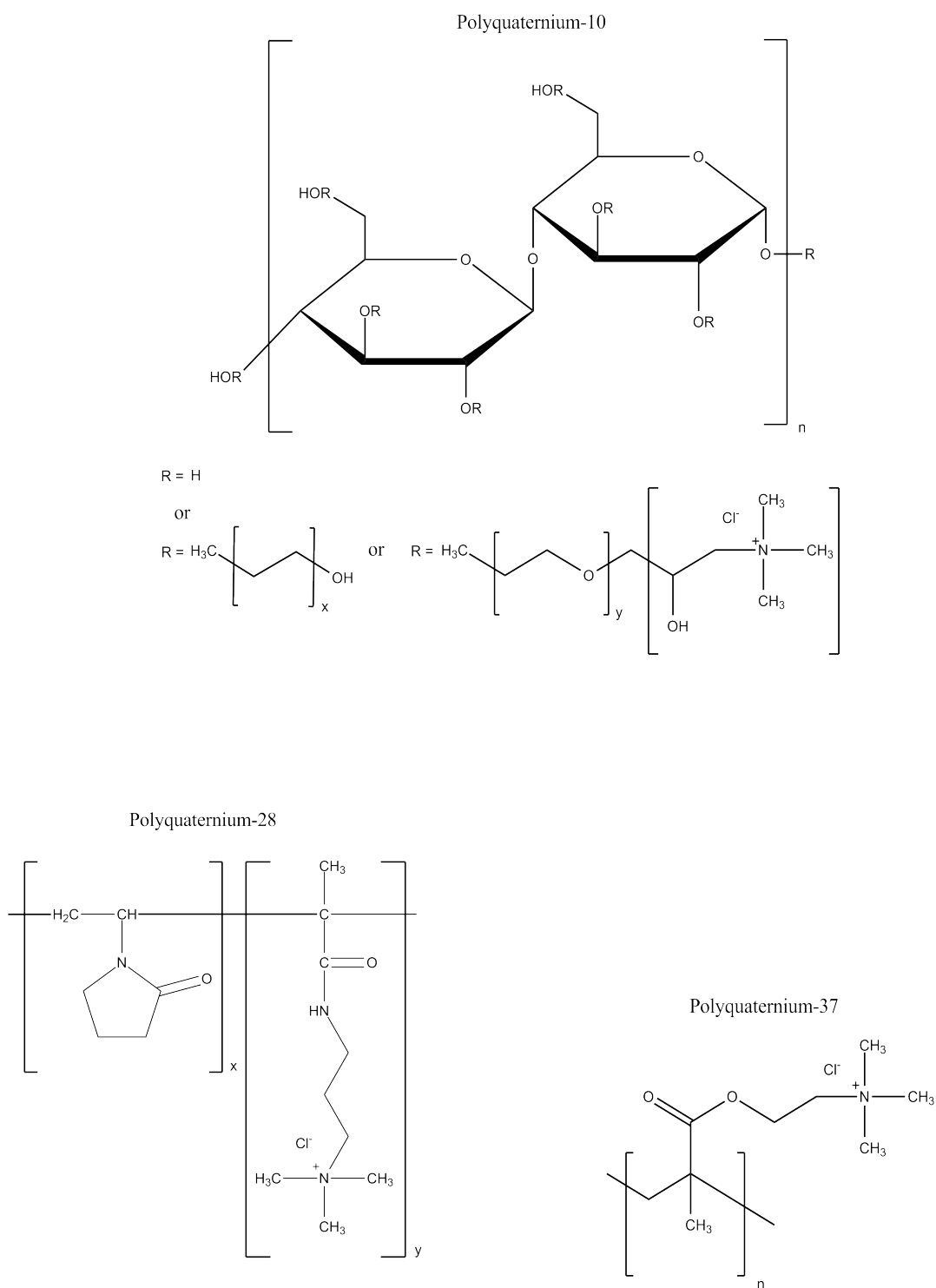


Figure 4. 2 b. Polyquaternium compounds used in this study (continued).

It is suggested in the literature that molecular weight is a significant factor in the antimicrobial activity of a quaternary ammonium compound (Engler *et al.*, 2011). Therefore the Mw of the compounds used in this study were determined by gel permeation chromatography size exclusion chromatography (SEC). The relevance of the size of these compounds will be evaluated in Section 4. 3.

Table 4. 2. Molecular weight (Mw) of polyquaternium compounds.

Polyquaternium	Molecular weight (Mw) (kDa)
Polyquaternium-4	460
Polyquaternium-6	12
Polyquaternium-6	38
Polyquaternium-6	400
Polyquaternium-10	750
Polyquaternium-28	990
Polyquaternium-37	1900

Alongside the PQs, the proprietary antimicrobial Byotrol™ was also tested against *E. coli* K12, and clinical isolates of *E. coli*, *K. pneumoniae* and *P. aeruginosa*. Byotrol™ contains a mixture of QACs (benzalkonium chloride and didecyl dimethyl ammonium chloride) and a polymeric biguanide (polyhexamethylene biguanide). A more in-depth introduction to Byotrol™ is given in Section 4. 4 where there is further analysis of this compound.

These compounds were added with the bacterial inoculum at 0 hours and incubated for 18 hours at 37°C. A summary showing the MIC and biofilm inhibitory concentrations of the polyquaterniums and Byotrol™ are presented in Table 4. 3 and Table 4. 4 respectively. Dose response data for planktonic and biofilm cells are shown in Figure 4. 3 to Figure 4. 16. All data represent the mean of over 24 replicates, involving a minimum of 3 biological replicates for each strain.

Table 4. 3. The minimum inhibitory concentration (MIC) of polyquaternium (PQ) compounds and Byotrol™ for the planktonic growth of *E. coli* K12 and the clinical isolates of *E. coli*, *K. pneumoniae* and *P. aeruginosa*.

	Minimum inhibitory concentration (MIC) (µg/mL)			
	<i>E. coli</i> K12	<i>E. coli</i> clinical isolate	<i>K. pneumoniae</i> clinical isolate	<i>P. aeruginosa</i> clinical isolate
PQ-4	2000	1000	>5000	5000
PQ-6*	15	15	30	30
PQ-7	5000	5000	5000	5000
PQ-10	5000	5000	5000	5000
PQ-28	>5000	>5000	>5000	>5000
PQ-37	>1000	>1000	>1000	>1000
Byotrol™	3	3	15	15

*PQ-6 is a 12 kDa compound.

Table 4. 4. The minimum biofilm inhibitory concentration of polyquaternium (PQ) compounds and Byotrol™ for the biofilm growth of *E. coli* K12 and the clinical isolates of *E. coli*, *K. pneumoniae* and *P. aeruginosa*.

	Minimum biofilm inhibitory concentration (µg/mL)			
	<i>E. coli</i> K12	<i>E. coli</i> clinical isolate	<i>K. pneumoniae</i> clinical isolate	<i>P. aeruginosa</i> clinical isolate
PQ-4	1000	1000	>5000	5000
PQ-6*	15	15	30	30
PQ-7	>5000	>5000	>5000	>5000
PQ-10	>5000	>5000	>5000	>5000
PQ-28	2000	5000	>5000	>5000
PQ-37	1000	>1000	>1000	>1000
Byotrol™	3	5	15	30

*PQ-6 is a 12 kDa compound.

It is clear from the results presented in Table 4. 3 and Table 4. 4 that as the molecular weight increased, the antimicrobial activity of the compounds decreased. The compounds with the most inhibitory action were Polyquaternium-6 (PQ-6) and Byotrol™. Interestingly, Polyquaternium-7 (PQ-7), which is a copolymer with repeating units of PQ-6 and acrylamide, had an MIC of greater than 5 mg/mL and also did not inhibit biofilm formation at the same concentration (Table 4. 3). PQ-7 consists of the relatively antimicrobial PQ-6 as one of its monomer units (Figure 4. 1 a), however when PQ-6 is co-polymerised with acrylamide to make PQ-7, it has a reduced antimicrobial effect than PQ-6 alone.

The MIC and minimum biofilm inhibitory concentrations were greater than 1 mg/mL for the other polyquaternium compounds tested and were therefore not considered to be active as antimicrobials. The dose response results for each of these compounds against the planktonic and biofilm growth of each organism used in this study are shown in Figure 4. 3 to Figure 4. 16.

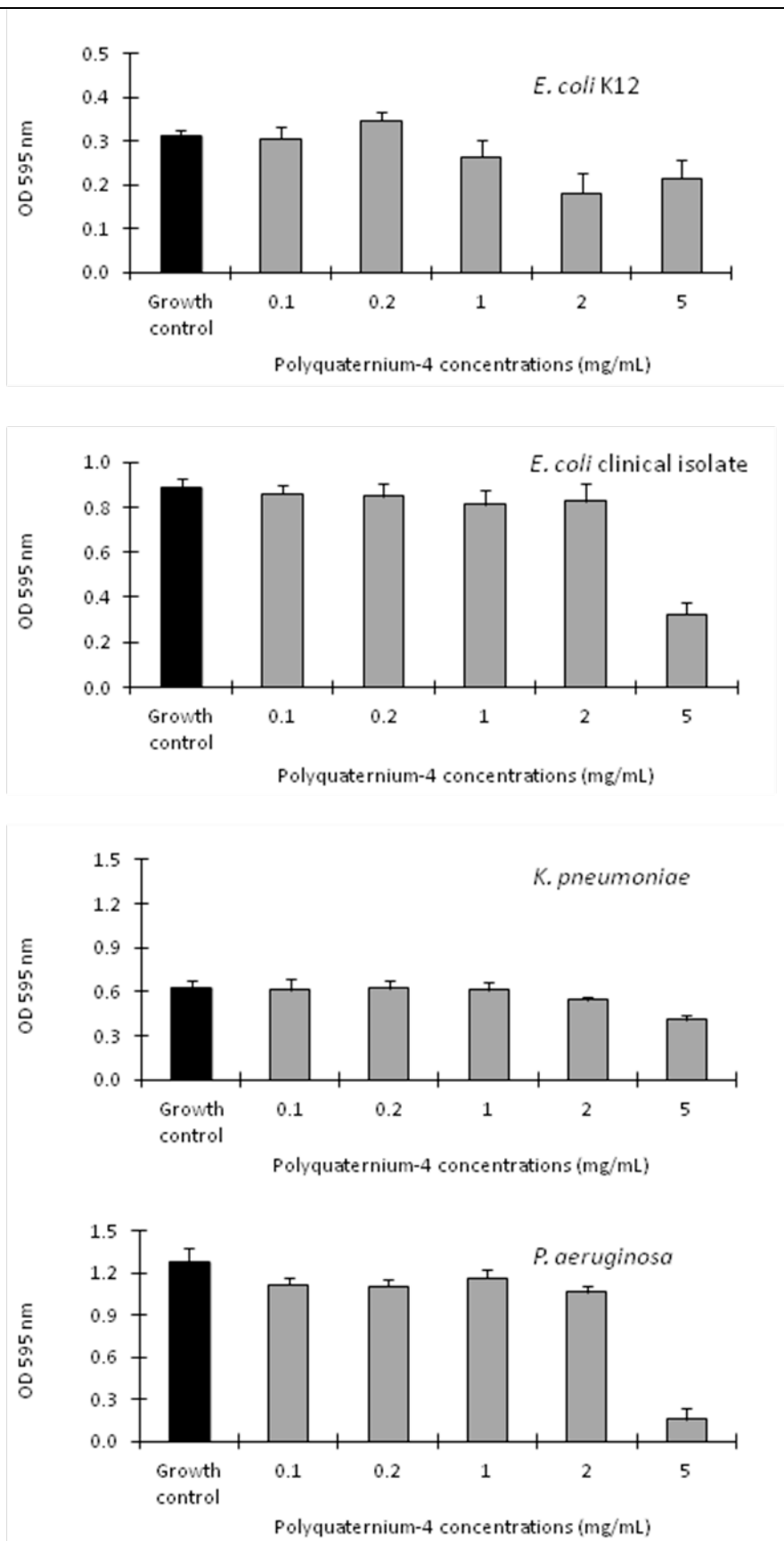


Figure 4. 3. The dose response of Polyquaternium-4 against the planktonic cells of *E. coli* K12 and clinical isolates of *E. coli*, *K. pneumoniae* and *P. aeruginosa*, grown for 18 hours.

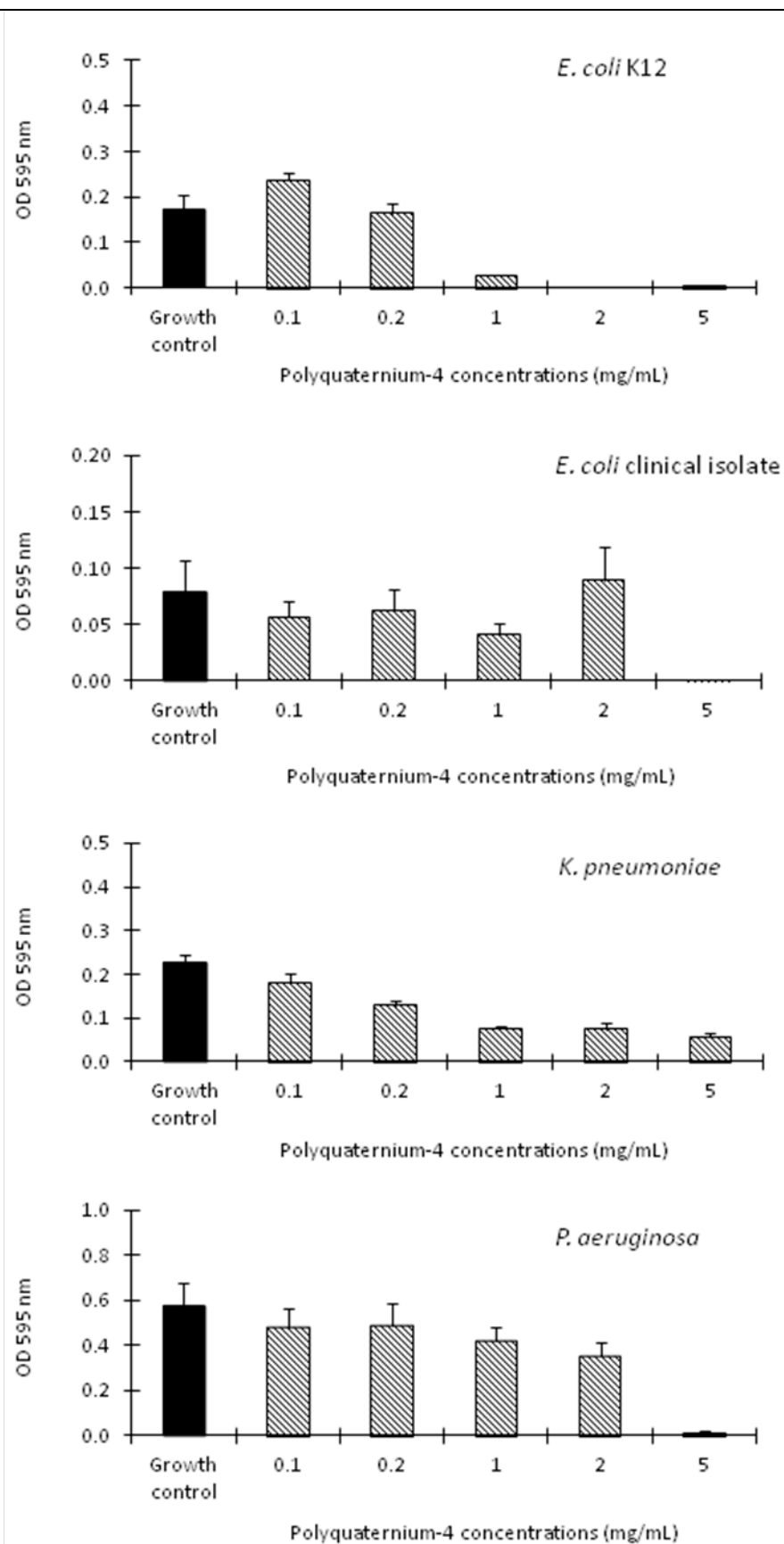


Figure 4. 4. The dose response of Polyquaternium-4 against the biofilm cells of *E. coli* K12 and clinical isolates of *E. coli*, *K. pneumoniae* and *P. aeruginosa*, grown for 18 hours.

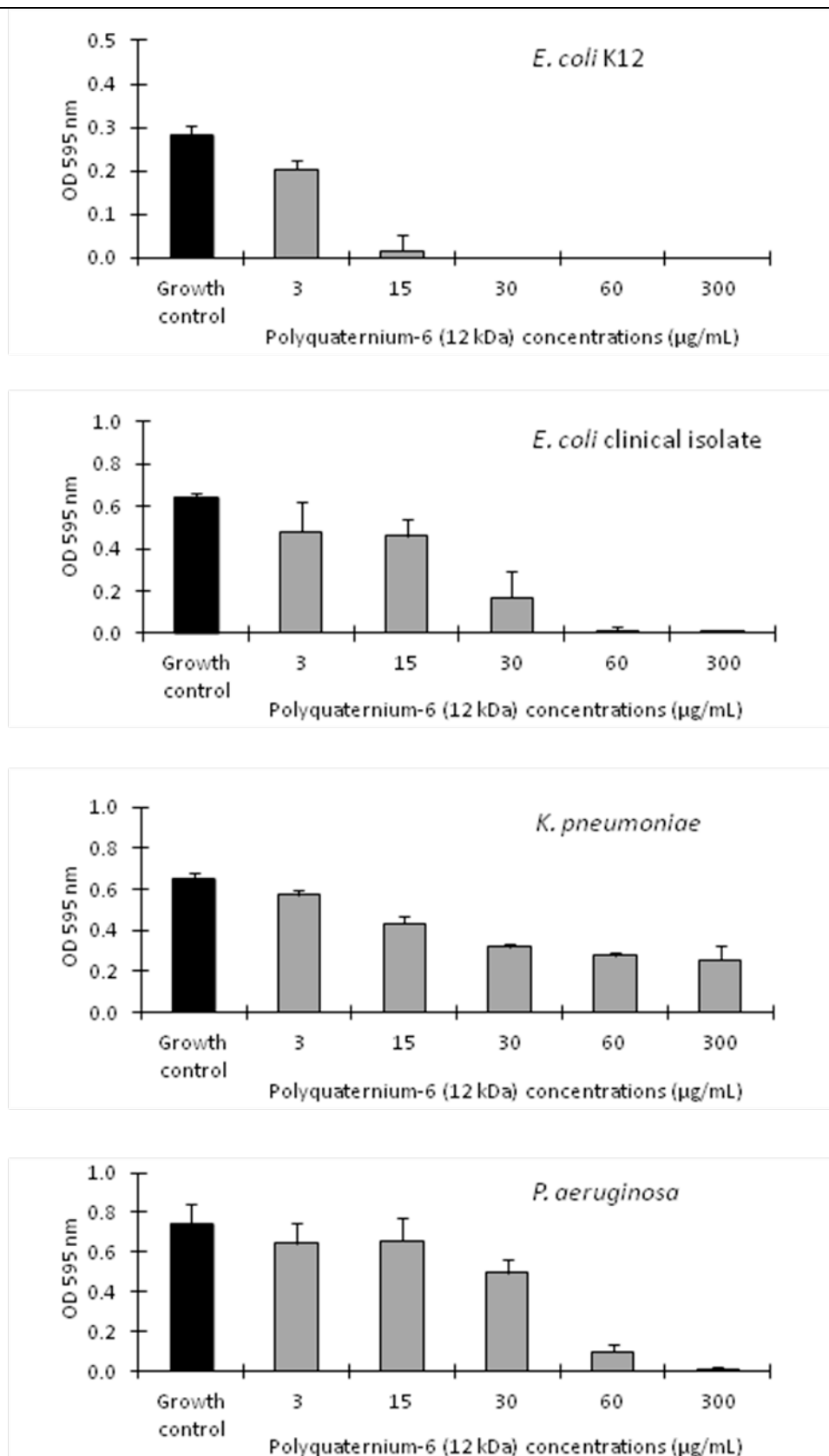


Figure 4. 5. The dose response of Polyquaternium-6 (12 kDa) against the planktonic cells of *E. coli* K12 and clinical isolates of *E. coli*, *K. pneumoniae* and *P. aeruginosa*, grown for 18 hours.

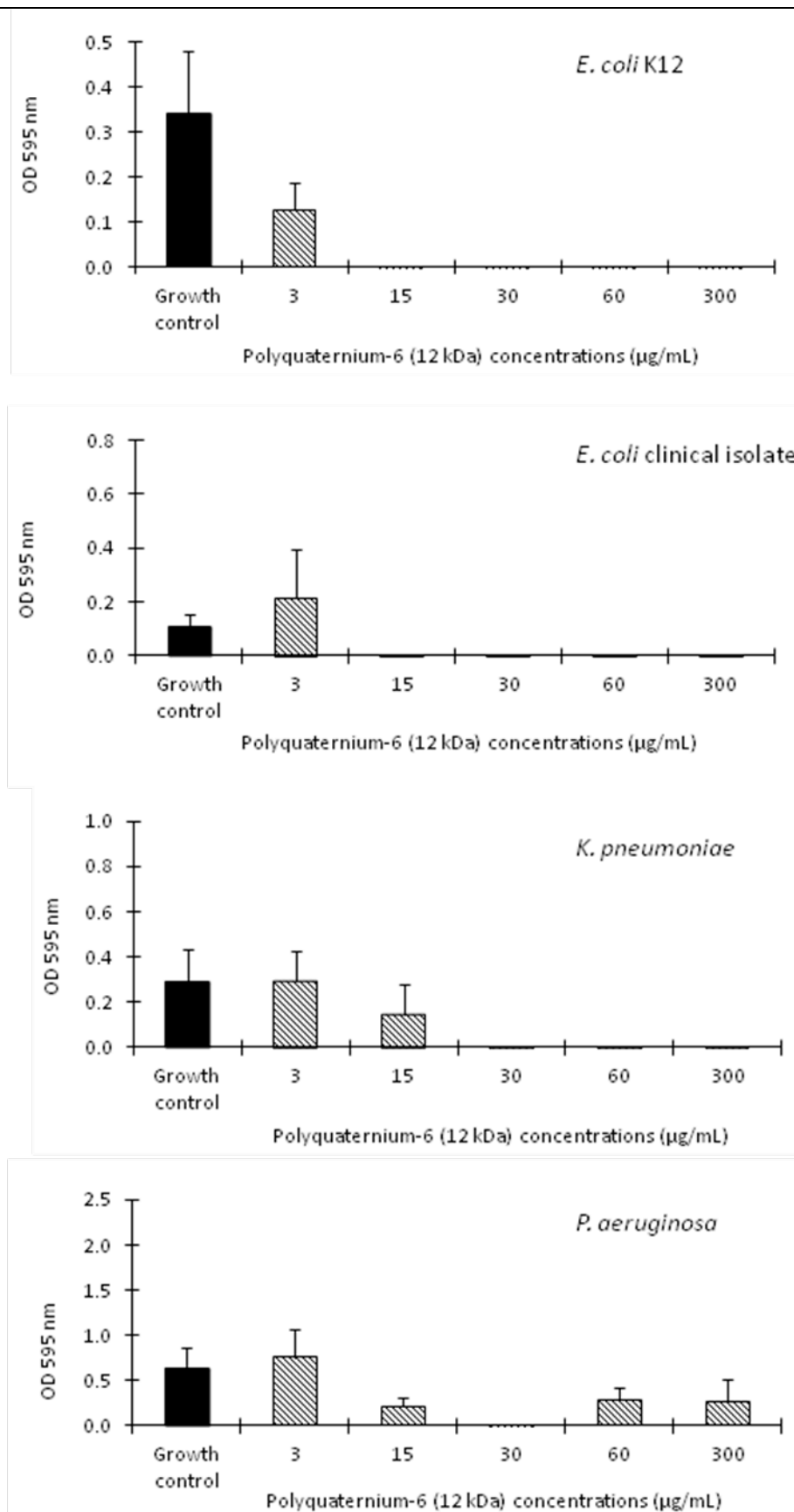


Figure 4. 6. The dose response of Polyquaternium-6 (12 kDa) against the biofilm cells of *E. coli* K12 and clinical isolates of *E. coli*, *K. pneumoniae* and *P. aeruginosa*, grown for 18 hours.

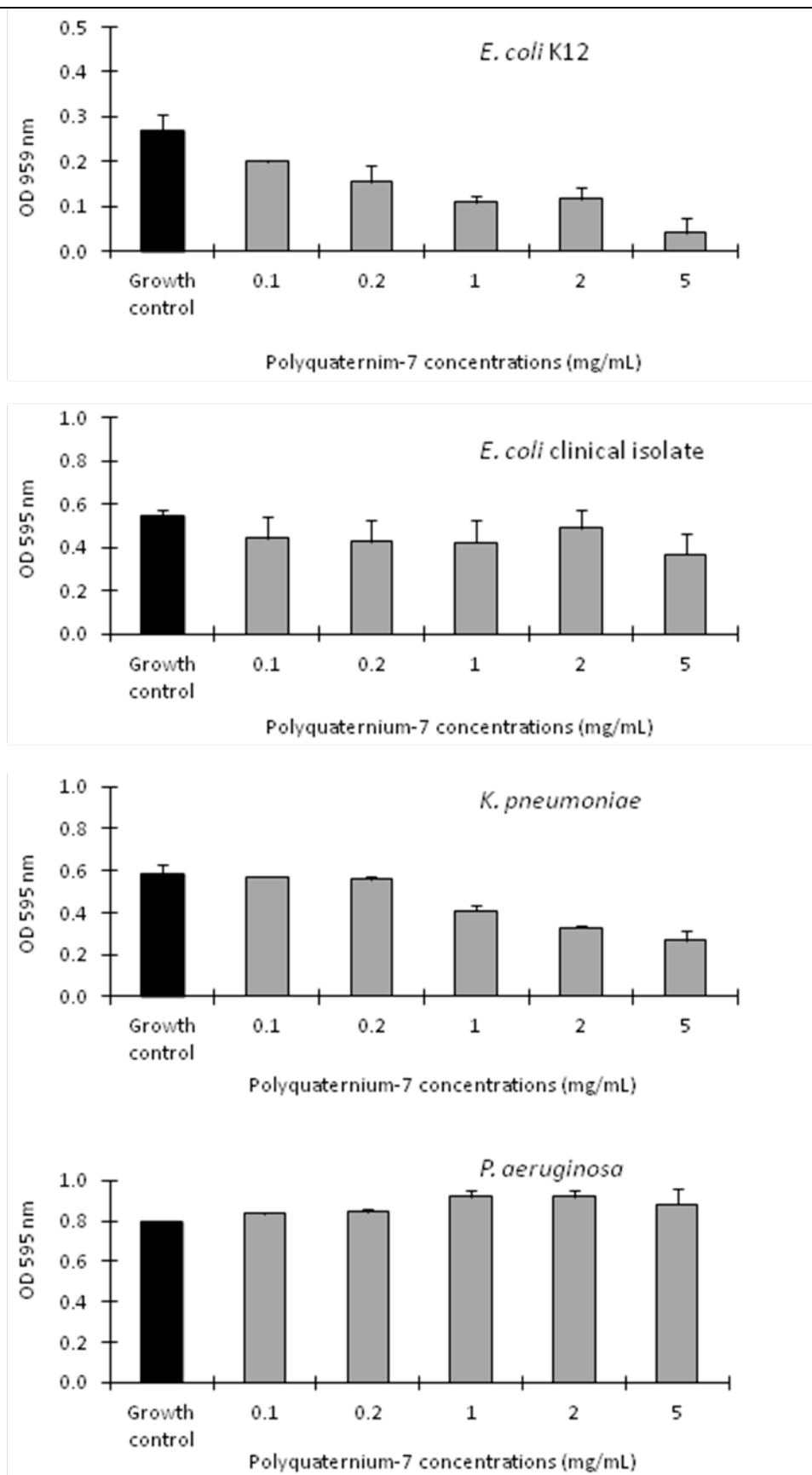


Figure 4. 7. The dose response of Polyquaternium-7 against the planktonic cells of *E. coli* K12 and clinical isolates of *E. coli*, *K. pneumoniae* and *P. aeruginosa*, grown for 18 hours.

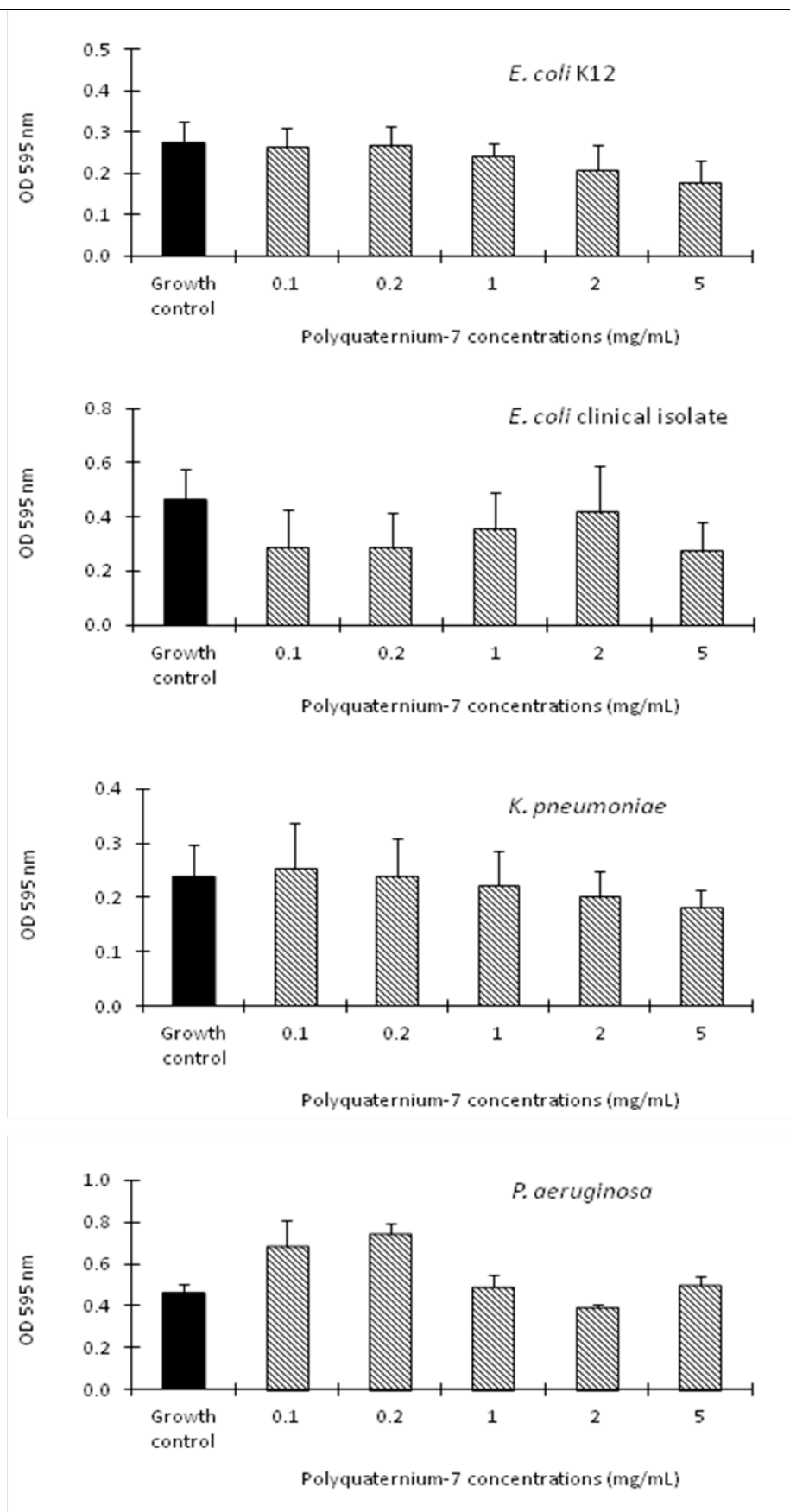


Figure 4. 8. The dose response of Polyquaternium-7 against the biofilm cells of *E. coli* K12 and clinical isolates of *E. coli*, *K. pneumoniae* and *P. aeruginosa*, grown for 18 hours.

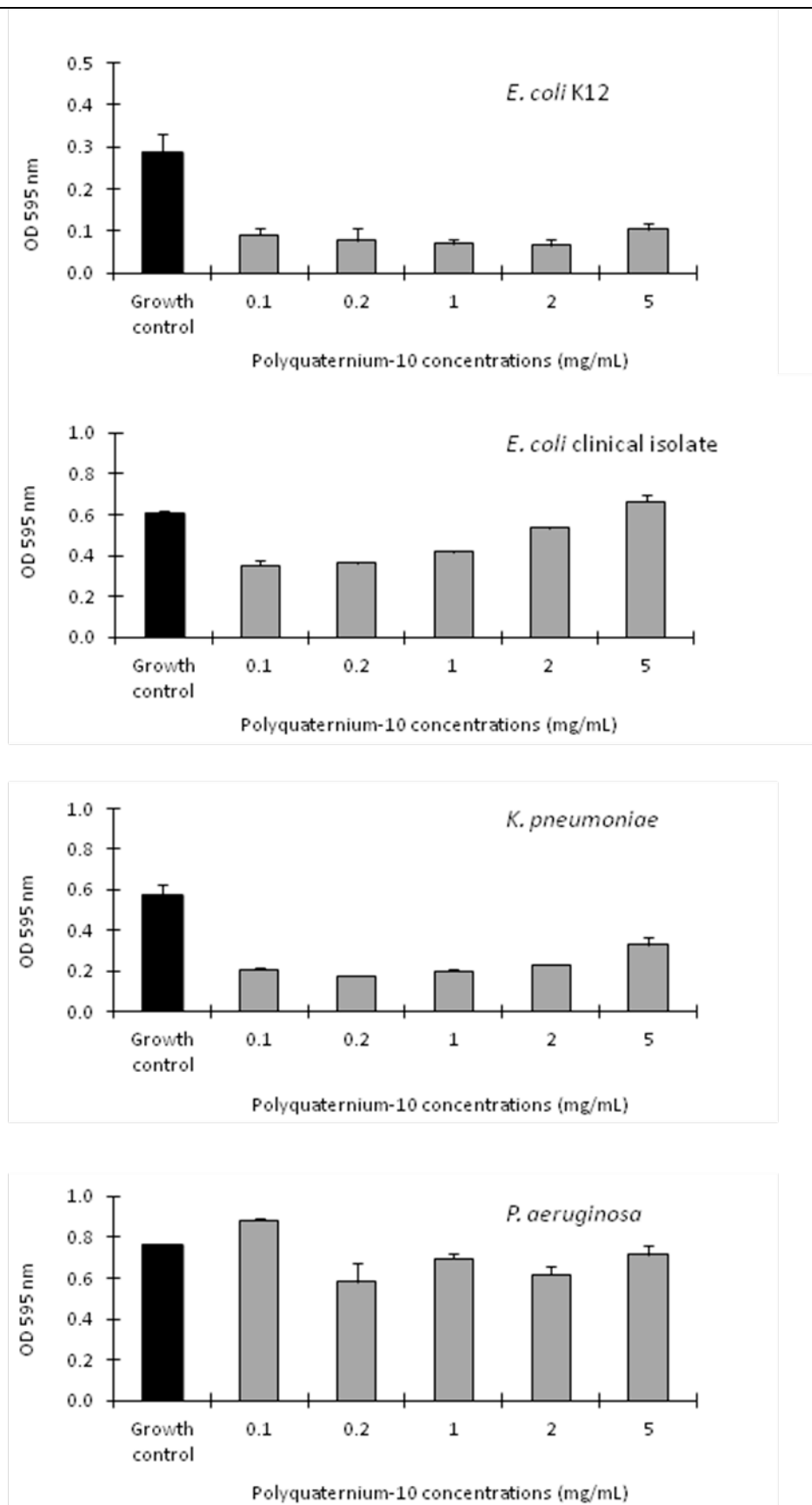


Figure 4. 9. The dose response of Polyquaternium-10 against the planktonic cells of *E. coli* K12 and clinical isolates of *E. coli*, *K. pneumoniae* and *P. aeruginosa*, grown for 18 hours.

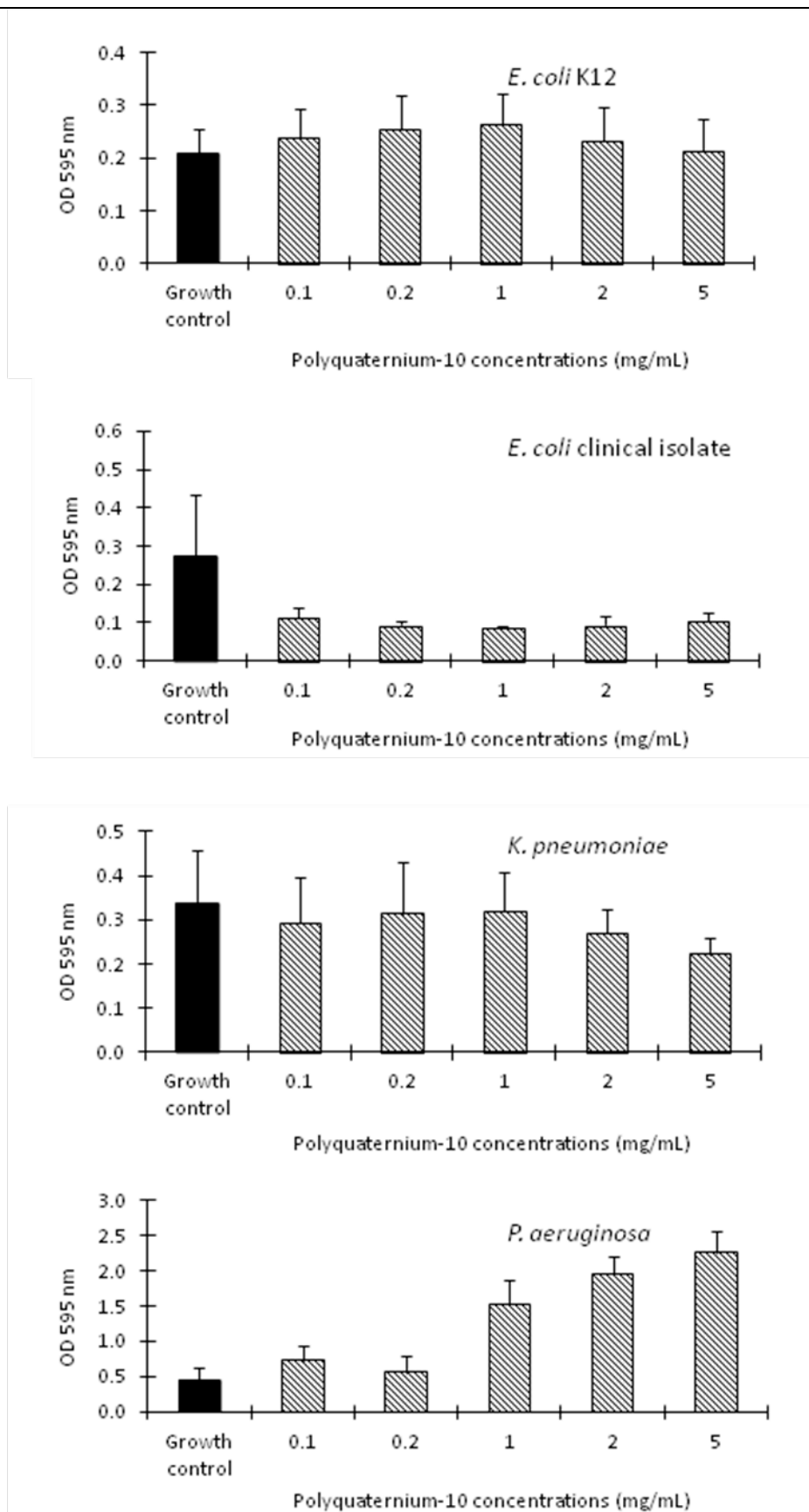


Figure 4. 10. The dose response of Polyquaternium-10 against the biofilm cells of *E. coli* K12 and clinical isolates of *E. coli*, *K. pneumoniae* and *P. aeruginosa*, grown for 18 hours.

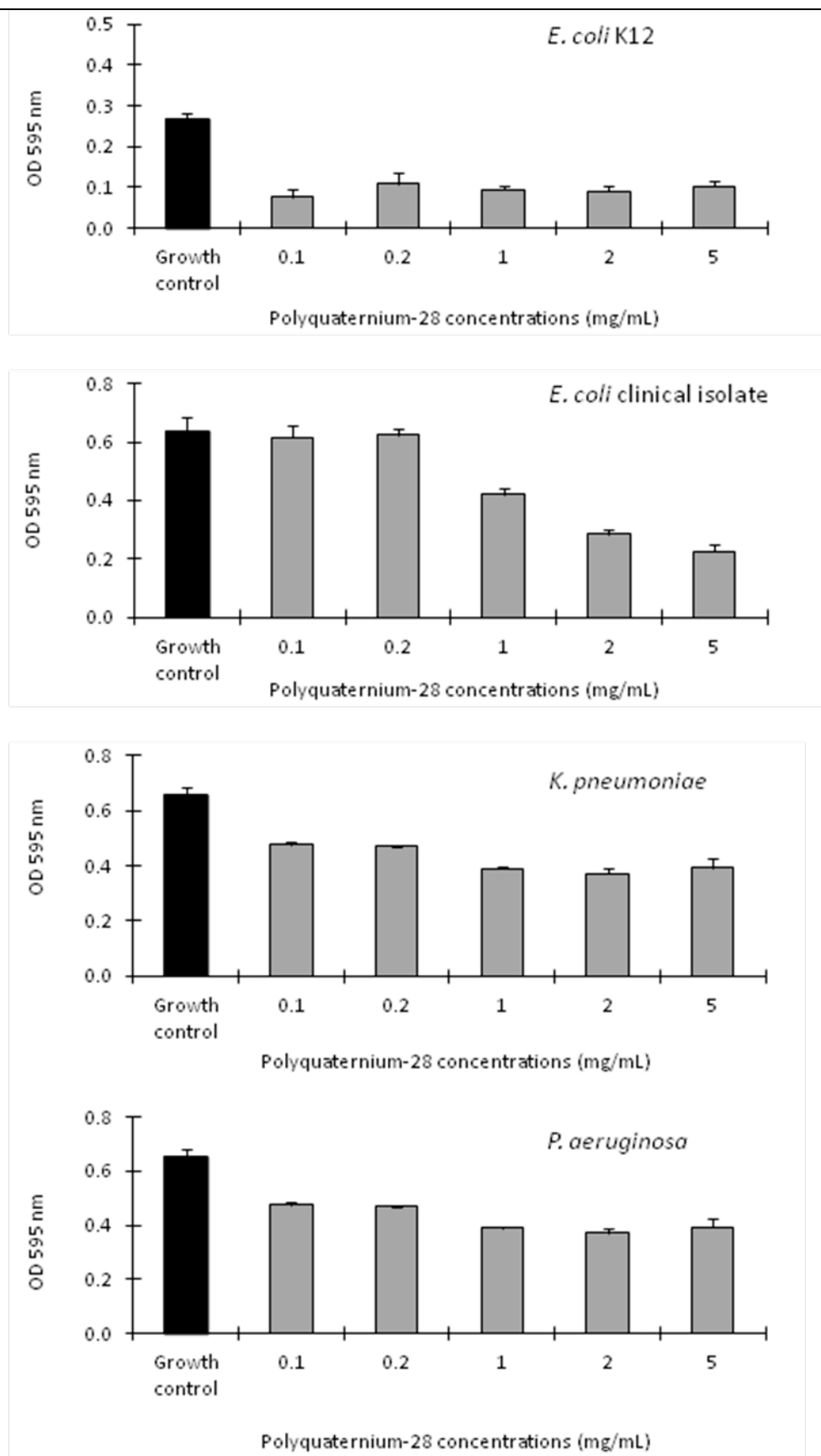


Figure 4. 11. The dose response of Polyquaternium-28 against the planktonic cells of *E. coli* K12 and clinical isolates of *E. coli*, *K. pneumoniae* and *P. aeruginosa*, grown for 18 hours.

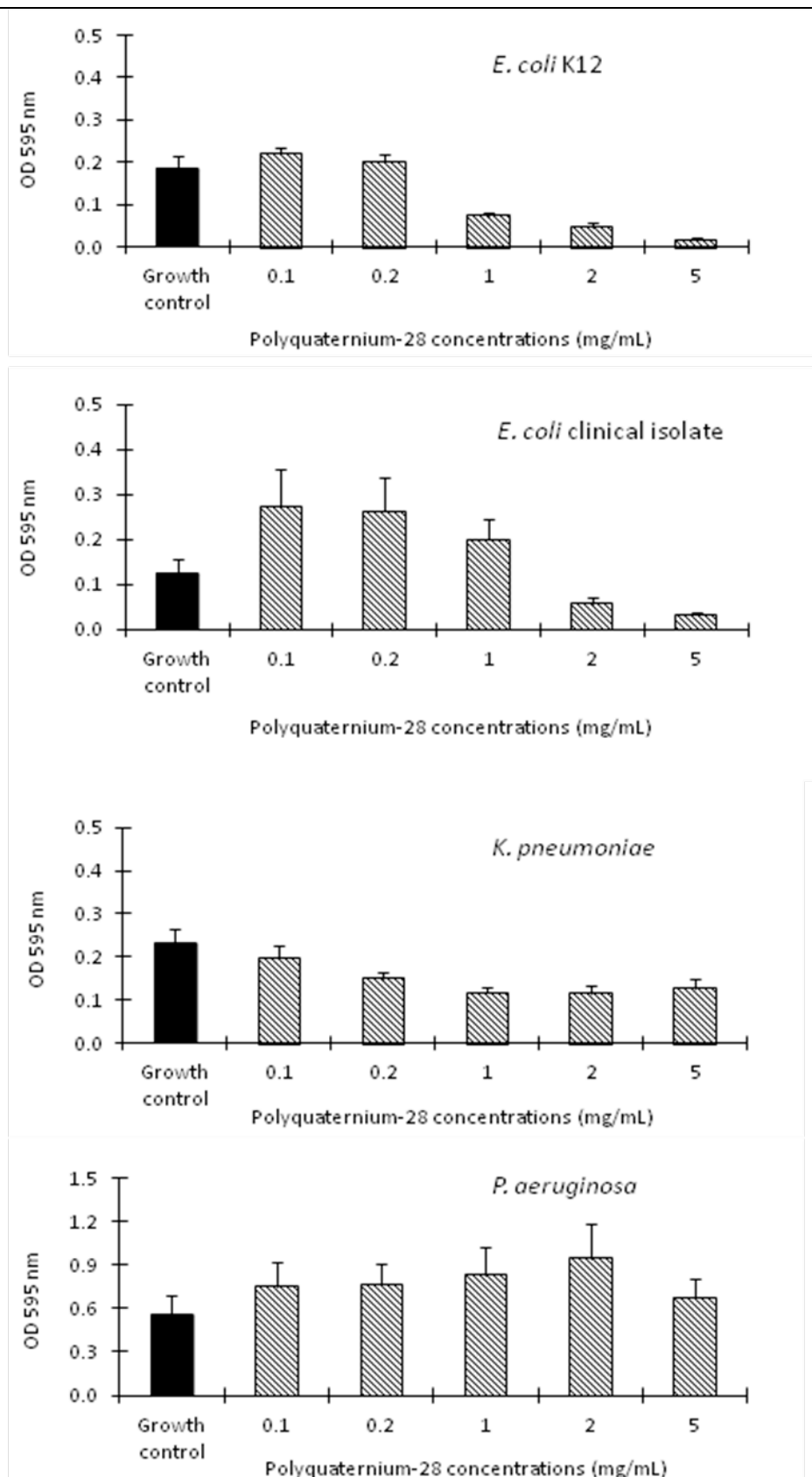


Figure 4. 12. The dose response of Polyquaternium-28 against the biofilm cells of *E. coli* K12 and clinical isolates of *E. coli*, *K. pneumoniae* and *P. aeruginosa*, grown for 18 hours.

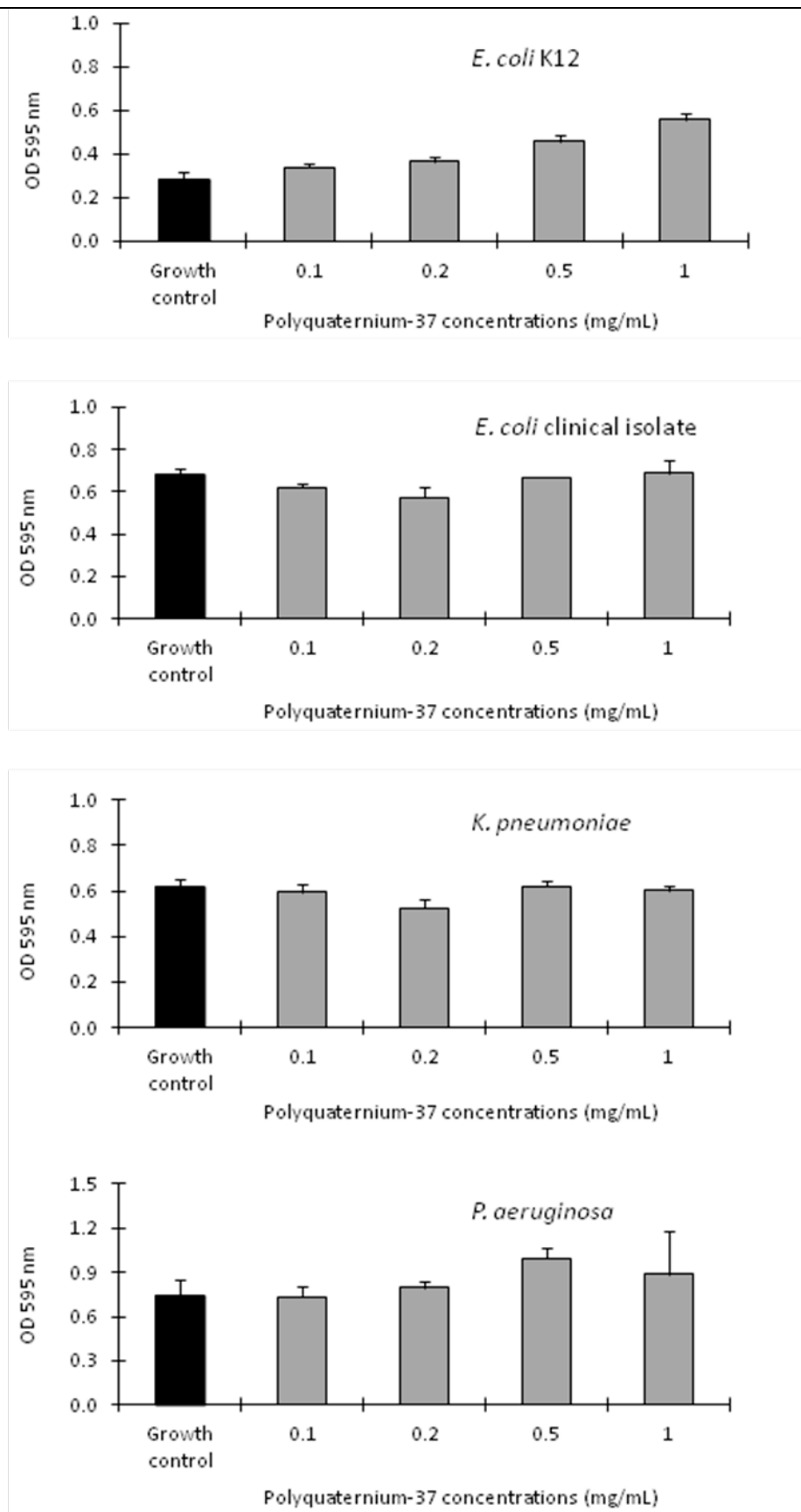


Figure 4. 13. The dose response of Polyquaternium-37 against the planktonic cells of *E. coli* K12 and clinical isolates of *E. coli*, *K. pneumoniae* and *P. aeruginosa*, grown for 18 hours.

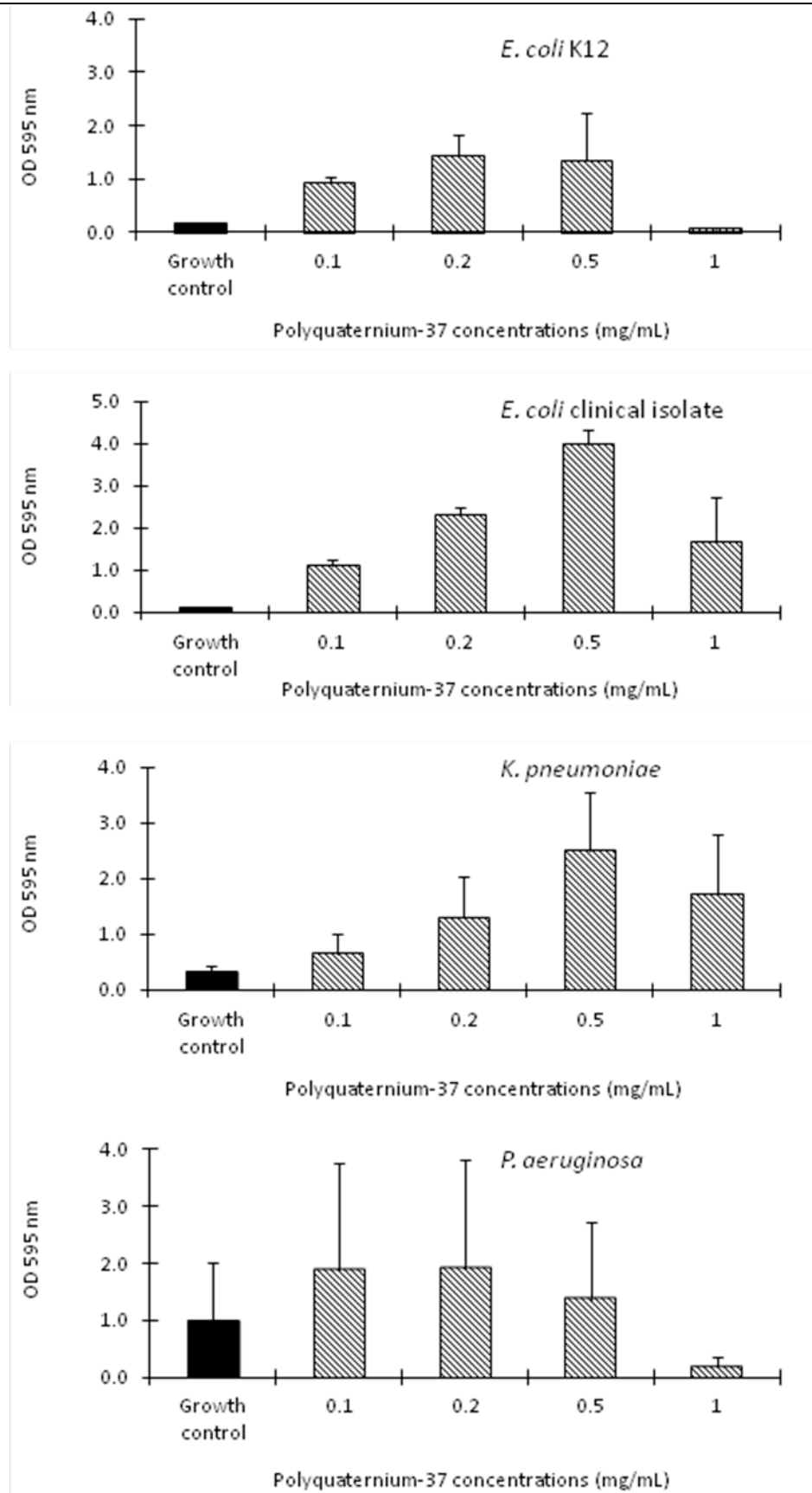


Figure 4. 14. The dose response of Polyquaternium-37 against the planktonic cells of *E. coli* K12 and clinical isolates of *E. coli*, *K. pneumoniae* and *P. aeruginosa*, grown for 18 hours.

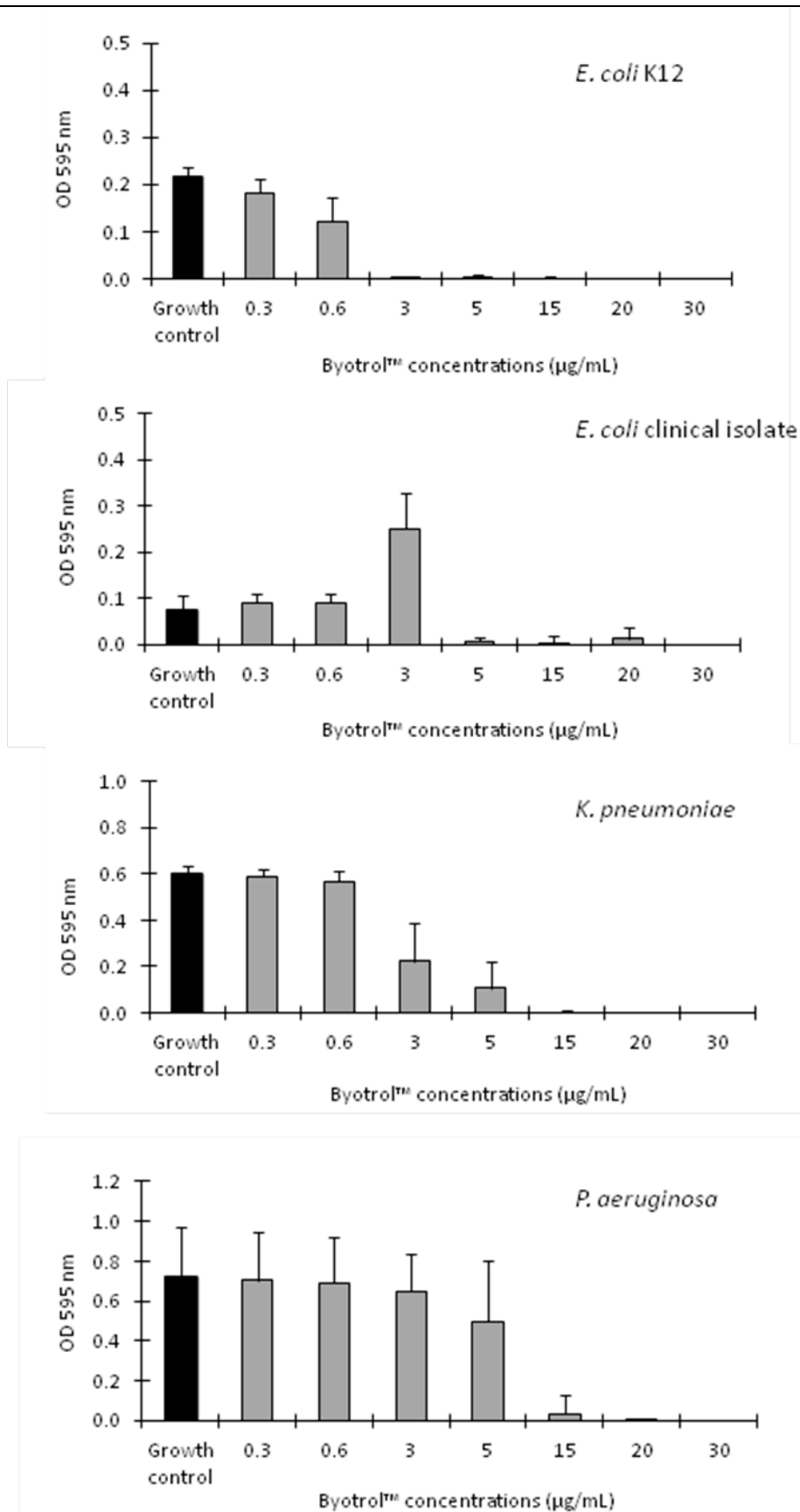


Figure 4.15. The dose response of Byotrol™ against the planktonic cells of *E. coli* K12 and clinical isolates of *E. coli*, *K. pneumoniae* and *P. aeruginosa*, grown for 18 hours.

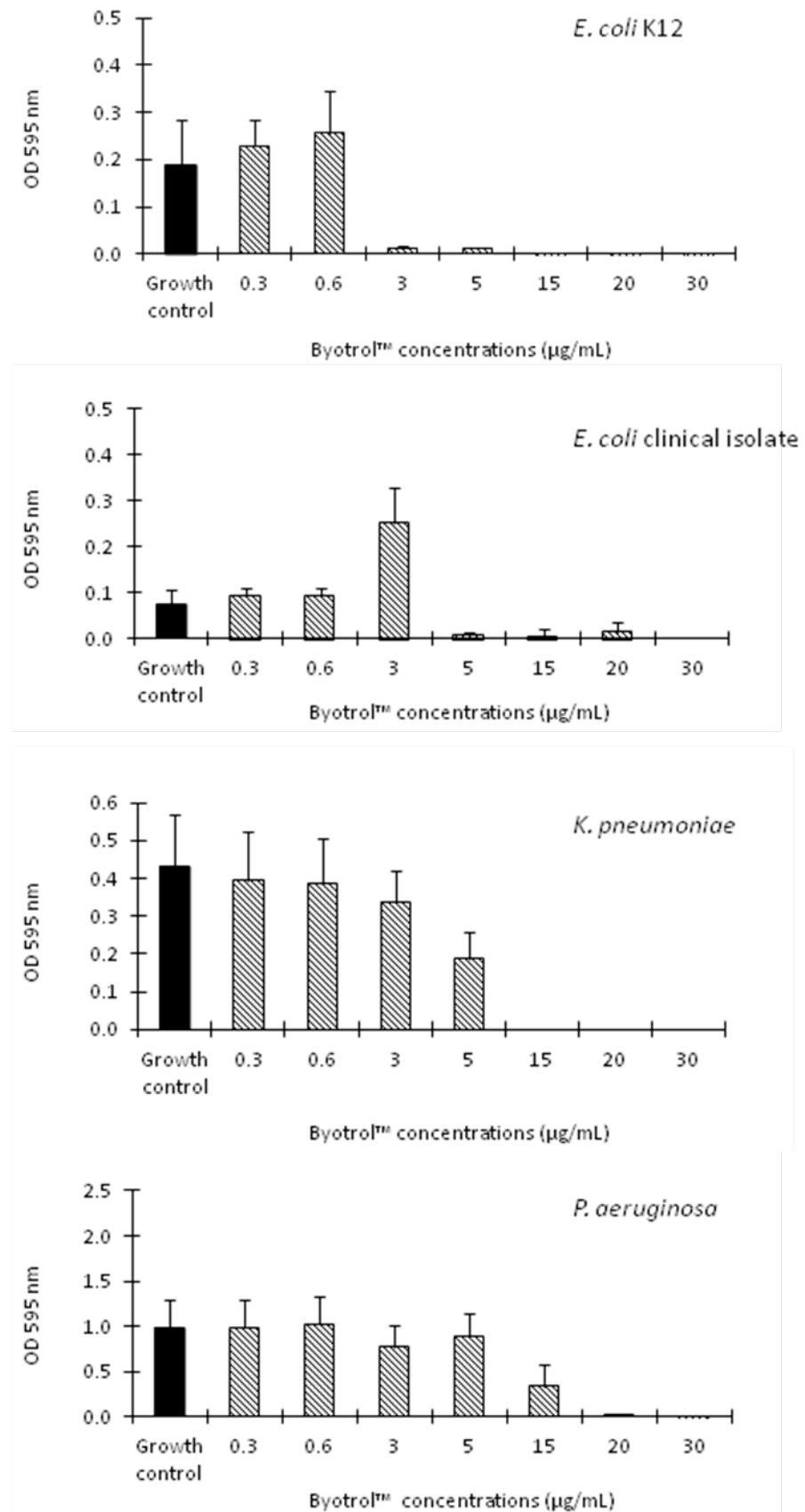


Figure 4. 16. The dose response of Byotrol™ against the biofilm cells of *E. coli* K12 and clinical isolates of *E. coli*, *K. pneumoniae* and *P. aeruginosa*, grown for 18 hours.

4.3. The susceptibility of bacteria to Polyquaternium-6 (PQ-6)

As PQ-6 (12 kDa) demonstrated the most antimicrobial activity of the polyquaternium compounds tested in this study, this was studied in more detail. There is evidence to suggest that increasing molecular weights may alter the antimicrobial effect of a polyquaternium (Engler *et al.*, 2011). To determine the effect of increasing molecular weights on bacterial growth, a range of molecular weights of PQ-6 were synthesised by Peter Wills at the Organic Material Innovation Centre (OMIC), University of Manchester. The 3 molecular weights of PQ-6 tested were 12 kDa, 38 kDa, and 400 kDa. Increasing concentrations of PQ-6 were tested against the bacterial isolates used in this study which were grown under static conditions at 37°C for 18 hours. The results, summarised in Table 4. 5 and Table 4. 6 show that as the molecular weight increased, the antimicrobial effect decreased. The dose response results for PQ-6 (12 kDa) against planktonic growth and biofilm growth are shown in Figure 4. 5 and Figure 4. 6; and for PQ-6 (38 kDa) and PQ-6 (400 kDa) in Figure 4. 17 to Figure 4. 20.

To confirm the inhibitory effects observed for PQ-6 (12 kDa), viable cell counts and bright-field microscopy were performed. The viable cell counts (Figure 4. 21) validate the MIC results (Table 4. 3) for the planktonic phenotype of bacteria treated with PQ-6 (12 kDa). The microscopy results (Figure 4. 22) also validate the minimum biofilm inhibitory concentration (Table 4. 4) results for the biofilm phenotype of bacteria grown treated with PQ-6 (12 kDa). The viable cell counts and bright field microscopy results correlate with the MIC and biofilm inhibition trend of inhibition demonstrated with PQ-6 (12 kDa).

Table 4. 5. The minimum inhibitory concentration of increasing molecular weights of Polyquaternium-6 (PQ-6) compounds for the planktonic growth of *E. coli* K12 and the clinical isolates of *E. coli*, *K. pneumoniae* and *P. aeruginosa*.

	Minimum inhibitory concentration (MIC) ($\mu\text{g/mL}$)			
	<i>E. coli</i> K12	<i>E. coli</i> clinical isolate	<i>K. pneumoniae</i> clinical isolate	<i>P. aeruginosa</i> clinical isolate
PQ-6 12 kDa	15	15	30	30
PQ-6 38 kDa	20	20	20	20
PQ-6 400 kDa	20	50	50	100

Table 4. 6. The minimum biofilm inhibitory concentration of increasing molecular weights of Polyquaternium-6 (PQ-6) compounds for the planktonic growth of *E. coli* K12 and the clinical isolates of *E. coli*, *K. pneumoniae* and *P. aeruginosa*.

	Minimum biofilm inhibitory concentration ($\mu\text{g/mL}$)			
	<i>E. coli</i> K12	<i>E. coli</i> clinical isolate	<i>K. pneumoniae</i> clinical isolate	<i>P. aeruginosa</i> clinical isolate
PQ-6 12 kDa	15	15	30	30
PQ-6 38 kDa	20	30	200	60
PQ-6 400 kDa	20	100	400	100

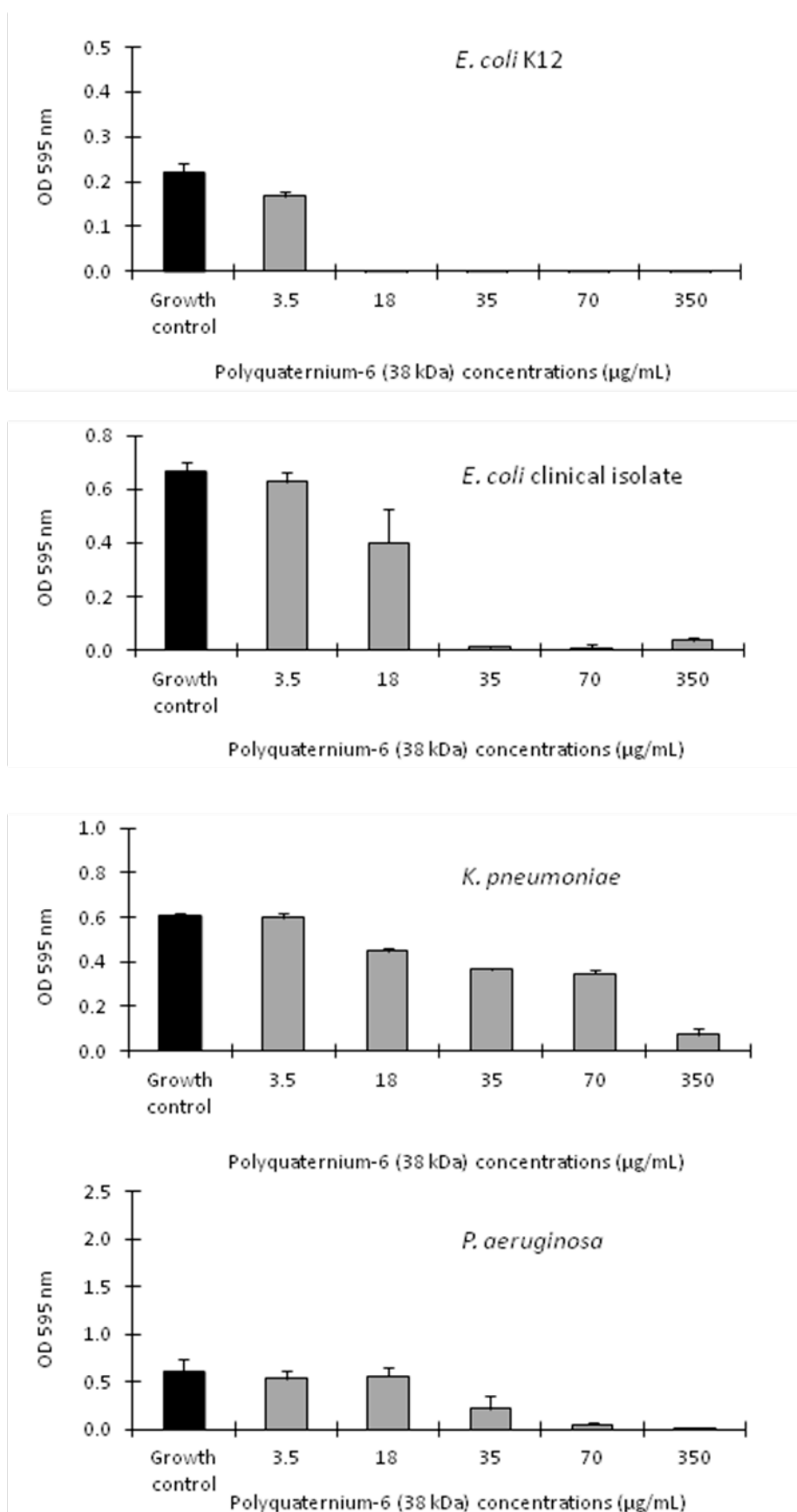


Figure 4. 17. The dose response of Polyquaternium-6 (38 kDa) against the planktonic cells of *E. coli* K12 and clinical isolates of *E. coli*, *K. pneumoniae* and *P. aeruginosa*, grown for 18 hours.

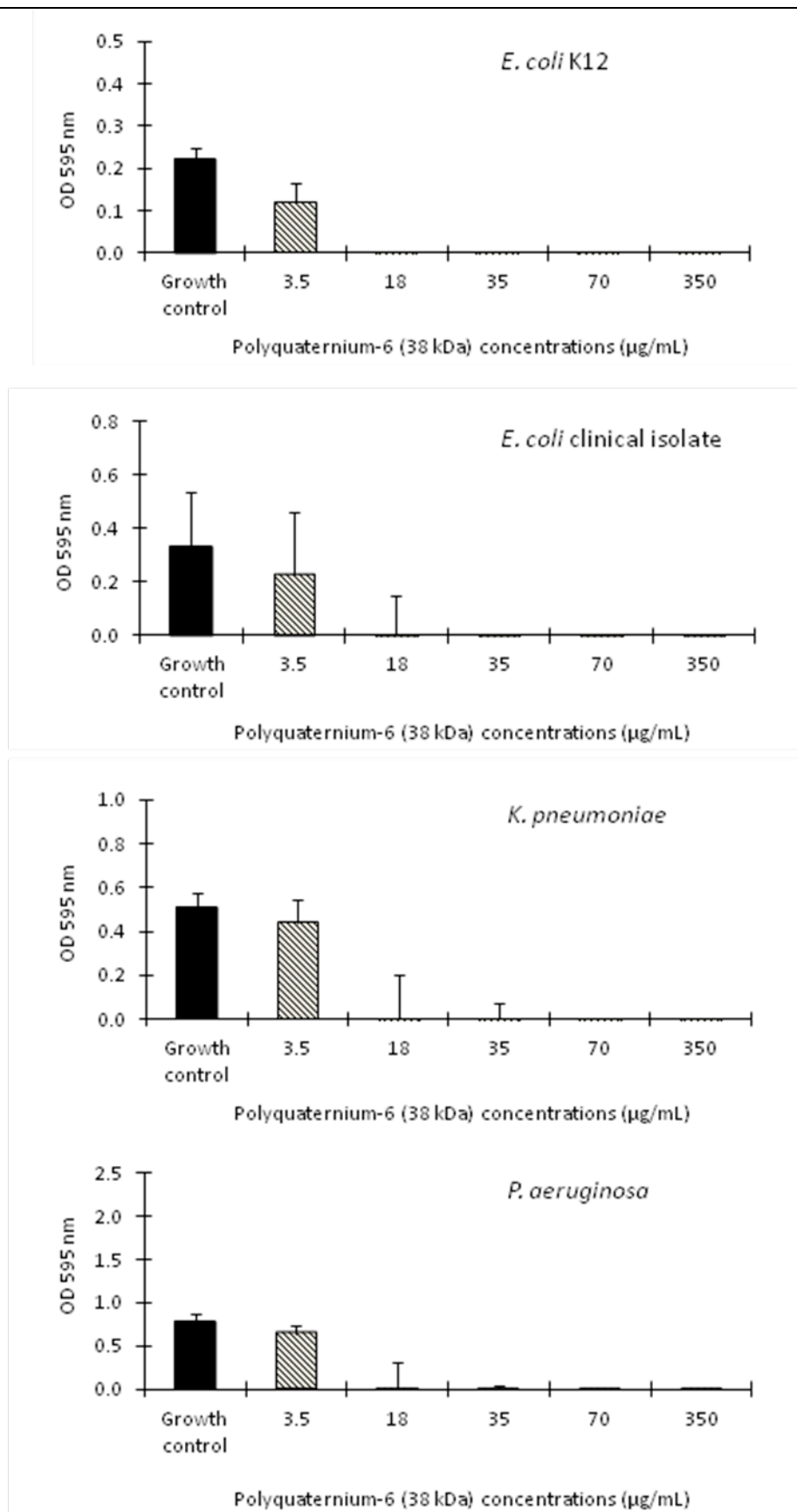


Figure 4. 18. The dose response of Polyquaternium-6 (38 kDa) against the biofilm cells of *E. coli* K12 and clinical isolates of *E. coli*, *K. pneumoniae* and *P. aeruginosa*, grown for 18 hours.

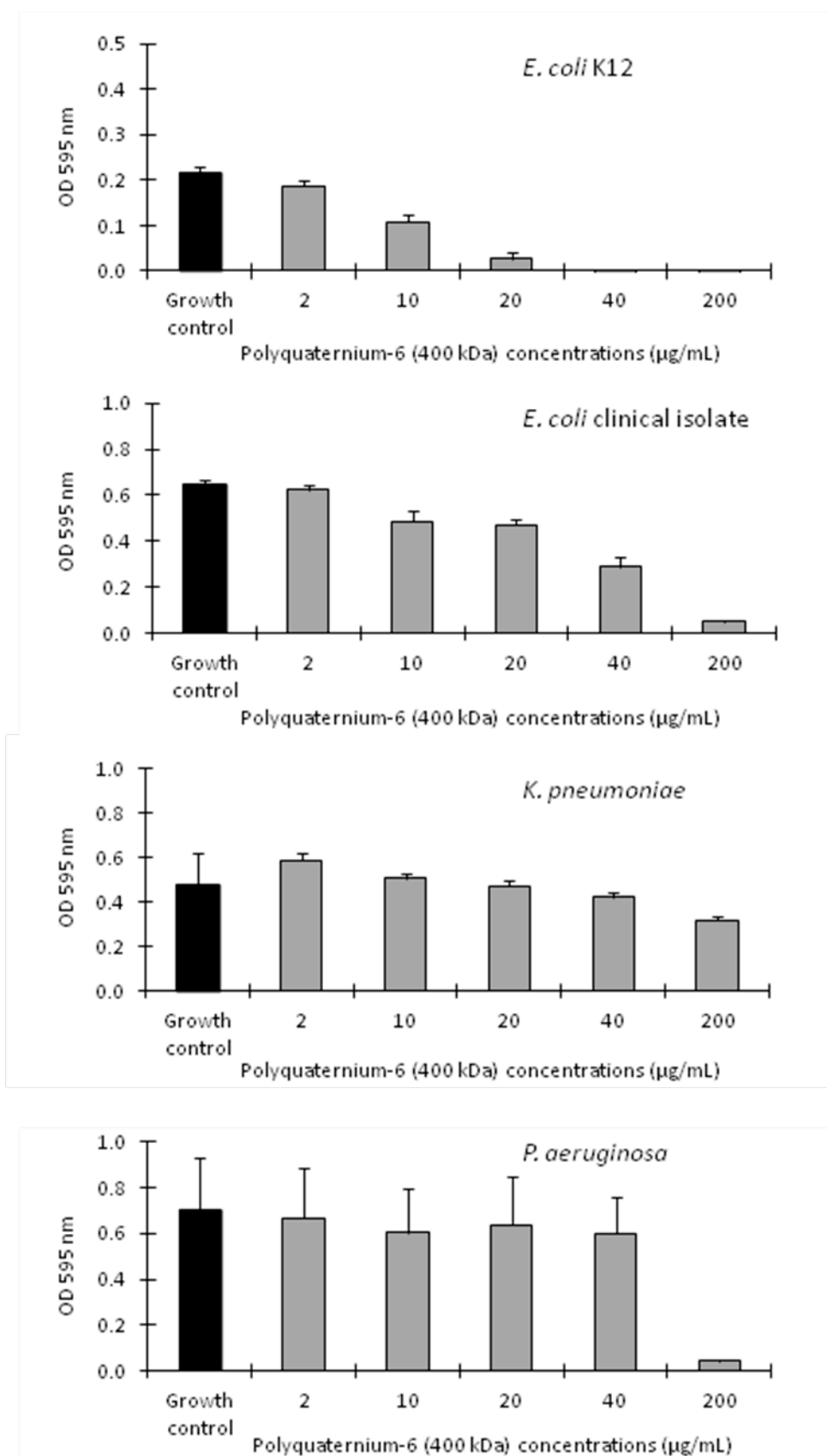


Figure 4. 19. The dose response of Polyquaternium-6 (400 kDa) against the planktonic cells of *E. coli* K12 and clinical isolates of *E. coli*, *K. pneumoniae* and *P. aeruginosa*, grown for 18 hours.

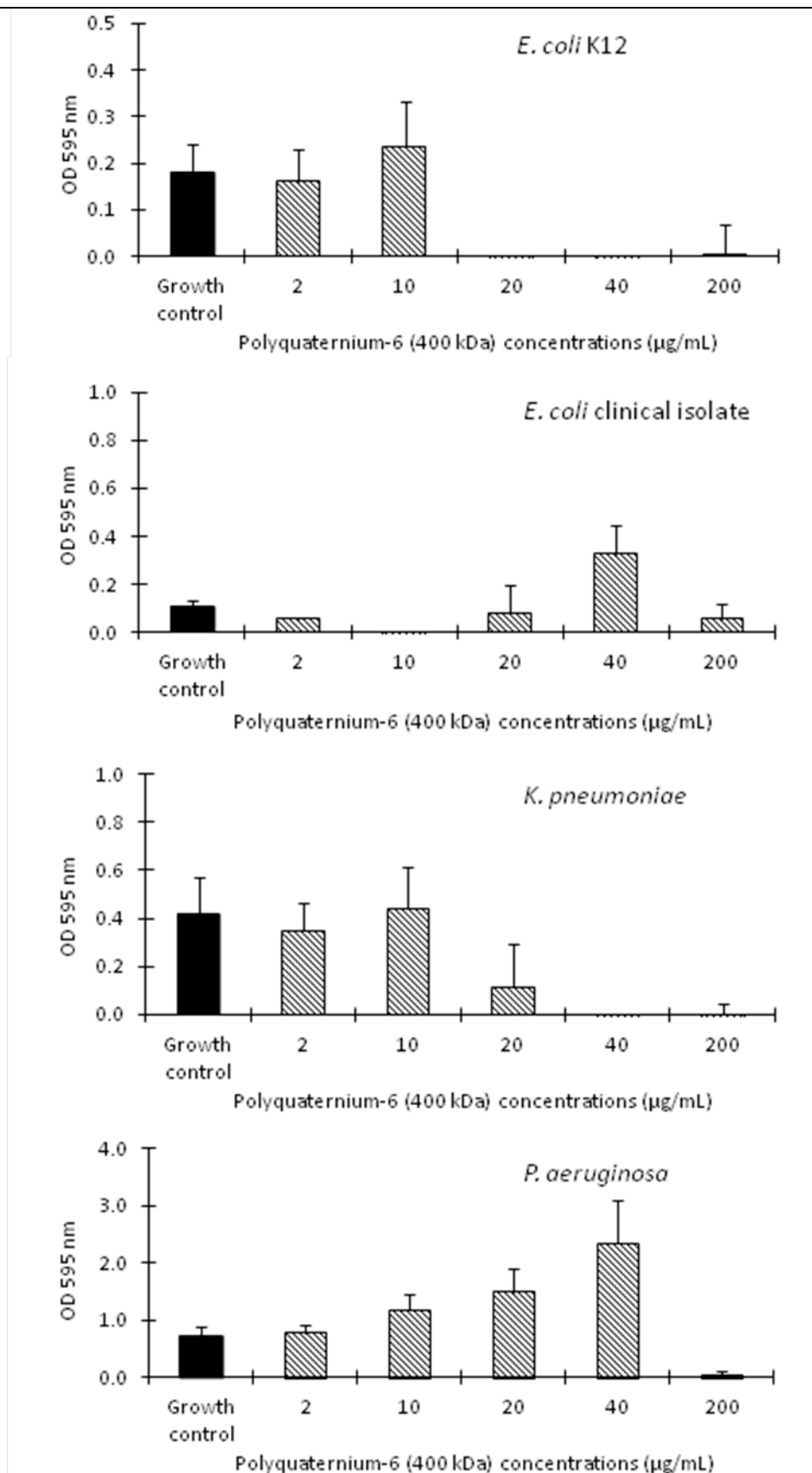


Figure 4. 20. The dose response of Polyquaternium-6 (400 kDa) against the biofilm cells of *E. coli* K12 and clinical isolates of *E. coli*, *K. pneumoniae* and *P. aeruginosa*, grown for 18 hours.

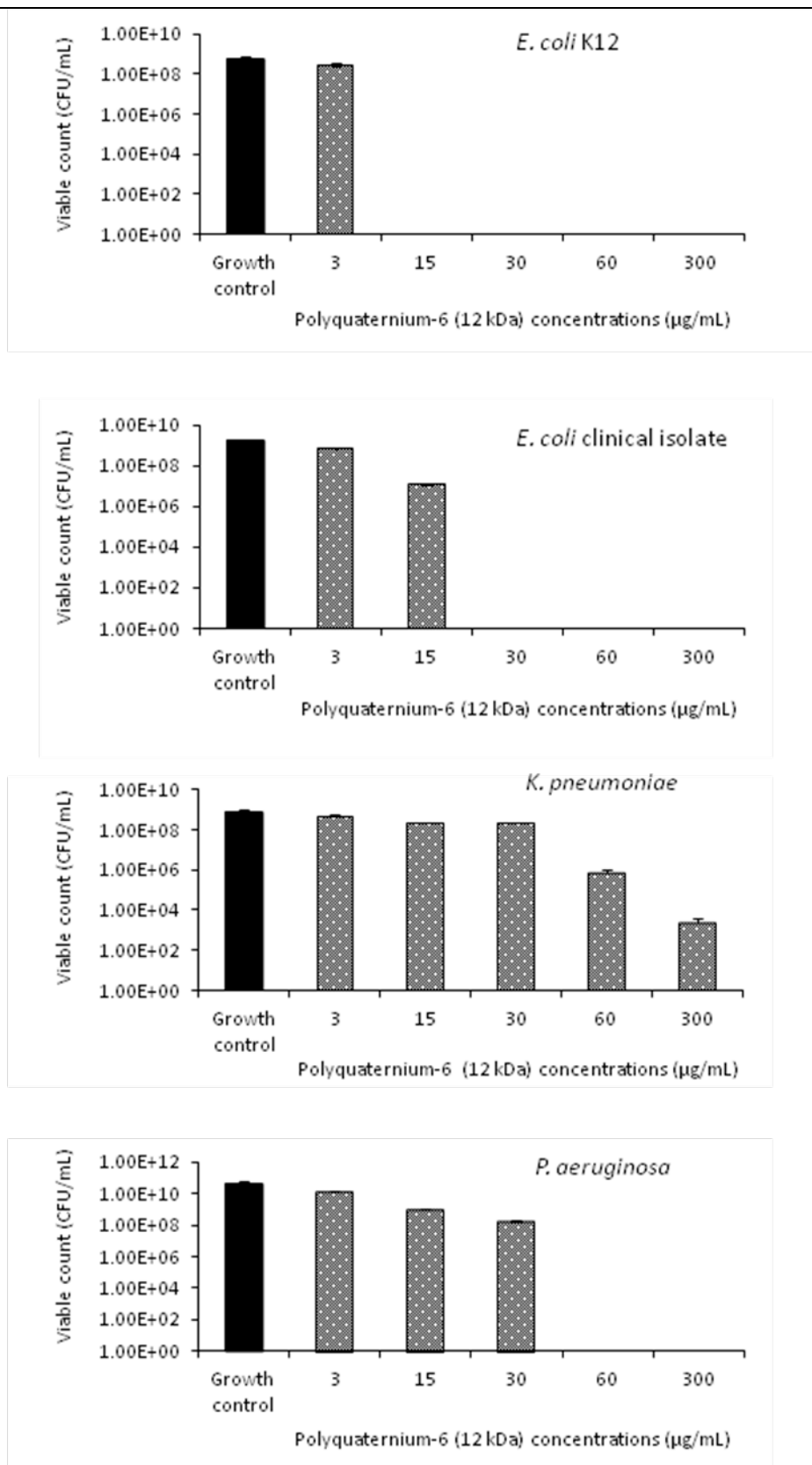


Figure 4. 21. Viable cell counts determining the activity of increasing concentrations of Polyquaternium-6 (12 kDa) against the planktonic cells of *E. coli* K12 and the clinical isolates of *E. coli*, *K. pneumoniae* and *P. aeruginosa* grown for 18 hours. Growth is presented as the colony forming units/mL (CFU/mL) from an average of a minimum of 3 biological replicates. Error bars indicate the standard deviation.

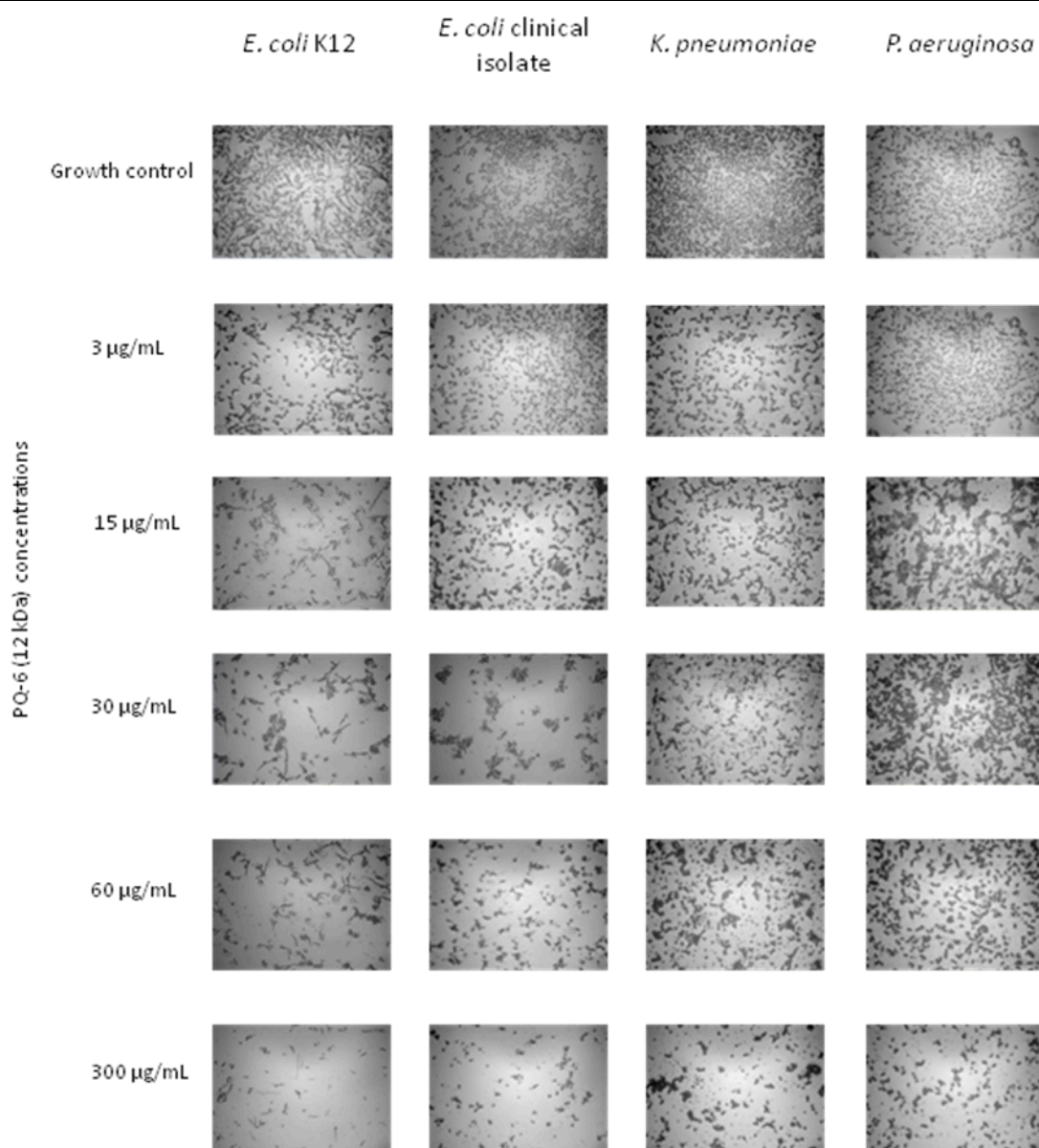
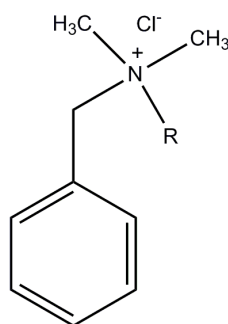


Figure 4. 22. Bright field microscopy of biofilms treated with Polyquaternium-6 (12 kDa) Bright field microscopy images (100x magnification) showing the effects of increasing concentrations of Polyquaternium-6 on the biofilm formation of *E. coli* K12 and the clinical isolates of *E. coli*, *K. pneumoniae* and *P. aeruginosa* grown for 18 hours and stained with crystal violet.

4.4. The susceptibility of bacteria to the proprietary antimicrobial Byotrol™ and its individual components: PHMB, BAC and DDQ

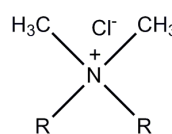
Byotrol™ is a commercially available solution and is the active ingredient in sanitisers, detergents and cleaning agents used in the domestic environment as well as the food industry and clinical setting. Byotrol™ consists of alkyl dimethyl benzyl ammonium chloride (BAC) (4%), didecyl dimethyl ammonium chloride (DDQ) (6%), and poly(hexamethylene biguanide) (PHMB) (10%). The structures of the constituents of Byotrol™ are shown in Figure 4. 23.

Alkyl dimethyl benzyl ammonium chloride (BAC)



R = Alkyl (C₁₂H₂₅, 70%; C₁₄H₂₉, 30%)

Didecyl dimethyl ammonium chloride (DDQ)



R = C₁₀H₂₁

Poly(hexamethylene biguanide) (PHMB)

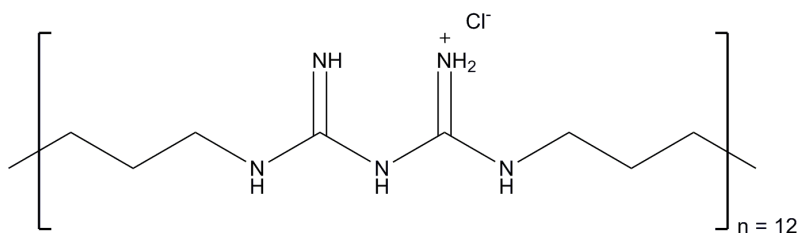


Figure 4. 23. The individual constituents of Byotrol™: BAC, DDQ and PHMB.

PHMB is a polymeric biguanide compound which has a hydrophobic backbone, off which are cationic groups that confer its antibacterial properties (Gilbert & Moore, 2005). Research on PHMB began during the 1940s and 1950s, and it is now commonly used in the domestic industry in cleaning solutions, disinfectant, as environmental biocides, in swimming pools for sanitisation and in a wide range of antiseptic materials and solutions including hand sanitisers. It is also present in commercially available wound dressings and contact lens solutions (Gilbert & Moore, 2005; Kim *et al.*, 2011). The mode of action of PHMB has the same overall effect as QACs in that the cell is perturbed and the cell content is released, however the mechanism is slightly different. The positively charged divalent cations (Mg^{2+} and Ca^{2+}) that stabilise the lipid bilayer are displaced by the charged nitrogen of the QAC, which, in effect, solubilises and disintegrates the bacterial outer membrane allowing entry into the cell (Wilkinson & Gilbert, 1987).

Benzalkonium chloride (BAC) and didecyl dimethyl ammonium chloride (DDQ, also known as DDAC) are quaternary ammonium surfactants in Byotrol™. The BAC used in this study has a 12-16 alkyl chain length, as this is known to be the optimum chain length for antimicrobial activity (Halvax *et al.*, 1990). BAC is currently the most widely used preservative in ophthalmic solutions due to its broad spectrum of activity and known chemical compatibility with many different classes of therapeutic agents, presumably due to its ability to perturb the bacterial membrane (Kaur *et al.*, 2009; Rolando *et al.*, 2011). It has also been investigated as a central venous catheter coating (Jaeger *et al.*, 2001). DDQ is also a widely used biocide in the environmental industries (Brooks, 2001). Ioannou and co-workers identified that DDQ can cause autolysis of *Staphylococcus aureus* at low concentrations (9-18 $\mu\text{g/mL}$), however they did not perform testing of this on Gram-negative organisms (Ioannou *et al.*, 2007).

The activity of Byotrol™ and its individual constituents (PHMB, BAC and DDQ) were tested against the planktonic and biofilm phenotypes of all the organisms used in this study. The results are summarised in Table 4. 7 and Table 4. 8 and details of the dose response data are displayed in Figure 4. 15 and Figure 4. 16. All data represent the mean of over 24 replicates, involving a minimum of 3 biological replicates for each strain.

Table 4. 7. Minimum inhibitory concentrations (MICs) of Byotrol™ and its constituents, PHMB, DDQ and BAC against *E. coli* K12 and the clinical isolates of *E. coli*, *K. pneumoniae* and *P. aeruginosa*.

	Minimum inhibitory concentration (MIC) (µg/mL)			
	<i>E. coli</i> K12	<i>E. coli</i> clinical isolate	<i>K. pneumoniae</i> clinical isolate	<i>P. aeruginosa</i> clinical isolate
Byotrol™	3	3	15	15
PHMB	15	60	100	200
DDQ	20	30	100	100
BAC	60	100	100	400

Table 4. 8. Minimum biofilm inhibitory concentrations of Byotrol™ and its constituents, PHMB, DDQ and BAC against *E. coli* K12 and the clinical isolates of *E. coli*, *K. pneumoniae* and *P. aeruginosa*.

	Minimum biofilm inhibitory concentration (µg/mL)			
	<i>E. coli</i> K12	<i>E. coli</i> clinical isolate	<i>K. pneumoniae</i> clinical isolate	<i>P. aeruginosa</i> clinical isolate
Byotrol™	3	5	15	20
PHMB	20	60	100	400
DDQ	20	30	30	200
BAC	60	100	60	400

Byotrol™ displayed antimicrobial activity against the planktonic and biofilm phenotypes. The MICs range from 3 µg/mL for planktonic *E. coli* K12 to 15 µg/mL for planktonic *P. aeruginosa* (Table 4. 7). The minimum biofilm inhibitory concentrations that range from 3 µg/mL for biofilm *E. coli* K12 to 20 µg/mL for biofilm *P. aeruginosa* (Table 4. 8). A comparison between the results in the two tables show that Byotrol™ displayed a much greater degree of antimicrobial activity than its individual constituents.

The antimicrobial activity of Byotrol™ against the bacterial isolates was validated by viable cell counts and bright field microscopy. Viable cell counts are a measure of planktonic cells (Figure 4. 24) therefore confirmed the inhibition of planktonic cells as shown by the MIC results (Table 4. 7); bright field microscopy shows an image of cells attached to a surface (Figure 4. 25) therefore validate biofilm formation as shown by the minimum biofilm inhibitory results (Table 4. 8). Although the viable cell counts were higher for all the bacteria in relation to the MIC results, apart from the *E. coli* clinical isolate that was the same (3 µg/mL); the trend was the same for all both the viable cell counts and MIC results. The results of the bright field microscopy showed a decrease in cell growth at 5 µg/mL, 20 µg/mL and 15 µg/mL for *E. coli* K12, the clinical isolates of *E. coli*, *K. pneumoniae* and *P. aeruginosa*, respectively (Figure 4. 25). The microscopy results demonstrated that as the concentration of Byotrol™ increased, the number of bacterial cells decreased (Figure 4. 25), which correlate with the minimum biofilm inhibitory concentrations shown in Table 4. 7.

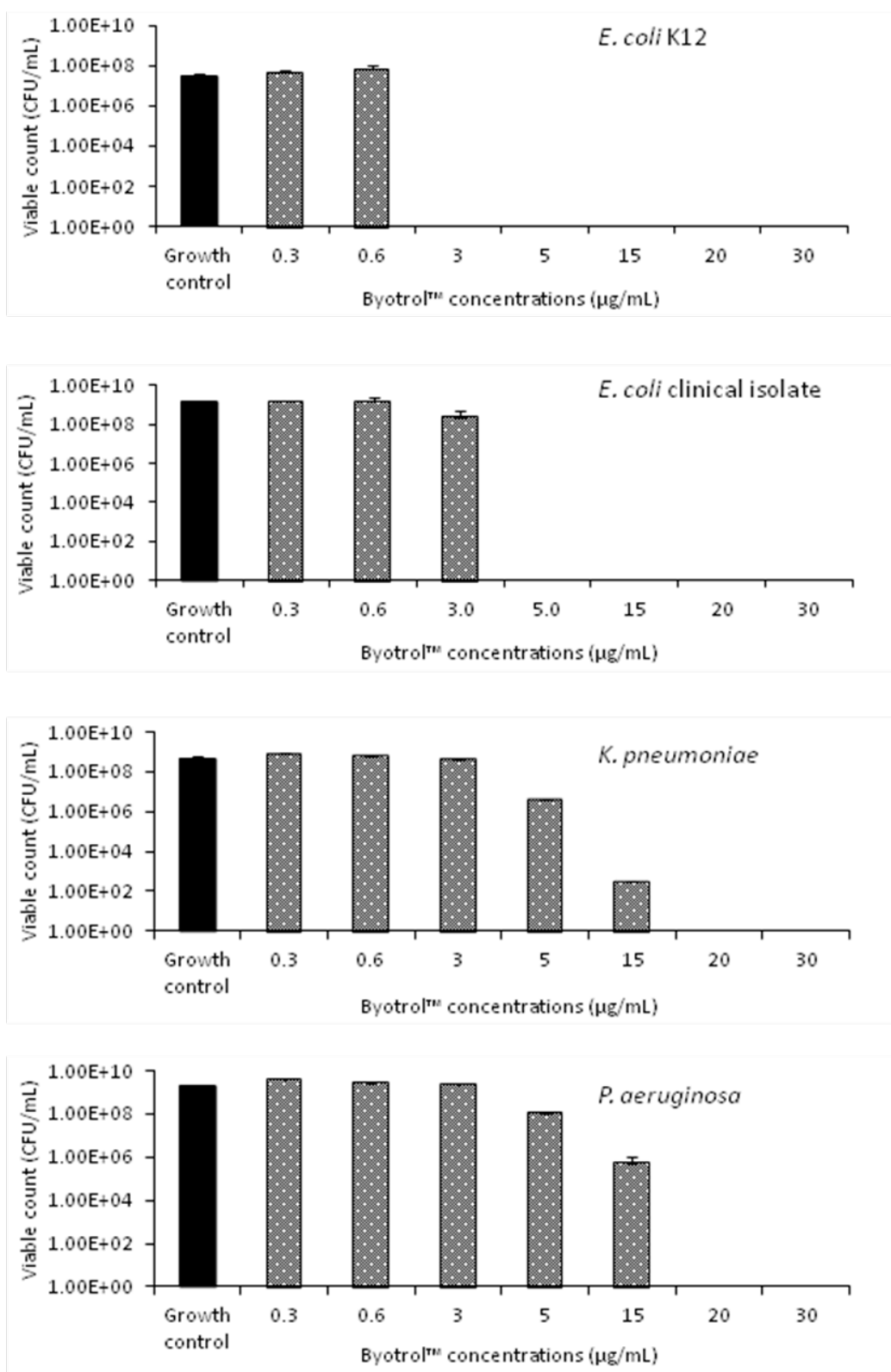


Figure 4. 24. Viable cell counts determining the activity of increasing concentrations of Byotrol™ against the planktonic cells of *E. coli* K12 and the clinical isolates of *E. coli*, *K. pneumoniae* and *P. aeruginosa* grown for 18 hours. Growth is presented as the colony forming units/mL (CFU/mL) from an average of a minimum of 3 biological replicates. Error bars indicate the standard deviation.

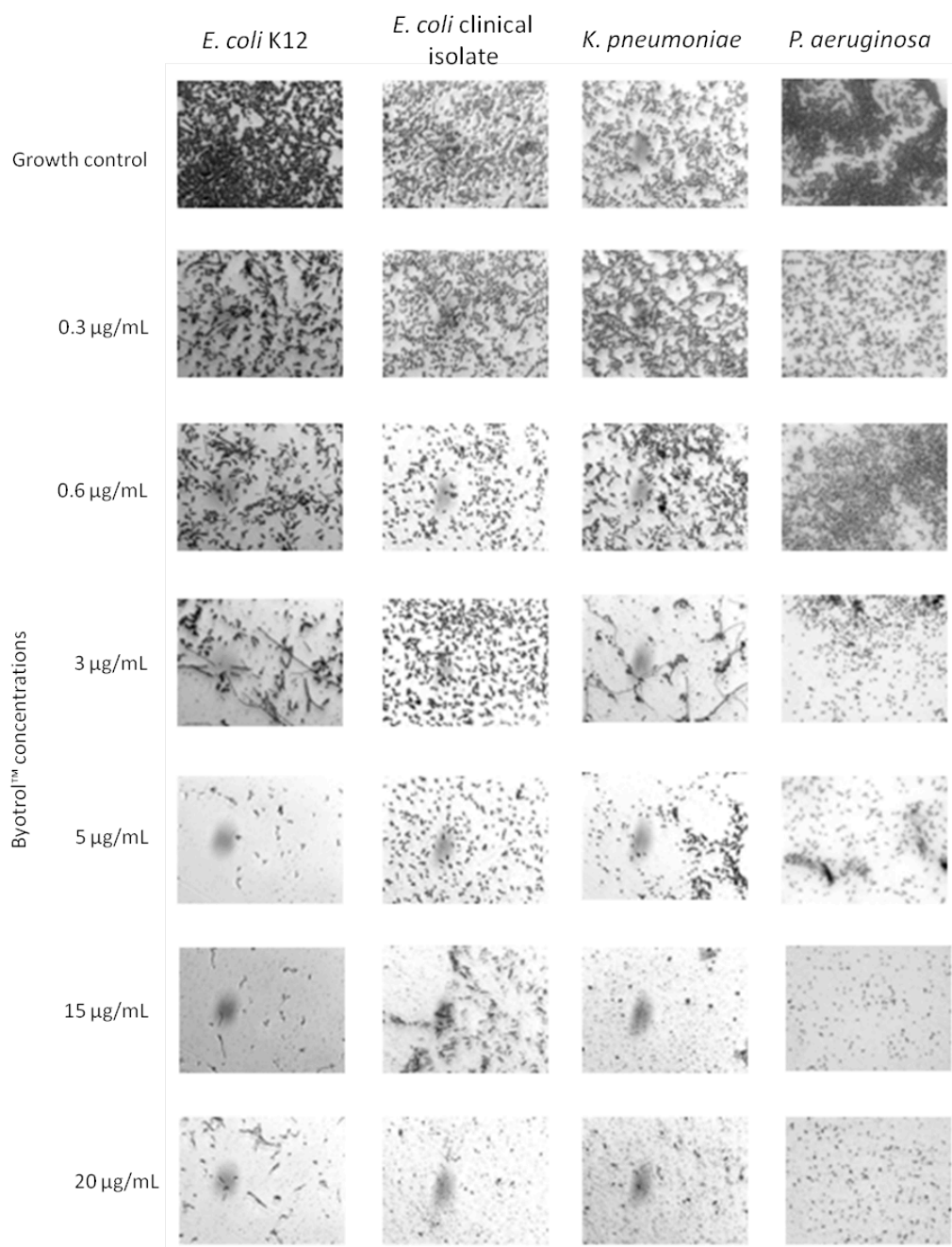


Figure 4. 25. Bright field microscopy of biofilms treated with Byotrol™. Bright field microscopy images (100x magnification) showing the effects of increasing concentrations of Byotrol™ on the biofilm formation of *E. coli* K12 and the clinical isolates of *E. coli*, *K. pneumoniae* and *P. aeruginosa* grown for 18 hours and stained with crystal violet.

4. 4. 1. Pre-coating a surface with Byotrol™

In order to test the effect of Byotrol™ on initial bacterial attachment, Byotrol™ was coated onto a glass surface (Figure 4. 26) and a polystyrene microtitre plate surface (Figure 4. 27) prior to the introduction of inoculum. Pre-treating a glass surface also enabled the visualisation of the coating with atomic force microscopy (Section 4. 4. 1. 2). These data suggest that there was little difference between pre-coating a glass surface and pre-coating a polystyrene microtitre plate. On both the glass surface and microtitre plate the inhibitory concentration for *E. coli* K12 and *E. coli* clinical isolate was 400 µg/mL, for *K. pneumoniae* the inhibitory concentration was 1 mg/mL and for *P. aeruginosa* is greater than 1 mg/mL.

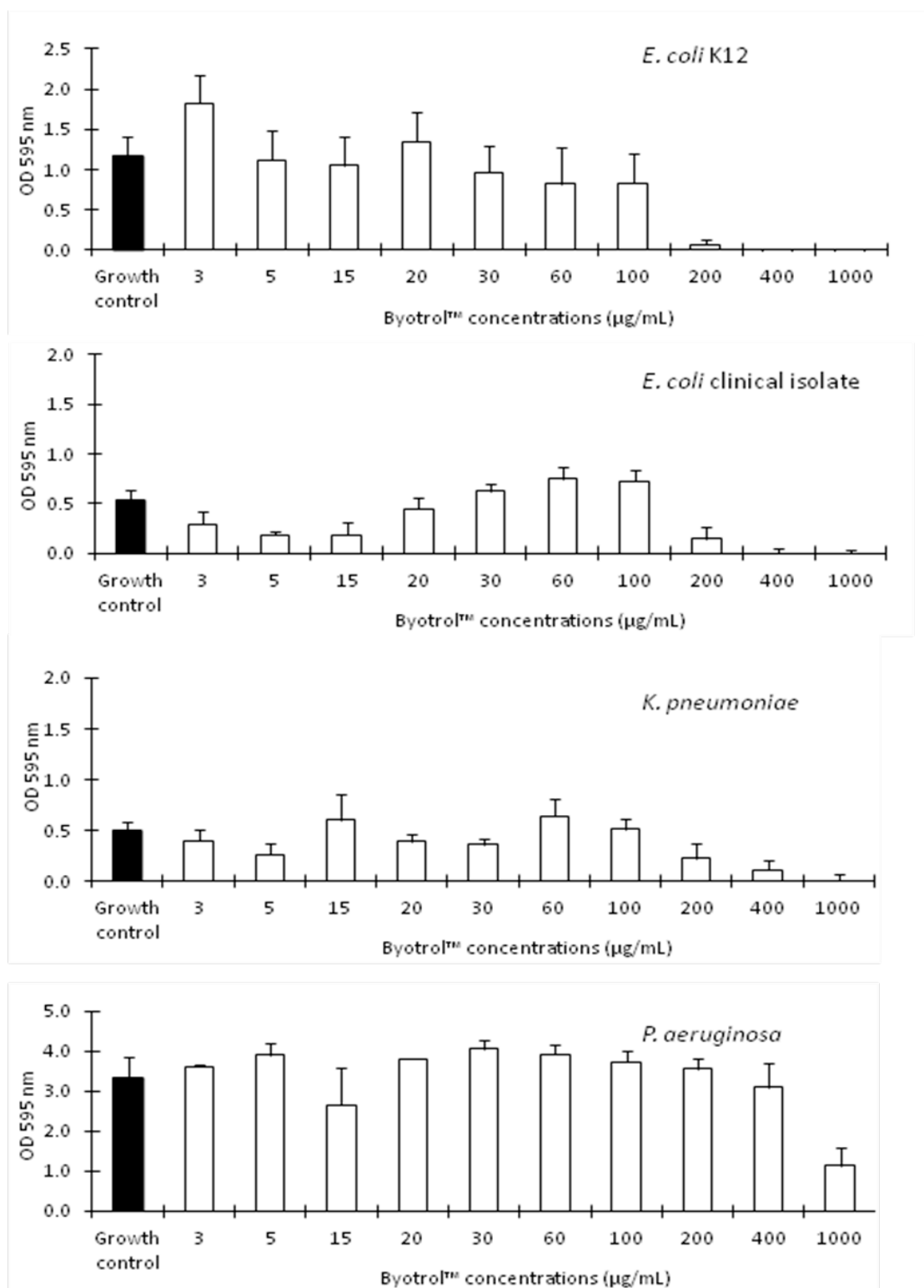


Figure 4.26. The effects of a Byotrol™ coated glass surface on biofilm development. A glass surface was pre-coated with Byotrol™ for 18 hours and seeded with *E. coli* K12 and the clinical isolates of *E. coli*, *K. pneumoniae* and *P. aeruginosa* for 8 hours. The extent of biofilm formation was determined by crystal violet staining. The absorbance values of the solubilised stain displayed represent the mean of over 24 experiments, involving a minimum of 3 biological replicates for each strain. Error bars indicate the standard error of the mean.

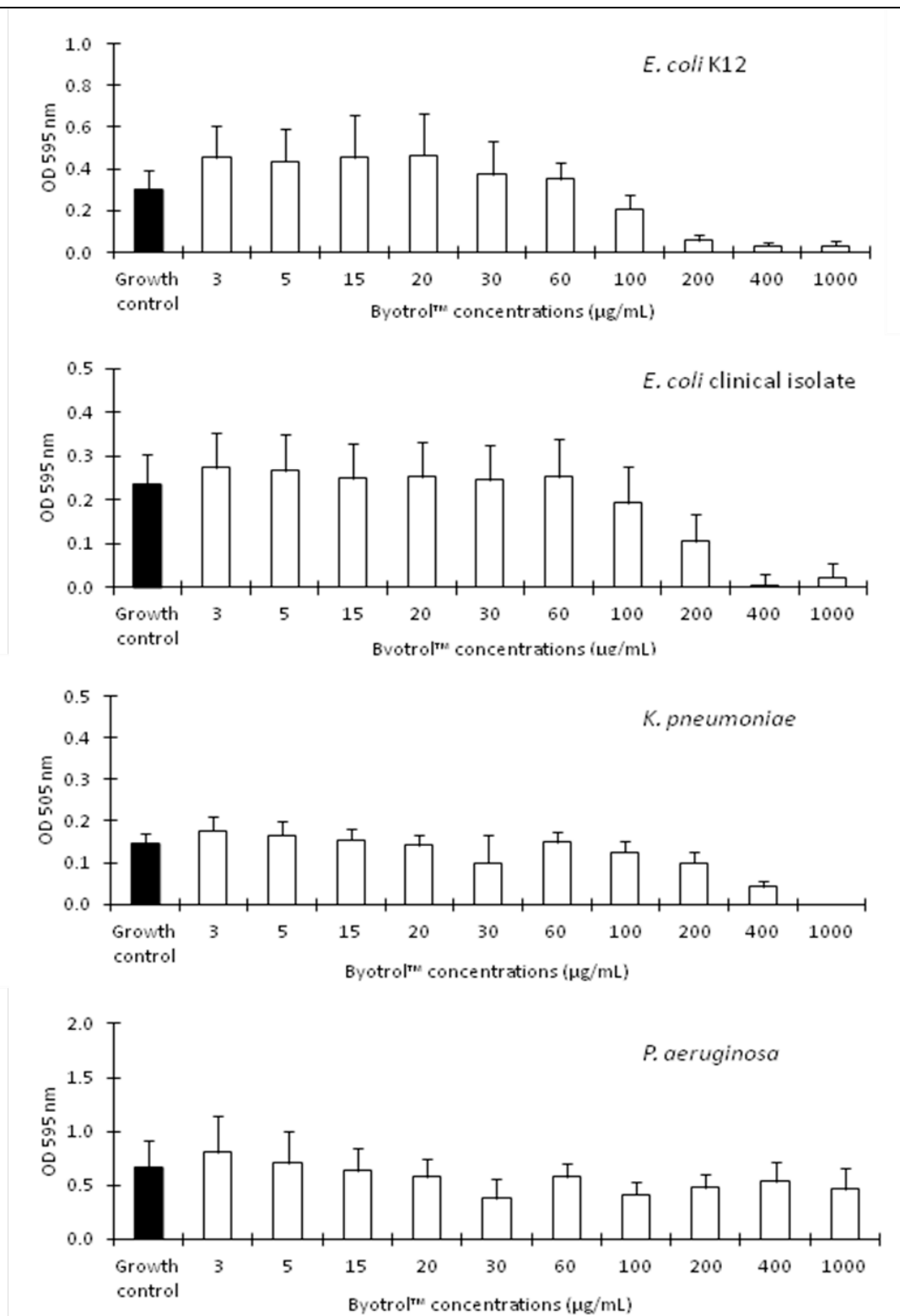


Figure 4. 27. The effects of a Byotrol™ coated polystyrene surface on biofilm development.

A microtitre plate was pre-coated with Byotrol™ for 18 hours and seeded with *E. coli* K12 and the clinical isolates of *E. coli*, *K. pneumoniae* and *P. aeruginosa* for 8 hours. The extent of biofilm formation was determined by crystal violet staining. The absorbance values of the solubilised stain displayed represent the mean of over 24 experiments, involving 3 biological replicates for each strain. Error bars indicate the standard error of the mean.

4. 4. 1. 2. Atomic force microscopy of a glass surface pre-coated with Byotrol™

Non-contact atomic force microscopy (AFM) was performed on a surface with increasing concentrations of Byotrol™ (Figure 4. 28). This was to confirm how evenly a surface was being coated by Byotrol™, thereby providing an insight into the mode of action of Byotrol™ as a potential antimicrobial coating. AFM also gave an indication of the depth of the coating. The results demonstrate that there was full coverage of the surface at both concentrations (Figure 4. 28 a). A scratch showed the depth of the coating at 5 µg/mL Byotrol™ to be approximately 20 nm, and approximately 60 nm with a 1 mg/mL coating of Byotrol™. It was clear that as the concentration of Byotrol™ increased, the coating depth increased. (Figure 4. 28 b). Inhibition is greatest when the surface is fully and evenly coated.

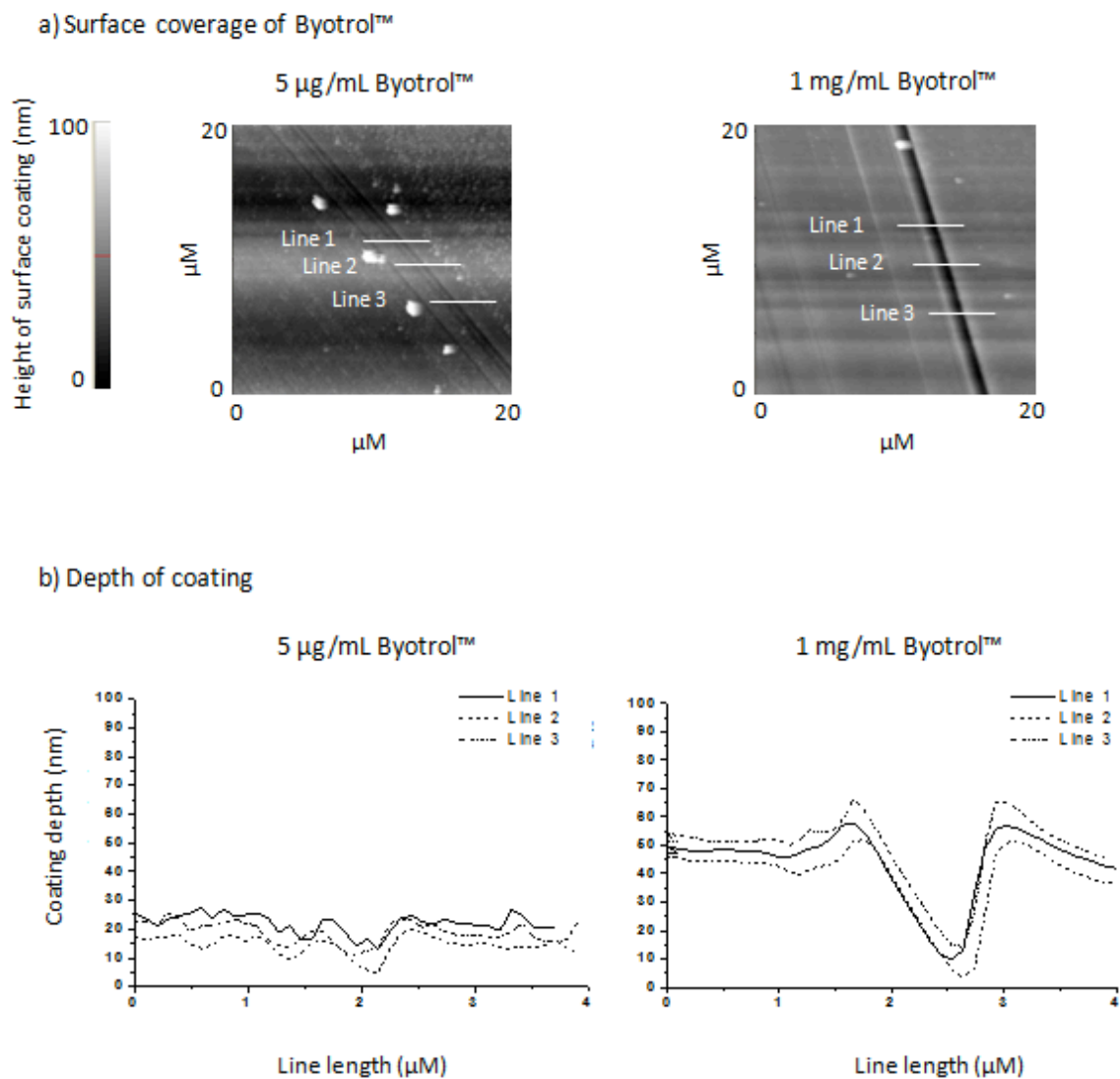


Figure 4. 28. The coating potential of Byotrol™: **a)** atomic force microscopy images of a glass surface coated with 5 µg/mL and 1 mg/mL Byotrol™ for 18 hours; **b)** a scratch was made across the surface to indicate the depth of the coatings. The film depth was determined by measuring the distance across the scratches in 3 distinct areas.

4.4.2. Eradication of an established biofilm with Byotrol™: MBEC assay system

The MIC and microtitre plate biofilm formation assays used in this study have tested the effect of QACs and Byotrol™ in suspension against planktonic cells. This has been useful in identifying antimicrobials that inhibit planktonic cells, which subsequently reduce the number of viable cells remaining to establish a biofilm. Of the bacterial inhibitors tested, Byotrol™ was proven to be superior. It was therefore useful to determine if Byotrol™ was capable of removing an established biofilm, as this may increase its use in the clinical environment.

The MBEC (minimum biofilm eradication concentration) assay system is the first high throughput method that has been developed which tests the susceptibility of established biofilms to antimicrobials, as well as giving an MIC for the planktonic growth which is shed from a biofilm (Ceri *et al.*, 1999). This was determined for Byotrol™. Biofilms were allowed to grow on pegs for 18 hours, challenged with Byotrol™ for 18 hours and surviving biofilm cells were allowed to recover in fresh media for 18 hours. The pegs with biofilm growth were stained and the stain solubilised. The MBEC value is defined as the minimum concentration of antimicrobial that inhibits the re-growth of biofilm cells in recovery media (Sawasdidoln *et al.*, 2010). The 'P-MIC', the minimum inhibitory concentration of the cells which were shed from the pegs during challenge with Byotrol™ (Sawasdidoln *et al.*, 2010), was also determined (Figure 4. 30). The MBEC results showed some residual crystal violet staining of Byotrol™ on the pegs at 1 mg/mL, however the P-MIC data clearly demonstrated that biofilm was eradicated (Figure 4. 30), and generally there was a similar trend between this and the MBEC. As the literature suggests, once a biofilm is established, it is more difficult to eradicate (Lewis, 2001). The eradication of an 18 hour biofilm with Byotrol™ gave an MBEC which was approximately 40-60% higher than the P-MIC and minimum biofilm inhibitory concentrations.

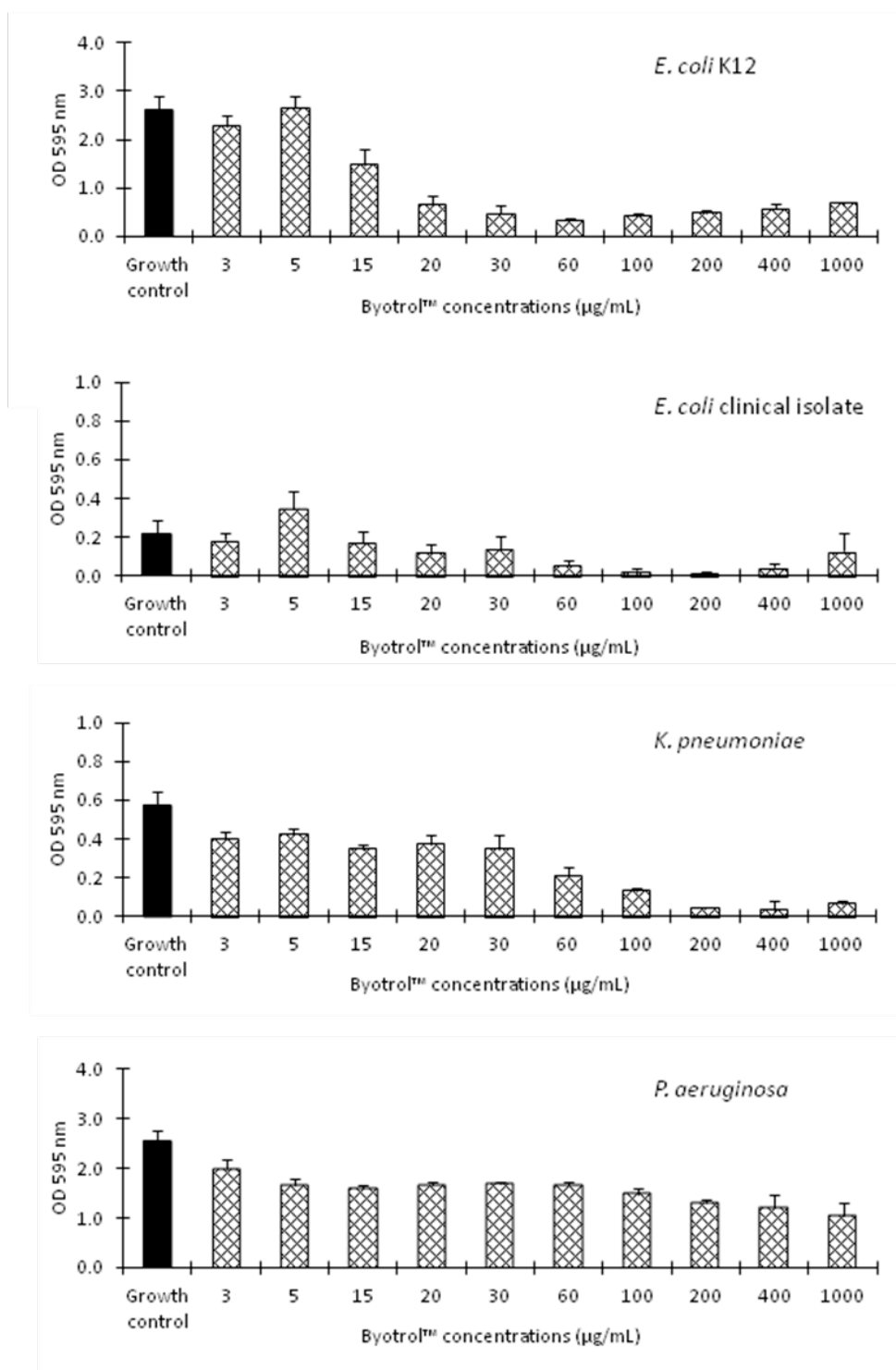


Figure 4. 29. Eradication of an 18 hour biofilm: Minimum biofilm eradication concentration (MBEC) determining the activity of increasing concentrations of Byotrol™ on a biofilm grown on polystyrene pegs for 18 hours and treated with Byotrol™ for 18 hours under static conditions at 37°C. Bacterial cells were allowed to recover in fresh media for 18 hours. The extent of biofilm formation was determined by crystal violet staining and solubilised. The absorbance values of the solubilised stain displayed represent the mean of over 24 experiments, involving a minimum of 3 biological replicates for each strain. Error bars indicate the standard error of the mean.

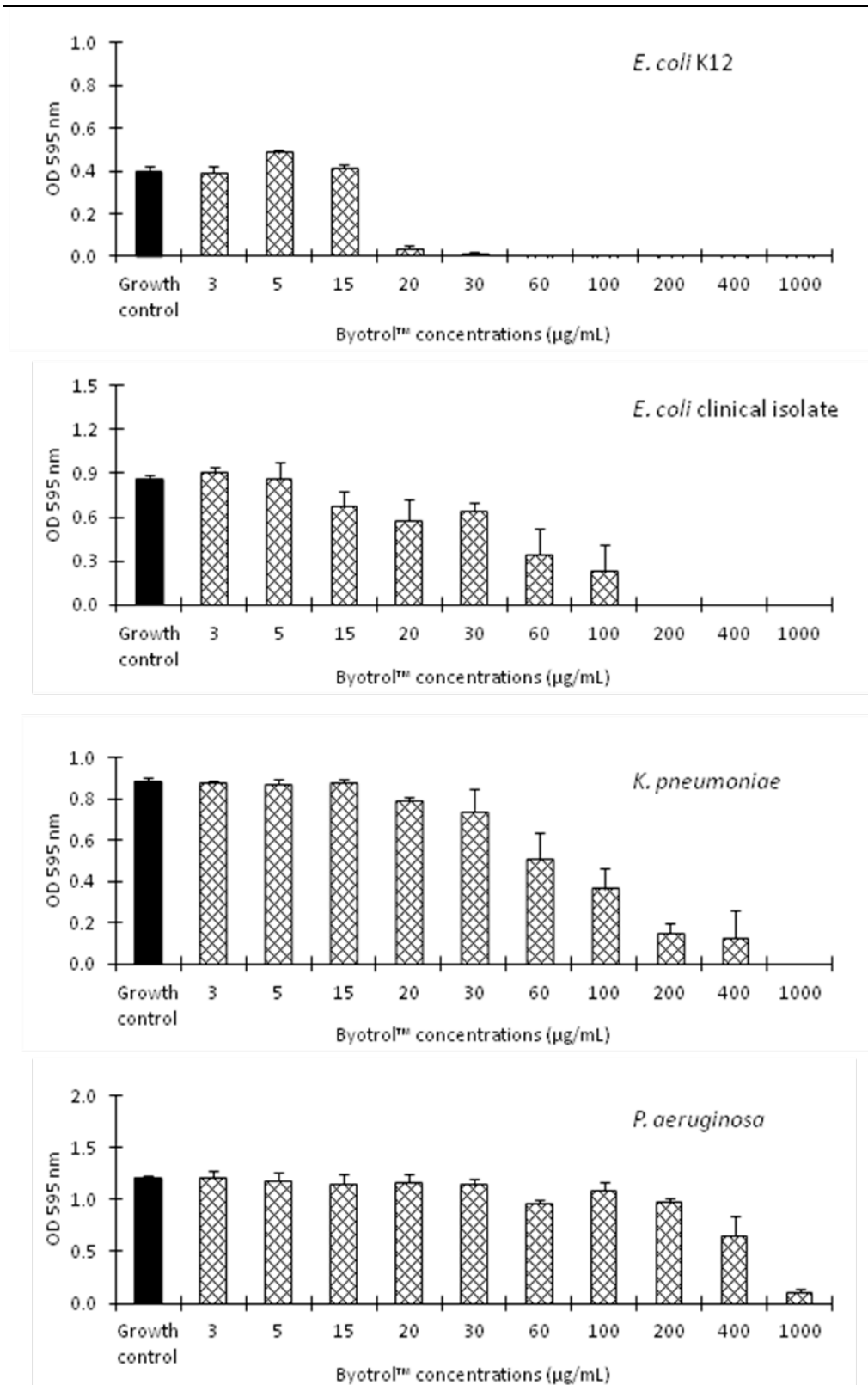


Figure 4. 30. P-MIC for planktonic cells shed from a biofilm: The activity of increasing concentrations of Byotrol™ on a biofilm grown on polystyrene pegs for 18 hours and treated with Byotrol™ for 18 hours under static conditions at 37°C. The growth of planktonic cells shed from the biofilm grown on the pegs was determined by reading the absorbance. The absorbance values represent the mean of over 24 experiments, involving minimum of 3 biological replicates for each strain. Error bars indicate the standard error of the mean.

4. 5. Discussion

Biofilm formation on the surface of urinary catheters is a great expense to the health service (Polonio *et al.*, 2001). Due to the inherent resistance of bacteria to conventional antimicrobials, colonised catheters routinely have to be removed to reduce the risk of systemic infection (Trautner & Darouiche, 2004). The overall outcome of this research should be to support efforts designed to reduce the incidence of CAUTI and prolong the life of a urinary catheter.

4. 5. 1. The difference between *E. coli*, *K. pneumoniae* and *P. aeruginosa*

For all of the compounds tested, there was a trend whereby the *E. coli* laboratory strain was the most sensitive, followed by the *E. coli* clinical isolate, *K. pneumoniae* and then finally, *P. aeruginosa*. Genes that confer fitness to bacteria may be deleted or become non-functioning as a result of serial passage of laboratory strains over the years (Koskiniemi *et al.*, 2012), and this may be why the laboratory strain of *E. coli* was more sensitive to the compounds tested. Most of the QACs showed less inhibition against *P. aeruginosa*. Biocides that have a broad spectrum of activity and non-specific mode of action may cause non-specific resistance mechanisms, for example, in *P. aeruginosa*, the hyper-expression of multidrug efflux pumps. This may explain the increased tolerance of *P. aeruginosa* to biocides. There may also be changes to the outer membrane which reduces the permeability of the membrane to the biocide (Gilbert, 2005). Previous studies have found that *P. aeruginosa* has a higher Mg²⁺ content compared to other Gram-negative bacteria, which increases the outer membrane stability, as divalent cations increase lipopolysaccharide-lipopolysaccharide interactions. In comparison to the PQs tested, the marginally higher MIC of Byotrol™ for *P. aeruginosa* compared to that of the other organisms does not alter the fact that Byotrol™ was still the most superior inhibitor tested in this study.

4. 5. 2. The effect of molecular weight on inhibition of bacterial growth

There was a correlation between molecular weight and antimicrobial activity for the compounds tested in this study. The increasing molecular weights tested for PQ-6 demonstrated that the higher the molecular weight, the lower its inhibitory activity. A reduction in inhibitory activity of higher molecular weight compounds compared to

lower molecular weight compounds can be explained by understanding the relationship between the polycations on a polymer chain, and the counter-ions associated with the cations. It has been suggested that there is a link between the conformation of PQ-6 in solution and its corresponding MICs, as the molecular weight of the PQ-6 effects the molecule's conformation (Peter Wills, personal communication). Lower molecular weight samples (12 kDa and 38 kDa) are suggested to be in a more rod like conformation compared to the higher molecular weight (400 kDa) sample, suggested to be in a more coil like conformation. With this in mind, it was proposed that when the conformation of PQ-6 is more coil-like compared to a rod-based conformation, some poly-cations would be less accessible to the bacteria (Figure 4. 31). In addition to this, the conformation of the molecule can also affect its charge density properties, with the coil conformation believed to enhance the counter ion condensation phenomena, thereby reducing the full antimicrobial potential of the positive charge (Wills, 2013).

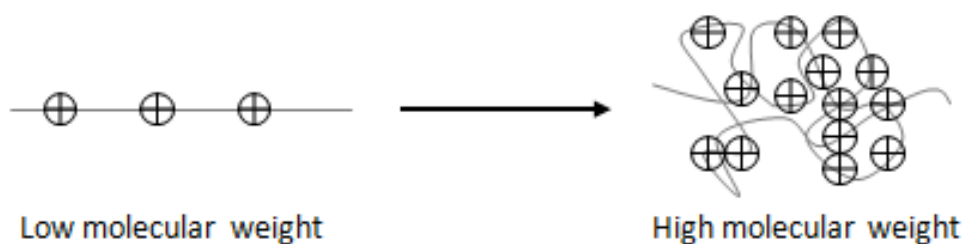


Figure 4. 31. The folding effect of polyquaterniums as the polymer chain length increases and the molecular weight increases. The positive charges are closer together when a polymer folds, and this reduces its antimicrobial effect, as the positive charge is sequestered by the counter-ion.

In this study, the difference between the polyquaterniums and PHMB should have been greater, given the known antimicrobial effect of PHMB (Allen *et al.*, 2006; Gilbert *et al.*, 1990; Gilbert & Moore, 2005), however, there was only a 5-10 fold difference between PQ-6 (12 kDa compound) which has an MIC of 15-30 $\mu\text{g/mL}$ for all of the organisms tested, and PHMB which has an MIC of 15 $\mu\text{g/mL}$ for *E. coli* K12 and 200 $\mu\text{g/mL}$ for *P. aeruginosa* (Table 4. 7). This may be because of the molecular weight of PHMB used in this study was not high enough in relation to that of PQ-6. Gilbert and

co-workers have demonstrated that as the molecular weight of PHMB increases, the biocidal effect also increases (Gilbert *et al.*, 1990); Gilbert, 2005).

4. 5. 3. Validation of MIC and minimum biofilm inhibitory concentrations

For the most inhibitory compounds, Byotrol™ and PQ-6 (12 kDa), MIC and minimum biofilm inhibitory concentrations were validated with viable cell counts and bright field microscopy. The level of planktonic cells was proportional to the biofilm cells that adhered to the microtitre plate surface (Ymele-Leki & Ross, 2007). It was therefore important to validate the MIC with the viable cell count of planktonic cells. The viable cell counts of bacteria grown treated with Byotrol™ showed a positive correlation with the MIC results. Lower MIC values in relation to the viable cell counts are to be expected as the viable cell count will show greater sensitivity to growth than an OD measurement of the turbidity of bacterial growth. Biofilm growth can be validated by microscopy, as the bacterial cells are attached to the glass surface. Microscopy was performed for PQ-6 (12 kDa) and Byotrol™. The images presented were a representative of at least 3 replicates and inhibition of growth was compared to the growth control by visual inspection. In all cases, the minimum biofilm inhibitory concentration and the reduction in cells shown by the microscopy images were complementary.

4. 5. 4. The effect of Byotrol™ on bacterial growth

PHMB was the most potent of all the individual cationic biocides tested in the current study. This is the main active component in Byotrol™; therefore it is unsurprising that the Byotrol™ solution was by far the most efficacious antimicrobial tested against all of the organisms in this study.

In the literature, PHMB had an MIC of 3.5 µg/mL for a strain of *E. coli* K12 (Allen *et al.*, 2006). In the current study, the MIC for *E. coli* K12 was 15 µg/mL (Table 4. 7), suggesting that the strains tested in the study by Allen and co-workers may have a greater tolerance, or the PHMB is of a higher molecular weight.

The testing of polyquaterniums and Byotrol™ to determine the MIC and minimum biofilm inhibitory concentration was performed by growing bacteria in a suspension of media containing the cationic compound. This suggests that these compounds may be

killing planktonic bacteria before cells are able to attach to the surface to form a biofilm. Pre-coating the surface of a glass slide and microtitre plate determined whether cells that come into contact with the surface are inhibited from proliferating.

Like-for-like concentrations used for pre-coating a surface with Byotrol™ and in suspension demonstrated that pre-coating was not as effective against planktonic cells as indicated by the pre-coating data and the MIC results. Pre-coating was also not as effective as the inhibition against an established biofilm, as demonstrated by the MBEC assay. This may be because PHMB adheres to the surface with the highest affinity (Borkovec & Papastavrou, 2008), leaving BAC and DDQ to go back into solution. Although PHMB is active on the surface as a coating, it has greater potency when in solution with BAC and DDQ, as the Byotrol™ MIC results showed. DDQ and BAC in solution, without PHMB, are also not as effective as inhibitors. Therefore, it may be that the lower level of inhibition on a pre-treated surface may be due to PHMB, BAC and DDQ not forming a lasting and permanent film on the surface of the glass. Once the bacterial suspension is added to the pre-coated surface, PHMB, BAC and DDQ may return to solution allowing bacteria to adhere to the surface. Also, when pre-coating the surface with Byotrol™, the suspension was decanted after 18 hours and only the compounds that were attracted to the surface in that time would dry to form a coating. Therefore, if it is the case that Byotrol™ is re-suspended after pre-coating, the concentration of Byotrol™ in the bacterial suspension would be lower than the concentration of Byotrol™ used to determine the MIC and microtitre plate biofilm formation assay. These factors may explain the reason for the higher concentrations required to inhibit bacterial growth when a surface is coated with Byotrol™.

As the Byotrol™ formulation was the compound that demonstrated the greatest antimicrobial activity of the compounds tested in this study, this was taken forward for proteomic and transcriptomic analysis against *E. coli* K12. This further investigation would elucidate the effect that Byotrol™ has on the transcription and translation by bacteria, that is related to bacterial growth, metabolism and survival.

Chapter 5

Proteomic analysis of the *E. coli* K12 in response to Byotrol™

5. 1. Proteomic analysis of *E. coli* K12

Proteomics is the large scale study of the structure, function and interactions of proteins in a cell (Tyers & Mann, 2003). Unlike genomic and transcriptomics analysis, the analysis of a bacterial cell's proteome is the most accurate and direct method to yield a picture of that organism's living state at a given time point, under specific conditions (Lubec *et al.*, 1999).

5. 1. 2. Two-dimensional gel electrophoresis (2DGE)

The 2DGE technique enables the separation of a large number of proteins from the whole bacterial cell to a unique spot in the acrylamide gel that is related to its mass and charge. The protein can then be excised and identified by mass spectrometry. 2DGE also offers the advantage of easy identification of multiple post-translational modifications of a protein, seen as a 'spot train' on gels (Suh *et al.*, 2008).

5. 1. 2. 1. Isoelectric focussing: the separation of proteins in the first dimension

In the first dimension, proteins migrate through a strip of acrylamide gel along which is a pH gradient. Electrolytes are added to assist protein migration. A protein, which is in a pH range below its *pI* will be positively charged and will migrate to the cathode, and a negatively charged protein will migrate towards the electrode. Once the protein reaches its *pI*, or the point at which the net charge of the protein is zero, it will cease to migrate. In this way the proteins are separated according to their *pI* in the first dimension.

5. 1. 2. 2. SDS PAGE: the separation of proteins in the second dimension

In the second dimension, proteins are separated at 90° to the first dimension. The protein complexes are denatured by SDS (sodium dodecyl sulphate), which also gives all of the proteins a net negative charge, so when a current is passed through the gel, the proteins will migrate to the cathode. Separation of proteins in this dimension is based on the mass of the protein. This method of protein resolution maximises the separating power of 2DGE to identify the largest possible number of proteins extracted from the bacterial cell.

5. 1. 2. 3. *Visualisation of resolved proteins*

There are 3 common ways to visualise proteins. The first is the colloidal Coomassie blue staining which has a detection limit of approximately 50 ng protein, it is the least sensitive stain used. The second is silver staining, which can detect proteins with 10-100 fold greater sensitivity than Coomassie blue staining. Finally, a molecular probe based dye, Sypro[®] Ruby, allows for fluorescence detection of proteins and is the most sensitive of the 3 stains. Sypro[®] Ruby can enable visualisation of even very low concentrations of proteins with a lower detection limit of 0.25 – 1 ng protein. Sypro[®] Ruby staining also has a wider linear dynamic range for better quantification (Berggren *et al.*, 2000). Silver staining is used in this study for its higher sensitivity than Coomassie blue staining at a relatively low cost in relation to Sypro[®] Ruby stain.

In this chapter, the application of 2DGE to study the differential expression of proteins between *E. coli* K12 isolates in the biofilm and planktonic phenotypic states will be discussed. Byotrol[™] was determined to be the most successful inhibitor of *E. coli* K12 bacterial growth (Chapter 4); therefore both the biofilm and planktonic phenotypes were studied with and without the treatment of Byotrol[™] at sub-minimum inhibitory concentrations (sub-MIC) at 24 hours growth. The expression of proteins from the planktonic phenotype was also studied at mid-exponential phase (5 hours growth) as this was when cells were most actively growing. The different growth conditions described for proteomic analysis in this chapter are summarised diagrammatically in Figure 5. 1.

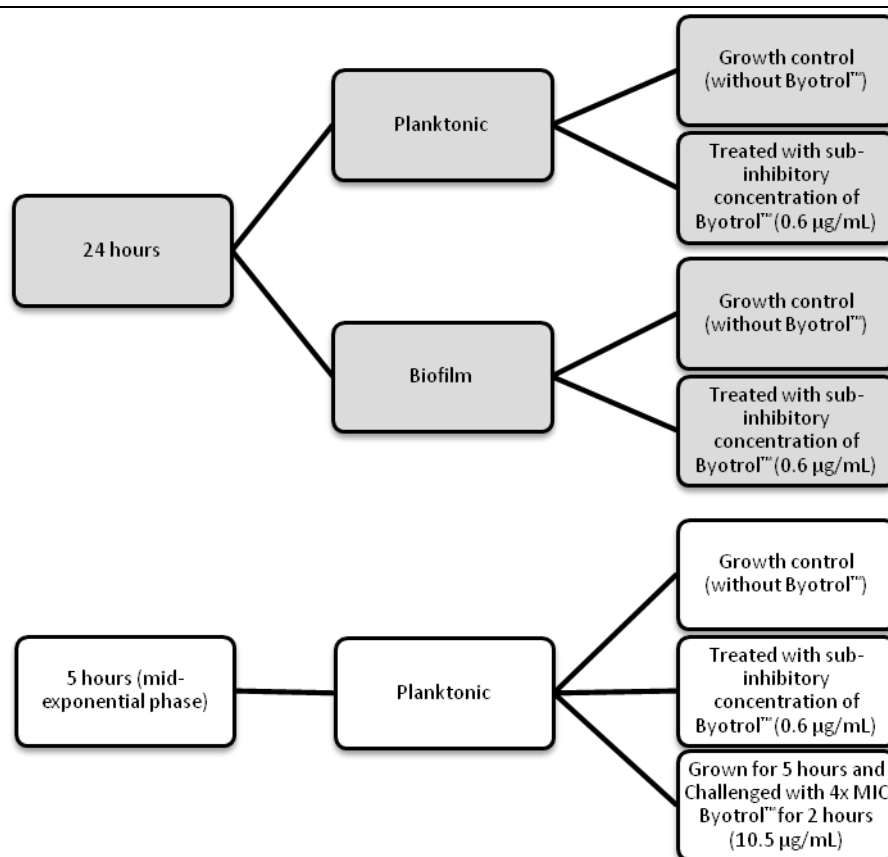


Figure 5. 1. Diagram outlining the growth conditions for *E. coli* K12 cells from which proteins were extracted for analysis.

5. 2. Optimisation of 2DGE

Optimisation of the 2DGE method was imperative in order to obtain reproducible gels. The factors optimised were the extraction buffer, the IPG strips for first dimension separation and the percentage SDS-polyacrylamide gel.

5. 2. 1. Optimisation to reduce horizontal protein streaking and increased protein resolution in 2DGE

In the early separations, a large accumulation of protein at the anode was observed along with significant horizontal streaking (Figure 5. 2 and Figure 5. 3 a). Dithiothreitol (DTT), although required for efficient protein resolution, can have an adverse effect if the concentration is not optimised. DTT is a reducing agent for 2DGE, used in the rehydration buffer and prior to alkylation, as it cleaves the inter-molecular disulfide bonds, thereby achieving protein unfolding (Gundry *et al.*, 2009). To ascertain the optimum concentration of DTT to use in the rehydration buffer that is used to extract

bacterial whole cell protein, a range of DTT concentrations were investigated. The proteins extracted were then subjected to IEF on individual 17 cm, pH 3-10 IPG strips (Figure 5. 2). 1.0 – 0.1% DTT did not facilitate complete separation of proteins in the first dimension. 0.05% DTT concentration allowed for the greatest resolution of proteins.

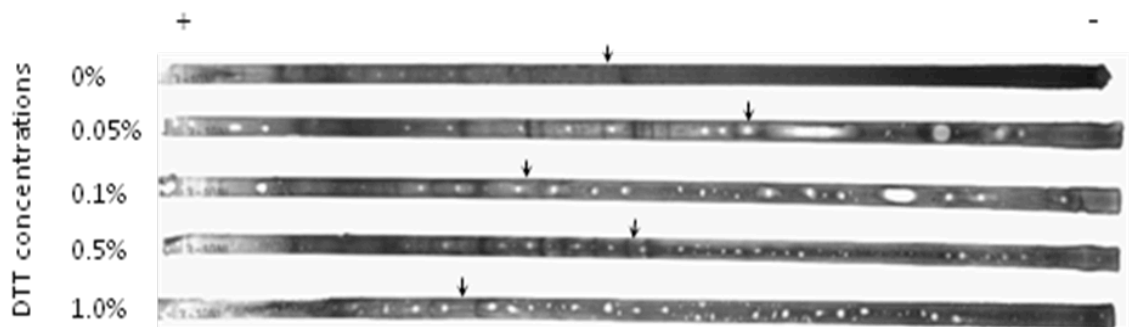


Figure 5. 2. Optimisation of the DTT concentration used for protein extraction. 200 μg of protein extracted from planktonic cells grown for 24 hours using an extraction buffer with a range of DTT concentrations were resolved on 17 cm, pH 3-10 IPG strips. Arrows indicates the furthest distance to which the proteins are resolved.

The second dimension separation was performed to determine if the 0.05% DTT concentration reduced horizontal streaking in the SDS-polyacrylamide gel. A comparison between proteins extracted in a buffer with 1.0% DTT and a buffer with 0.05% DTT is demonstrated in Figure 5. 3.

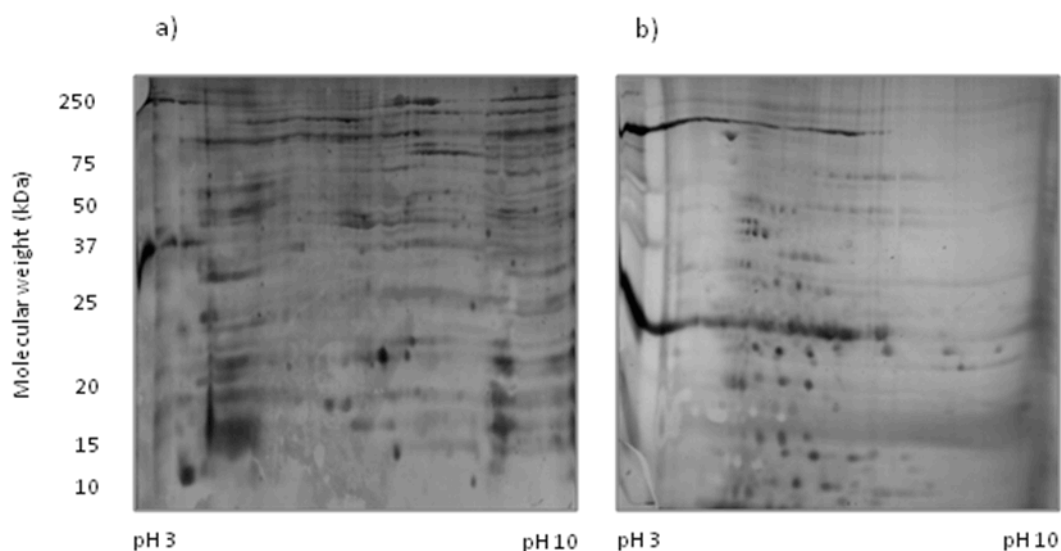


Figure 5. 3. 2DGE optimisation of DTT concentration.

a) proteins extracted with 1.0% DTT. **b)** proteins extracted with 0.05% DTT. 200 μg of protein extracted from planktonic cells grown for 24 hours, resolved by isoelectric focussing on a 17 cm, pH 3-10 IPG strip and then on a 10% SDS-PAGE gel. Proteins were visualised by silver staining.

It is clear that the reduced concentration of DTT reduced horizontal protein streaking; therefore 0.05% DTT concentration was used in the rehydration buffer for all future protein extractions. The dark horizontal streaks that can be seen in Figure 5. 3 b) are due to excess protein marker loading.

5. 2. 2. Optimisation of IPG strip pH range

Although the 0.05% DTT facilitated the best resolution in the first dimension on the pH 3-10 IPG strip, the proteins still did not migrate along the maximum length of the strip to the highest pH (pH 10). Two gels that demonstrate how proteins are more concentrated around a narrow pH range, are shown in Figure 5. 4. A majority of the proteins, which were focussed over the pH 3-10 range and resolved in the second dimension separation, had an iso-electric point within the pH 5-8 range. An IPG strip with a pH 5-8 range has greater resolving power and therefore would increase the number of protein spots that are able to be visualised. For these reasons, 17 cm IPG strips with a narrow pH range of 5-8 were used in future protein separations. In most cases proteins are visible up to approximately 100 kDa in the second dimension.

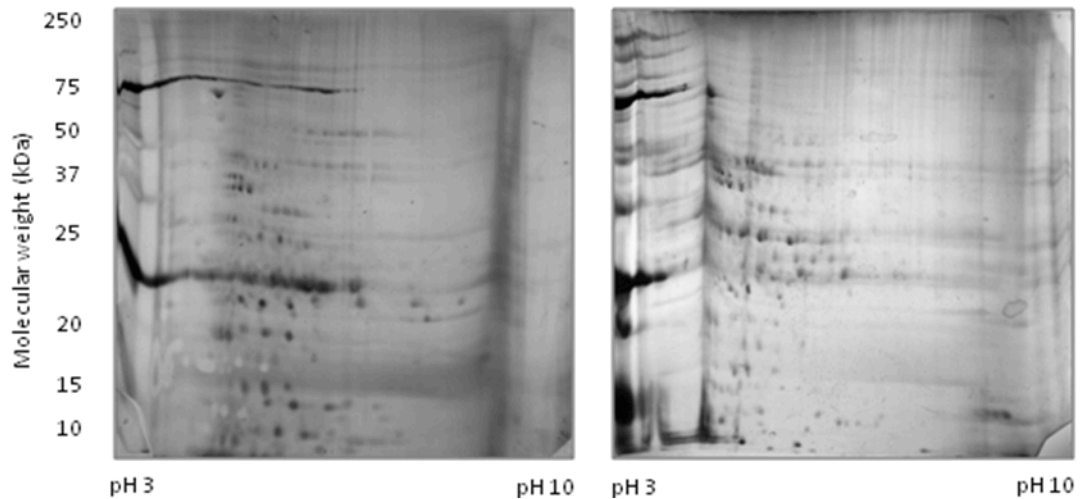


Figure 5. 4. 2DGE of proteins using 17 cm, pH 3-10 IPG strips. 200 μ g of protein extracted from planktonic cells grown for 24 hours, resolved by isoelectric focussing and then on a 10% SDS-PAGE gel. Proteins were visualised by silver staining. Each gel represents a separate biological replicate.

5. 3. Proteomic comparison of planktonic and biofilm cells grown for 24 hours (growth controls)

Proteins were extracted from *E. coli* K12 planktonic cells and biofilm cells both grown for 24 hours. As these were growth controls, they were grown in the absence of Byotrol™. Figure 5. 5 shows a comparison between 3 replicate gels for each of the two phenotypes. The gels demonstrated that there was good overall reproducibility between biological and technical replicates. Reproducibility is critical for an accurate comparison of differentially expressed proteins.

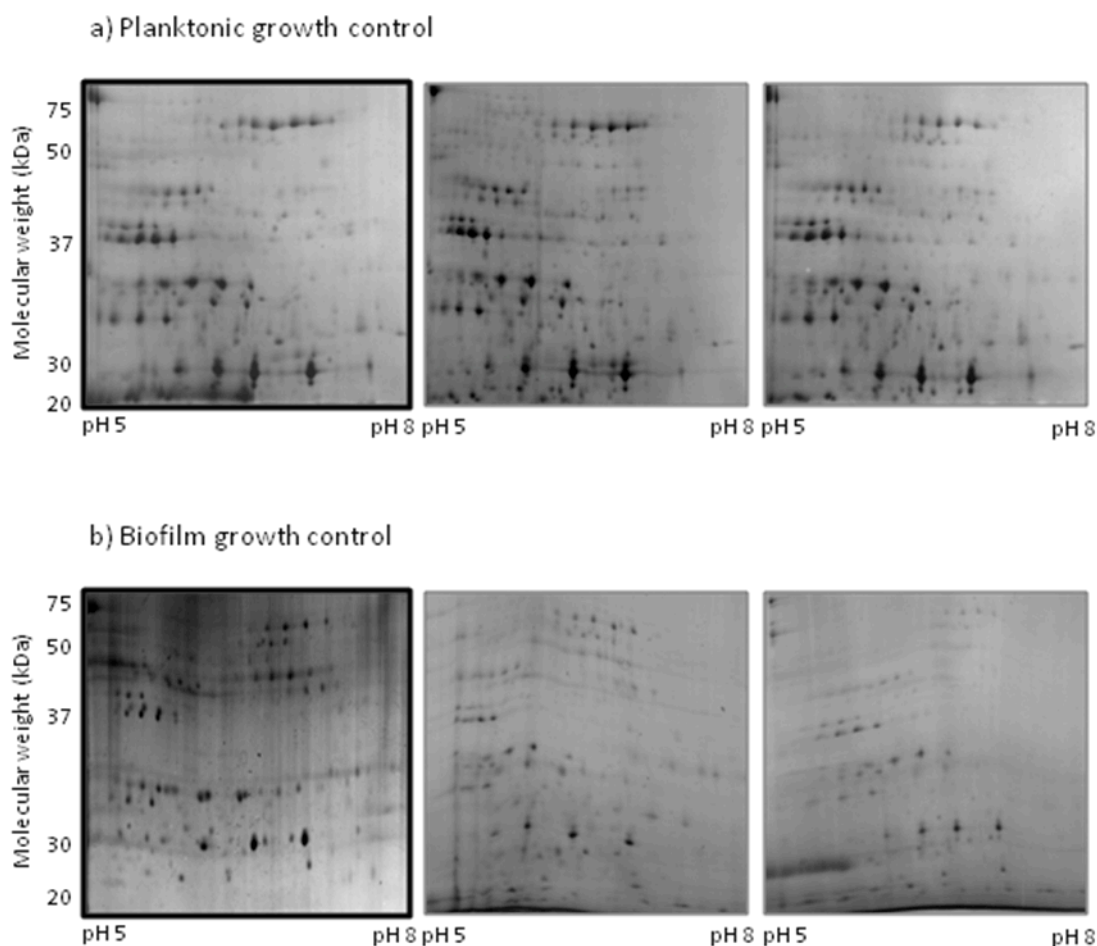


Figure 5. 5. Replicate gels displaying resolved proteins extracted from planktonic and biofilm cells of *E. coli* K12 demonstrate reproducibility.

a) 3 replicate gels of proteins extracted from planktonic cells grown for 24 hours (growth control); **b)** 3 replicate gels of proteins extracted from biofilm cells grown for 24 hours (growth control). All proteins were separated using iso-electric focussing in the first dimension, 10% SDS-PAGE in the second dimension and visualised by silver staining.

A comparison between the two phenotypes, shown in Figure 5. 5, revealed several proteins that were differentially expressed between bacteria in the planktonic phenotype and biofilm phenotype grown for 24 hours. Representative gels from Figure 5. 5 are enlarged in Figure 5. 6 for a clearer visualisation of the differentially expressed proteins. Differentially expressed proteins of the planktonic and biofilm phenotypes are labelled with numbered white arrows, which correspond to the protein name as described in Table 5. 1. Circled proteins are landmark proteins used to orientate the gels and for reference points. The landmark protein identified is phosphoglycerate kinase (labelled ‘a’ on the figures). For all of the gels, any small differences in expression levels are not

statistically significant when using the Student's unpaired *t*-test. The areas where differentially expressed proteins are situated in the gels are highlighted in the white boxed areas and are enlarged in Figure 5. 7 and Figure 5. 8 for a more clear visualisation of the differentially expressed proteins.

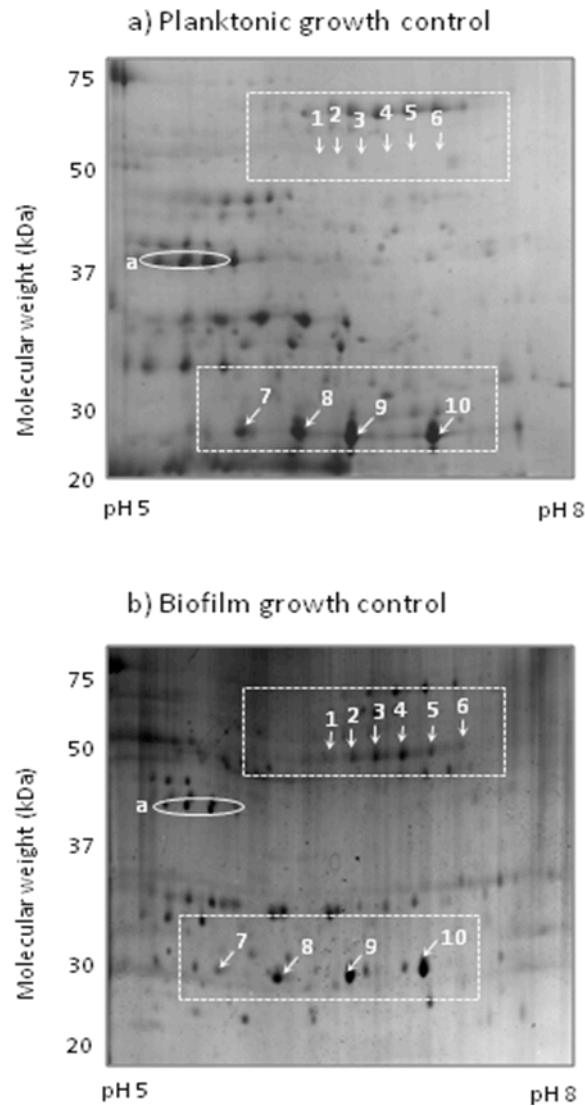


Figure 5. 6. Identification of differentially expressed proteins extracted from the growth controls of the planktonic and biofilm phenotypes of *E. coli* K12: **a)** proteins extracted from planktonic cells grown for 24 hours (growth control); **b)** proteins extracted from biofilm cells grown for 24 hours (growth control). Numbered white arrows indicate proteins which are differentially expressed. Proteins in the white circle (a) are landmark proteins.

The identification of differentially expressed proteins was achieved by mass spectrometry. The results are presented in Table 5. 1. The greater the number of peptides that match a protein, the higher the chances are that the protein identification is accurate. The standard practice is to assume that greater than 2 matched peptides are considered fully identified. A working group for the standardisation of protein identification have acknowledged that this method is, in most cases, likely to generate true positive results (Carr *et al.*, 2004). The proteins identified as differentially expressed between the planktonic and biofilm phenotypes were tryptophanase and D-ribose binding periplasmic protein. As with all of the proteins identified in this study, by comparing the experimental *pI* (isoelectric point) and molecular weight (Mw) with the predicted *pI* and Mw, a confirmation of protein identity can be made. These results showed a good correlation between the experimental and predicted *pI* and Mw in all of the proteins identified. The range for the experimental *pI* is due to the different isoforms of the protein.

Table 5. 1. The identification of differentially expressed proteins by mass spectrometry. Proteins were identified after extraction from the planktonic and biofilm phenotypes of *E. coli* K12 grown for 24 hours. The protein label corresponds to numbering in the gels in Figure 5. 7 and Figure 5. 8. The protein name and accession number were taken from a search on the UniProt *E. coli* K12 database. The number of matched peptides were derived from the number of peptides which accurately matched the protein sequence, a number >2 is considered to be fully identified. The predicted *pI* (isoelectric point) and *Mw* (molecular weight) were derived from the Compute *pI/Mw* tool (ExpASy, SIB Bioinformatics Resource Portal). The experimental *pI* and *Mw* were derived from the gels.

Protein Label	Protein name (UniProt accession number)	Number of matched peptides	Predicted/ Experimental <i>pI</i>	Predicted/ Experimental <i>Mw</i> (Da)
1-6	Tryptophanase (TNA _A _ECOLI)	6, 8, 12, 9, 10, 7 respectively	5.88/ ~6.2-7	52773.46/ ~50000
7-10	D-ribose binding periplasmic protein (RBSB_ECOLI)	12, 16, 12, 15 respectively	6.85/ ~6-6.8	30950.48/ ~22000

Figure 5. 7 and Figure 5. 8 show the enlarged detail of regions with differentially expressed proteins from Figure 5. 6. The differentially expressed proteins were quantified and the results are represented in Table 5. 2.

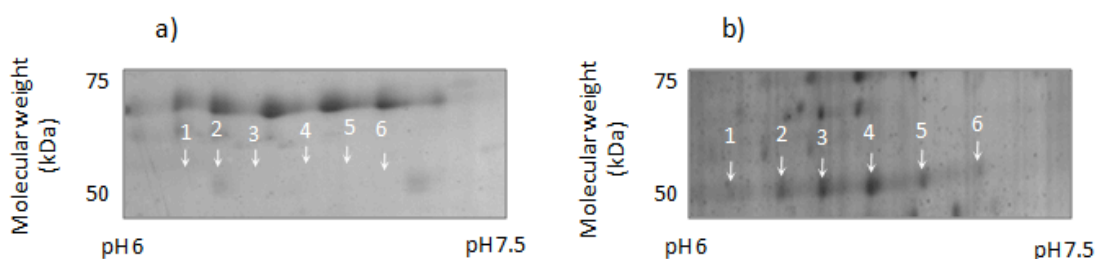


Figure 5. 7. The enlarged detail of tryptophanase up-regulated in the biofilm phenotype when compared to the planktonic phenotype of *E. coli* K12: **a)** tryptophanase extracted from planktonic cells grown for 24 hours; **b)** tryptophanase extracted from biofilm cells grown for 24 hours. Differentially expressed proteins are indicated with numbered arrows.

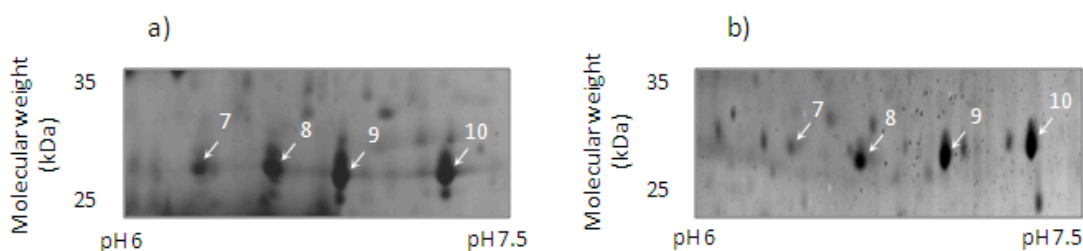


Figure 5. 8. The enlarged detail of D-ribose periplasmic binding protein down-regulated in the biofilm phenotype when compared to the planktonic phenotype of *E. coli* K12: **a)** D-ribose periplasmic binding protein extracted from planktonic cells grown for 24 hours; **b)** D-ribose periplasmic binding protein extracted from biofilm cells grown for 24 hours. Differentially expressed proteins are indicated with numbered arrows.

For all differentially expressed proteins identified in this study, a statistical comparison was performed using the unpaired *t*-test as described in Section 2. 21. 16. *t*-values <0.05 were considered to be statistically different, thereby disproving the null hypothesis which states that protein expression for the two phenotypes or the different conditions, are not different.

Tryptophanase was up-regulated in the planktonic phenotype grown for 24 hours, D-ribose binding periplasmic protein was down-regulated in the same phenotype.

Table 5. 2. Statistical analysis of differentially expressed proteins extracted from the planktonic and biofilm phenotypes of *E. coli* K12 grown for 24 hours. Protein labels correspond to numbering in Figure 5. 7 and Figure 5. 8. The fold induction and repression of proteins in the biofilm phenotype is calculated by using the integrated density values of proteins differentially expressed in the biofilm growth control in relation to the planktonic growth control. *t*-values were calculated using the unpaired two-tailed *t*-test. A *t*-value of <0.05 is considered statistically significant.

Protein Label	Protein name	Integrated density value		Fold induction (+)/ repression (-)	<i>t</i> -value
		Planktonic growth control	Biofilm growth control		
	Landmark protein	57838	58741	1.02	0.93
1-6	Tryptophanase	-6351	11368	-1.8 (+)	<0.0001
7-10	D-ribose binding periplasmic protein	62858	28058	0.4 (-)	<0.0001

5. 4. Proteomic comparison of planktonic cells grown with and without Byotrol™ (growth control) for 24 hours.

Proteins were extracted from *E. coli* K12 planktonic cells grown with and without Byotrol™ (Figure 5. 9). Planktonic cells grown with Byotrol™ were treated with a sub-minimum inhibitory concentration (sub-MIC) of Byotrol™ (0.6 µg/mL) for 24 hours at 37°C (Figure 5. 9 b). Figure 5. 9 shows a comparison of 3 replicate gels for each of the growth conditions. The gels demonstrated that there was good reproducibility between replicates. Representative gels are enlarged in Figure 5. 10 for a clearer visualisation of differentially expressed proteins.

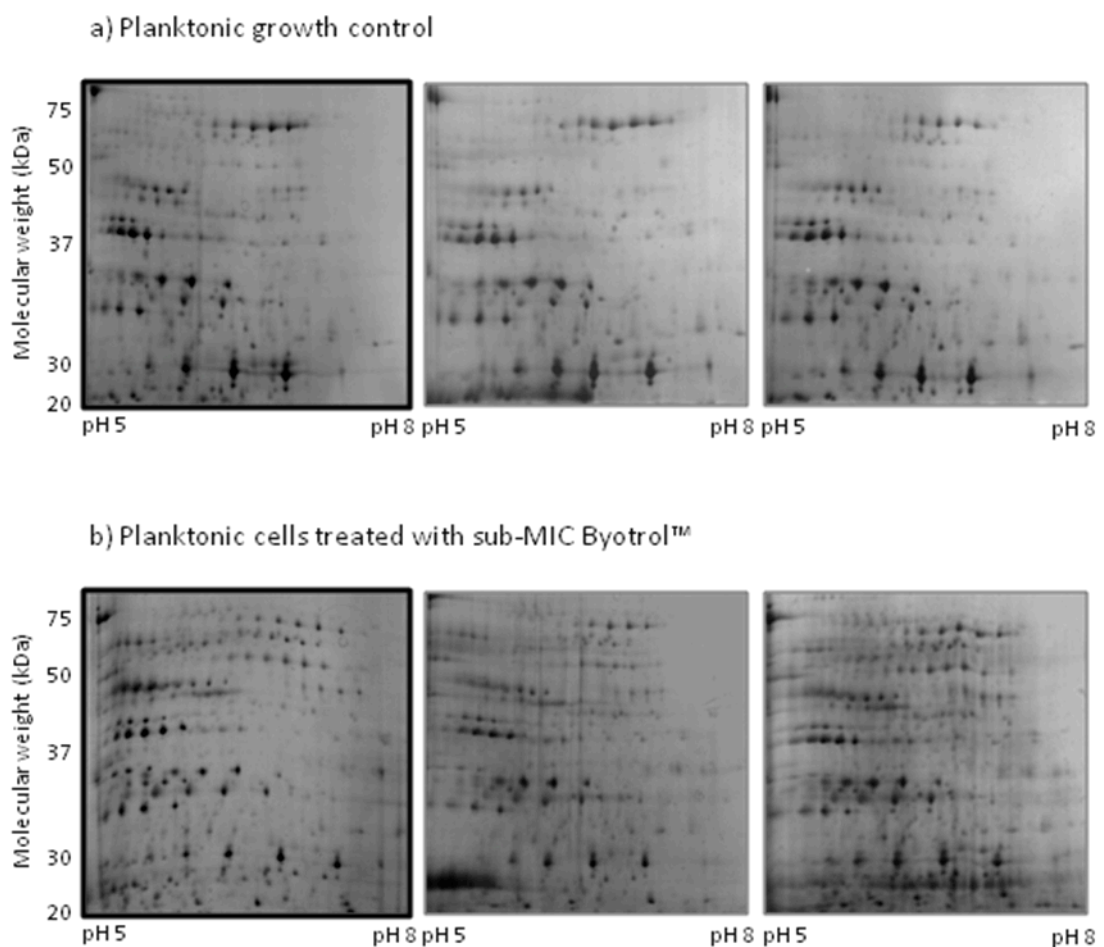


Figure 5. 9. Replicate gels displaying resolved proteins extracted from planktonic cells of *E. coli* K12 grown **a)** without Byotrol™ (growth control) and **b)** with sub-MIC Byotrol™ 24 hours. All proteins were separated using iso-electric focussing in the first dimension and 10% SDS-PAGE in the second dimension and visualised by silver staining.

A comparison between the 2 growth conditions shown in Figure 5. 9 revealed differentially expressed proteins in the planktonic phenotype with and without Byotrol[™]. Numbered white arrows correspond to the protein name as described in

Table 5. 3. Circled proteins are landmark proteins (labelled 'a' on the figures). The white boxed areas with differentially expressed proteins are enlarged in Figure 5. 11 and Figure 5. 12.

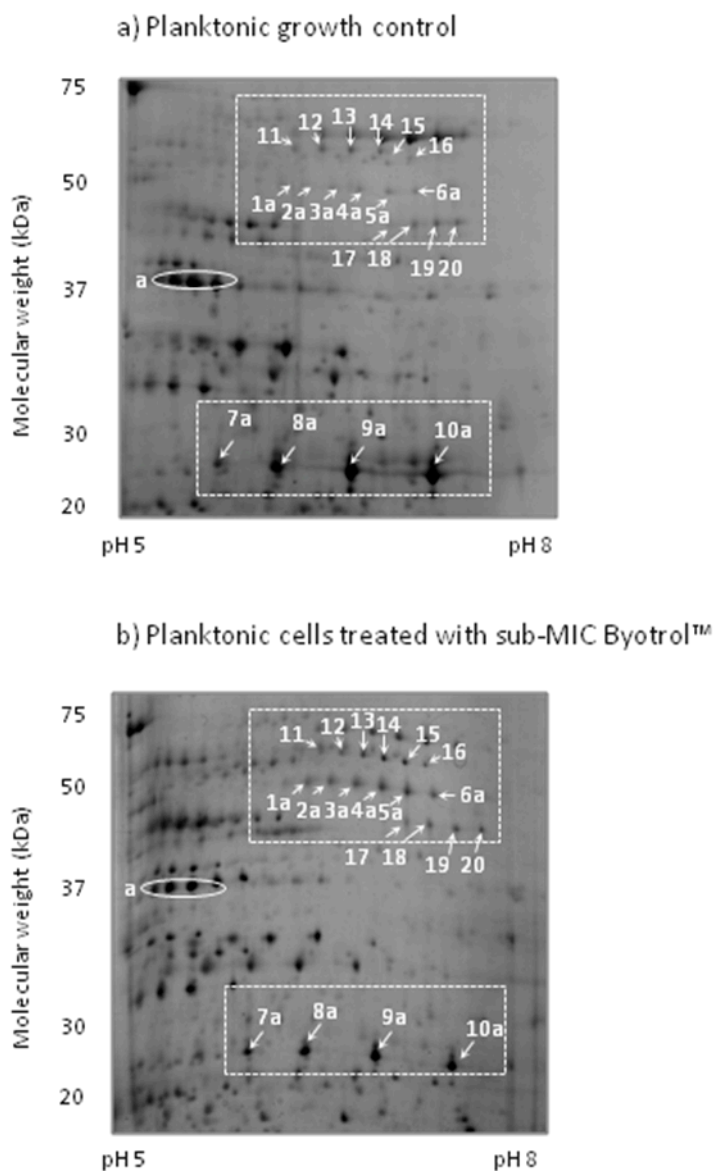


Figure 5. 10. Identification of differentially expressed proteins extracted from planktonic cells grown for 24 hours **a)** without Byotrol™ (growth control) and **b)** treated with Byotrol™. Numbered white arrows indicate differentially expressed proteins. Proteins in the white circle (a) are landmark proteins.

Differentially expressed proteins identified by mass spectrometry were tryptophanase, D-ribose binding periplasmic protein, dihydrolipoyl dehydrogenase and serine hydroxymethyltransferase (Table 5. 3). There was a good correlation between the predicted and experimental *pI* and *M_w*, therefore confirming protein identity. The range for the experimental *pI* is likely to be due to the different isoforms of the protein.

Table 5.3. Identification of differentially expressed proteins by mass spectrometry. Proteins were identified from 2DGE analysis of the planktonic phenotypes of *E. coli* K12 grown with and without Byotrol™ for 24 hours. The protein label corresponds to numbering in the gels in Figure 5. 10. The protein name and accession number were taken from a search on the UniProt *E. coli* K12 database. The number of matched peptides were derived from the number of peptides which accurately matched the protein sequence, a number >2 is considered to be fully identified. The predicted pI (isoelectric point) and Mw (molecular weight) were derived from the Compute pI/Mw tool (ExpASY, SIB Bioinformatics Resource Portal). The experimental pI and Mw were derived from the gels.

Protein Label	Protein name (UniProt accession number)	Number of matched peptides	% coverage	Predicted/ Experimental pI	Predicted/ Experimental Mw (Da)
1a-6a	Tryptophanase (TNAA_ECOLI)	6, 8, 12, 9, 10, 7	9-18%	5.88/ ~6.2-7	52773.46/ ~50000
7a-10a	D-ribose binding periplasmic protein (RBSB_ECOLI)	12, 16, 12, 15	35-57%	6.85/ ~6-6.8	30950.48/ ~22000
11-16	Dihydrolipoyl dehydrogenase (DLDH_ECOLI)	5-12	11-26%	5.79/ ~6	50688.49/ ~50000
17-20	Serine hydroxymethyl-transferase (D3QN42_ECOC B)	8-10	17-19%	6.03/ ~6.5	45316.59/ ~43000

Differentially expressed proteins in Figure 5. 10 were highlighted in the white boxed areas and enlarged in Figure 5. 11 and Figure 5. 12 for closer visualisation. The differentially expressed proteins were quantified statistically and described in Figure 5. 5.

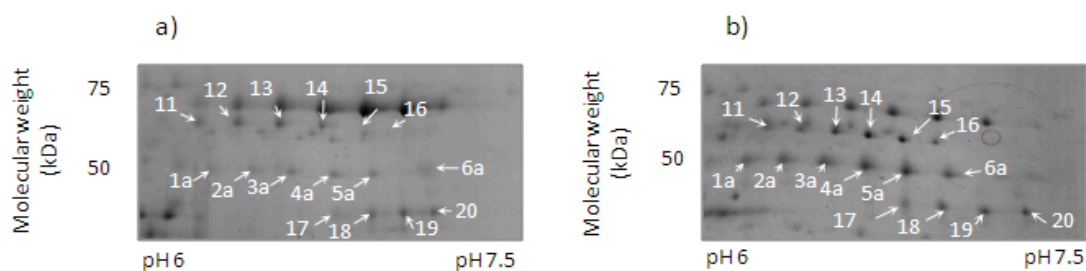


Figure 5. 11. The enlarged detail of up-regulated proteins identified in the planktonic phenotype of *E. coli* K12 grown for 24 hours when **a)** treated with Byotrol™, compared to **b)** *E. coli* K12 planktonic cells grown without Byotrol™ (growth control). Numbered white arrows indicate proteins which are differentially expressed.

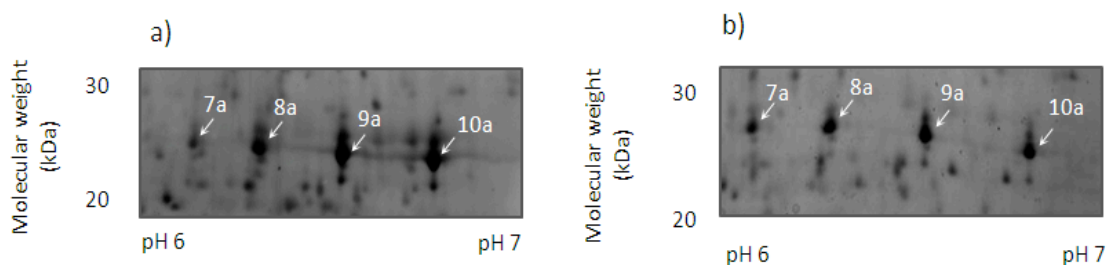


Figure 5. 12. The enlarged detail of down-regulated proteins identified in the planktonic phenotype of *E. coli* K12 cells grown for 24 hours **a)** without Byotrol™ (growth control) and **b)** treated with Byotrol™. Numbered white arrows indicate proteins which are differentially expressed.

Statistical analysis confirmed that the identified proteins were all up-regulated in the planktonic phenotype treated with sub-MIC Byotrol™ for 24 hours, with the exception of D-ribose binding periplasmic protein which was down-regulated (Table 5. 4).

Table 5. 4. The statistical analysis of differentially expressed proteins extracted from the planktonic phenotypes of *E. coli* K12 grown with and without Byotrol™ for 24 hours.

Protein labels correspond to numbering in Figure 5. 11 and Figure 5. 12. The fold induction and repression of proteins in the planktonic phenotype were calculated by using the integrated density values of proteins differentially expressed under the two conditions. *t*-values were calculated using the unpaired two-tailed *t*-test. A *t*-value of <0.05 is considered statistically significant.

Protein Label	Protein name	Integrated density value		Fold induction (+)/repression (-)	<i>t</i> -value
		Planktonic growth control	Planktonic treated with Byotrol™		
	Landmark protein	57838	30172	0.52	0.09
1a-6a	Tryptophanase	-5025	25636	-5.1 (+)	<0.0001
7a-10a	D-ribose binding periplasmic protein	68861	101529	1.5 (+)	<0.0001
11-16	Dihydrolipoyl dehydrogenase	3746	21467	5.7 (+)	0.003
17-20	Serine hydroxymethyl-transferase	2784	17139	6.2 (+)	0.004

5. 5. Proteomic comparison of planktonic and biofilm cells treated with sub-MIC Byotrol™ for 24 hours

Proteins were extracted from *E. coli* K12 planktonic cells and biofilm cells treated for 24 hours with sub-MIC Byotrol™. Figure 5. 13 shows a comparison between a minimum of 3 replicate gels for each of the growth conditions. The gels demonstrated that there is good overall reproducibility between biological and technical replicates. Representative gels are enlarged in Figure 5. 14.

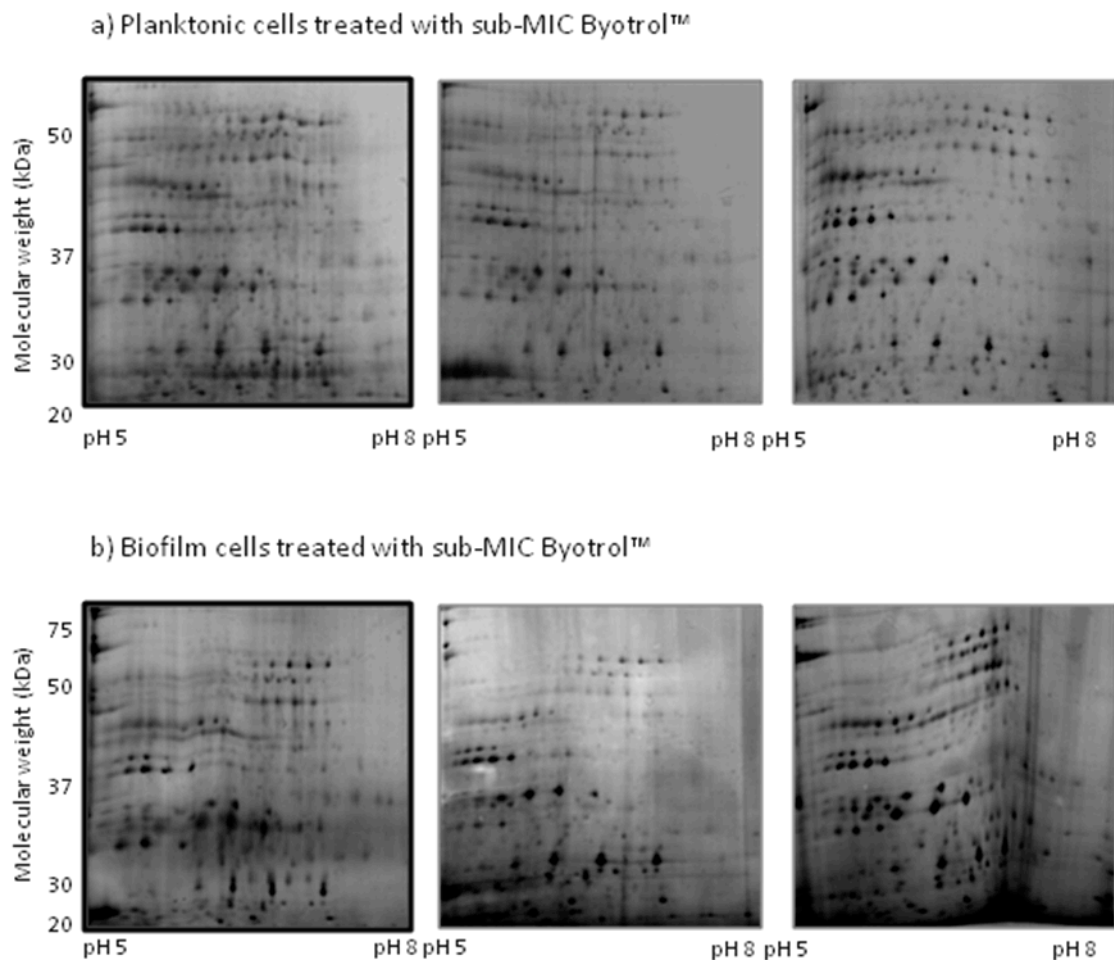


Figure 5. 13. Replicate gels displaying resolved proteins extracted from **a)** planktonic and **b)** biofilm cells of *E. coli* K12 treated with sub-MIC Byotrol™ for 24 hours. All proteins were separated using iso-electric focussing in the first dimension, 10% SDS-PAGE in the second dimension and visualised by silver staining.

Figure 5. 14 shows differentially expressed proteins between the planktonic and biofilm phenotypes treated with sub-MIC Byotrol™ grown for 24 hours. The proteins that were consistently differentially expressed across 3 replicate gels are annotated with numbered white arrows. Circled proteins are landmark proteins (labelled 'a' on the figures). Differentially expressed proteins are highlighted in the white boxes and are enlarged in Figure 5. 15 for closer visualisation.

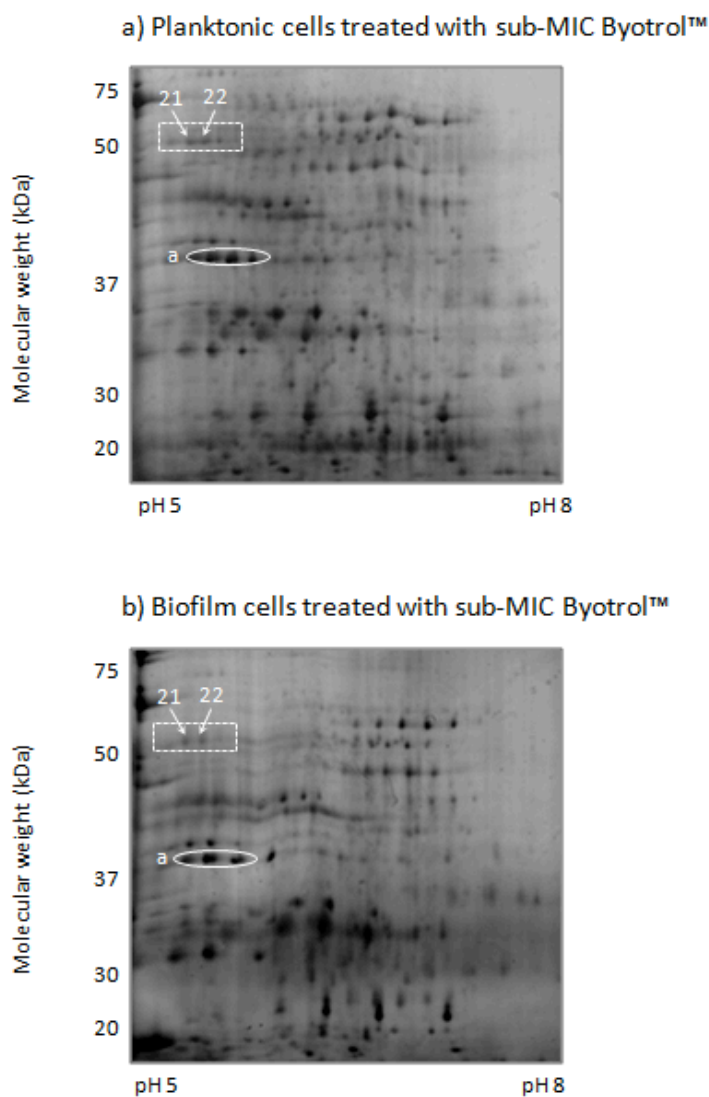


Figure 5. 14. Identification of differentially expressed proteins extracted from **a)** planktonic and **b)** biofilm cells treated with sub-MIC Byotrol™ for 24 hours. Numbered white arrows indicate proteins which are differentially expressed. Proteins in the white circle (a) are landmark proteins.

Proteins were identified by comparing the experimental *pI* and Mw with the predicted *pI* and Mw. Table 5. 5 shows that there is good correlation between the experimental and predicted *pI* and Mw in all of the proteins identified. The differentially expressed proteins were quantified statistically and described in Table 5. 6.

Table 5. 5. The identification of differentially expressed proteins by mass spectrometry. Proteins were identified from 2DGE analysis of the planktonic and biofilm phenotypes of *E. coli* K12 grown for 24 hours. The protein label corresponds to numbering in the gels in Figure 5. 14. The protein name and accession number were taken from a search on the UniProt *E. coli* K12 database. The number of matched peptides were derived from the number of peptides which accurately matched the protein sequence, a number >2 is considered to be fully identified. The predicted pI and Mw (molecular weight) were derived from the Compute pI /Mw tool (ExPASy, SIB Bioinformatics Resource Portal). The experimental pI and Mw were derived from the gels.

Protein Label	Protein name (UniProt accession number)	Number of matched peptides	% coverage	Predicted/ Experimental pI	Predicted/ Experimental Mw (Da)
21, 22	Lactaldehyde dehydrogenase (ALDA_ECOLI)	16, 2	5%, 35%	5.07/ ~5	52272.79/ ~55000



Figure 5. 15. The enlarged detail of lactaldehyde dehydrogenase up-regulated in **a)** planktonic cells of *E. coli* K12 when compared to **b)** biofilm cells treated with sub-MIC Byotrol™ for 24 hours. Numbered white arrows indicate differentially expressed proteins.

Table 5. 6 shows that lactate dehydrogenase was down-regulated in the biofilm phenotype treated with sub-MIC Byotrol™ for 24 hours.

Table 5. 6. The statistical analysis of differentially expressed proteins extracted from the planktonic and biofilm phenotypes of *E. coli* K12 treated with sub-MIC Byotrol™ for 24 hours.

Protein labels correspond to numbering in Figure 5. 15. The fold induction and repression of proteins in the biofilm phenotype were calculated by using the integrated density values of proteins differentially expressed under the two conditions. *t*-values were calculated using the unpaired two-tailed *t*-test. A *t*-value of <0.05 is considered statistically significant.

Protein Label	Protein name	Integrated density value		Fold induction (+)/repression (-)	<i>t</i> -value
		Planktonic treated with Byotrol™	Biofilm treated with Byotrol™		
	Landmark protein	50321	36122	0.72	0.22
21, 22	Lactaldehyde dehydrogenase	27405	9309	3 (-)	0.01

5. 6. Proteomic comparison of planktonic cells grown to mid-exponential phase (5 hours), with and without Byotrol™

Proteins were extracted from planktonic cells of *E. coli* K12 grown to mid-exponential phase (5 hours) and treated for 5 hours with sub-MIC Byotrol™ (0.6 µg/mL). Planktonic cells were also grown for 5 hours and challenged for 2 hours with 4 times the MIC of Byotrol™ (10.5 µg/mL). This was performed to allow comparison with the experiments described in Chapter 6, where RNA extracted from these same cells grown under the same conditions have been analysed to identify differentially expressed genes.

Figure 5. 16 shows a comparison between 3 replicate gels for each of the growth conditions, of which representative gels are enlarged in Figure 5. 17. The gels demonstrated good overall reproducibility between biological and technical replicates. Proteins identified as differentially expressed across the replicates are annotated with numbered white arrows. Circled proteins are landmark proteins (labelled 'a' on the figures). Differentially expressed proteins were situated in the gels are highlighted in the white boxed areas and are enlarged in Figure 5. 18 and Figure 5. 19 for closer visualisation of the differentially expressed proteins.

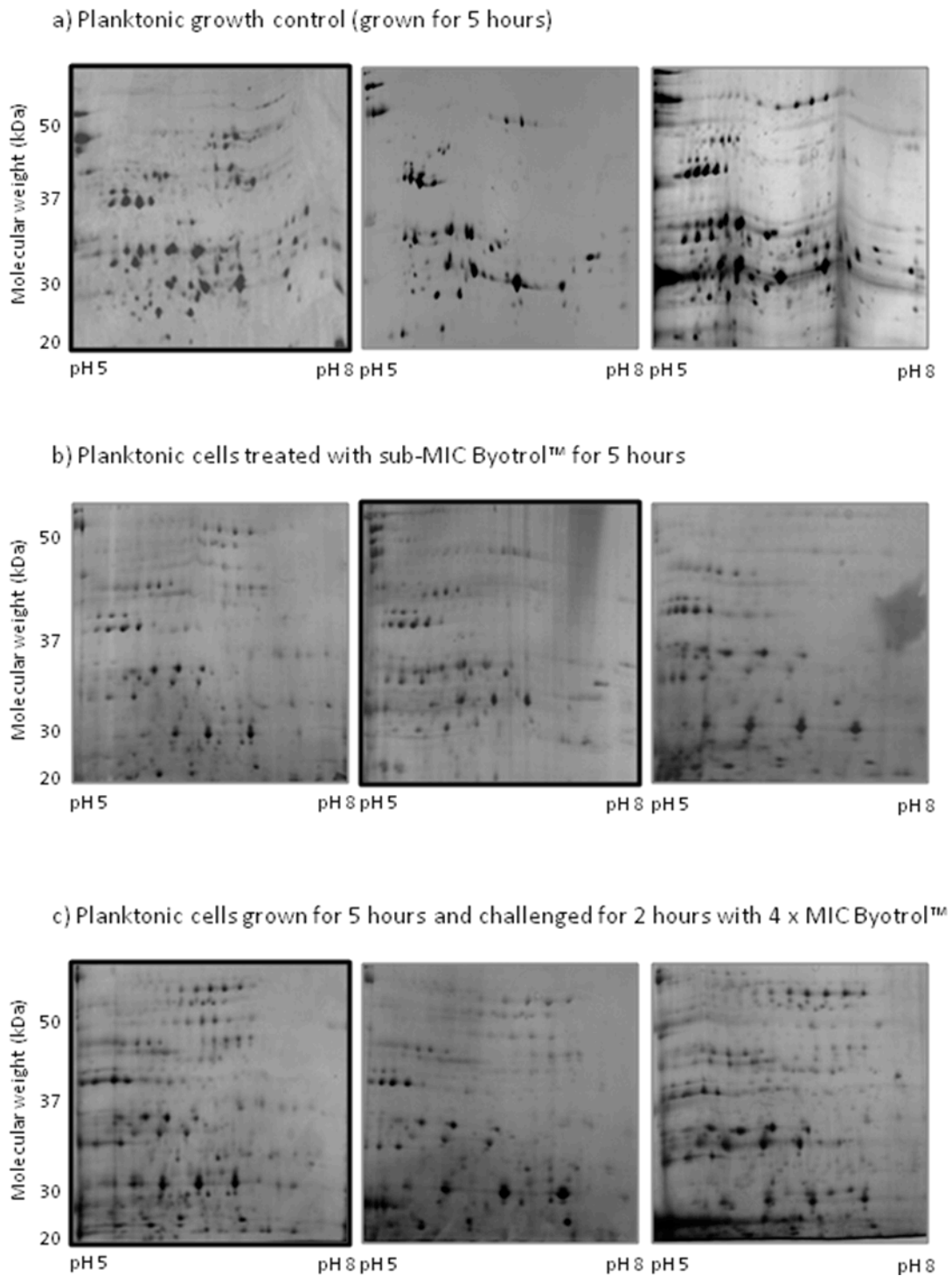


Figure 5. 16. Replicate gels displaying resolved proteins extracted from the planktonic phenotype of *E. coli* K12 grown under 3 conditions: **a)** growth to mid-log phase (5 hours); **b)** growth treated with sub-MIC Byotrol™ (0.6 µg/mL) for 5 hours; **c)** growth for 5 hours, challenged for 2 hours with 4 times MIC Byotrol™ (10.5 µg/mL). All proteins were separated using iso-electric focussing in the first dimension, 10% SDS-PAGE in the second dimension and visualised by silver staining.

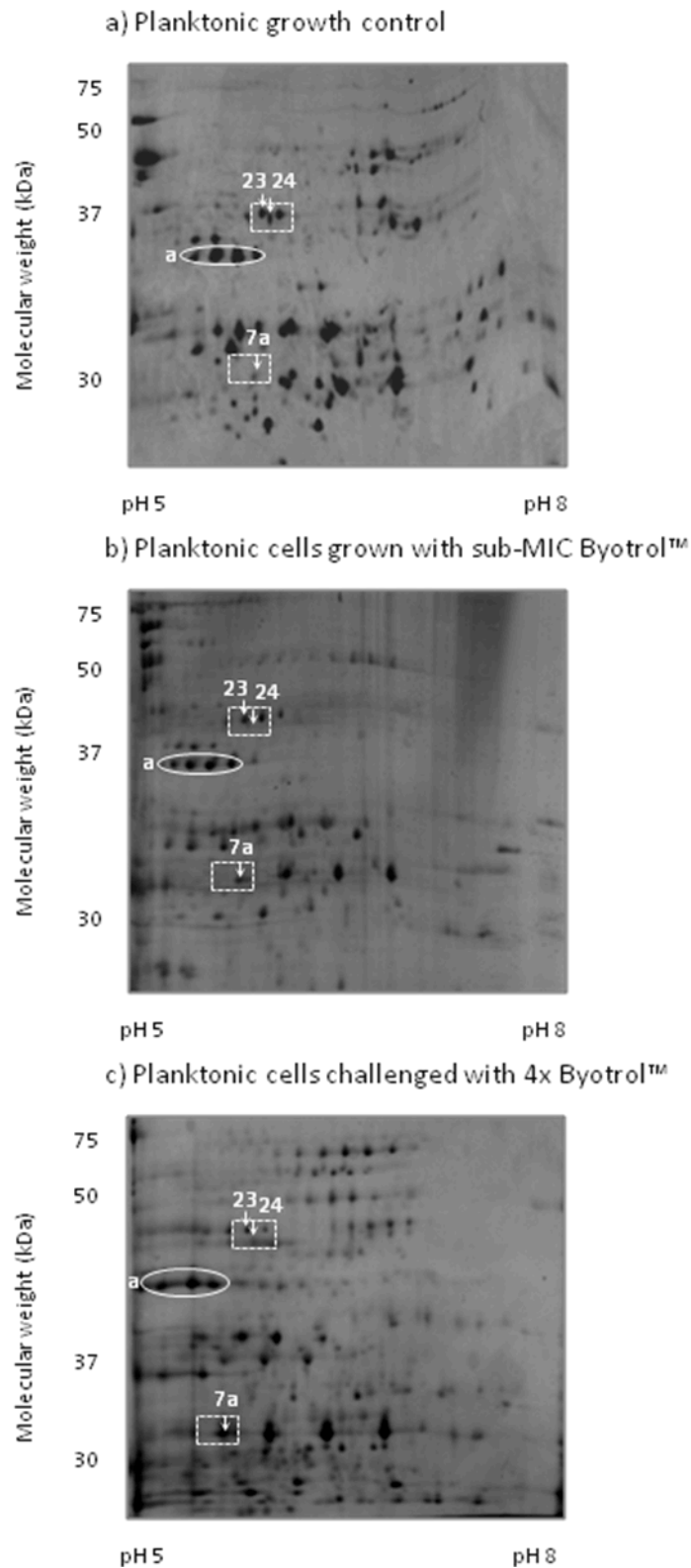


Figure 5. 17. Identification of differentially expressed proteins extracted from the planktonic phenotype of *E. coli* K12 grown under 3 conditions: **a)** growth to mid-log phase (5 hours); **b)** growth treated with sub-MIC Byotrol™ (0.6 µg/mL) for 5 hours; **c)** growth for 5 hours, challenged for 2 hours with 4 times MIC Byotrol™ (10.5 µg/mL). Differentially expressed proteins are indicated with numbered arrows. Proteins in the white circle (a) are landmark proteins. The white boxed areas are enlarged in Figure 5. 18 and Figure 5. 19.

Table 5. 5 shows that there was good correlation between the experimental and predicted *pI* and *Mw* in all of the proteins analysed by mass spectrometry, which therefore confirmed protein identity.

Table 5. 7. Identification of differentially expressed proteins by mass spectrometry. Proteins were identified from 2DGE analysis of the planktonic phenotype of *E. coli* K12 grown to mid-exponential phase (5 hours) under 3 growth conditions. The protein label corresponds to numbering on the gels in Figure 5. 18 and Figure 5. 19. The protein name and accession number were taken from a search on the UniProt *E. coli* K12 database. The number of matched peptides were derived from the number of peptides which accurately match the protein sequence, a number >2 is considered to be fully identified.

Protein Label	Protein name (UniProt accession number)	Number of matched peptides	% coverage	Predicted/ Experimental <i>pI</i>	Predicted/ Experimental <i>Mw</i> (Da)
23	Enolase (ENO_ECOLI)	9	19%	5.32/ ~5.8	45654.95/ ~43000
24	Glucose-1-phosphatase (AGP_ECOLI)	7	7%	5.48/ ~5.8	45682.91/ ~43000
7a	D-ribose binding periplasmic protein (RBSB_ECOLI)	9	35%	6.85/ ~6-6.8	30950.48/ ~22000

Figure 5. 18 and Figure 5. 19 show the enlarged regions containing differentially expressed proteins from Figure 5. 17. These proteins were quantified and described in Table 5. 8.

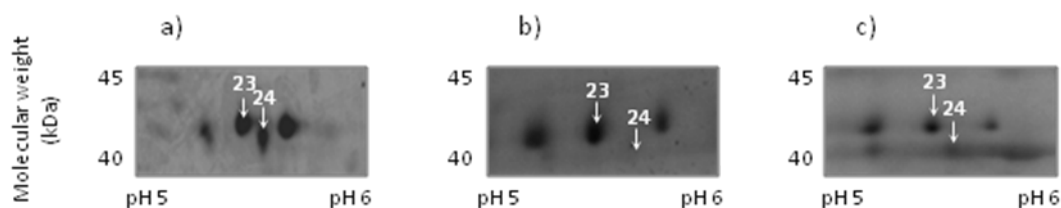


Figure 5. 18. The enlarged detail of differentially expressed proteins of the planktonic phenotype of *E. coli* K12 grown **a)** to mid-exponential phase (5 hours) without Byotrol™; **b)** to mid-exponential phase (5 hours) with sub-MIC Byotrol™; **c)** to mid-exponential phase (5 hours) without Byotrol™ and challenged for 2 hours with 4 times MIC (10.5 μg/mL) Byotrol™. Numbered white arrows indicate differentially expressed proteins.

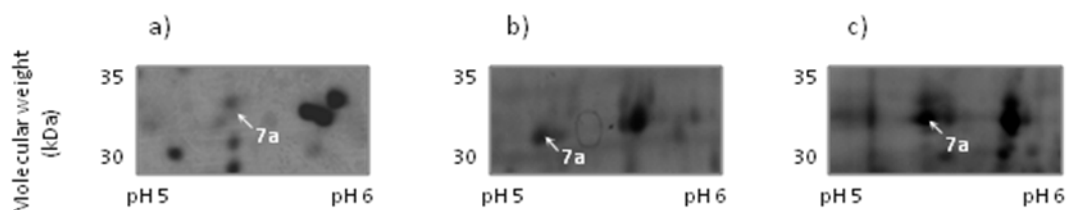


Figure 5. 19. The enlarged detail of differentially expressed proteins of the planktonic phenotype of *E. coli* K12 grown **a)** to mid-exponential phase (5 hours) without Byotrol™; **b)** to mid-exponential phase (5 hours) with sub-MIC Byotrol™; **c)** to mid-exponential phase (5 hours) without Byotrol™ and challenged for 2 hours with 4 times MIC (10.5 μg/mL) Byotrol™. Numbered white arrows indicate differentially expressed proteins.

Table 5. 8 shows a statistical comparison of the differentially expressed proteins extracted from *E. coli* K12 when grown under the 3 growth conditions. Although enolase and D-ribose binding periplasmic protein showed a difference in mean spot density (according to the integrated density value), the *t*-value suggested that the difference was not statistically significant (Table 5. 8). Glucose-1-phosphatase was significantly down-regulated when planktonic cells were treated with Byotrol™ for 5 hours, however appeared not to be down-regulated when challenged with Byotrol™ for 2 hours.

Table 5. 8. The statistical analysis of differentially expressed proteins extracted from the planktonic phenotype of *E. coli* K12 grown for 5 hours. Protein labels correspond to numbering in Figure 5. 18 and Figure 5. 19. The fold induction and repression of proteins in the biofilm phenotype were calculated by using the integrated density values of proteins differentially expressed under the two conditions. *t*-values were calculated using the unpaired two-tailed *t*-test. A *t*-value of <0.05 is considered statistically significant.

Protein Label	Integrated density value		Fold induction (+)/ repression (-)	<i>t</i> -value	
	Growth control	Byotrol™ Challenge			
Growth control vs Cells treated with Byotrol™					
Landmark protein	43535	26935	0.62	0.49	
23	27983	-63162	-0.4 (-)	0.23	
24	24763	7281	3.4 (-)	0.05	
7a	48894	12006	4.1 (-)	0.30	
Growth control vs Cells challenged with Byotrol™					
Landmark protein	43535		48337	1.11	0.69
23	27983		22272	1.3 (-)	0.36
24	24763		23142	1.1 (-)	0.8
7a	48894		45066	1.1 (-)	0.88
Cells treated with Byotrol™ vs Cells challenged with Byotrol™					
Landmark protein		26935	48337	1.79	0.28
23		-63162	22272	1.3 (+)	0.25
24		7281	23142	-17.7 (+)	0.05
7a		12006	45066	1.8 (+)	0.24

A summary comparing the differentially expressed proteins in relation to the growth control are displayed in Table 5. 9.

Table 5. 9. Comparison of protein expression changes between the different growth conditions and phenotypes of *E. coli* K12: ↑ indicates the up-regulation of the protein in relation to the growth control; ↓ indicates the down-regulation of the protein in relation to the growth control; – indicates no difference in expression in relation to the growth control.

Protein name	24 hours growth		Mid-exponential phase growth (5 hours)	
	Planktonic Byotrol™ treated	Biofilm Byotrol™ treated	Planktonic Byotrol™ treated	Challenge (2 hours)
Tryptophanase	↑	↓	–	–
D-ribose periplasmic binding protein	↑	↑	↑	↓
Serine hydroxymethyltransferase	↑	–	–	–
Lactaldehyde dehydrogenase	↑	–	–	–
Dihydrolipoyl dehydrogenase	↑	–	–	–
Glucose-1-phosphatase	–	–	↓	–

5. 7. Discussion

This chapter describes the use of proteomics to evaluate the effect that sub-MIC Byotrol™ concentrations have on *E. coli* K12 protein expression. 2DGE revealed that 6 proteins were differentially expressed between the planktonic and biofilm phenotypes, grown with and without Byotrol™.

The main artifact which was consistently observed during protein separation was the horizontal ‘spot trains’, more accurately termed ‘charge trains’ in this instance. These are individual protein spots with the same identity, but with different charges. Spot trains represent isoforms often formed by post-translational modifications (PTMs), or conformers that are proteins that have different conformations which separate to different isoelectric points in the first dimension (Deng *et al.*, 2012). PTMs commonly refer to phosphorylation and glycosylation (Rabilloud, 1996), however, glycosylated proteins often have an increased size and lower pI, so proteins resolve with different masses and charges. Other PTMs include deamination, desulfuration, protein acylation and alkylation, which result in minor changes in the charge of a protein. A possible explanation for the charge trains observed in the gels from this study could be oxidation (Kleinert *et al.*, 2007; Perdivara *et al.*, 2010). Oxidation is a common problem with proteins rich in cysteine residues, which appears to be the case for tryptophanase and D-ribose periplasmic subunit (Arnitz *et al.*, 2006), and possibly for the other proteins identified. Oxidation can be limited by the addition of the reducing agent dithiothreitol (DTT) that prevents protein folding by limiting disulfide bond formation by cysteine residues (Gundry *et al.*, 2009). Although standard protocols suggest that 10-20 minutes for reduction and alkylation is sufficient, Galvani and co-workers suggested that charge trains were due to incomplete reduction and alkylation, and recommended performing these steps for 6 hours (Galvani *et al.*, 2001). In fact, the same group suggested that reduction and alkylation at just the step after isoelectric focussing was far from being optimal (Herbert *et al.*, 2001).

With the early separations performed in this study, the concentration of DTT in the rehydration buffer was too high. This resulted in accumulation of proteins at the anode and increased horizontal streaking. A reason for this may be due to the thiol groups of DTT being ionised at high pH during IEF, causing DTT to migrate towards the electrode. This may have resulted in lower concentrations of DTT in the gel, so proteins

became less soluble as they reformed disulfide bonds (Herbert *et al.*, 1998), thereby reducing protein migration to the cathode. To overcome this Gorg and co-workers (1995) suggested adding DTT to the electrode wick at the cathode during IEF. However, if the concentration of DTT is too high there may be excessive electroendosmosis (the counter-flow of water ions) which can cause protein precipitation leading to horizontal streaking (Hoving *et al.*, 2002). By using a lower concentration of DTT in the rehydration buffer there was reduced horizontal streaking and sharper spots, this phenomenon was also observed by Valcu & Schlink (2006). Herbert and co-workers (1998) suggest replacing DTT with the non-ionic reducing agent tributyl phosphine (TBP) which is altogether possibly a better alternative.

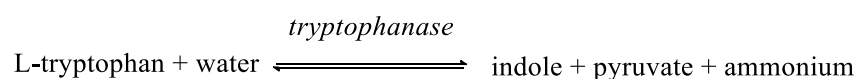
Despite the charge trains, which are often observed with 2DGE, differentially expressed proteins were evident from the gels. The proteins identified were all metabolic enzymes (Zhang *et al.*, 2007).

5. 7. 1. Landmark protein: phosphoglycerate kinase

Proteins consistently expressed at the same level under all growth conditions were identified on each gel in order to ensure gels were loaded equally, and to locate the proteins expressed despite any inconsistencies in the protein resolution. The landmark protein identified was phosphoglycerate kinase. This is a highly conserved protein and is not susceptible to protease cleavage (Young *et al.*, 2007). This protein is essential to the growth of all organisms, and in *E. coli* is responsible for the degradation of glucose and binding of ATP in the glycolysis pathway (Song *et al.*, 2012).

5. 7. 2. Tryptophanase and indole production

Tryptophanase catalyses the following reaction:



There was an increase in tryptophanase when planktonic cells were treated with a sub-inhibitory concentration of Byotrol™ for 24 hours, suggesting that tryptophanase may be

important in cell survival. Studies have suggested that indole induces proteins that play a role in enabling the cell to survive (Hu *et al.*, 2010; Lee *et al.*, 2010).

Although tryptophanase was over-expressed in planktonic cells treated with Byotrol™, tryptophanase was not over-expressed when biofilm cells were treated with Byotrol™ for 24 hours, which may be because Byotrol™ was not entering the biofilm matrix in sufficient quantities to have a detectable effect on tryptophanase expression.

Tryptophanase was over-expressed in biofilm cells grown for 24 hours without Byotrol™. In addition to this, tryptophanase was also induced in the stationary phase of planktonic growth when cells were grown for 7 hours (5 hours growth plus 2 hours challenge) (Figure 5. 17). This correlates to the results where tryptophanase was over-expressed in biofilm cells because when cells enter stationary phase, the cells are thought to reflect the state of the biofilm phenotype (Zhang *et al.*, 2007).

Tryptophanase may be a useful target for bacterial growth inhibition and biofilm inhibition as it was over-expressed when the cell was under stress and when cells had been growing for a longer period, especially as it is known that indole, which is the product of the reaction that tryptophanase catalyses, is important in regulating biofilm formation (Lee *et al.*, 2007a). Indole represses bacterial motility and controls biofilm formation by inducing *sdiA* (quorum sensing signal autoinducer-I, a LuxR homolog), therefore is considered to be an extracellular signalling molecule (Wang *et al.*, 2001). There is evidence to suggest that a mutant strain of *E. coli* deficient of tryptophanase was unable to form a biofilm on polystyrene or adhere to human pneumocyte cells (Di Martino *et al.*, 2002). Interestingly, Domka and co-workers found that although *P. aeruginosa* did not produce indole, its ability to form a biofilm increased in the presence of indole, as its motility was repressed (Domka *et al.*, 2006; Lee *et al.*, 2007a). This would be consistent with the knowledge that *P. aeruginosa* does not require motility once attachment to a surface occurs (Klausen *et al.*, 2003).

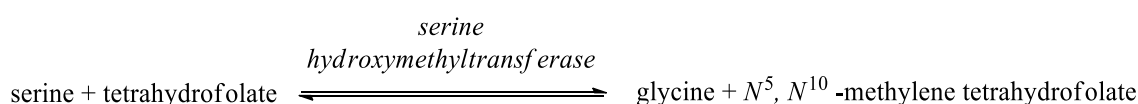
5. 7. 3. D-ribose periplasmic binding protein

D-ribose periplasmic binding protein (*rbsB*) was down-regulated in the biofilm phenotype suggesting that *rbsB* is not essential to biofilm growth. This was consistent with the results of this laboratory previously (Orme, 2006). It was however up-regulated

in the planktonic phenotype treated with a sub-inhibitory concentration of Byotrol™ at both mid-exponential phase of growth (5 hours) and 24 hours of growth, therefore may be important in cell survival under antimicrobial stress. The function of rbsB is to bind D-ribose and recognise substrates such as carbohydrates for transport and chemotaxis across the cytoplasmic membrane. This system is similar for other sugars such as L-arabinose and D-galactose, and is also known as an osmotic stress sensitive transport system (Binnie *et al.*, 1992).

5. 7. 4. Serine hydroxymethyltransferase

When planktonic cells were under the antimicrobial stress of Byotrol™ for 24 hours, serine hydroxymethyltransferase were up-regulated. This is an enzyme that catalyses the following reaction:



Serine and glycine are essential amino acids. The up-regulation of serine hydroxymethyltransferase may indicate that cells required amino acids for protein synthesis and cell repair when under the stress of Byotrol™.

5. 7. 5. Lactaldehyde dehydrogenase

Lactaldehyde dehydrogenase expression increased in the planktonic phenotype when cells were under the antimicrobial stress of Byotrol™ for 24 hours. The catalytic function of lactaldehyde dehydrogenase is to convert lactaldehyde to lactate, which is subsequently converted to pyruvate, especially when oxygen is in short supply (Di Costanzo *et al.*, 2007). An increase of lactaldehyde dehydrogenase in the planktonic phenotype when the cell was under the antimicrobial stress of Byotrol™ may be due to the cell's need to produce pyruvate. Pyruvate is an intermediate in several metabolic pathways. The majority of pyruvate is converted to acetyl-coenzyme A (acetyl coA), which is key to cell metabolism and ATP production (Castano-Cerezo *et al.*, 2009). Therefore the products of lactaldehyde dehydrogenase catalysis facilitate processes that are usually required for cell growth, but may be used for cell repair (Zhang & Rock,

2009) when a cell is under attack from an antimicrobial such as Byotrol™, whose mode of action compromises the integrity of the cell membrane (Berney *et al.*, 2006).

5. 7. 6. Dihydrolipoyl dehydrogenase

Dihydrolipoyl dehydrogenase was up-regulated in planktonic cells treated with Byotrol™ for 24 hours. This enzyme is part of a complex that consists of 3 enzymes that transform pyruvate to acetyl-coenzyme A (acetyl coA) via pyruvate decarboxylation. This enzyme is therefore an essential part of the citric acid cycle and important in ATP production. Acetyl coA, the product of dihydrolipoyl dehydrogenase, is also important in peptidoglycan synthesis and therefore the bacterial cell up-regulates the production of acetyl coA to aid in cell wall repair (Liu *et al.*, 2012). Cell wall repair may be important when the cell is under the stress of Byotrol™, as its primary mode of action is likely to be cell wall perturbation.

5. 7. 7. Glucose-1-phosphatase

Glucose-1-phosphatase was repressed when *E. coli* K12 was treated with Byotrol™ for 5 hours. Glucose-1-phosphatase is a key enzyme found in the periplasm that is required for the growth of *E. coli* as it is the main glucose scavenger. This enzyme is involved in the catabolism of glucose-1-phosphate to glucose and phosphate (Lee *et al.*, 2003). Its repression suggests that the cell may not require the function of this enzyme under stress as it is not actively growing so the need for glucose as a carbon source is reduced. Glucose-1-phosphatase was not repressed when the cells were challenged with Byotrol™ for 2 hours suggesting treatment with Byotrol™ for 2 hours was not long enough to have an effect on the production of glucose-1-phosphatase.

5. 7. 8. Conclusion

The proteins identified were all metabolic enzymes (Zhang *et al.*, 2007), being involved particularly in protein synthesis and cellular repair, however the over-expression of the enzyme tryptophanase may be significant in the production of indole, a known global regulator of essential stress related functions. When indole is induced in *E. coli*, biofilm formation is reportedly decreased by down-regulating motility; acid resistance decreases and amino acid synthesis is up-regulated (Hirawaka *et al.*, 2010; Lee *et al.*, 2007a). The

influence that indole has on bacterial metabolism and stress response is shown in Figure 5. 20. The regulation by indole on other cellular processes is described in more detail in Chapter 7.

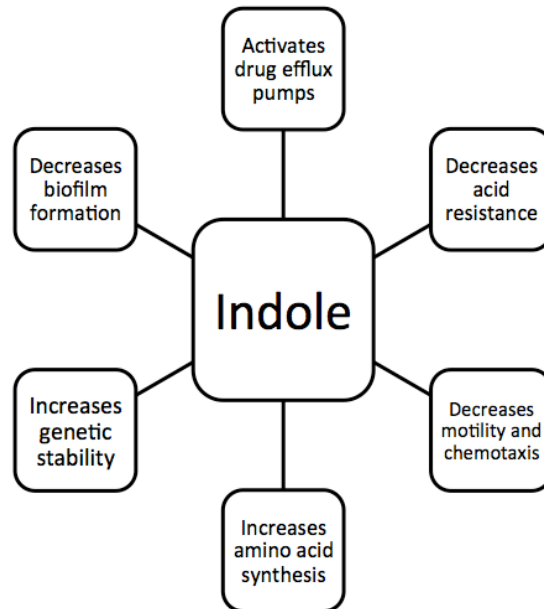


Figure 5. 20. Indole as a global regulator of cellular functions in *E. coli*.

Chapter 6

Transcriptomic analysis of

***E. coli* K12 in response to Byotrol™**

6. 1. An introduction to RNA-seq

Prior to the advent of RNA-Seq, also called Whole Transcriptome Shot-gun Sequencing (WTSS), microarrays were the gold standard for transcriptomic studies. Microarrays are chips or solid supports, which carry a large array of immobilised probes. The probes can be genomic DNA, cDNA or oligonucleotides of known sequence to which target cDNA or genomic DNA of unknown or known sequence hybridises. Target-probe hybridisation is detected by chemluminescence- or fluorophore-labelled targets with each experimental sample labelled to produce different colours. This enables the target to be identified based on the sequence of the probe to which it is hybridised and the intensity of emitted light can be used to quantify the expression levels of the target. Expression patterns can be compared with other microarray expression patterns to determine differential expression (Hegde *et al.*, 2000).

Microarrays are designed for comparative studies, however they only provide limited information about absolute gene expression levels. This is due to cross-hybridisation causing high background levels and differences in hybridisation efficiencies and specificities for different probes (Royce *et al.*, 2007).

RNA-seq is a relatively new approach, which has been developed to characterise the transcriptome profile of a population of cells (Wang *et al.*, 2009). The transcriptome refers to all the RNA molecules in a cell, including mRNA, non-coding RNA such as tRNA and rRNA and small RNAs. Transcriptomics involves high-throughput technology, which is relatively low in cost, given the vast amount of data generated and the great capacity to recover a variety of information. The RNA-seq method was used in this chapter to quantify the differential expression levels of genes under different conditions (Wang *et al.*, 2009b).

Using high-throughput deep-sequencing technologies, RNA-seq is sensitive to the level of single transcript resolution, and offers accurate quantification of transcript expression levels, which has not been possible to the same resolution previously with microarrays (Su *et al.*, 2011; Wang *et al.*, 2009b; Wilhelm *et al.*, 2010). The technology is sensitive enough to differentiate between paralogous sequences (i.e. duplicated genes that have different positions on the same genome) (Fu *et al.*, 2009). In relation to microarrays, it

is suggested that RNA-seq also has a lower level of background signal (Kogenaru *et al.*, 2012).

6. 1. 1. Principles of RNA-Seq

The sequencing depth or library size is the term used to describe the total number of sequence reads which map to the genome that are produced during a sequencing run. The gene length is the number of base pairs of a gene and the gene counts refer to the number of reads that match to a gene (Figure 6. 1). Also, the greater the gene or transcript length, the greater the number of reads that have the potential to match to the gene. The expression of a gene is directly proportional to the number of reads that map to that gene (Marioni *et al.*, 2008). Therefore, normalisation is required in order to account for the fact that a gene may appear to be up-regulated within a sample as demonstrated by a high count, when in fact the transcripts for a gene may appear to represent a greater proportion of the library than any other individual gene. Likewise, if the library size is larger in one sample than another, then it may automatically generate more reads for a particular gene than a sample where the library size is smaller.

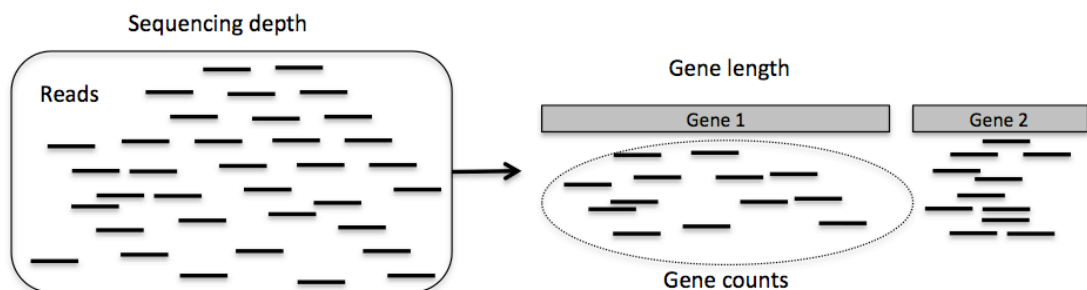


Figure 6. 1. Illustration of the terms used to describe the principles of RNA-Seq. The number of reads is related to the sequencing depth. Each read is mapped to a reference genome and the number of genes that map to a gene is referred to as the gene count. The gene count is related to the length of the gene.

6.2. Global gene expression of *E. coli* K12 when treated and challenged with Byotrol™

The high throughput sequence data generated using Illumina technology was used to identify many differentially expressed transcripts from three growth conditions: i) Growth control: *E. coli* K12 growth control, cells grown to mid-exponential phase (5 hours); ii) Treated: *E. coli* K12 grown in the presence of sub-inhibitory concentrations of Byotrol™ to mid-exponential phase (5 hours); and iii) Challenge: *E. coli* K12 cells grown to mid-exponential phase (5 hours) and challenged with 4 times the MIC of Byotrol™ for 2 hours.

The Illumina sequencing platform generated 69.4 MB sequence data containing a total of 48,656,483 (representing 4,816,532,343 bp), 39,978,722 (3,942,347,192 bp) and 32,541,123 (3,196,309,920 bp) high quality reads in the growth control, Byotrol™ treated and challenged cells, respectively.

Analysis of the sequences using the MG-RAST server and CLC workbench demonstrated that, for the growth control, Byotrol™ treated and challenged cells, a total of 34,635,530, 26,435,638 and 20,940,394 reads, respectively, mapped to the *E. coli* K12 sub-strain MG1655 complete genome database. A detailed breakdown of the sequenced data for each of the growth conditions is outlined in Figures 6. 2 to 6. 7.

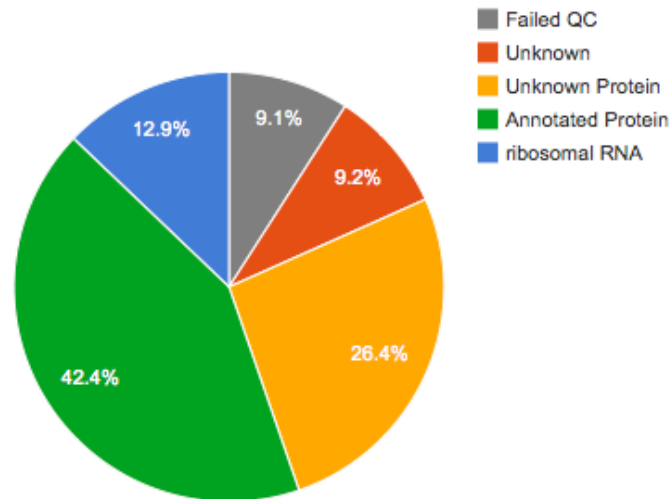


Figure 6. 2. Breakdown of *E. coli* K12 growth control sequences into 5 distinct categories.

4,421,979 sequences (9.1%) failed to pass the quality control (QC) pipeline. Of the sequences that passed QC, 6,259,053 sequences (12.9%) contained ribosomal RNA genes. Of the remainder, 20,636,885 sequences (42.4%) contained predicted proteins with known functions and 12,845,010 sequences (26.4%) contained predicted proteins with unknown function. 4,493,556 sequences (9.2%) had no rRNA genes or predicted proteins.

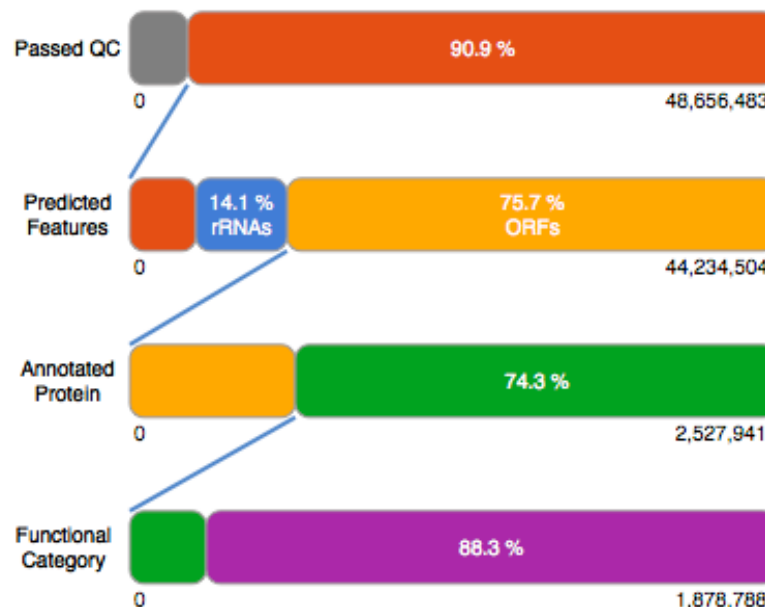


Figure 6. 3. Analysis flowchart with detailed breakdown of sequences of *E. coli* K12 growth control.

4,421,979 sequences failed quality control. Of the 44,234,504 sequences that passed quality control, 33,481,895 (75.7%) produced a total of 2,527,941 predicted protein coding regions. Of these predicted protein features, 1,878,788 (74.3% of features) were assigned an annotation using at least one of the MG-RAST protein databases (M5NR) and 649,153 (25.7% of features) had no significant similarities to the protein database (orfans). 1,658,571 features (88.3% of annotated features) were assigned to functional categories.

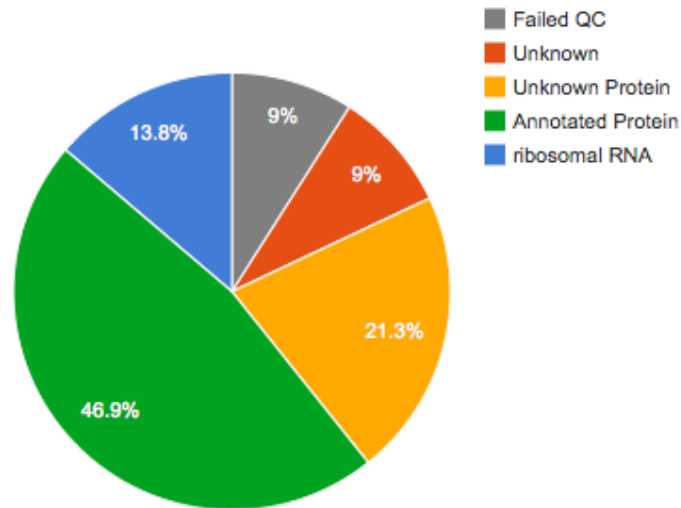


Figure 6. 5. Breakdown of sequences of *E. coli* K12 cells treated with sub-MIC Byotrol™, into 5 distinct categories (treated).

3,611,687 sequences (9.0%) failed to pass the quality control (QC) pipeline. Of the sequences that passed QC, 5,509,164 sequences (13.8%) contained ribosomal RNA genes. Of the remainder, 18,766,468 sequences (46.9%) contained predicted proteins with known functions and 8,510,610 sequences (21.3%) contained predicted proteins with unknown function. 3,580,793 sequences (9.0%) had no rRNA genes or predicted proteins.

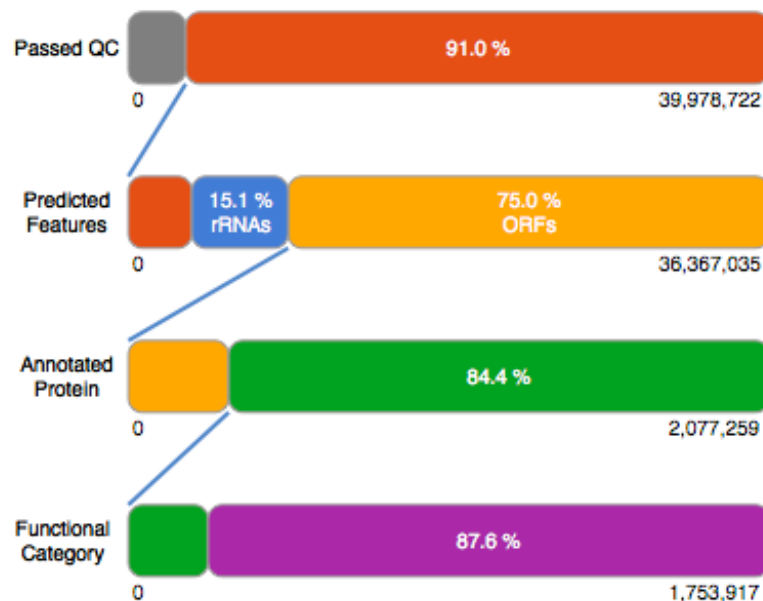


Figure 6. 4. Analysis flowchart with detailed breakdown of sequences of *E. coli* K12 treated with sub-MIC Byotrol™ (treated).

3,611,687 sequences failed quality control. Of the 36,367,035 sequences that passed quality control, 27,277,078 (75.0%) produced a total of 2,077,259 predicted protein coding regions. Of these predicted protein features, 1,753,917 (84.4% of features) were assigned an annotation using at least one of the MG-RAST protein databases (M5NR) and 323,342 (15.6% of features) had no significant similarities to the protein database (orfans). 1,535,923 features (87.6% of annotated features) were assigned to functional categories.

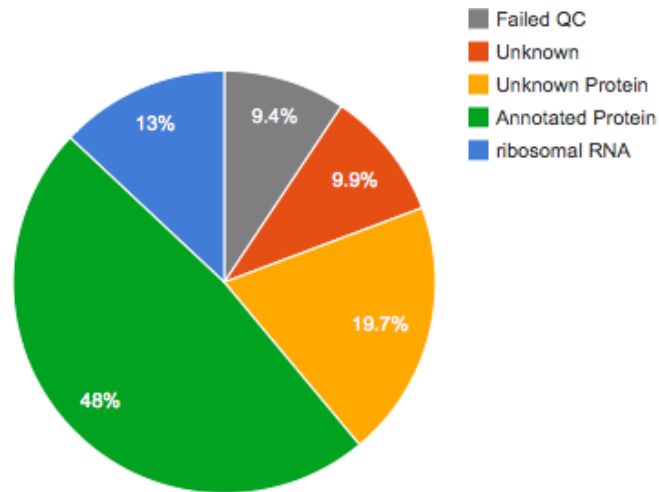


Figure 6. 7. Breakdown of *E. coli* K12 cells grown to mid-exponential phase and challenged with 4 times MIC Byotrol™ 2 hours, into 5 distinct categories (challenge). 3,044,869 sequences (9.4%) failed to pass the quality control (QC) pipeline. Of the sequences that passed QC, 4,232,575 sequences (13.0%) contained ribosomal RNA genes. Of the remainder, 15,634,805 sequences (48.0%) contained predicted proteins with known functions and 6,399,633 sequences (19.7%) contained predicted proteins with unknown function. 3,229,241 sequences (9.9%) had no rRNA genes or predicted proteins.

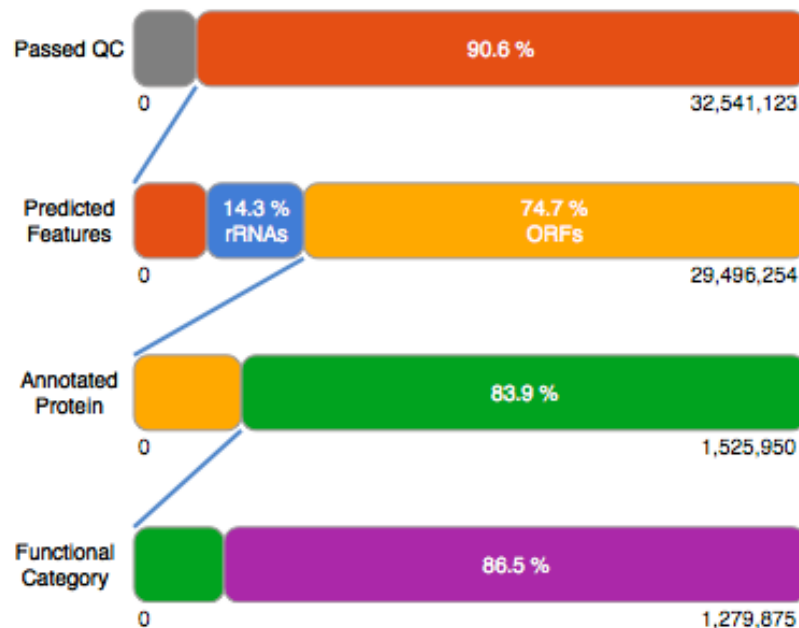


Figure 6. 6. Analysis flowchart with detailed breakdown of sequences of *E. coli* K12 grown to mid-exponential phase and challenged with 4 times MIC Byotrol™ 2 hours (challenge).

3,044,869 sequences failed quality control. Of the 29,496,254 sequences that passed quality control, 22,034,438 (74.7%) produced a total of 1,525,950 predicted protein coding regions. Of these protein features, 1,279,875 (83.9% of features) were assigned an annotation using at least one of the MG-RAST protein databases (M5NR) and 246,075 (16.1% of features) had no significant similarities to the protein database (orfans). 1,106,640 features (86.5% of annotated features) were assigned to functional categories.

6.3. Genes differentially expressed in response to Byotrol™

Bacteria differentially express a number of genes to enable the cell to adapt to any changes in environmental conditions, including stresses, in order to survive or grow optimally. A description of genes induced or repressed in response to the stress stimulus from the biocide Byotrol™, are presented.

Relative gene expression was determined through the following comparisons: growth control vs. treated; treated vs. challenge; and growth control vs. challenge. RNA-seq analysis revealed that sequence reads mapped to a total of 4496 genes in all three conditions.

The proportion of differentially expressed genes compared to the total number of genes (4496 genes) is presented diagrammatically in Figure 6. 8. Genes were considered differentially expressed if the fold change was ≥ 2 for up-regulated genes or ≤ 2 for down-regulated genes (Yu, *et al.*, 2011). 4345 genes were differentially expressed in the growth control cells when compared to the challenged cells and 151 genes were not differentially expressed. 3904 genes were differentially expressed in the cells treated with Byotrol™ when compared to cells challenged with Byotrol™ and 592 were not differentially expressed and 3862 genes were differentially expressed when growth control cells were compared to cells challenged cells, whereas 634 genes were not differentially expressed.

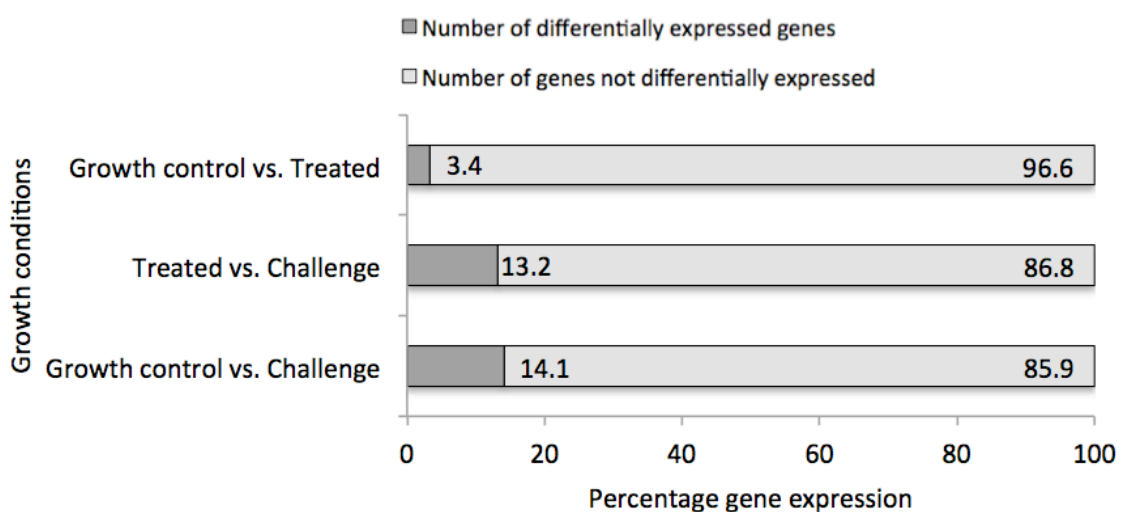


Figure 6. 8. Total number of differentially expressed genes (fold change of ≤ 2 and ≥ 2) in the three different growth conditions: growth control, cells treated with Byotrol™ (treated) and cells challenged with Byotrol™ for 2 hours after 5 hours of growth (challenge).

Of the genes that were differentially expressed, the number of genes which had a fold change of ≤ 5 and ≥ 5 were of most interest as these were considered highly differentially expressed (Yu, *et al.*, 2011). The number of genes that were significantly differentially expressed in this category (p -value 0.001) is presented in Figure 6. 9.



Figure 6. 9. Venn diagram demonstrating the distribution of highly differentially expressed genes (fold change of ≤ 5 and ≥ 5) when compared across the different growth conditions (growth control, *E. coli* K12 cells treated with sub-MIC Byotrol™ and *E. coli* K12 cells challenged with 4 times MIC Byotrol™).

Figure 6. 9 shows 12 genes were differentially expressed in the growth control compared to treated cells, 105 genes were differentially expressed in the growth control compared to challenge cells and 118 genes were differentially expressed in treated cells compared to challenge cells. No genes were differentially expressed in all three conditions or in the growth control when compared to both the treated cells and challenge cells. However 74 genes were differentially expressed in cells challenged compared to the growth control and treated cells. 7 genes were differentially expressed in treated cells compared to the growth control and challenge cells.

Of the differentially expressed genes in the growth control compared to treated cells, 10 genes were observed to be up-regulated and 2 genes were down-regulated. In the challenge cells compared to treated cells, 46 genes were up-regulated and 72 were down-regulated. Finally a comparison of the challenge cells and growth control identified 40 genes that were up-regulated and 65 genes that were down-regulated (Figure 6. 10). The genes that are up and down-regulated are elaborated on in greater detail in Table 6. 3 to Table 6. 8.

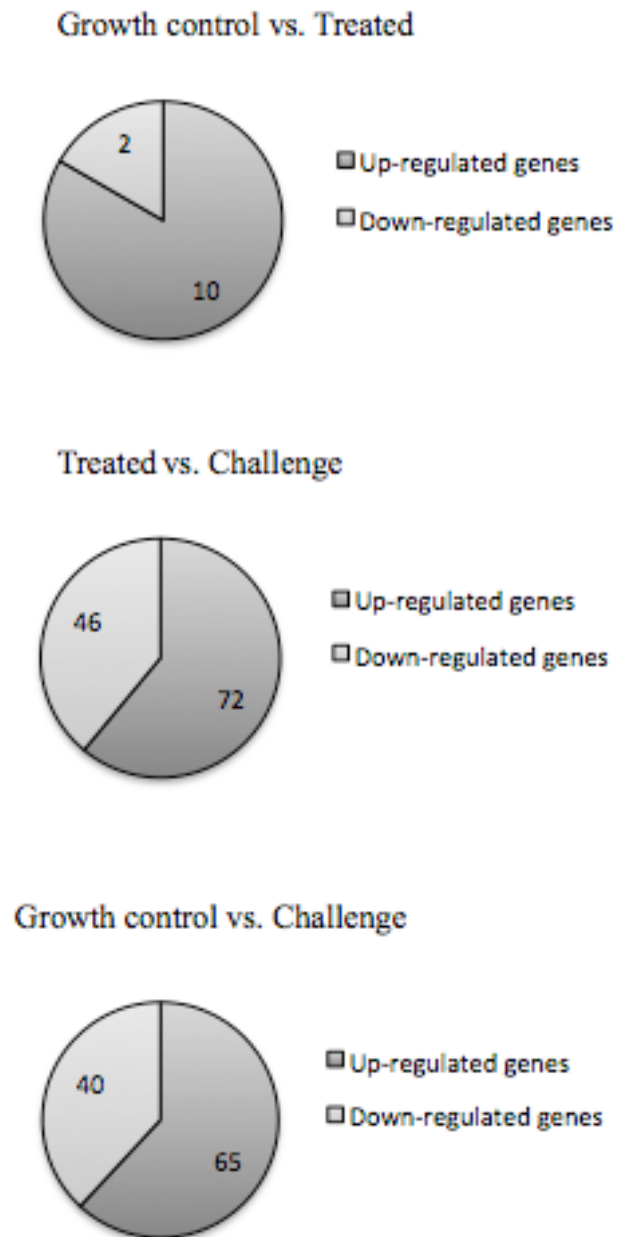


Figure 6. 10. Proportion of up and down regulated genes as a total of the genes differentially expressed (fold change of ≤ 5 and ≥ 5) under the three different growth conditions

6.4. Classification of differentially expressed genes according to function

Genes that are differentially expressed can be classified according to their function. Classification of the differentially expressed genes in functional groups revealed which functional groups of genes were most affected during exposure to Byotrol™. Also, an indication of the number of genes most significantly altered in relation to the three growth conditions (growth control, Byotrol™ treated and challenged cells), are summarised in Tables 6. 1 and 6. 2, and presented graphically in Figure 6. 11.

The data displayed in Tables 6. 1 and 6. 2 and Figure 6. 11 demonstrate that although a greater variety of gene functions were up-regulated when cells were treated or challenged with Byotrol™, a greater number of genes were down-regulated for specific gene functions, namely flagella synthesis and ion transport, specifically iron. A greater number of genes involved in transcription regulation were up-regulated in cells challenged with Byotrol™.

Across all of the gene functions, there were a greater number of genes that were differentially expressed in cells challenged with Byotrol™ when compared to the growth control and Byotrol™ treated cells. An exception to this was the up-regulation of genes in Byotrol™ treated cells in comparison to the growth control. These genes are involved in protein synthesis, antibiotic resistance or membrane biosynthesis and DNA synthesis.

Genes and operons relating to these functional groups will be discussed according to their differential expression.

Table 6. 1. Classification of genes up-regulated in response to Byotrol™ according to their function.

Gene function	Number of genes up-regulated in treated cells compared to growth control		Number of genes up-regulated in challenged cells compared to growth control		Number of genes up-regulated in challenged cells compared to both growth control and treated		Total genes (number)	Total genes (%)
	Number of genes up-regulated in treated cells compared to growth control	Number of genes up-regulated in challenged cells compared to treated cells	Number of genes up-regulated in challenged cells compared to growth control	Number of genes up-regulated in challenged cells compared to both growth control and treated	Total genes (number)	Total genes (%)		
Function unknown/Protein uncharacterised	2	7	8	13	30	36		
Transport	1	6	0	3	10	12		
Transcription regulation	0	2	0	7	9	11		
Protein synthesis	2	1	1	2	6	7		
DNA replication and synthesis	1	2	2	1	6	7		
Ion transport, binding and metabolism	0	1	1	2	4	5		
Stress response	0	0	1	3	4	5		
Energy production	0	1	0	3	4	5		
Metabolism	1	0	0	3	4	5		
Cell adhesion	0	1	0	2	3	4		
Carbohydrate metabolism	0	0	0	2	2	2		
Antibiotic resistance/membrane biosynthesis	1	0	0	0	1	1		
Flagellum biosynthesis/chemotaxis	0	0	0	1	1	1		
Toxin metabolism	0	0	0	0	0	0		

Table 6. 2. Classification of genes down-regulated in response to Byotrol™ according to their gene function.

Gene function	Number of genes down-regulated in treated cells compared to growth control	Number of genes down-regulated in challenged cells compared to treated cells	Number of genes down-regulated in challenged cells compared to growth control	Number of genes down-regulated in challenged cells compared to both growth control and treated	Total genes (number)	Total genes (%)
Ion transport, binding and metabolism	0	3	9	2	14	24
Flagellum biosynthesis/chemotaxis	0	1	2	10	13	22
Carbohydrate metabolism	0	4	3	0	7	12
Function unknown/Protein uncharacterised	0	4	1	1	6	10
Protein synthesis	0	1	3	0	4	7
DNA replication and synthesis	0	0	1	3	4	7
Transcription regulation	0	1	1	2	4	7
Antibiotic resistance/membrane biosynthesis	0	1	0	0	1	2
Toxin metabolism	0	1	0	0	1	2
Stress response	0	0	1	0	1	2
Energy production	0	1	0	0	1	2
Metabolism	0	1	0	0	1	2
Transport	0	1	0	0	1	2
Cell adhesion	0	0	0	0	0	0

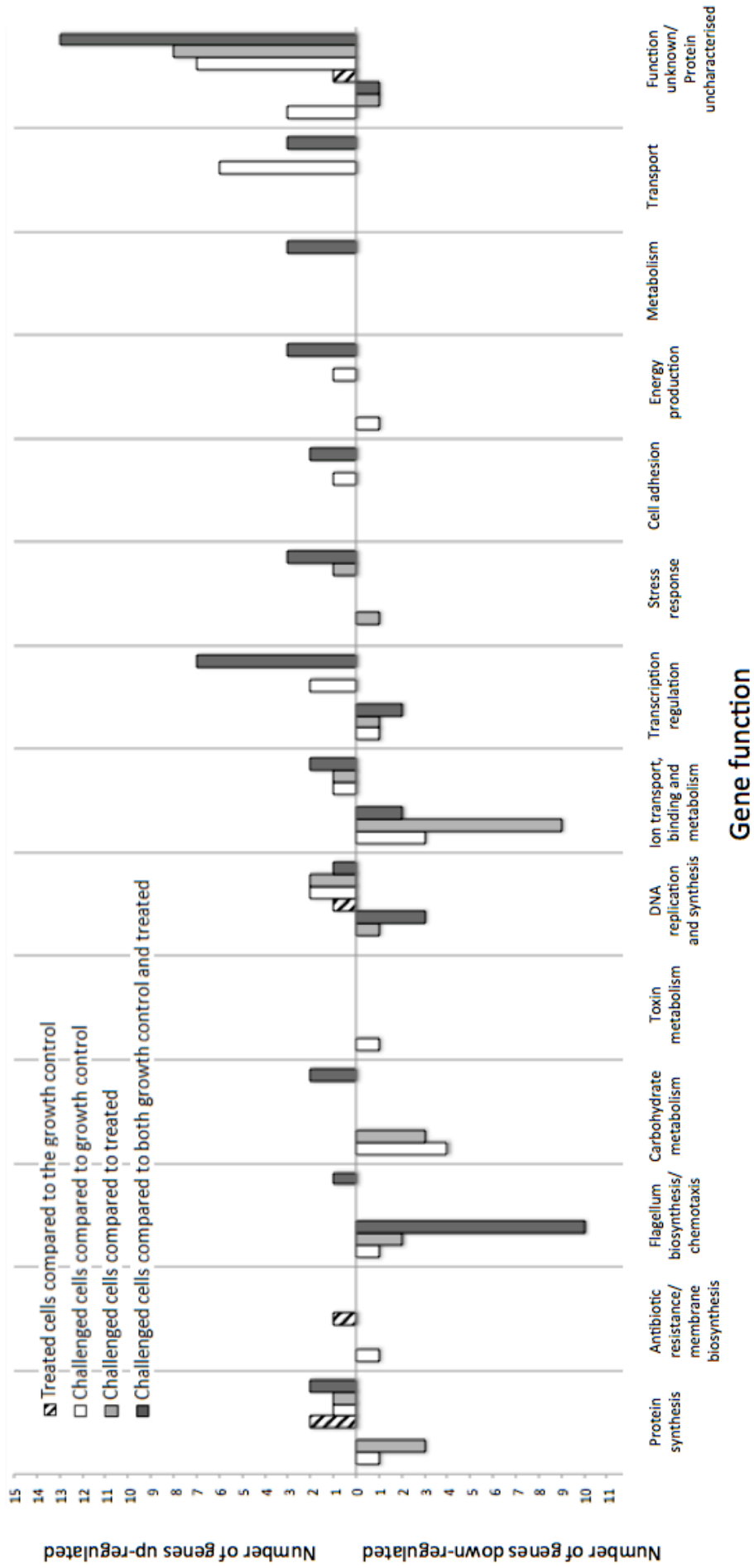


Figure 6. 11. Number of genes up and down-regulated when compared to the different growth conditions, categorised according to gene function.

6.5. Genes differentially expressed in *E. coli* K12 cells treated with Byotrol™ compared to the growth control

In cells treated with a sub-inhibitory concentration of Byotrol™ for 5 hours, 10 genes were up-regulated in comparison to the growth control (Table 6. 3). The gene with the greatest fold change was *tnaC* (~100-fold up-regulated). When up-regulated, *tnaC* enables the transcription of the enzyme tryptophanase, which in turn catalyses the reaction producing indole and the amino acid tryptophan (Lee *et al.*, 2007a). Although a majority of the genes that were up-regulated in the treated cells compared to the growth control have an unknown function, the characterised genes encode proteins which are involved in protein synthesis, such as *tnaC* and DNA replication, such as *ybbW*.

In cells treated with a sub-inhibitory concentration of Byotrol™ for 5 hours, 2 genes were down-regulated in comparison to the growth control (Table 6. 3). The gene with the greatest fold change of down-regulated genes was *cysW* (~33-fold down-regulated), which is involved in sulphate transport.

Table 6. 3. Genes in *E. coli* K12 that were differentially expressed in response to treatment with Byotrol™ compared to the growth control. Genes with a fold change ≥ 5 and ≤ 5 are displayed.

Gene	UniProt accession number	Function and/or product	Fold Change ^a	<i>p</i> -value ^b
<i>tnaC</i>	P0AD89	Leader peptide in tryptophanase biosynthesis	102.48	1.69E-06
<i>hyi</i>	P30147	Hydroxypyruvate isomerase	15.1	4.04E-07
<i>gudP</i>	Q46916	D-glucarate transporter	14.42	2.56E-11
<i>glxR</i>	P77161	Cyclic AMP receptor	13.49	3.00E-04
<i>ybbW</i>	P75712	Purine and pyrimidine transporter	9.37	5.64E-04
<i>gcl</i>	P0AEP7	Glyoxylate carboligase	8.91	1.13E-06
<i>ykgS</i>		Uncharacterised	7.08	1.28E-04
<i>wcaD</i>	P71238	Putative colanic acid polymerase	6.48	8.01E-07
<i>gudX</i>	Q46915	D-glucarate dehydratase	5.63	1.17E-04
<i>appC</i>	P26459	Cytochrome bd-II oxidase subunit I	5.53	9.81E-09
<i>cysW</i>	P0AEB0	Membrane-bound sulphate transport protein	-32.86	2.96E-11
<i>ydjO</i>	P0AD89	Uncharacterised protein	-6.92	8.78E-03

^a Fold change based on normalised values; ^b *p*-value (≤ 0.001).

6. 6. Genes differentially expressed in *E. coli* K12 cells challenged with Byotrol™ compared to cells treated with Byotrol™

6. 6. 1. Genes up-regulated in *E. coli* K12 cells challenged with Byotrol™ compared to cells treated with Byotrol™

In mid-exponential phase cells that were challenged with Byotrol™ for 2 hours, 76 genes were up-regulated in comparison to cells treated with Byotrol™ for 5 hours (Table 6. 4). The gene with the greatest fold change was *yadN*, a fimbria protein, which was up-regulated 75 times more than in cells treated with Byotrol™. A majority of genes up-regulated have an unknown function or have not been characterised, however overall, genes involved in transport were up-regulated under these conditions. This includes genes of the *cys* operon, involved in sulphate transport and genes of the *lsr* operon, involved in the uptake of autoinducer-2 (AI-2).

Table 6. 4. Genes in *E. coli* K12 up-regulated in response to challenge with Byotrol™ compared to treatment with Byotrol™. Genes with a fold change ≥ 5 are displayed.

Gene	UniProt Entry	Function and/or product	Fold Change ^a	p-value ^b
<i>yadN</i>	P37050	Putative fimbrial-like protein	75.05	4.38E-03
<i>yjfl</i>		Inner membrane protein	36.6	1.19E-09
<i>cysU</i>	P16701	Sulphate transport system permease protein	22.15	2.22E-16
<i>napD</i>	P0A9I5	Twin-arginine signal-peptide-binding chaperone for NapA	20.42	2.21E-12
<i>fixB</i>	P31574	Flavoprotein subunit required for anaerobic carnitine metabolism	20.37	3.64E-11
<i>gspC</i>	P45757	Component of GspC-O secreton complex	17.49	3.73E-14
<i>iraM</i>	P75987	RpoS stabiliser during Mg ²⁺ starvation	17.06	1.48E-10
<i>cysW</i>	P0AEB0	Membrane-bound sulphate transport protein	16.78	5.41E-06
<i>fdrA</i>	Q47208	Multicopy suppressor of dominant negative ftsH mutations	16.64	2.20E-04
<i>lsrA</i>	P77257	Autoinducer-2 import ATP-binding protein	16.04	8.88E-16
<i>cysA</i>	P16676	Sulphate-transporting ATPase	15.85	6.76E-11
<i>yjfJ</i>	P0AF78	Predicted transcriptional regulator effector protein	14.23	1.26E-06
<i>ydjO</i>		Function unknown	13.94	3.04E-05
<i>pspD</i>	P0AFV8	Peripheral inner membrane phage-shock protein	13.83	9.33E-15
<i>elfA</i>	P75855	FimA homolog, predicted fimbrial-like adhesin protein	13.73	3.23E-10
<i>napB</i>	P0ABL3	Periplasmic nitrate reductase, cytochrome c ₅₅₀ protein	13.3	1.25E-08
<i>cysD</i>	P21156	Sulphate adenylyltransferase	13.2	8.54E-13
<i>csgD</i>	P52106	Transcriptional activator for <i>csgBA</i> and other genes	12.25	9.95E-04
<i>ymgC</i>	P75994	Function unknown	11.24	1.15E-06
<i>lsrC</i>	P76141	Component of LsrA/LsrC/LsrD/LsrB ABC transporter, Autoinducer-2 (AI-2) uptake	11.04	5.75E-06
<i>pspC</i>	P0AFN2	PspC transcriptional regulator; toxin of a PspC-PspB toxin-antitoxin pair	10.73	8.88E-16
<i>napG</i>	P0AAL3	Quinol dehydrogenase	10.57	4.21E-05
<i>ivbL</i>	P03061	<i>ilvB</i> operon leader peptide	10.23	6.66E-16
<i>fixC</i>	P68644	Carnitine metabolism	9.57	1.83E-03
<i>yhaI</i>	P64592	Function unknown	9.53	5.56E-06
<i>ygiL</i>	P39834	Predicted fimbrial-like adhesin protein	9.46	1.40E-04
<i>yegJ</i>	P76334	Function unknown	8.79	2.56E-04
<i>yigG</i>	P27843	Required for swarming phenotype	8.29	6.71E-03
<i>umuD</i>	P0AG11	DNA polymerase V subunit	8.09	6.19E-04
<i>agaV</i>	P42904	N-acetylgalactosamine-specific enzyme IIB component of phosphotransferase system (PTS)	7.88	4.77E-05
<i>yiaO</i>	P37676	Extracytoplasmic solute receptor protein	7.76	2.28E-05
<i>ariR</i>	P75993	RcsB connector protein for biofilm and acid resistance regulation	7.39	5.77E-11
<i>paaZ</i>	P77455	Enoyl-CoA hydratase	7.29	2.34E-04
<i>leuB</i>	P30125	Component of 3-isopropylmalate dehydrogenase	7.22	1.18E-10
<i>matA</i>	P71301	Putative transcriptional regulator for mat genes (malonyl-CoA decarboxylase)	7.06	5.43E-06
<i>ycaL</i>	P43674	putative heat shock protein	7.03	1.48E-04
<i>fadM</i>	P77712	Acyl-CoA thioester hydrolase	6.95	2.74E-07

^a Fold change based on normalised values; ^b p-value (≤ 0.001).

Table 6. 4. Continued.

Gene	UniProt Entry	Function and/or product	Fold Change^a	p-value^b
<i>yrhB</i>	P46857	Stable heat shock chaperone	6.86	5.82E-03
<i>cysN</i>	P23845	Gtp subunit of ATP sulfurylase	6.83	5.51E-13
<i>nanC</i>	P69856	Probable N-acetylneuraminic acid outer membrane channel protein	6.64	7.18E-06
<i>yhiL</i>	P37629	Putative dehydrogenase with NAD(P) binding	6.31	6.14E-05
<i>lsrB</i>	P76142	Autoinducer-2-binding protein LsrB	6.24	5.26E-13
<i>ygbJ</i>	Q46888	Putative dehydrogenase with NAD(P) binding	6.16	4.70E-06
<i>sbp</i>	P0AG78	Periplasmic sulphate-binding protein	6.16	7.82E-09
<i>agaA</i>	P42906	Putative N-acetylgalactosamine-6-phosphate deacetylase	6.13	3.36E-04
<i>yagH</i>	P77713	Predicted xylosidase/arabinosidase	6.13	1.11E-15
<i>ygbL</i>	Q46890	Putative aldolase class 2 protein	6.06	1.24E-03
<i>psuK</i>	P30235	Pseudouridine kinase	6	1.53E-06
<i>lsrR</i>	P76141	Transcriptional regulator LsrR	5.9	1.78E-15
<i>ybfG</i>	P37003	Uncharacterised protein	5.85	8.89E-04
<i>bssR</i>	P0AA Y1	Biofilm regulator	5.79	2.54E-06
<i>yngI</i>	A5A611	Uncharacterised protein	5.75	1.17E-05
<i>napC</i>	P0ABL5	Cytochrome c-type protein	5.71	8.28E-13
<i>yiiE</i>	P0ADQ5	Putative transcriptional regulator	5.7	8.20E-03
<i>yfhL</i>	P52102	Ferredoxin-like protein	5.69	7.92E-08
<i>ydeJ</i>	P0ACW0	Uncharacterised protein	5.68	1.52E-10
<i>thiC</i>	P30136	Phosphomethylpyrimidine synthase	5.65	4.15E-14
<i>bioA</i>	P12995	Adenosylmethionine-8-amino-7-oxononanoate aminotransferase	5.65	1.31E-03
<i>ybbD</i>	P33669	Uncharacterised protein	5.57	6.79E-03
<i>nudI</i>	P52006	Nucleoside triphosphatase	5.56	2.65E-05
<i>ydeO</i>	P76135	HTH-type transcriptional regulator	5.54	2.01E-03
<i>ilvN</i>	P0ADF8	Acetolactate synthase isozyme 1 small subunit	5.47	9.77E-13
<i>yagG</i>	P75683	CP4-6 prophage sugar transporter	5.4	1.05E-09
<i>pspF</i>	P37344	DNA-binding transcriptional activator	5.39	1.41E-08
<i>yjbM</i>	P32694	Function unknown	5.36	4.76E-08
<i>yjhP</i>	P39367	Phage-like element, predicted methyltransferase	5.35	1.44E-06
<i>envR</i>	P0ACT2	DNA-binding transcriptional regulator	5.31	3.21E-03
<i>ygaQ</i>	P76616	Uncharacterised protein	5.26	9.21E-04
<i>yncJ</i>	P64459	Uncharacterised protein	5.15	6.88E-06
<i>recN</i>	P05824	DNA repair protein	5.11	1.57E-11
<i>ybfO</i>	P77779	Uncharacterised protein	5.09	4.82E-05
<i>yeiL</i>	P0A9E9	DNA-binding transcriptional activator of stationary phase nitrogen survival	5.05	1.80E-03

^a Fold change based on normalised values; ^b p-value (≤ 0.001).

6. 6. 2. Genes down-regulated in *E. coli* K12 cells challenged with Byotrol™ compared to cells treated with Byotrol™

In cells challenged with 4 times MIC Byotrol™ for 2 hours after growth for 5 hours, 47 genes were down-regulated in comparison to cells treated with Byotrol™ for 5 hours (Table 6. 5). The gene most greatly down-regulated was *flgB* (~32-fold) which encodes the basal-body of flagella. Other genes associated with the synthesis of flagella were also down-regulated, including *flgC* (~21-fold), *flgD* (~11-fold), *flgE* (~9-fold), *flgF* (~6-fold), *fliA* (~16-fold), *fliM* (~9-fold), *fliF* (~6-fold). The genes encoding components of flagella are shown in Figure 6. 12. Also down-regulated under these conditions was *tnaC* (~12-fold), the gene encoding the leader peptide of the tryptophanase operon *tnaCAB*.

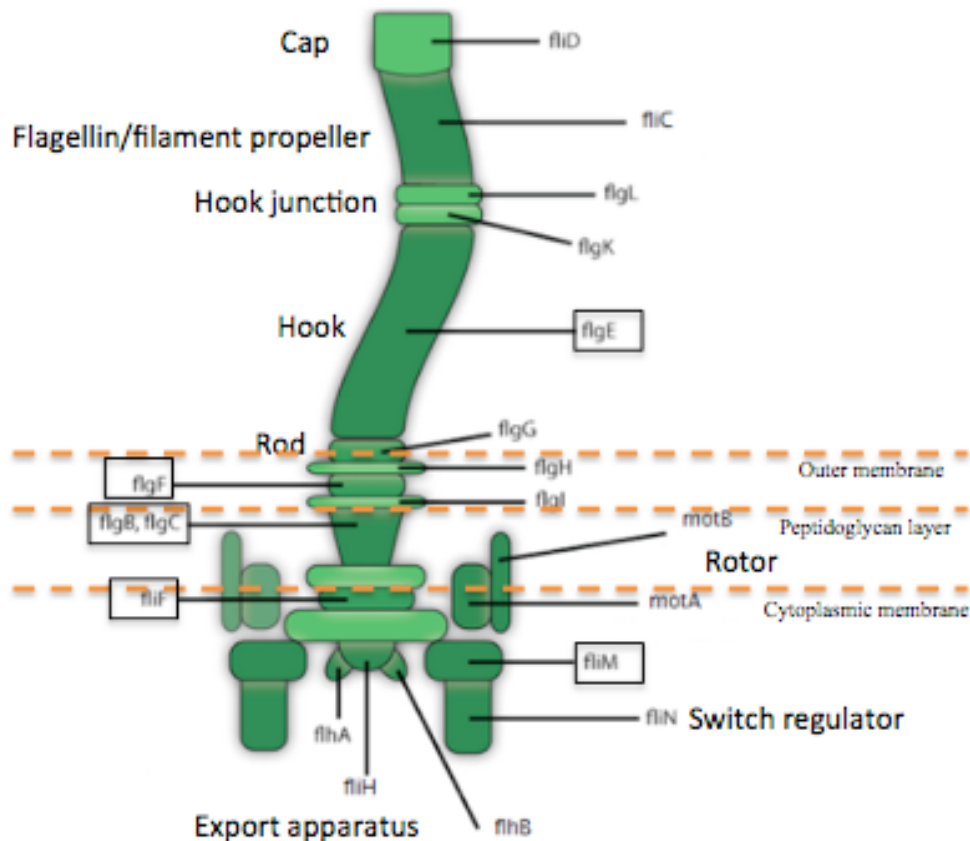


Figure 6. 12. Components of flagella and the genes involved in the synthesis of flagella apparatus. Genes highlighted within a box are those that are differentially expressed in the current study (Image adapted from California, 2012).

Table 6. 5. Genes in *E. coli* K12 down-regulated in response to challenge with Byotrol™ in comparison to cells treated with Byotrol™. Genes with a fold change ≤ 5 are displayed.

Gene	UniProt Entry	Function and/or product	Fold Change^a	p-value^b
<i>flgB</i>	P0ABW9	Flagellar basal-body rod protein FlgB	-31.58	1.95E-03
<i>hdeD</i>	P0AET5	Acid-resistance membrane protein	-22.02	2.38E-08
<i>yhiD</i>	P0AFV2	Putative Mg ²⁺ transport inner membrane ATPase	-21.58	9.09E-06
<i>ydiY</i>	P76206	Putative outer membrane protein, acid inducible	-21.28	4.00E-15
<i>flgC</i>	P0ABX2	Flagellar basal-body rod protein	-21.04	7.46E-05
<i>fes</i>	P13039	Enterochelin esterase	-17.59	1.63E-13
<i>fliA</i>	P0AEM6	Component of RNA polymerase sigma 28	-16.36	2.03E-05
<i>alsK</i>	P32718	D-allose kinase	-15.73	2.33E-14
<i>hyi</i>	P30147	Hydroxypyruvate isomerase	-15.66	3.66E-07
<i>glxR</i>	P77161	Tartronate semialdehyde reductase, NADH-dependent	-14.93	2.57E-04
<i>bglJ</i>	P39404	Transcriptional activator protein	-13.37	1.63E-13
<i>entB</i>	P0ADI4	Isochorismatase	-12.84	1.40E-13
<i>tnaC</i>	P0AD89	Tryptophanase leader peptide	-11.77	1.97E-05
<i>nrdF</i>	P37146	Ribonucleoside-diphosphate reductase 2 subunit beta	-11.72	1.07E-11
<i>flgD</i>	P75936	Basal-body rod modification protein	-10.69	1.46E-05
<i>rpiB</i>	P37351	Allose 6-phosphate isomerase	-9.57	8.42E-09
<i>gudP</i>	Q46916	Probable glucarate transporter	-9.28	3.33E-10
<i>flgE</i>	P50610	Flagellar hook subunit protein	-9.18	3.22E-15
<i>entS</i>	P24077	Enterobactin exporter	-8.88	2.66E-13
<i>fliM</i>	P06974	Flagellar motor switch protein	-8.73	7.92E-03
<i>entH</i>	P0A8Y8	Thioesterase	-8.09	7.25E-13
<i>arnC</i>	P77757	Undecaprenyl phosphate-L-Ara4FN transferase	-7.9	4.60E-04
<i>nrdI</i>	P0A772	Protein that stimulates ribonucleotide reduction	-7.87	6.97E-07
<i>mcrC</i>	P15006	McrBC restriction endonuclease	-7.83	4.78E-06
<i>gadE</i>	P63204	Transcriptional regulator	-7.44	8.86E-10
<i>mdtE</i>	P37636	Multidrug resistance protein	-7.26	2.76E-06
<i>ais</i>	C4ZU94	Lipopolysaccharide core heptose(II)-phosphate phosphatase	-7.22	5.69E-03
<i>gcl</i>	P0AEP7	Component of glyoxylate carboligase	-7.15	3.18E-06
<i>arnD</i>	P76472	Probable 4-deoxy-4-formamido-L-arabinose-phosphoundecaprenol deformylase	-6.99	9.42E-04
<i>arnA</i>	P77398	Bifunctional polymyxin resistance protein	-6.92	6.60E-08
<i>gudD</i>	P0AES2	Glucarate dehydratase	-6.78	1.55E-15
<i>yfaH</i>	P45505	Uncharacterised protein	-6.46	9.25E-05
<i>fecR</i>	P23485	Regulation of iron dicitrate transport	-6.45	9.42E-05
<i>cspA</i>	P0A9X9	Cold shock protein	-6.45	3.46E-06
<i>fliF</i>	P25798	Flagellar basal body M-ring protein	-6.44	4.38E-04
<i>fepC</i>	P23878	Component of ferric enterobactin ABC transporter	-6.29	8.10E-10
<i>iap</i>	P10423	Alkaline phosphatase isozyme conversion protein	-6.1	1.91E-09
<i>flgF</i>	P75938	Flagellar basal-body rod protein	-6.08	6.22E-03
<i>pyrI</i>	P0A7F3	Aspartate carbamoyltransferase regulatory chain	-5.99	5.66E-07
<i>fecl</i>	P23484	Probable RNA polymerase sigma factor	-5.94	1.21E-05
<i>fhuD</i>	P07822	Ferric hydroxamate uptake protein D	-5.7	1.17E-05
<i>gadC</i>	P63235	Extreme acid sensitivity protein	-5.62	1.22E-09
<i>yjdP</i>	Q6BEX5	Uncharacterised protein	-5.38	1.23E-12
<i>kdpA</i>	P03959	Potassium-transporting ATPase A chain	-5.22	8.72E-04
<i>uraA</i>	P0AGM7	Uracil transporter	-5.19	1.01E-05
<i>ydhO</i>	P76190	Endopeptidase	-5.13	5.55E-16

6. 7. Genes differentially expressed in *E. coli* K12 cells challenged with Byotrol™ compared to the growth control

6. 7. 1. Genes up-regulated in *E. coli* K12 cells challenged with Byotrol™ compared to the growth control

In cells challenged with 4 times MIC Byotrol™ for 2 hours after 5 hours of growth, 65 genes were down-regulated in comparison to the growth control (Table 6. 6). Many of the genes differentially expressed under these conditions have an unknown function, however the characterised protein that was most highly over-expressed was *csgD* (25 fold), which is involved in transcriptional regulation. Genes of the *lsr* operon were up-regulated in cells challenged with Byotrol™, namely *lsrA* (~11-fold), *lsrB* (~5-fold), *lsrC* (~11.5-fold) and *lsrR* (~6.5-fold). The gene with the highest fold change was *iraM*, which is up-regulated when magnesium ions are not present, thereby inducing RpoS.

Table 6. 6. Genes in *E. coli* K12 that were up-regulated in response to challenge with Byotrol™ compared to the growth control. Genes with a fold change greater 5 compared to untreated cells are displayed.

Gene	Uniprot Entry	Function and/or product	Fold Change ^a	<i>p</i> -value ^b
<i>iraM</i>	P75987	RpoS stabiliser during Mg ²⁺ starvation	36.17	1.85E-11
<i>yjbS</i>	P58036	Function unknown	27.19	7.92E-03
<i>csgD</i>	P52106	DNA-binding transcriptional activator in two-component regulatory system	25.39	4.44E-04
<i>yjfI</i>	P0AF76	Inner membrane protein	21.72	3.40E-09
<i>ariR</i>	P75993	RcsB connector protein for biofilm and acid resistance regulation	16.58	1.77E-13
<i>rrsA</i>		rRNA	16.28	2.22E-04
<i>yjfJ</i>	P0AF78	Predicted transcriptional regulator effector protein	16.26	9.00E-07
<i>pspD</i>	P0AFV8	Peripheral inner membrane phage-shock protein	16.1	3.55E-15
<i>ymgC</i>	P75994	Function unknown	15.36	4.49E-07
<i>ymgI</i>	A5A611	Function unknown	15.27	1.95E-07
<i>rrlG</i>		rRNA	15.14	3.37E-03
<i>gspC</i>	P45757	Protein secretion protein for export	14.94	8.84E-14
<i>elfA</i>	P75855	Predicted fimbrial-like adhesion protein	14.61	2.45E-10
<i>yegJ</i>	P76334	Function unknown	14.29	9.05E-05
<i>rrlE</i>		rRNA	12.84	3.60E-03
<i>pspC</i>	P0AFN2	Transcriptional regulator	12.06	4.44E-16
<i>napD</i>	P0A9I5	Twin-arginine signal-peptide-binding chaperone for NapA	12	2.77E-11
<i>fixB</i>	P31574	Flavoprotein subunit required for anaerobic carnitine metabolism	11.98	3.47E-10

^a Fold change based on normalised values; ^b *p*-value (≤ 0.001).

Table 6. 6. Continued.

Gene	Uniprot Entry	Function and/or product	Fold Change ^a	p-value ^b
<i>lsrC</i>	P77672	Autoinducer-2 (AI-2) uptake ABC transporter	11.59	4.97E-06
<i>ydeJ</i>	P0ACW0	Function unknown	11.56	1.50E-13
<i>yhaI</i>	P64592	Predicted inner membrane protein	10.84	3.59E-06
<i>lsrA</i>	P77257	Autoinducer-2 (AI-2) uptake; essential for aerobic growth	10.84	1.53E-14
<i>ycaL</i>	P43674	Putative heat shock protein	9.67	5.45E-05
<i>leuB</i>	P30125	Beta-Isopropylmalate dehydrogenase	8.71	2.24E-11
<i>ygbJ</i>	Q46888	Putative dehydrogenase with NAD(P) binding	8.35	9.51E-07
<i>matA</i>	P71301	Putative transcriptional regulator for mat genes (fimbrillin genes)	8.16	2.76E-06
<i>yedN</i>	P76321	Function unknown	7.83	5.78E-05
<i>fdrA</i>	Q47208	Protein transporter	7.77	9.02E-04
<i>napB</i>	P0ABL3	Small subunit of periplasmic nitrate reductase	7.67	1.79E-07
<i>nanC</i>	P69856	N-acetylneuraminic acid outer membrane channel protein	7.52	3.88E-06
<i>recN</i>	P05824	Protein used in recombination and DNA repair	7.16	1.53E-13
<i>ygbL</i>	Q46890	Predicted class II aldolase	7.02	8.09E-04
<i>agaV</i>	P42904	N-acetylgalactosamine-specific enzyme IIB component of phosphotransferase system (PTS)	6.83	8.08E-05
<i>ygiL</i>	P39834	Predicted fimbrial-like adhesin protein	6.68	3.82E-04
<i>yccJ</i>	P0AB14	Function unknown	6.64	8.47E-10
<i>yedR</i>	P76334	Inner membrane protein	6.59	1.32E-07
<i>agaA</i>	P42906	Predicted truncated N-acetylgalactosamine-6-phosphate deacetylase	6.54	2.67E-04
<i>yegP</i>	P76402	Conserved protein	6.51	1.53E-09
<i>lsrR</i>	P76141	<i>lsrACDBFGE</i> operon regulator for autoinducer-2 (AI-2) uptake	6.45	4.44E-16
<i>yhiL</i>	P37629	Uncharacterised protein	6.32	6.12E-05
<i>bioA</i>	P12995	Adenosylmethionine-8-amino-7-oxononanoate aminotransferase	6.28	9.35E-04
<i>yohC</i>	P0AD17	Predicted inner membrane protein	6.16	1.18E-03
<i>hokD</i>	P0ACG6	Small toxic membrane polypeptide	6.06	3.57E-03
<i>ibpB</i>	P0C058	Heat-inducible protein of HSP20 family	5.86	2.67E-11
<i>yagH</i>	P77713	Predicted xylosidase/arabinosidase	5.83	2.66E-15
<i>yagG</i>	P75683	Predicted sugar transporter	5.8	4.72E-10
<i>napG</i>	P0AAL3	Quinol dehydrogenase	5.62	3.37E-04
<i>ilvN</i>	P0ADF8	Acetohydroxy acid synthase	5.57	7.39E-13
<i>paaZ</i>	P77455	Enoyl-CoA hydratase	5.51	6.16E-04
<i>enu</i>	P64467	Origin of replication (OriC) binding protein	5.38	3.68E-06
<i>rcnA</i>	P76425	Probable nickel and cobalt efflux system	5.35	5.89E-07
<i>ybfG</i>	P37003	Uncharacterised protein	5.3	1.25E-03
<i>pspF</i>	P37003	DNA-binding transcriptional activator	5.28	1.73E-08
<i>yeiL</i>	P0A9E9	DNA-binding transcriptional activator of stationary phase nitrogen survival	5.23	1.59E-03
<i>lsrB</i>	P76142	Autoinducer-2 (AI-2) uptake	5.15	8.53E-12
<i>astE</i>	P76215	Succinylglutamate desuccinylase	5.13	2.47E-09
<i>yjbM</i>	P32694	Function unknown	5.08	7.99E-08
<i>proW</i>	P14176	High-affinity transport for glycine, betaine, and proline	5.07	1.51E-03
<i>ygbK</i>	Q46889	Function unknown	5.04	1.90E-08
<i>ydaF</i>	P0ACW0	Rac prophage putative protein	5.01	7.31E-03
<i>yfdF</i>	P76505	Uncharacterised protein	5	1.89E-09

^a Fold change based on normalised values; ^b p-value (≤ 0.001).

6. 7. 2. Genes down-regulated in *E. coli* K12 cells challenged with Byotrol™ compared to the growth control

In cells challenged with 4 times MIC Byotrol™ for 2 hours, 40 genes were down-regulated in comparison to the growth control (Table 6. 7). The gene with the greatest fold change was *flgB*, which encodes a flagellar protein, and as for the *E. coli* K12 cells treated with Byotrol™ when compared to cells challenged with Byotrol™, other genes involved in flagella synthesis and motility were also down-regulated (genes of the *flg* operon and *fli* operon). The subsequent characterised proteins also down-regulated were associated with the *als* operon, which encode components of the D-allose ABC transporter. Ion transport, flagellar synthesis, carbohydrate metabolism and protein synthesis were all down-regulated functions when challenged cells were compared to the growth control.

Table 6. 7. Genes in *E. coli* K12 that were down-regulated in response to challenge with Byotrol™ compared to the growth control. Genes with a fold change greater 5 compared to untreated cells are displayed.

Gene	UniProt Entry	Function and/or product	Fold Change ^a	p-value ^b
<i>flgB</i>	P0ABW9	Flagellar basal-body rod protein FlgB	-24.35	7.33E-03
<i>fes</i>	P13039	Enterochelin esterase	-20.5	7.77E-16
<i>alsA</i>	P32721	Component of D-allose ABC transporter	-18.94	1.46E-12
<i>alsC</i>	P32720	Component of D-allose ABC transporter	-17.5	2.15E-06
<i>ydiY</i>	P76206	Uncharacterised protein	-16.85	6.92E-12
<i>alsE</i>	P32719	Allose-6-P 3-epimerase	-15.11	7.77E-16
<i>nrdF</i>	P37146	Ribonucleoside diphosphate reductase 2	-14.86	3.66E-15
<i>arnC</i>	P77757	Undecaprenyl phosphate-L-Ara4FN transferase	-14.69	1.66E-07
<i>ais</i>	C4ZU94	Lipopolysaccharide core heptose(II)-phosphate phosphatase	-13.63	2.56E-05
<i>flgC</i>	P0ABX2	Flagellar basal-body rod protein FlgC	-11.5	5.86E-03
<i>fliA</i>	P0AEM6	Component of RNA polymerase sigma 28	-11.42	6.27E-04
<i>arnA</i>	P77398	Bifunctional polymyxin resistance protein	-10.46	7.23E-13
<i>entH</i>	P0A8Y8	Thioesterase	-9.9	2.22E-16
<i>arnD</i>	P76472	Probable 4-deoxy-4-formamido-L-arabinose-phosphoundecaprenol deformylase	-9.59	3.79E-05
<i>nrdI</i>	P0A772	Flavotoxin required for NrdEF cluster assembly	-9.55	1.47E-08
<i>entS</i>	P24077	Component of EntS-TolC Enterobactin Efflux Transport System	-8.21	4.25E-12
<i>flgE</i>	P50610	Flagellar hook subunit protein	-7.5	7.02E-12
<i>fepC</i>	P23878	Component of ferric enterobactin ABC transporter	-7.47	3.16E-12
<i>fecI</i>	P23484	RNA polymerase, sigma19 factor	-7.46	2.18E-07
<i>tdcE</i>	P42632	Pyruvate formate-lyase	-7.45	1.42E-10
<i>fecR</i>	P23485	Transmembrane signal transducer for ferric citrate transport	-7.14	2.62E-05
<i>flgD</i>	P75936	Flagellar biosynthesis, initiation of hook assembly	-6.87	1.37E-03
<i>entA</i>	P15047	Component of 2,3-dihydro-2,3-dihydroxybenzoate dehydrogenase	-6.67	1.23E-08
<i>bglJ</i>	P39404	BglJ transcriptional regulator	-6.64	3.98E-06
<i>ygfF</i>	P52037	Putative NAD(P) binding oxidoreductase	-6.53	9.28E-10
<i>yfaH</i>	P45505	Function unknown	-6.35	1.15E-04
<i>ynjE</i>	P78067	Thiosulphate sulfur transferase	-6.28	3.38E-11
<i>mcrC</i>	P15006	MrcC subunit of 5-methylcytosine restriction system	-6.23	1.08E-04
<i>tdcD</i>	P11868	Propionate kinase, anaerobic	-6.21	3.96E-05
<i>fliF</i>	P25798	Flagellar basal body M-ring protein	-6.2	6.36E-04
<i>alsB</i>	P39265	Periplasmic Allose-binding protein	-6.14	9.46E-10
<i>rbsR</i>	P0ACQ0	Transcriptional repressor for the ribose <i>rbsDACBK</i> operon	-5.78	5.00E-15
<i>uraA</i>	P0AGM7	Uracil permease	-5.71	1.88E-06
<i>yqgC</i>	P64570	Function unknown	-5.58	2.10E-13
<i>arnB</i>	P77690	UDP-4-amino-4-deoxy-L-arabinose synthase	-5.52	6.00E-09
<i>fhuD</i>	P07822	Ferric hydroxamate uptake protein D	-5.36	2.99E-05
<i>ydhO</i>	P76190	Endopeptidase	-5.34	1.11E-16
<i>exbD</i>	P0ABV2	Biopolymer transport protein ExbD	-5.3	4.44E-16
<i>fepG</i>	P23877	Ferrienterobactin transporter	-5.2	5.43E-04
<i>fhuB</i>	P06972	Ferrichrome-dependent iron uptake	-5.13	2.87E-10

^a Fold change based on normalised values; ^b p-value (≤ 0.001).

The data displayed in Tables 6. 3 to 6. 7 outline the number genes that were up and down-regulated in each condition. There are, however, genes that were up-regulated in one condition but down-regulated in another and these are detailed in Table 6. 8. Of the two comparisons (treated vs. growth control and challenge vs. treated), overall, genes were most greatly differentially expressed in cells treated with Byotrol™ when compared to the growth control.

Table 6. 8. Genes up-regulated in one growth condition and down-regulated in another.

Gene	UniProt entry	Gene function	Fold change expression in treated cells compared to growth control	Fold change expression in challenged cells compared to treated	Fold change expression in challenged cells compared to growth control
<i>cysW</i>	P0AEB0	Sulphate transport protein	-32.86	+16.78	ND*
<i>gcl</i>	P0AEP7	Glyoxylate carboligase	+8.91	-7.15	ND*
<i>glxR</i>	P77161	2-hydroxy-3-oxopropionate reductase	+13.49	-14.93	ND*
<i>gudP</i>	Q46916	D-glucarate transporter	+14.42	-9.28	ND*
<i>tnaC</i>	P0AD89	Tryptophanase leader peptide	+102.48	-11.77	ND*
<i>hyi</i>	P30147	Hydroxypyruvate isomerase	+15.1	-15.66	ND*
<i>tnaC</i>	P0AD89	Tryptophanase leader peptide	+102.48	-11.77	ND*
<i>ydjO</i>	P76210	Unknown function	-6.92	+13.94	ND*

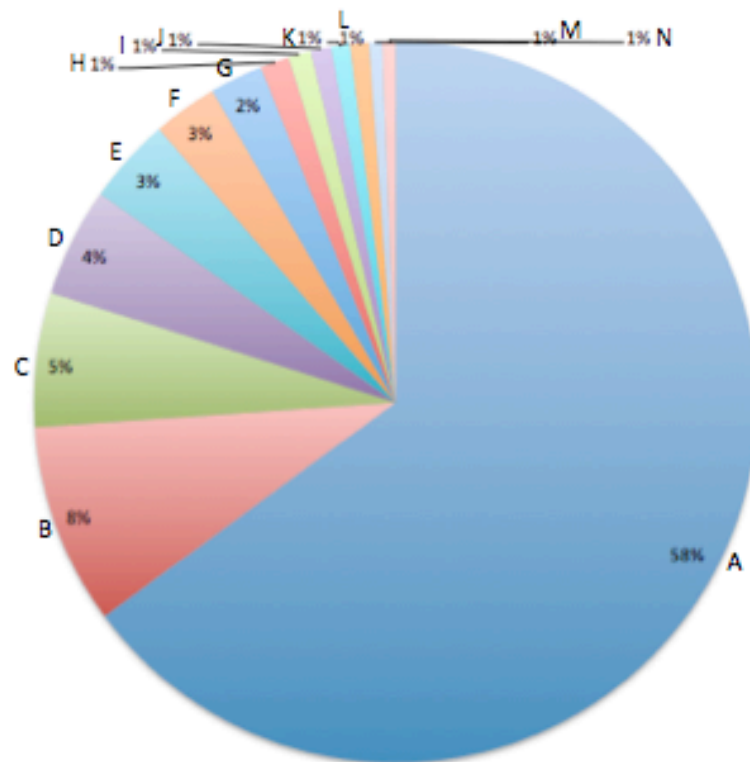
*‘ND’ No Difference.

6. 8. Unmapped reads

The data shows that the total number of unmapped reads were approximately 14 million (29% of total reads), 13.5 million (34% of total reads) and 11.6 million (36% of total reads) for the growth control, treated and challenge cells, respectively. An NCBI BLAST search of the unmapped reads for *E. coli* K12 growth control cells revealed the identity of the complete genomes or complete sequences to which the unmapped reads align (Figure 6. 13). The greatest proportion of the unmapped reads aligned to the *E. coli* APEC 078 genome (58%), followed by 8% of the unmapped reads that map to the *E. coli* K12 F plasmid. The number of reads which map to each of the genomes and sequences identified are displayed in Table 6. 9.

Table 6. 9. Genomes and sequences identified by BLAST to which unmapped reads align and the range of hits (reads) to the genome or sequence.

Genomes and sequences identified by BLAST to which unmapped reads align	Highest number of reads	Lowest number of reads
<i>Escherichia coli</i> APEC O78, complete genome	12467	24
<i>Escherichia coli</i> K-12 plasmid F DNA, complete sequence	155	1
<i>Salmonella enterica</i> subsp. enterica serovar Typhi str. Ty21a, complete genome	14354	100
<i>Escherichia coli</i> P12b, complete genome	9359	38
<i>Escherichia coli</i> O104:H4 str. 2009EL-2071, complete genome	979	45
<i>Salmonella enterica</i> subsp. enterica serovar Heidelberg plasmid pSH696_117, complete sequence	102	29
<i>Escherichia coli</i> Xuzhou21, complete genome	14354	70
<i>Escherichia coli</i> Vir68 plasmid pVir68, complete sequence	100	5
<i>Escherichia coli</i> DH1 (ME8569) DNA, complete genome	1133	10
<i>Escherichia coli</i> strain 3A11 plasmid pHN3A11, complete sequence	115	73
<i>Escherichia coli</i> plasmid pEC_L46, complete sequence	100	100
<i>Escherichia coli</i> W, complete genome	3461	80
<i>Escherichia coli</i> O25b:ST131 str. JIE186 plasmid pJIE186-2, complete sequence	236	92
<i>Escherichia coli</i> O55:H7 str. RM12579 plasmid p12579_2, complete sequence	37	35



- A ■ *Escherichia coli* APEC O78, complete genome
- B ■ *Escherichia coli* K-12 plasmid F DNA, complete sequence
- C ■ *Salmonella enterica* subsp. *enterica* serovar Typhi str. Ty21a, complete genome
- D ■ *Escherichia coli* P12b, complete genome
- E ■ *Escherichia coli* O104:H4 str. 2009EL-2071, complete genome
- F ■ *Salmonella enterica* subsp. *enterica* serovar Heidelberg plasmid pSH696_117, complete sequence
- G ■ *Escherichia coli* Xuzhou21, complete genome
- H ■ *Escherichia coli* Vir68 plasmid pVir68, complete sequence
- I ■ *Escherichia coli* DH1 (ME8569) DNA, complete genome
- J ■ *Escherichia coli* strain 3A11 plasmid pHN3A11, complete sequence
- K ■ *Escherichia coli* plasmid pEC_L46, complete sequence
- L ■ *Escherichia coli* W, complete genome
- M ■ *Escherichia coli* O25b:ST131 str. JIE186 plasmid pJIE186-2, complete sequence
- N ■ *Escherichia coli* O55:H7 str. RM12579 plasmid p12579_2, complete sequence

Figure 6. 13. Identification of unmapped reads in *E. coli* K12 growth control cells.

6. 9. Discussion

The presence of the biocide Byotrol™ evoked many genome-wide expression changes covering a variety of functional gene groups in *E. coli* K12. The induction and repression of a diverse group of genes occurred when cells are both treated with Byotrol™ for the duration of growth to mid-log phase at sub-inhibitory concentrations, and challenged with the biocide for 2 hours at 4 times the MIC.

6. 9. 1. Genes up-regulated in response to Byotrol™

6. 9. 1. 1. *Up-regulation of genes associated with transcriptional regulation and DNA binding*

Allen and co-workers (2006) found that PHMB, which is the main biocidal component in Byotrol™, degrades the DNA of the cell. It is therefore not surprising that the cell's response to the presence of PHMB, is to protect the DNA. In this study, *recN* and *umu* genes were induced. These genes are involved in DNA shielding (Allen *et al.*, 2006). *RecN* is a unique DNA repair gene, which is related to *recA* (Meddows *et al.*, 2005), also identified by Allen and co-workers as being up-regulated in the presence of PHMB (Allen *et al.*, 2006). *UmuD* is another gene whose protein product is involved in DNA repair and which is regulated by RecA. When DNA is damaged, the cell attempts to continue DNA synthesis by producing single stranded DNA, which in turn permits the formation of RecA. The production of RecA leads to the expression of the *umuDC* operon (Ohta *et al.*, 1999). This operon may be utilised in the recombinational repair of DNA which has been damaged, and increases protein stability, although exactly how proteins are stabilised is unclear (Frank *et al.*, 1996). The RecN protein is induced when the cell is exposed to DNA damaging agents, whereby RecN forms oligomers that interact with the DNA, protecting it from exonucleases (McKenzie *et al.*, 2000).

6. 9. 1. 2. *Up-regulation of genes involved in protein synthesis*

Sulphur is an essential element that is required for the biosynthesis of certain proteins as it is a component of some amino acids (Fuentes *et al.*, 2007; Mendez *et al.*, 2011). The *cys* operons encode sulphur-containing amino acids such as methionine and cysteine, which may be required for protein repair after biocidal damage (Mendez *et al.*, 2011). In

In addition to this, in sulphur containing nucleic acids, di-sulphide bonds are repaired under stress, and these di-sulphide bonds are important in maintaining DNA stability under changes in the pH of the environment (Dolinnai & Borisova, 2000). In cells treated with Byotrol™ there was an up-regulation of genes associated with sulphate binding and transport, namely *cysA*, *cysD*, *cysU*, *cysW*. Gunasekera and co-workers also described the *cys* gene clusters as being related to stress response in *E. coli* K12, particularly to heat shock, however it is postulated that genes that are associated with a specific stress response such as heat, may also be induced in other stress conditions (Gunasekera *et al.*, 2008). In addition to this, cysteine is a precursor of glutathione, which is important as a defence against oxidative stress by maintaining a reduced environment in the cytosol. Exactly how this is achieved has not been studied in great detail, but there is definite induction of glutathione upon oxidative stress (Carmel-Harel & Storz, 2000).

6. 9. 1. 3. Up-regulation of genes specific to stress response

The phage shock protein (Psp) stress response system is responsible for repairing damage to the inner membrane of the cell and maintenance of the proton-motive force across the inner membrane (Brissette *et al.*, 1990). The *pspC*, *pspD* and *pspF* genes were up-regulated in cells challenged with Byotrol™. Although Psp is induced in response to phage shock, it is also up-regulated under other conditions including secretin production, blockage of protein export or phospholipid biosynthesis, extreme osmotic or heat shock and high ambient pH (Huvet *et al.*, 2011). It may be for this reason that it was induced at high concentrations of Byotrol™.

IraM was up-regulated (~36-fold) when cells were challenged with Byotrol™ compared to the growth control. *iraM* is involved in the induction of σ^S (RpoS) sub-unit of RNA polymerase particularly upon magnesium ion (Mg^{2+}) starvation (Hengge-Aronis, 2002). QACs act by displacing the Mg^{2+} ions that stabilise the outer membrane of *E. coli*, consequently, the cell wall is perturbed causing cell lysis (Gilbert & Moore, 2005). At bactericidal concentrations, PHMB also causes DNA damage (Allen *et al.*, 2006). RpoS is rapidly induced upon stress, including osmotic stress, DNA damage, nutrient deprivation, heat and cold shock and acid shock (Battesti *et al.*, 2011), furthermore, RpoS may be induced as a stress response which induces biofilm related genes, as RpoS

is essential for biofilm formation (Hengge-Aronis, 2002). The induction of biofilm formation as a stress response will be discussed further in Section 6.9.5.

The small heat shock protein of *E. coli*, IbpB, was also up-regulated in cells challenged with Byotrol™ (~6-fold). The *ibpB* gene is up-regulated under antimicrobial stress as well as elevated temperatures and acts as an anti-oxidant (Hansen *et al.*, 2004). The role of IbpB, with the assistance of other chaperones, is to re-fold denatured proteins and prevent their aggregation (Veinger *et al.*, 1998).

6.9.1.4. Up-regulation of genes involved in quorum sensing

Quorum sensing is the cell-cell signalling mechanism used by bacteria to control gene expression in response to cell density, which can regulate bacterial pathogenicity by regulating the coordinated expression of virulence factors, toxin production, motility and biofilm formation. In the current study, the *lsr* operon was up-regulated when cells were treated and challenged with Byotrol™ compared the growth control. Autoinducer-2 (AI-2), a signalling molecule used for bacterial intercellular communication, is transported into the cell via the genes encoded by the *lsr* operon, therefore it is likely that the AI-2 is still effectively internalised under biocidal stress. Previous studies have found that AI-2 production is directly related to growth rate (DeLisa *et al.*, 2001; Ren *et al.*, 2004a). Cells that are in the exponential phase of growth have an increasing level of AI-2 (Ren *et al.*, 2004a). DeLisa and co-workers also found that AI-2 expression was closely affected by environmental stress such as changes in levels of glucose, oxygen, extreme temperature, ethanol stress and oxidative stress and observed an initial decrease in AI-2 followed by oscillating levels particularly in the presence of ethanol and heat stress (Zhang *et al.*, 2007). *lsr* up-regulation may be continuous in response to Byotrol™, however, with regard to the relationship between growth rate, ethanol and heat stress, and AI-2 expression, the up-regulation of the *lsr* operon in the current study may be a snapshot of AI-2 gene regulation, and perhaps if gene expression was studied at various time points for a longer period, an oscillating pattern of *lsr* gene expression may also have been observed.

6. 9. 1. 5. Up-regulation of pili and curli fimbriae genes

The study by Allen and co-workers, as with the current study, demonstrated that pili and curli fimbriae genes were up-regulated, which was exemplified by the up-regulation of *elfA* (a *fimA* homolog), *ygiL* and *csgD*, when cells were treated and challenged with Byotrol™. *csgD* was up-regulated ~36-fold in cells challenged with Byotrol™ when compared to the growth control. *csgD* is the master regulator for adhesive curli fimbriae expression and is necessary for transcription of the first operon which encodes *csgBAC*, as well as the second operon encoding the *csgDEFG* operon (Gophna *et al.*, 2001). *csgD* may be up-regulated because the pili and fimbriae are suggested to be important in cell aggregation; it is possible that increased cell aggregation will protect cells in the middle of the aggregate from the damaging effects of the biocide (Allen *et al.*, 2006). It is also possible that the up-regulation of fimbriae genes is due to the up-regulation of RpoS (Section 6. 9. 1. 3), as curli expression is dependent on RpoS (Arnqvist *et al.*, 1994; Barnhart & Chapman, 2006).

6. 9. 2. Genes down-regulated in response to Byotrol™

In a comparison of the genes expressed by the *E. coli* K12 growth control and the genes expressed when cells are treated or challenged with Byotrol™, a greater proportion were down-regulated in the challenged cells. These will be discussed further in the following sections.

6. 9. 2. 1. Down-regulation of genes involved in flagellar synthesis

Flagella are required for motility and chemotaxis in *E. coli* (Vladimirov *et al.*, 2010; Zhao *et al.*, 2007). In the current study, the *flgB*, *flgC*, *flgD* and *flgE* genes of the flagella-associated operon *flgBCDEFGHIJKL* were down-regulated in cells both treated and challenged with Byotrol™, as were genes of the *fli* operon involved in the synthesis of structural components of flagella. Furthermore, *matA*, which is a repressor of flagellar genes, was up-regulated when cells were challenged with Byotrol™, although perhaps not induced at sub-inhibitory concentrations of Byotrol™ when cells were treated with Byotrol™. It is likely that the whole operon was down-regulated but as Allen and co-workers (2006) suggest, perhaps due to differences in transcript stability, not all of the genes were reverse transcribed. Previous studies have also demonstrated that genes associated with flagella synthesis are down-regulated in the presence of

PHMB (Allen *et al.*, 2006), which suggests that motility was not the main priority of *E. coli* when under the stress the Byotrol™. There is also a suggestion by Allen and co-workers (2006) that cellular damage caused by PHMB forces the *E. coli* to switch from flagella synthesis to curli synthesis, as curli fimbriae allow the cells to aggregate in order to protect themselves from PHMB damage.

6. 9. 2. 2. Down-regulation of genes involved in central metabolism

An important feature of the stress response is conservation of energy (Weber *et al.*, 2005). Gene expression studies show a repression of genes associated with cell growth when cells are under stress (Barker *et al.*, 2001; Weber *et al.*, 2005). This is exemplified by the D-allose (*als*) operon, which is involved in carbohydrate metabolism. D-allose can be utilised by *E. coli* as a carbon source, and therefore, when growth is repressed as a stress response, this operon is not required, as growth is not the cell's priority under conditions of stress (Kim *et al.*, 1997).

6. 9. 2. 3. Down-regulation of genes involved in iron transfer

Iron is an essential microelement for bacteria for aerobic metabolism and growth (Ouyang & Isaacson, 2006; Vagralli, 2009) and bacteria produce mechanisms of iron uptake called siderophores, which, under iron starvation scavenge iron from the environment (Andrews *et al.*, 2003). In *E. coli*, there are a number of iron transport systems which are involved in the transport of ferrichrome and ferric-hydroxamate, ferric-enterobactin (FeEnt), and ferric-citrate (Ouyang & Isaacson, 2006); Waldron & Robinson, 2009). These pathways were all down-regulated in *E. coli* K12 when challenged with Byotrol™.

Enterobactin, encoded by the *ent* operon, is one of the major siderophores of *E. coli* (Ehmann *et al.*, 2000). The proteins encoded by the *fep* operon as well as *fes* are involved in the transport of FeEnt into the bacterial cell. FepA facilitates the initial binding of FeEnt, FepB transports FeEnt across the periplasmic membrane, FepD and FepG are cytoplasmic transmembrane proteins that receive FeEnt from FepB, which is facilitated by FepC (Raymond *et al.*, 2003). Overall, in cells challenged with Byotrol™ compared to the growth control and also when cells challenged with Byotrol™ were compared to cells treated with Byotrol™, the *fep* operon and *fes* were down-regulated

along with the *ent* genes which encode enterobactin (-20.5 to -5.2-fold down-regulation).

Although iron is essential for growth in bacteria, there is an optimum intracellular concentration, which is different for each species. If the intracellular concentration of iron is too high, it may lead to oxidative damage caused by free radicals within the bacterial cell (Andrews *et al.*, 2003). As the action of Byotrol™ is likely to result in damage of the outer membrane, perhaps the need for chelating iron and transporting it across the membrane is reduced.

As with the transport of iron, many genes associated with the cytoplasm and periplasm which have transport and binding functions, were down-regulated in cells challenged with Byotrol™ when compared to the growth control and treated cells. This may also be due to the damage caused by biocidal action to the outer membrane of the bacterial cell whereby the activities of transport systems across the membrane are disturbed or required to a lesser degree than when the membrane is intact (Torres *et al.*, 2001).

6. 9. 2. 4. Down-regulation of specific stress response genes

The *gad* genes form two operons: the *gadA* operon and the *gadBC* operon. *gadA* and *gadB* encode isoforms of glutamate decarboxylase and *gadC* encodes glutamate γ -amino butyric acid (GABA), a membrane associated antiporter that exchanges exogenous glutamate for intracellular GABA (Castanie-Cornet & Foster, 2001). *GadE* is required for the activation of *gadA* and *gadBC* expression, therefore if *gadE* is down-regulated, *gadA* and *gadBC* are also down-regulated (Hirakawa *et al.*, 2010). Previous studies have demonstrated that the acid-resistance genes *gadA*, *gadB* and *gadE* (previously *yhiE*), and *hdeD* are up-regulated in low pH environments and under continuous heat stress, however, they are down-regulated under osmotic stress (Gunasekera *et al.*, 2008; Tucker *et al.*, 2002). In the current study, the *gad* operons and *hdeD* were also down-regulated in the presence of biocidal stress, particularly when cells were challenged with Byotrol™ compared to cells treated with Byotrol™. The exact function of the protein product of *hdeD* is unclear, however as for the *gad* operons, *hdeD* is involved in acid-resistance. Lee and co-workers suggest that AI-2 has a regulatory effect on *gad* and *hde* expression, whereby AI-2 repressed the expression of the *gad* and *hde* genes 6-18-fold (Lee *et al.*, 2007a).

The cold shock protein encoded by *cspA* was down-regulated (-6.45-fold) in cells challenged with Byotrol™ compared to cells treated with Byotrol™. *cspA* encodes a protein that has a function related to the adaptation to adverse conditions and a previous study has found that this protein is up-regulated in the presence of biocidal stress, particularly BAC, in *E. coli* and *Salmonella* biofilms (Mangalappalli-Illathu & Korber, 2006). It is possible that the down-regulation of *cspA* in cells challenged with Byotrol™, which was demonstrated by this current study, is due to the high concentrations used. The up-regulation of the cold shock protein may only occur when cells are exposed to an optimum sub-lethal concentration, therefore as the concentration of the biocide increases, the expression of the cold shock protein is induced up to a certain concentration of biocide, after which the biocide concentration increases to a level whereby the cold shock protein is not required.

6. 9. 3. Correlation of gene expression with protein expression

6. 9. 3. 1. D-ribose periplasmic binding protein

In the current study, *rbsR* was down-regulated (~6-fold) in cells challenged with Byotrol™ when compared to both the growth control and Byotrol™ treated cells. This gene encodes a DNA binding transcriptional repressor, RsbR, which represses the transcription of the ribose operon (*rbsDACBK*) (Mauzy & Hermodson, 1992; Shimada *et al.*, 2013). When *rbsR* is down-regulated, the ribose operon continues to be functional, which correlates with the up-regulation of RsbB protein, as discussed in Chapter 5, Section 5. 7. 3. However, *rbsB* was not observed to be up-regulated in the transcriptomics data of the current study, the reason for which is unclear.

6. 9. 3. 2. Tryptophanase and indole production

In cells treated with Byotrol™ the expression of *tnaC* was up-regulated (~100-fold) in relation to the growth control. However when cells were challenged, the expression of *tnaC* was down-regulated (~11-fold). *tnaC* encodes the leader peptide in the *tnaCAB* operon, involved in tryptophan and indole metabolism. *tnaC* may be induced when cells are continuously under the pressure of growing in the presence of an inhibitor, as amino acids such as tryptophan are required for growth and protein repair, which is paramount to cell survival under such conditions. However, when cells are transiently or acutely

challenged with a biocide as they are when challenged with Byotrol™, this amino acid may not be as essential to survival in the short term. Instead other functions such as the up-regulation of fimbriae take priority, as discussed in Section 6.9.1.5. Indole is the product of tryptophan catalysis and therefore tryptophanase regulation has an effect on the production of indole. As discussed previously, indole is a known global regulator in *E. coli* of genes associated with acid stress and motility (Hirakawa *et al.*, 2010). Therefore, as indole is expressed in cells treated with Byotrol™, motility is down-regulated, but also, as indole is repressed in cells challenged with Byotrol™, acid-resistance is also repressed. The up-regulation of tryptophanase gene expression correlates with the up-regulation of tryptophanase protein expression in treated cells, as discussed in Chapter 5, Section 5.7.2.

6.9.4. Genes both up and down-regulated under the same condition

When grouping genes into the functional categories of protein synthesis, flagella synthesis, DNA replication, ion transport, transcription regulation and energy production, it is clear that some genes are up-regulated and others from the same group are down-regulated even though cells were exposed to the same growth condition. For example, in cells challenged with Byotrol™ compared to the cells treated with Byotrol™, stress response genes were both up and down-regulated. The *ibpB* gene involved in stress response was up-regulated (~6-fold), the *hdeD* gene encoding a membrane protein involved in acid-resistance, is a stress response protein which was down-regulated (~22-fold). This apparently conflicting trend in the differential expression of genes according to their function is most likely due to the way in which genes were grouped into very broad functional categories. The grouping does not account for the complexity involved in the regulation of genes for a particular function.

6.9.5. Induction of biofilm-related genes under stress

The induction of RpoS which in turn may be related to the up-regulation of fimbriae curli (Barnhart & Chapman, 2006), which are known to be induced during the early stages of biofilm formation (Blumer *et al.*, 2005), may suggest that planktonic cells were up-regulating genes related to biofilm formation. Tryptophanase was also down-regulated in challenged cells (~11-fold), thereby repressing the production of indole. Indole is known to inhibit biofilm formation (Lee *et al.*, 2007b), therefore the repression

of indole may encourage biofilm formation. AI-2 and RpoS were also up-regulated, both proteins regulate biofilm forming genes (Barnhart & Chapman, 2006; Li *et al.*, 2007). Furthermore, previous studies have suggested that when biofilm forming genes are up-regulated, acid-resistance genes are down-regulated (Lee *et al.*, 2007a), which was also demonstrated in this study, whereby *gad* and *hde* genes were down-regulated. Perhaps biocidal damage induced biofilm formation as a stress response (Landini, 2009; Shemesh *et al.*, 2010).

6.9.6. Greater differential expression of genes in cells challenged with Byotrol™ compared to cells treated with Byotrol™

The continuous presence of an antimicrobial is thought to induce a stress response, as demonstrated with the cells treated with sub-MIC Byotrol™ for 5 hours. However genes expressed when cells are in this state of stress are thought to be up or down-regulated initially, but then settle into a steady state (Gunasekera *et al.*, 2008). However, an acute or short period of stress, as demonstrated with the cells challenged with 4 times Byotrol™ for 2 hours after growth for 5 hours, requires the cell to induce genes associated with shock response (Gunasekera *et al.*, 2008). Perhaps for this reason, a greater number of differentially expressed genes are observed in the cells challenged with Byotrol™ in comparison to the cells treated with Byotrol™ for 5 hours at a sub-inhibitory concentration.

6.9.7. Unmapped reads

Approximately 30% of the sequence reads obtained in the current study did not map to the reference *E. coli* K12 genome. The particular strain of *E. coli* K12 MG1655 used in this current study carries an XL-1 blue phage and therefore contains a Lambda cloning vector. Perhaps some of the unmapped reads map to this vector. The high percentage of unmapped reads which mapped to the *E. coli* APEC 078 strain and the high number of reads against the *E. coli* Xuzhou, an O157:H7 strain, as well as the other strains identified by the BLAST search, indicated that there was some environmental or sampling contamination. Previously published RNA-Seq data also produced approximately 5-20% unmapped reads (Wang *et al.*, 2009b; Yi *et al.*, 2011). A study which has evaluated the identity of unmapped reads concluded that commonly, the

reason for unmapped reads is due to rRNA which has not been successfully removed (Yi *et al.*, 2011).

Chapter 7

General Discussion and Future Work

The purpose of the studies presented in this thesis was to identify a novel cationic antimicrobial compound that has the potential for the treatment or prevention of infections caused by Gram-negative uropathogens. As part of this, data to better understand how a selected antimicrobial might perform as a catheter coating, and as an antimicrobial against an established biofilm is presented. Also, studies to elucidate the biological response of *E. coli*, the most common cause of CAUTI, to a selected antimicrobial, are presented. Genes and proteins that were differentially expressed demonstrated how these bacteria adapt to certain antimicrobial stresses.

There is no doubt that an established and mature biofilm is difficult to treat. There is a need to understand the behaviour of mature biofilms, as the treatment challenges of this stage of the biofilm phenotype are significantly more diverse and different to a young biofilm. However, intervening at the early stages of biofilm development and inhibiting planktonic cells before they are able to attach to a surface is most desirable. For this reason the inhibition of viable planktonic bacteria that could potentially attach to the surface was evaluated at 18 hours with the microtitre plate biofilm formation assay and at 8 hours for the pre-coating assay.

A study by Amin and co-workers (2009) revealed that the Gram-negative bacteria *E. coli*, *K. pneumoniae* and *P. aeruginosa*, as well as *Enterobacter* spp. are the most commonly isolated organisms from a colonised urinary catheter (Amin & Wareham, 2009). Crystalline biofilms commonly caused by *P. mirabilis* and *K. pneumoniae* are a common problem for catheterised patients, and are notoriously difficult to treat. However, as *K. pneumoniae* is the second most prevalent organism isolated from a CAUTI after *E. coli*, the latter was prioritised for use in the current study. Although coagulase-negative staphylococci such as *S. epidermidis* are a cause of CAUTI, they are often contaminants of a catheter when the device is being inserted, also, Gram-positive bacteria account for less than 3% of CAUTI (Hooton *et al.*, 2010). This being the case, Gram-positive bacteria were not tested in this study. The effect of antimicrobials against a mixed population of bacterial species relevant to UTI has also not been studied. Studying mixed populations is always a challenge and something that surely all biofilm researchers aspire to investigate once the challenges of mono-culture biofilms have been overcome and a greater understanding of biofilm behaviour is gained from single species biofilms.

7. 1. **The search for a novel cationic antimicrobial**

During the course of the current study, natural compounds and QACs were tested for their antimicrobial potential. The initial search for natural compounds such as polyamines was abandoned in the light of the fact that QACs, with their stable cationic charge, would likely be superior, providing antimicrobial action at lower concentrations. The antibacterial properties of a QAC depends on the size (molecular weight), the length of hydrophobic chains in the quaternary ammonium groups, and the counter-anion (Chen *et al.*, 2000). Of the QACs tested, as described in Chapter 4, many did not display inhibitory activity against planktonic or biofilm cells. In fact, this was also demonstrated when the natural polyamines were quaternised (Chapter 3). The counter ion associated with the quaternary ammonium group of the quaternised polyamines is iodide (I⁻), which may result in quenching of the positive charge associated with the nitrogen group, as iodide is such a large negatively charged ion. The current study did demonstrate that, overall, low molecular weight cationic polyquaterniums are better inhibitors than the higher molecular weight compounds tested, as described in Chapter 4. The current study also supports the theory associated with the antimicrobial activity of quaternary ammonium compounds and poly-cationic compounds in relation to molecular weight, which is based on a bell-shaped curve, whereby very low and very high molecular weight compounds have less antimicrobial activity (Chen *et al.*, 2000). This suggests it may be possible to identify a compound that displays optimal characteristics for potent antimicrobial activity.

Of the antimicrobials screened in the current study, Byotrol™, a novel formulation of QACs and PHMB described in Chapter 4, displayed the greatest antimicrobial activity both in suspension and as a coating, inhibiting the growth of planktonic cells and early biofilm growth of Gram-negative uropathogenic organisms. However, as well as screening for inhibitory compounds using the MIC assay and microtitre plate biofilm formation assay, bacteria were also exposed for 8 hours to a surface pre-coated with Byotrol™. This assay attempted to determine if bacteria were likely to be killed upon contact with a Byotrol™ coated surface, rather than in suspension as was the case for the microtitre plate biofilm formation assay (Chapter 4, Section 4. 2). For the pre-coating of a microtitre plate, Byotrol™ was dried onto the surface. This method of coating may be temporary as Byotrol™ may come away from the surface once a suspension of bacteria is added, as Byotrol™ is soluble in water. In addition to this, it was difficult to quantify

the exact concentration of Byotrol™ that was coated onto the surface as much of it was decanted, therefore it is likely that the concentrations adhered to the surface were lower than what was initially dispensed onto the surface. Even given these limitations with the method of pre-coating used in this study, it was useful for gaining an initial understanding of Byotrol™'s pre-coating potential and activity as a coating. In order to ensure that a sufficient amount of Byotrol™ had coated a surface, AFM was used. This confirmed that a solution with a concentration of 1 mg/mL Byotrol™, when dispensed onto a surface, was still sufficient to cover a surface consistently. Also, initial AFM results demonstrated that there was a greater thickness in the coating as the concentration increased, which suggests that a higher concentration of Byotrol™ on a surface may have a longer lasting effect than lower concentrations, however further replicates would need to be performed to confirm this fully.

In order to place these findings in context with the clinical situation whereby the catheter will be exposed to urine under flow, a method to coat the surface of a catheter more permanently would need to be employed. The stability and lifetime of this coating under flow would also be an important factor in the success of Byotrol™ as a catheter coating. It would be sensible to presume that the more stable the coating, the longer the catheter's lifetime would be. That being the case, any uroepithelial cell toxicity associated with long-term use of Byotrol™ would also need to be assessed. It should be noted that PHMB, the most potent antimicrobial compound in the Byotrol™ formulation, is already widely used in the environmental and clinical setting, including wound care dressings and contact lens solutions (Kingsley & Kiernan, 2013). Although PHMG (polyhexamethyleneguanide hydrochloride) is no longer approved for use, the safety aspects of continued use of PHMB is still under investigation. A detailed review of the studies surrounding the alleged carcinogenic nature of PHMB has concluded that the effect is minimal at the concentrations tested. In addition to this, it may be that the manner in which PHMB is applied, has an impact on how adverse the effects of PHMB is on health (Agency, 2011). The United States Environmental Protection Agency has noted that PHMB does not have adverse effects to human health. In addition to this, Materials Safety and Data Sheets for PHMB outline that there is not a great risk of toxicity by PHMB (Appendix E. 1). Tests with PHMB against mammalian cells and in studies with human participants also did not show significant adverse effects (EPA, 2004a; EPA, 2004b), and given the concentrations that are proposed to be used, it is not likely that cytotoxicity will be a major cause for concern.

7. 2. The effects of Byotrol™ on the biological pathways of *E. coli*

In this study, technology to elucidate both protein and mRNA expression was important, as no one approach will facilitate a comprehensive understanding of a cell's physiology and adaptability under antimicrobial stress. Transcriptomics enables the study of the transcriptome of a cell, a dynamic entity that reflects a snapshot of the organism's response to a changing environment (Zhang *et al.*, 2010a). Proteomics is a direct method to yield a picture of an organism's living state at a given time point, under specific conditions (Lubec *et al.*, 1999). Researchers have used various proteomic and transcriptomic technologies to understand the metabolic activity of bacterial cells that are under the stress of an external factor such as antimicrobials.

In comparison to the high throughput and relatively low cost of transcriptomics, proteomics is far more time consuming and has many limitations. The challenges of proteomics include the low level of coverage of information retrieved due to variations in protein hydrophobicity, protein stability and abundance, protein size and charge and modifications of proteins caused by components in the various buffers and reagents required for growth of cells, extraction, purification and resolution (Hedge, 2003). The challenges associated with proteomics make the steps involved difficult to standardise and fully control (Koomen *et al.*, 2008). 2DGE although notoriously difficult to reproduce, often with low resolution and low detection limits, is the most common way to analyse whole cell protein (Meleady, 2011; Sauer, 2003). The main limitation of 2DGE is the inter-gel variation. Newer technologies have helped to overcome some of the limitations of 2DGE, for example, fluorescently tagged proteins enable higher detection levels and greater sensitivity the gold standard of which is two dimensional difference gel electrophoresis (2D-DIGE) (May *et al.*, 2012). 2D-DIGE allows for the comparison of up to three different protein samples, each labelled with different fluorescent dyes. The samples are then resolved simultaneously on the same 2D gel (Alban *et al.*, 2003).

The use of an internal control is what brings 2D-DIGE into its element. An internal control is a reference control, which involves pooling all of the samples at equal concentrations and labelling them with one fluorescent dye. This internal standard is run with the individual samples on the same gel. By comparing the sample protein spot to its corresponding reference spot, a true measure of induced biological change can be

elucidated (Marouga *et al.*, 2005). This is not possible with 2DGE whereby only one sample can be resolved per gel.

Despite any limitations of 2DGE, the importance of proteomics should not be underestimated. Proteins are the functional components of cells, therefore an understanding of which proteins are expressed and repressed under different conditions and during expression of different phenotypes, provides us with more practical and applicable information than can be predicted by the mRNA expression levels alone (Gygi *et al.*, 1999; Zhang *et al.*, 2010b).

As RNA-seq is still a relatively new technology, and under development, it presents some challenges. In order to construct a cDNA library, several stages are involved, including the fragmentation of large mRNA or cDNA molecules so that they can be processed by deep-sequencing technologies (Wang *et al.*, 2009b). For this current study, the Illumina Sequencing system was used, which produces short reads (100 bp). Another, more practical challenge is related to bioinformatics. RNA-Seq produces a very large volume of data, which can be difficult to process on some systems so the appropriate hardware and software that can handle this type of data should be considered before starting analysis (Wang *et al.*, 2009b).

Although transcriptomics is not without its flaws, as described, it is extremely sensitive, with the capacity to detect even low abundance transcripts and subtle changes in mRNA expression (Lundberg *et al.*, 2010). The relatively new RNA-Seq technology is continually being assessed to identify and remove any limitations, however, to date, this technology is by far the best method to analyse the transcript of a cell (Lopez-Casado *et al.*, 2012).

A greater number of transcripts were identified as differentially expressed compared to the number of proteins. This may be because of the limitations of the proteomic technique employed, which therefore did not reveal a significant proportion of the proteins that had been expressed. It is also important to consider that cellular gene transcripts are not necessarily translated into proteins. In the current study there was a positive correlation between the up-regulation of genes transcribed and the over-expression of proteins, i.e. the proteins that were identified as over-expressed when

treated or challenged with Byotrol™ have corresponding genes that were also up-regulated.

Proteomics and transcriptomics have revealed that the enzyme tryptophanase, encoded by *tnaCAB* was differentially expressed. Tryptophanase is responsible for the metabolism of indole, a known gene regulator of acid resistance, biofilm formation and motility in *E. coli* (Hirakawa *et al.*, 2010), which may be potentially important for biofilm and planktonic survival in the presence of Byotrol™. The importance of the proteins identified as differentially expressed in planktonic and biofilm growth when treated and challenged with Byotrol™ would have to be validated by western blot. Likewise, differentially expressed genes identified by RNA-seq, such as those identified as being important in transcription regulation, fimbriae synthesis, stress response, and the induction of biofilm related genes need to be validated with quantitative-reverse transcriptase PCR (q-rtPCR) and their protein products, validated by western blot analysis.

7. 3. Proposals for use of Byotrol™ as a novel catheter coating

A catheter surface itself contributes to the effectiveness of adherence of bacteria to the material, and the organism's ability to produce the necessary components of a biofilm (Ryder, 2005). Therefore, current therapeutic options to reduce the formation of biofilms on catheter surfaces include using new material surfaces that are inherently more resistant to bacterial adhesion. Products being developed for a suitable catheter material should have the following criteria: they should be biocompatible, flexible, comfortable for the patient, durable, strong, have a low coefficient of friction and minimise bacterial adhesion and catheter encrustation. A hydrogel that coats a silicone or latex catheter would appear to fit these criteria (Cox *et al.*, 1989; Zhu & Marchant, 2011).

Hydrogels are synthetic, three dimensional, cross-linked polymer networks that are ideal as drug delivery systems (Gou *et al.*, 2008). Therefore, not only do the inherent properties of hydrogels reduce adhesion of bacteria, but they can also be manipulated to allow the incorporation of inhibitors into their structure, which can be released in a controlled manner. Hydrogels are sensitive to external parameters such as pH and

temperature, so, depending on the overall charge of the hydrogel, the degree of cross-linking and the conditions of its external environment, the hydrophobicity of the hydrogel will alter and an embedded drug can be released (Satish *et al.*, 2006). Hydrogels have already been used for the incorporation of antimicrobial agents including chlorohexidine, benzalkonium chloride, triclosan and silver, either alone, or in combination (Stickler, 2000; Fontana *et al.*, 2006). Future work could therefore assess Byotrol™'s potential as an antimicrobial incorporated into a hydrogel surface, however, perhaps due to the size of PHMB, the degree of polymer cross-linking would have to be adjusted. Also, exactly how the main components of Byotrol™ adhere to a surface would have to be investigated in greater depth.

7. 4. Conclusion

The investigations in the current work presented here have provided an important insight into the effect that a range of antimicrobial compounds have on the growth of planktonic cells and on the initial stages of biofilm formation. From these investigations, the current study has highlighted the inhibitory potential of a novel cationic biocide, Byotrol™, and has demonstrated the global gene expression response and protein complement of *E. coli* during exposure Byotrol™. This has strengthened the understanding of how bacteria can adapt and survive to biocidal stress, and this information can be used to develop strategies to prevent or better manage CAUTI.

References

- Absolom, D. R. (1988).** The Role of Bacterial Hydrophobicity in Infection - Bacterial Adhesion and Phagocytic Ingestion. *Can J Microbiol* **34**, 287-298.
- Agarwal, J., Srivastava, S. & Singh, M. (2012).** Pathogenomics of uropathogenic *Escherichia coli*. *Indian J Med Microbiol* **30**, 141-149.
- Agency, E. C. (2011).** Annex 2 - Comments and response to the opinion proposing harmonised classification and labelling at community level of PHMB pp. 83.
- Ahamed, M., AlSalhi, M. S. & Siddiqui, M. K. J. (2010).** Silver nanoparticle applications and human health. *Clinica Chimica Acta* **411**, 1841-1848.
- Ahearn, D. G., Grace, D. T., Jennings, M. J., Borazjani, R. N., Boles, K. J., Rose, L. J., Simmons, R. B. & Ahanotu, E. N. (2000).** Effects of hydrogel/silver coatings on in vitro adhesion to catheters of bacteria associated with urinary tract infections. *Curr Microbiol* **41**, 120-125.
- Ahlstrom, B., Chelminska-Bertilsson, M. Thompson, R.A. & Edebo, L. (1995).** Long-chain alkanoylcholines, a new category of soft antimicrobial agents that are enzymatically degradable. *Antimicrob Agents Chemother* **39**, 50-55.
- Alban, A., David, S. O., Bjorkesten, L., Andersson, C., Sloge, E., Lewis, S. & Currie, I. (2003).** A novel experimental design for comparative two-dimensional gel analysis: two-dimensional difference gel electrophoresis incorporating a pooled internal standard. *Proteomics* **1**, 36-44.
- Allen, M. J., White, G. F. & Morby, A. P. (2006).** The response of *Escherichia coli* to exposure to the biocide polyhexamethylene biguanide. *Microbiology* **152**, 989-1000.
- Allepuz-Palau, A., Rossello-Urgell, J., Vaque-Rafart, J., Hermosilla-Perez, E., Arribas-Llorente, J. L., Sanchez-Paya, J. & Lizan-Garcia, M. (2004).** Evolution of closed urinary drainage systems use and associated factors in Spanish hospitals. *J Hosp Infect* **57**, 332-338.
- Allon, M. (2003).** Prophylaxis against dialysis catheter-related bacteremia with a novel antimicrobial lock solution. *Clin Infect Dis* **36**, 1539-1544.
- Amin, A. K. & Wareham, D. W. (2009).** Plasmid-mediated quinolone resistance genes in Enterobacteriaceae isolates associated with community and nosocomial urinary tract infection in East London, UK. *Int J Antimicrob Agents* **34**, 490-491.
- Anderl, J. N., Franklin, M. J. & Stewart, P. S. (2000).** Role of antibiotic penetration limitation in *Klebsiella pneumoniae* biofilm resistance to ampicillin and ciprofloxacin. *Antimicrob Agents Chemother* **44**, 1818-1824.
- Anderson, G. G., Palermo, J. J., Schilling, J. D., Roth, R., Heuser, J. & Hultgren, S. J. (2003).** Intracellular bacterial biofilm-like pods in urinary tract infections. *Science* **301**, 105-107.
- Andreessen, L., Wilde, M. H. & Herendeen, P. (2012).** Preventing catheter-associated urinary tract infections in acute care: the bundle approach. *J Nurs Care Qual* **27**, 209-217.

- Andrews, S. C., Robinson, A. K. & Rodriguez-Quinones, F. (2003).** Bacterial iron homeostasis. *FEMS Microbiol Rev* **27**, 215-237.
- Arnitz, R., Sarg, B., Ott, H. W., Neher, A., Lindner, H. & Nagl, M. (2006).** Protein sites of attack of N-chlorotaurine in *Escherichia coli*. *Proteomics* **6**, 865-869.
- Arnqvist, A., Olsen, A. & Normark, S. (1994).** Sigma S-dependent growth-phase induction of the *csgBA* promoter in *Escherichia coli* can be achieved in vivo by sigma 70 in the absence of the nucleoid-associated protein H-NS. *Mol Microbiol* **13**, 1021-1032.
- Atiyeh, B. S., Costagliola, M., Hayek, S. N. & Dibo, S. A. (2007).** Effect of silver on burn wound infection control and healing: Review of the literature. *Burns* **33**, 139-148.
- Banerjee, I., Pangule, R. C. & Kane, R. S. (2011).** Antifouling Coatings: Recent Developments in the Design of Surfaces That Prevent Fouling by Proteins, Bacteria, and Marine Organisms. *Adv Mater* **23**, 690-718.
- Barker, M. M., Gaal, T. & Gourse, R. L. (2001).** Mechanism of regulation of transcription initiation by ppGpp. II. Models for positive control based on properties of RNAP mutants and competition for RNAP. *J Mol Biol* **305**, 689-702.
- Barnhart, M. M. & Chapman, M. R. (2006).** Curli biogenesis and function. *Annu Rev Microbiol* **60**, 131-147.
- Barrios, A. F., Zuo, R., Ren, D. & Wood, T. K. (2006).** Hha, YbaJ, and OmpA regulate *Escherichia coli* K12 biofilm formation and conjugation plasmids abolish motility. *Biotechnol Bioeng* **93**, 188-200.
- Barrow, G. I. & Feltham, R. K. A. (2003).** *Cowan and Steel's manual for the identification of medical bacteria*. Cambridge: Cambridge University Press.
- Battesti, A., Majdalani, N. & Gottesman, S. (2011).** The RpoS-Mediated General Stress Response in *Escherichia coli*. *Annu Rev Microbiol* **65**, 189-213.
- Berggren, K., Chernokalskaya, E., Steinberg, T. H., Kemper, C., Lopez, M. F., Diwu, Z., Haugland, R. P. & Patton, W. F. (2000).** Background-free, high sensitivity staining of proteins in one- and two-dimensional sodium dodecyl sulfate-polyacrylamide gels using a luminescent ruthenium complex. *Electrophoresis* **21**, 2509-2521.
- Berney, M., Weilenmann, H. U. & Egli, T. (2006).** Flow-cytometric study of vital cellular functions in *Escherichia coli* during solar disinfection (SODIS). *Microbiol-SGM* **152**, 1719-1729.
- Binnie, R. A., Zhang, H., Mowbray, S. & Hermodson, M. A. (1992).** Functional Mapping of the Surface of *Escherichia-Coli* Ribose-Binding Protein - Mutations That Affect Chemotaxis and Transport. *Protein Sci* **1**, 1642-1651.

- Bjarnsholt, T., Jensen, P. O., Burmolle, M. & other authors (2005).** Pseudomonas aeruginosa tolerance to tobramycin, hydrogen peroxide and polymorphonuclear leukocytes is quorum-sensing dependent. *Microbiol-SGM* **151**, 373-383.
- Bjerrum, L., Grinsted, P., Hyltoft, P. P. & Sogaard, P. (1999).** Validity of susceptibility testing of uropathogenic bacteria in general practice. *Br J Gen Pract* **49**, 821-822.
- Black, D. S., Kelly, A. J., Mardis, M. J. & Moyed, H. S. (1991).** Structure and Organization of Hip, an Operon That Affects Lethality Due to Inhibition of Peptidoglycan or DNA-Synthesis. *J Bacteriol* **173**, 5732-5739.
- Blumer, C., Kleefeld, A., Lehnen, D. & other authors (2005).** Regulation of type 1 fimbriae synthesis and biofilm formation by the transcriptional regulator LrhA of Escherichia coli. *Microbiology* **151**, 3287-3298.
- Bockelmann, U., Janke, A., Kuhn, R., Neu, T. R., Wecke, J., Lawrence, J. R. & Szewzyk, U. (2006).** Bacterial extracellular DNA forming a defined network-like structure. *FEMS Microbiol Lett* **262**, 31-38.
- Boks, N. P., Norde, W., van der Mei, H. C. & Busscher, H. J. (2008).** Forces involved in bacterial adhesion to hydrophilic and hydrophobic surfaces. *Microbiol-SGM* **154**, 3122-3133.
- Boles, B. R., Thoendel, M. & Singh, P. K. (2005).** Rhamnolipids mediate detachment of Pseudomonas aeruginosa from biofilms. *Mol Microbiol* **57**, 1210-1223.
- Bologna, R. A., Tu, L. M., Polansky, M., Fraimow, H. D., Gordon, D. A. & Whitmore, K. E. (1999).** Hydrogel/silver ion-coated urinary catheter reduces nosocomial urinary tract infection rates in intensive care unit patients: a multicenter study. *Urology* **54**, 982-987.
- Bordi, C. & de Bentzmann, S. (2011).** Hacking into bacterial biofilms: a new therapeutic challenge. *Ann Intensive Care* **1**, 19.
- Borkovec, M. & Papastavrou, G. (2008).** Interactions between solid surfaces with adsorbed polyelectrolytes of opposite charge. *Curr Opin Colloid Interface Sci* **13**, 429-437.
- Brackman, G., Cos, P., Maes, L., Nelis, H. J. & Coenye, T. (2011).** Quorum Sensing Inhibitors Increase the Susceptibility of Bacterial Biofilms to Antibiotics In Vitro and In Vivo. *Antimicrob Agents Chemother* **55**, 2655-2661.
- Bradford, M. M. (1976).** Rapid and Sensitive Method for Quantitation of Microgram Quantities of Protein Utilizing Principle of Protein-Dye Binding. *Anal Biochem* **72**, 248-254.
- Bradshaw, J. P. (2003).** Cationic antimicrobial peptides - Issues for potential clinical use. *Biodrugs* **17**, 233-240.
- Brissette, J. L., Russel, M., Weiner, L. & Model, P. (1990).** Phage shock protein, a stress protein of Escherichia coli. *Proc Natl Acad Sci U S A* **87**, 862-866.

- Brito, P. H., Rocha, E. P., Xavier, K. B. & Gordo, I. (2013).** Natural genome diversity of AI-2 quorum sensing in *Escherichia coli*: conserved signal production but labile signal reception. *Genome Biol Evol* **5**, 16-30.
- Brooks, K. M. (2001).** Literature Review and Assessment of the Environmental Risks Associated With the Use of ACQ Treated Wood Products in Aquatic Environments. Vancouver: Western Wood Preservers Institute.
- Brown, M. R. W. & Smith, A. W. (2003).** Antimicrobial agents and biofilms. In *Medical implications of biofilms*, pp. 36-48. Cambridge, UK: Cambridge University Press.
- Burrell, R. E. (2003).** A scientific perspective on the use of topical silver preparations. *Ostomy Wound Manage* **49**, 19-24.
- Busscher, H. J., van der Mei, H. C., Allison, D. G., Gilbert, P., Lappin-Scott, H. M. & Wilson, M. (2000).** Initial microbial adhesion events; mechanisms and implications. In *Community structure and co-operation in biofilms: fifty-ninth symposium of the Society for General Microbiology, held at the University of Exeter, September 2000*, pp. 25-32. Cambridge: Cambridge University Press for the Society for General Microbiology.
- California, U. o. S. (2012).** iGEM. University of California: University of Southern California.
- Carmel-Harel, O. & Storz, G. (2000).** Roles of the glutathione- and thioredoxin-dependent reduction systems in the *Escherichia coli* and *saccharomyces cerevisiae* responses to oxidative stress. *Annu Rev Microbiol* **54**, 439-461.
- Carr, S., Aebersold, R., Baldwin, M., Burlingame, A., Clauser, K. & Nesvizhskii, A. (2004).** The need for guidelines in publication of peptide and protein identification data - Working group on publication guidelines for peptide and protein identification data. *Mol Cell Proteomics* **3**, 531-533.
- Castanie-Cornet, M. P. & Foster, J. W. (2001).** *Escherichia coli* acid resistance: cAMP receptor protein and a 20 bp cis-acting sequence control pH and stationary phase expression of the *gadA* and *gadBC* glutamate decarboxylase genes. *Microbiology* **147**, 709-715.
- Castano-Cerezo, S., Pastor, J. M., Renilla, S., Bernal, V., Iborra, J. L. & Canovas, M. (2009).** An insight into the role of phosphotransacetylase (*pta*) and the acetate/acetyl-CoA node in *Escherichia coli*. *Microb Cell Fact* **8**.
- Cerca, N., Martins, S., Cerca, F., Jefferson, K. K., Pier, G. B., Oliveira, R. & Azeredo, J. (2005).** Comparative assessment of antibiotic susceptibility of coagulase-negative staphylococci in biofilm versus planktonic culture as assessed by bacterial enumeration or rapid XTT colorimetry. *J Antimicrob Chemother* **56**, 331-336.
- Ceri, H., Olson, M. E., Stremick, C., Read, R. R., Morck, D. & Buret, A. (1999).** The Calgary Biofilm Device: New technology for rapid determination of antibiotic susceptibilities of bacterial biofilms. *J Clin Microbiol* **37**, 1771-1776.

- Chen, C. Z. S., Beck-Tan, N. C., Dhurjati, P., van Dyk, T. K., LaRossa, R. A. & Cooper, S. L. (2000).** Quaternary ammonium functionalized poly(propylene imine) dendrimers as effective antimicrobials: Structure-activity studies. *Biomacromolecules* **1**, 473-480.
- Cho, Y. W., Park, J. H., Kim, S. H. & other authors (2003).** Gentamicin-releasing urethral catheter for short-term catheterization. *J Biomater Sci, Polym Ed* **14**, 963-972.
- CLSI (2009).** Methods for dilution antimicrobial susceptibility tests for bacteria that grow aerobically; approved standard - 8th edition. Wayne, PA: Clinical and Laboratory Standards Institute.
- Codling, C. E., Maillard, J. Y. & Russell, A. D. (2003a).** Performance of contact lens disinfecting solutions against *Pseudomonas aeruginosa* in the presence of organic load. *Eye Cont Lens* **29**, 100-102.
- Codling, C. E., Maillard, J. Y. & Russell, A. D. (2003b).** Aspects of the antimicrobial mechanisms of action of a polyquaternium and an amidoamine. *J Antimicrob Chemother* **51**, 1153-1158.
- Cohen, P. & Dawe, S. (2009).** Aseptic technique and urinary catheter care policy: North East London NHS Foundation Trust.
- Cornia, P. B., Amory, J. K., Fraser, S., Saint, S. & Lipsky, B. A. (2003).** Computer-based order entry decreases duration of indwelling urinary catheterization in hospitalized patients. *Am J Med* **114**, 404-407.
- Costerton, J. W., Cheng, K. J., Geesey, G. G., Ladd, T. I., Nickel, J. C., Dasgupta, M. & Marrie, T. J. (1987).** Bacterial biofilms in nature and disease. *Annu Rev Microbiol* **41**, 435-464.
- Costerton, J. W., Lewandowski, Z., Debeer, D., Caldwell, D., Korber, D. & James, G. (1994).** Biofilms, the Customized Microniche. *J Bacteriol* **176**, 2137-2142.
- Costerton, J. W., Lewandowski, Z., Caldwell, D. E., Korber, D. R. & Lappin-Scott, H. M. (1995).** Microbial biofilms. *Annu Rev Microbiol* **49**, 711-745.
- Costerton, J. W., Stewart, P. S. & Greenberg, E. P. (1999).** Bacterial biofilms: A common cause of persistent infections. *Science* **284**, 1318-1322.
- Costerton, J. W. (2007a).** *The Biofilm Primer*. Berlin, Heidelberg: Springer-Verlag Berlin Heidelberg.
- Costerton, J. W. (2007b).** Microbiology of the healthy human body. In *The Biofilm Primer*, pp. 109-113. Berlin, Heidelberg: Springer-Verlag Berlin Heidelberg.
- Cox, A. J., Millington, R. S., Hukins, D. W. & Sutton, T. M. (1989).** Resistance of catheters coated with a modified hydrogel to encrustation during an in vitro test. *Urol Res* **17**, 353-356.

- Cravens, D. D. & Zweig, S. (2000).** Urinary catheter management. *Am Fam Physician* **61**, 369-376.
- Danhorn, T. & Fuqua, C. (2007).** Biofilm formation by plant-associated bacteria. *Annu Rev Microbiol* **61**, 401-422.
- Dasgupta, N., Wolfgang, M. C., Goodman, A. L., Arora, S. K., Jyot, J., Lory, S. & Ramphal, R. (2003).** A four-tiered transcriptional regulatory circuit controls flagellar biogenesis in *Pseudomonas aeruginosa*. *Mol Microbiol* **50**, 809-824.
- Dave, R. N., Joshi, H. M. & Venugopalan, V. P. (2011).** Novel Biocatalytic Polymer-Based Antimicrobial Coatings as Potential Ureteral Biomaterial: Preparation and In Vitro Performance Evaluation. *Antimicrob Agents Chemother* **55**, 845-853.
- Davies, D. G. (2000).** Physiological events in biofilm formation. In *Community structure and co-operation in biofilms Society for General Microbiology Symposium*, pp. 47. Edited by D. G. Allison, Gilbert, P., Lappin-Scott, H. M. and Wilson, M.: Cambridge University Press.
- Dawson, C. C., Intapa, C. & Jabra-Rizk, M. A. (2011).** "Persisters": Survival at the Cellular Level. *PLoS Pathog* **7**.
- de Kievit, T. R. & Iglewski, B. H. (2003).** Quorum sensing and microbial biofilms. In *Medical implications of biofilms*, pp. 18-24. Cambridge, UK ; New York: Cambridge University Press.
- Deighton, M. A., Capstick, J., Domalewski, E. & van, N. T. (2001).** Methods for studying biofilms produced by *Staphylococcus epidermidis*. *Methods Enzymol* **336**, 177-195.
- DeLisa, M. P., Valdes, J. J. & Bentley, W. E. (2001).** Mapping stress-induced changes in autoinducer AI-2 production in chemostat-cultivated *Escherichia coli* K-12. *J Bacteriol* **183**, 2918-2928.
- Demling, R. H. (2001).** The role of silver in wound healing - Part 1: Effects of silver on wound management. *Wounds* **13**, 4-15.
- Deng, X., Hahne, T., Schroder, S., Redweik, S., Nebija, D., Schmidt, H., Janssen, O., Lachmann, B. & Watzig, H. (2012).** The challenge to quantify proteins with charge trains due to isoforms or conformers. *Electrophoresis* **33**, 263-269.
- Denyer, S. P. (1995).** Mechanisms of action of antimicrobial biocides. *Int Biodeterior Biodegrad* **36**, 227-245.
- Deupree, S. M. & Schoenfisch, M. H. (2009).** Morphological analysis of the antimicrobial action of nitric oxide on Gram-negative pathogens using atomic force microscopy. *Acta Biomater* **5**, 1405-1415.
- Di Costanzo, L., Gomez, G. A. & Christianson, D. W. (2007).** Crystal structure of lactaldehyde dehydrogenase from *Escherichia coli* and inferences regarding substrate and cofactor specificity. *J Mol Biol* **366**, 481-493.

- Di Martino, P., Merieau, A., Phillips, R., Orange, N. & Hulen, C. (2002).** Isolation of an *Escherichia coli* strain mutant unable to form biofilm on polystyrene and to adhere to human pneumocyte cells: involvement of tryptophanase. *Can J Microbiol* **48**, 132-137.
- Dolinnai, N. G. & Borisova, O. A. (2000).** [Sulfur-containing nucleic acids. Synthesis, chemical behavior in supramolecular biopolymer complexes, biological properties]. *Mol Biol (Mosk)* **34**, 931-945.
- Domka, J., Lee, J. & Wood, T. K. (2006).** YliH (BssR) and YceP (BssS) regulate *Escherichia coli* K-12 biofilm formation by influencing cell signaling. *Appl Environ Microbiol* **72**, 2449-2459.
- Dong, D., Huang, C., Park, J. H. & Wang, G. (2012).** Growth Inhibitory Levels of Salicylic Acid Decrease *Pseudomonas aeruginosa* fliC Flagellin Gene Expression. *J Exp Microbiol Immunol* **16**, 73-78.
- Donlan, R. M. (2001a).** Biofilms and device-associated infections. *Emerg Infect Dis* **7**, 277-281.
- Donlan, R. M. (2001b).** Biofilm formation: a clinically relevant microbiological process. *Clin Infect Dis* **33**, 1387-1392.
- Donlan, R. M. (2002).** Biofilms: Microbial life on surfaces. *Emerging Infect Dis* **8**, 881-890.
- Donlan, R. M. & Costerton, J. W. (2002).** Biofilms: Survival mechanisms of clinically relevant microorganisms. *Clin Microbiol Rev* **15**, 167-193.
- Doyle, R. J. (2000).** Contribution of the hydrophobic effect to microbial infection. *Microbes Infect* **2**, 391-400.
- Dromigny, J. A., Nabeth, P., Juergens-Behr, A. & Perrier-Gros-Claude, J. D. (2005).** Risk factors for antibiotic-resistant *Escherichia coli* isolated from community-acquired urinary tract infections in Dakar, Senegal. *J Antimicrob Chemother* **56**, 236-239.
- Ehmann, D. E., Shaw-Reid, C. A., Losey, H. C. & Walsh, C. T. (2000).** The EntF and EntE adenylation domains of *Escherichia coli* enterobactin synthetase: sequestration and selectivity in acyl-AMP transfers to thiolation domain cosubstrates. *Proc Natl Acad Sci USA* **97**, 2509-2514.
- Emori, T. G. & Gaynes, R. P. (1993).** An overview of nosocomial infections, including the role of the microbiology laboratory. *Clin Microbiol Rev* **6**, 428-442.
- Engler, A. C., Shukla, A., Puranam, S., Buss, H. G., Jreige, N. & Hammond, P. T. (2011).** Effects of Side Group Functionality and Molecular Weight on the Activity of Synthetic Antimicrobial Polypeptides. *Biomacromolecules* **12**, 1666-1674.
- EPA (2004a).** HQ-OPP-2004-0305-003, Overview of the PHMB preliminary risk assessment, August 2004.

- EPA (2004b)**. HQ-OPP-2004-0305-0011, Health Effects of PHMB in Humans, August 2004.
- Fakih, M. G., Pena, M. E., Shemes, S., Rey, J., Berriel-Cass, D., Szpunar, S. M., Savoy-Moore, R. T. & Saravolatz, L. D. (2010)**. Effect of Establishing Guidelines on Appropriate Urinary Catheter Placement. *Acad Emerg Med* **17**, 337-340.
- Fang, Z., Martin, J. & Wang, Z. (2012)**. Statistical methods for identifying differentially expressed genes in RNA-Seq experiments. *Cell Biosci* **2**, 26.
- Flemming, H., Wingender, J., Griebe, T. & Mayer, C. (2000)**. Physico-chemical properties of biofilms. In *Biofilms: recent advances in their study and control*, pp. 20. Australia: Harwood Academic Publishers.
- Flemming, H. C., Neu, T. R. & Wozniak, D. J. (2007)**. The EPS matrix: the "house of biofilm cells". *J Bacteriol* **189**, 7945-7947.
- Fox, C. L. (1968)**. Silver Sulfadiazine - a New Topical Therapy for Pseudomonas in Burns. *Arch Surg* **96**, 184-&.
- Frank, E. G., Gonzalez, M., Ennis, D. G., Levine, A. S. & Woodgate, R. (1996)**. In vivo stability of the Umu mutagenesis proteins: a major role for RecA. *J Bacteriol* **178**, 3550-3556.
- Franke, S., Grass, G. & Nies, D. H. (2001)**. The product of the ybdE gene of the Escherichia coli chromosome is involved in detoxification of silver ions. *Microbiol UK* **147**, 965-972.
- Fu, X., Fu, N., Guo, S. & other authors (2009)**. Estimating accuracy of RNA-Seq and microarrays with proteomics. *BMC Genomics* **10**.
- Fuentes, D. E., Fuentes, E. L., Castro, M. E., Perez, J. M., Araya, M. A., Chasteen, T. G., Pichuantes, S. E. & Vasquez, C. C. (2007)**. Cysteine metabolism-related genes and bacterial resistance to potassium tellurite. *J Bacteriol* **189**, 8953-8960.
- Fux, C. A., Stoodley, P., Hall-Stoodley, L. & Costerton, J. W. (2003)**. Bacterial biofilms: a diagnostic and therapeutic challenge. *Expert Rev Anti Infect Ther* **1**, 667-683.
- Galvani, M., Hamdan, M., Herbert, B. & Righetti, P. G. (2001)**. Alkylation kinetics of proteins in preparation for two-dimensional maps: A matrix assisted laser desorption/ionization-mass spectrometry investigation. *Electrophoresis* **22**, 2058-2065.
- Geng, V., Cobussen-Boekhorst, H., Farrell, J., Gea-Sanchez, M., Pearce, I., Schwennesen, T., Vahr, S. & Vandewinkel, C. (2012)**. Evidence-based guidelines for best practice in urological health care. Catheterisation: Indwelling catheters in adults: European Association of Urology Nurses.
- George, N., Faoagali, J. & Muller, M. (1997)**. Silvazine (TM) (silver sulfadiazine and chlorhexidine) activity against 200 clinical isolates. *Burns* **23**, 493-495.

- Getliffe, K. & Newton, T. (2006).** Catheter-associated urinary tract infection in primary and community health care. *Age Ageing* **35**, 477-481.
- Gilbert, P., Pemberton, D. & Wilkinson, D. E. (1990).** Synergism within Polyhexamethylene Biguanide Biocide Formulations. *J Appl Bacteriol* **69**, 593-598.
- Gilbert, P. (2005).** Cationic antiseptics: diversity of action under a common epithet. *J Appl Microbiol* **99**, 12.
- Gilbert, P. & Moore, L. E. (2005).** Cationic antiseptics: diversity of action under a common epithet. *J Appl Microbiol* **99**, 703-715.
- Gilbert, P. A.-T., A. (1985).** Antimicrobial activity of some alkytrimethylammonium bromides. *Lett Appl Microbiol* **1**, 4.
- Gillings, M. R., Duan, X. J., Hardwick, S. A., Holley, M. P. & Stokes, H. W. (2009a).** Gene cassettes encoding resistance to quaternary ammonium compounds: a role in the origin of clinical class 1 integrons? *ISME J* **3**, 209-215.
- Gillings, M. R., Holley, M. P. & Stokes, H. W. (2009b).** Evidence for dynamic exchange of qac gene cassettes between class 1 integrons and other integrons in freshwater biofilms. *FEMS Microbiol Lett* **296**, 282-288.
- Gophna, U., Barlev, M., Seiffers, R., Oelschlager, T. A., Hacker, J. & Ron, E. Z. (2001).** Curli fibers mediate internalization of Escherichia coli by eukaryotic cells. *Infect Immun* **69**, 2659-2665.
- Gorg, A., Boguth, G., Obermaier, C., Posch, A. & Weiss, W. (1995).** Two-dimensional polyacrylamide gel electrophoresis with immobilized pH gradients in the first dimension (IPG-Dalt): the state of the art and the controversy of vertical versus horizontal systems. *Electrophoresis* **16**, 1079-1086.
- Gorman, S. P. & Jones, D. S. (2003).** Biofilm complications of urinary tract devices. In *Medical implications of biofilms*, pp. 146. Cambridge, UK: Cambridge University Press.
- Gou, M., Li, X., Dai, M. & other authors (2008).** A novel injectable local hydrophobic drug delivery system: Biodegradable nanoparticles in thermo-sensitive hydrogel. *Int J Pharm* **359**, 228-233.
- Greenwood, D. (2007a).** *Medical microbiology : a guide to microbial infection : pathogenesis, immunity, laboratory diagnosis, and control*: Edinburgh ; New York : Churchill Livingstone/Elsevier.
- Greenwood, D. (2007b).** Bacterial pathogens and associated diseases. In *Medical microbiology : a guide to microbial infection : pathogenesis, immunity, laboratory diagnosis, and control*, pp. 287: Edinburgh ; New York : Churchill Livingstone/Elsevier.
- Gunasekera, T. S., Csonka, L. N. & Paliy, O. (2008).** Genome-wide transcriptional responses of Escherichia coli K-12 to continuous osmotic and heat stresses. *J Bacteriol* **190**, 3712-3720.

- Gundry, R. L., White, M. Y., Murray, C. I., Kane, L. A., Fu, Q., Stanley, B. A. & Van Eyk, J. E. (2009).** Preparation of proteins and peptides for mass spectrometry analysis in a bottom-up proteomics workflow. *Curr Protoc Mol Biol* **Chapter 10**, Unit10 25.
- Guo, S. & Dipietro, L. A. (2010).** Factors affecting wound healing. *J Dent Res* **89**, 219-229.
- Gygi, S. P., Rochon, Y., Franza, B. R. & Aebersold, R. (1999).** Correlation between protein and mRNA abundance in yeast. *Mol Cell Biol* **19**, 1720-1730.
- Halvax, J. J., Wiese, G., Arp, J. A., Vermeer, J. M. P., Vanbennekomp, W. P. & Bult, A. (1990).** Rapid-Determination of Benzalkonium Chloride in Pharmaceutical Preparations with Flow-Injection Liquid-Liquid-Extraction. *J Pharm Biomed Anal* **8**, 243-252.
- Hanna, H., Bahna, P., Reitzel, R., Dvorak, T., Chaiban, G., Hachem, R. & Raad, I. (2006).** Comparative in vitro efficacies and antimicrobial durabilities of novel antimicrobial central venous catheters. *Antimicrob Agents Chemother* **50**, 3283-3288.
- Hansen, C., Fu, A., Meng, Y., Okine, E., Hawken, R., Barris, W., Li, C. & Moore, S. S. (2004).** Gene expression profiling of the bovine gastrointestinal tract. *Genome* **47**, 639-649.
- Hardwick, S. A., Stokes, H. W., Findlay, S., Taylor, M. & Gillings, M. R. (2008).** Quantification of class 1 integron abundance in natural environments using real-time quantitative PCR. *FEMS Microbiol Lett* **278**, 207-212.
- Harrison, J. J., Stremick, C. A., Turner, R. J., Allan, N. D., Olson, M. E. & Ceri, H. (2010).** Microtiter susceptibility testing of microbes growing on peg lids: a miniaturized biofilm model for high-throughput screening. *Nature Protocols* **5**, 1236-1254.
- Hashmi, S., Kelly, E., Rogers, S. O. & Gates, J. (2003).** Urinary tract infection in surgical patients. *Am J Surg* **186**, 53-56.
- Hassett, D. J., Ma, J. F., Elkins, J. G. & other authors (1999).** Quorum sensing in *Pseudomonas aeruginosa* controls expression of catalase and superoxide dismutase genes and mediates biofilm susceptibility to hydrogen peroxide. *Mol Microbiol* **34**, 1082-1093.
- Hatt, J. K. & Rather, P. N. (2008).** Role of bacterial biofilms in urinary tract infections. *Curr Top Microbiol Immunol* **322**, 163-192.
- Haynie, S. L., Crum, G. A. & Doele, B. A. (1995).** Antimicrobial Activities of Amphiphilic Peptides Covalently Bonded to a Water-Insoluble Resin. *Antimicrob Agents Chemother* **39**, 301-307.
- He, G. X., Kuroda, T., Mima, T., Morita, Y., Mizushima, T. & Tsuchiya, T. (2004).** An H(+)-coupled multidrug efflux pump, PmpM, a member of the MATE family of transporters, from *Pseudomonas aeruginosa*. *J Bacteriol* **186**, 262-265.

- Hegde, P., Qi, R., Abernathy, K. Gay, C., Dharup, C., Gaspard, R., Hughes, J. E., Snesrud, E., Lee, N. & Quakenbush, J. (2000). A concise guide to cDNA microarray analysis. *Biotechniques* **29**, 548-550.
- Hengge-Aronis, R. (2002). Signal transduction and regulatory mechanisms involved in control of the sigma(S) (RpoS) subunit of RNA polymerase. *Microbiol Mol Biol Rev* **66**, 373-395.
- Herbert, B., Galvani, M., Hamdan, M., Olivieri, E., MacCarthy, J., Pedersen, S. & Righetti, P. G. (2001). Reduction and alkylation of proteins in preparation of two-dimensional map analysis: Why, when, and how? *Electrophoresis* **22**, 2046-2057.
- Herbert, B. R., Molloy, M. P., Gooley, A. A., Walsh, B. J., Bryson, W. G. & Williams, K. L. (1998). Improved protein solubility in two-dimensional electrophoresis using tributyl phosphine as reducing agent. *Electrophoresis* **19**, 845-851.
- Hetrick, E. M., Shin, J. H., Paul, H. S. & Schoenfisch, M. H. (2009). Anti-biofilm efficacy of nitric oxide-releasing silica nanoparticles. *Biomaterials* **30**, 2782-2789.
- Hirakawa, H., Hayashi-Nishino, M., Yamaguchi, A. & Nishino, K. (2010). Indole enhances acid resistance in Escherichia coli. *Microb Pathog* **49**, 90-94.
- Ho, T. D., Hastie, J. L., Intile, P. J. & Ellermeier, C. D. (2011). The Bacillus subtilis Extracytoplasmic Function sigma Factor sigma(V) Is Induced by Lysozyme and Provides Resistance to Lysozyme. *J Bacteriol* **193**, 6215-6222.
- Hoffmann, N., Lee, B., Hentzer, M., Rasmussen, T. B., Song, Z. J., Johansen, H. K., Givskov, M. & Hoiby, N. (2007). Azithromycin blocks quorum sensing and alginate polymer formation and increases the sensitivity to serum and stationary-growth-phase killing of Pseudomonas aeruginosa and attenuates chronic P-aeruginosa lung infection in Cfr(-/-) mice. *Antimicrob Agents Chemother* **51**, 3677-3687.
- Hooton, T. M. (2000). Pathogenesis of urinary tract infections: an update. *J Antimicrob Chemother* **46 Suppl 1**, 1-7.
- Hooton, T. M., Bradley, S. F., Cardenas, D. D. & other authors (2010). Diagnosis, Prevention, and Treatment of Catheter-Associated Urinary Tract Infection in Adults: 2009 International Clinical Practice Guidelines from the Infectious Diseases Society of America. *Clin Infect Dis* **50**, 625-663.
- Hoving, S., Gerrits, B., Voshol, H., Muller, D., Roberts, R. C. & van Oostrum, J. (2002). Preparative two-dimensional gel electrophoresis at alkaline pH using narrow range immobilized pH gradients. *Proteomics* **2**, 127-134.
- Hsueh, P. R., Teng, L. J., Yang, P. C., Chen, Y. C., Ho, S. W. & Luh, K. T. (1998). Persistence of a multidrug-resistant Pseudomonas aeruginosa clone in an intensive care burn unit. *J Clin Microbiol* **36**, 1347-1351.
- Hu, M. X., Zhang, C., Mu, Y. F., Shen, Q. W. & Feng, Y. J. (2010). Indole Affects Biofilm Formation in Bacteria. *Indian J Microbiol* **50**, 362-368.

- Hudault, S., Guignot, J. & Servin, A. L. (2001).** Escherichia coli strains colonising the gastrointestinal tract protect germfree mice against Salmonella typhimurium infection. *Gut* **49**, 47-55.
- Husain, M., Bourret, T. J., McCollister, B. D., Jones-Carson, J., Laughlin, J. & Vazquez-Torres, A. (2008).** Nitric oxide evokes an adaptive response to oxidative stress by arresting respiration. *J Biol Chem* **283**, 7682-7689.
- Hussain, M., Herrmann, M., von, E. C., Perdreau-Remington, F. & Peters, G. (1997).** A 140-kilodalton extracellular protein is essential for the accumulation of Staphylococcus epidermidis strains on surfaces. *Infect Immun* **65**, 519-524.
- Huvet, M., Toni, T., Sheng, X., Thorne, T., Jovanovic, G., Engl, C., Buck, M., Pinney, J. W. & Stumpf, M. P. (2011).** The evolution of the phage shock protein response system: interplay between protein function, genomic organization, and system function. *Mol Biol Evol* **28**, 1141-1155.
- Ikeda, T., Ledwith, A., Bamford, C. H. & Hann, R. A. (1984).** Interaction of a polymeric biguanide biocide with phospholipid membranes. *Biochim Biophys Acta* **769**, 57-66.
- Ingham, C., Buechner, M. & Adler, J. (1990).** Effect of outer membrane permeability on chemotaxis in Escherichia coli. *J Bacteriol* **172**, 3577-3583.
- Ioannou, C. J., Hanlon, G. W. & Denyer, S. P. (2007).** Action of disinfectant quaternary ammonium compounds against Staphylococcus aureus. *Antimicrob Agents Chemother* **51**, 296-306.
- Iyer, R. & Delcour, A. H. (1997).** Complex inhibition of OmpF and OmpC bacterial porins by polyamines. *J Biol Chem* **272**, 18595-18601.
- Iyer, R., Wu, Z., Woster, P. M. & Delcour, A. H. (2000).** Molecular basis for the polyamine-ompF porin interactions: inhibitor and mutant studies. *J Mol Biol* **297**, 933-945.
- Jachowicz, J., McMullen, R. & Prettypaul, D. (2008).** Alteration of skin mechanics by thin polymer films. *Skin Res Technol* **14**, 312-319.
- Jacobsen, S. M., Stickler, D. J., Mobley, H. L. T. & Shirliff, M. E. (2008).** Complicated catheter-associated urinary tract infections due to Escherichia coli and Proteus mirabilis. *Clin Microbiol Rev* **21**, 26-59.
- Jaeger, K., Osthaus, A., Heine, J., Ruschulte, H., Kuhlmann, C., Weissbrodt, H., Ganser, A. & Karthaus, M. (2001).** Efficacy of a benzalkonium chloride-impregnated central venous catheter to prevent catheter-associated infection in cancer patients. *Chemotherapy* **47**, 50-55.
- Janssens, J. C. A., Steenackers, H., Robijns, S. & other authors (2008).** Brominated Furanones Inhibit Biofilm Formation by Salmonella enterica Serovar Typhimurium. *Appl Environ Microbiol* **74**, 6639-6648.

- Jefferson, K. K. & Pier, G. B. (2003).** Pseudomonas aeruginosa biofilms in lung infections. In *Medical implications of biofilms*, pp. 293. Cambridge, UK: Cambridge University Press.
- Jefferson, K. K. (2004).** What drives bacteria to produce a biofilm? *FEMS Microbiol Lett* **236**, 163-173.
- Jenkins, A. T. A., Ffrench-Constant, R., Buckling, A., Clarke, D. J. & Jarvis, K. (2004).** Study of the attachment of Pseudomonas aeruginosa on gold and modified gold surfaces using surface plasmon resonance. *Biotechnol Progr* **20**, 1233-1236.
- Johnson, J. R. (1991).** Virulence factors in Escherichia coli urinary tract infection. *Clin Microbiol Rev* **4**, 80-128.
- Johnson, J. R., Delavari, P. & Azar, M. (1999).** Activities of a nitrofurazone-containing urinary catheter and a silver hydrogel catheter against multidrug-resistant bacteria characteristic of catheter-associated urinary tract infection. *Antimicrob Agents Chemother* **43**, 2990-2995.
- Johnson, J. R., Kuskowski, M. A. & Wilt, T. J. (2006).** Systematic review: antimicrobial urinary catheters to prevent catheter-associated urinary tract infection in hospitalized patients. *Ann Intern Med* **144**, 116-126.
- Jombo, G. T. A., Emanghe, U. E., Amefule, E. N. & Damen, J. G. (2012).** Nosocomial and community acquired uropathogenic isolates of Proteus mirabilis and antimicrobial susceptibility profiles at a university hospital in Sub-Saharan Africa. *Asian Pac J Trop Dis* **2**, 7-11.
- Jones, D. S., Garvin, C. P. & Gorman, S. P. (2004).** Relationship between biomedical catheter surface properties and lubricity as determined using textural analysis and multiple regression analysis. *Biomaterials* **25**, 1421-1428.
- Jones, L., Macdougall, N. & Sorbara, L. G. (2002).** Asymptomatic corneal staining associated with the use of balafilcon silicone-hydrogel contact lenses disinfected with a polyaminopropyl biguanide-preserved care regimen. *Opt Vis Sci* **79**, 753-761.
- Kal, A. J., van Zonneveld, A. J., Benes, V. & other authors (1999).** Dynamics of gene expression revealed by comparison of serial analysis of gene expression transcript profiles from yeast grown on two different carbon sources. *Mol Biol Cell* **10**, 1859-1872.
- Kariuki, S., Revathi, G., Corkill, J., Kiiru, J., Mwituria, J., Mirza, N. & Hart, C. A. (2007).** Escherichia coli from community-acquired urinary tract infections resistant to fluoroquinolones and extended-spectrum beta-lactams. *J Infect Dev Ctries* **1**, 257-262.
- Katsu, T., Nakagawa, H. & Yasuda, K. (2002).** Interaction between polyamines and bacterial outer membranes as investigated with ion-selective electrodes. *Antimicrob Agents Chemother* **46**, 1073-1079.
- Kaur, I. P., Lal, S., Rana, C., Kakkar, S. & Singh, H. (2009).** Ocular preservatives: associated risks and newer options. *Cut Ocul Toxicol* **28**, 93-103.

- Kazama, H., Hamashima, H., Sasatsu, M. & Arai, T. (1998).** Distribution of the antiseptic-resistance genes *qacE* and *qacE* delta 1 in gram-negative bacteria. *FEMS Microbiol Lett* **159**, 173-178.
- Keren, I., Kaldalu, N., Spoering, A., Wang, Y. & Lewis, K. (2004).** Persister cells and tolerance to antimicrobials. *FEMS Microbiol Lett* **230**, 13-18.
- Kil, K. S., Darouiche, R. O., Hull, R. A., Mansouri, M. D. & Musher, D. M. (1997).** Identification of a *Klebsiella pneumoniae* strain associated with nosocomial urinary tract infection. *J Clin Microbiol* **35**, 2370-2374.
- Kim, C., Song, S. & Park, C. (1997).** The D-allose operon of *Escherichia coli* K-12. *J Bacteriol* **179**, 7631-7637.
- Kim, S. Y., Lee, H. S., Hyun, J. J. & other authors (2011).** Comparison on the Efficacy of Disinfectants Used in Automated Endoscope Reprocessors: PHMB-DBAC versus Orthophthalaldehyde. *Clin Endosc* **44**, 109-115.
- Kingsley, A. & Kiernan, M. (2013).** Suprasorb X+PHMB Made Easy - Products for Practice. *Wounds UK* **9**, 1-4.
- Klausen, M., Heydorn, A., Ragas, P., Lambertsen, L., Aaes-Jorgensen, A., Molin, S. & Tolker-Nielsen, T. (2003).** Biofilm formation by *Pseudomonas aeruginosa* wild type, flagella and type IV pili mutants. *Mol Microbiol* **48**, 1511-1524.
- Kleinert, P., Kuster, T., Arnold, D., Jaeken, J., Heizmann, C. W. & Troxler, H. (2007).** Effect of glycosylation on the protein pattern in 2-D-gel electrophoresis. *Proteomics* **7**, 15-22.
- Knoll, B. M., Wright, D., Ellingson, L., Kraemer, L., Patire, R., Kuskowski, M. A. & Johnson, J. R. (2011).** Reduction of Inappropriate Urinary Catheter Use at a Veterans Affairs Hospital Through a Multifaceted Quality Improvement Project. *Clin Infect Dis* **52**, 1283-1290.
- Kogenaru, S., Qing, Y., Guo, Y. & Wang, N. (2012).** RNA-seq and microarray complement each other in transcriptome profiling. *BMC Genomics* **13**, 629.
- Kohler, T., Perron, G. G., Buckling, A. & van Delden, C. (2010).** Quorum sensing inhibition selects for virulence and cooperation in *Pseudomonas aeruginosa*. *PLoS Pathog* **6**, e1000883.
- Kokare, C. R., Chakraborty, S., Khopade, A. N. & Mahadik, K. R. (2009).** Biofilm: Importance and applications. *Indian J Biotechnol* **8**, 159-168.
- Koomen, J. M., Haura, E. B., Bepler, G. & other authors (2008).** Proteomic contributions to personalized cancer care. *Mol Cell Proteomics* **7**, 1780-1794.
- Koskiniemi, S., Sun, S., Berg, O. G. & Andersson, D. I. (2012).** Selection-Driven Gene Loss in Bacteria. *PLoS Genet* **8** e1002787.
- Kostakioti, M., Hadjifrangiskou, M., Cusumano, C. K., Hannan, T. J., Janetka, J. W. & Hultgren, S. J. (2012).** Distinguishing the Contribution of Type 1 Pili from That

of Other QseB-Misregulated Factors when QseC Is Absent during Urinary Tract Infection. *Infect Immun* **80**, 2826-2834.

Kostenko, V., Lyczak, J., Turner, K. & Martinuzzi, R. J. (2010). Impact of silver-containing wound dressings on bacterial biofilm viability and susceptibility to antibiotics during prolonged treatment. *Antimicrob Agents Chemother* **54**, 5120-5131.

Kucken, D., Feucht, H. H. & Kaulfers, P. M. (2000). Association of qacE and qacE Delta 1 with multiple resistance to antibiotics and antiseptics in clinical isolates of Gram-negative bacteria. *FEMS Microbiol Lett* **183**, 95-98.

Kuhnert, P., Boerlin, P. & Frey, J. (2000). Target genes for virulence assessment of Escherichia coli isolates from water, food and the environment. *FEMS Microbiol Rev* **24**, 107-117.

Kunin, C. M. & McCormack R.C. (1966). Prevention of Catheter-Induced Urinary-Tract Infections by Sterile Closed Drainage. *N Eng J Med* **274**, 1155-1161.

Kunin, C. M. (2009). Catheter-Associated Urinary Tract Infections: A Syllogism Compounded by a Questionable Dichotomy. *Clin Infect Dis* **48**, 1189-1190.

la Vega, A. L. & Delcour, A. H. (1996). Polyamines decrease Escherichia coli outer membrane permeability. *J Bacteriol* **178**, 3715-3721.

Landini, P. (2009). Cross-talk mechanisms in biofilm formation and responses to environmental and physiological stress in Escherichia coli. *Res Microbiol* **160**, 259-266.

Langsrud, S., Sundheim, G. & Borgmann-Strahsen, R. (2003). Intrinsic and acquired resistance to quaternary ammonium compounds in food-related Pseudomonas spp. *J Appl Microbiol* **95**, 874-882.

Laraki, N., Galleni, M., Thamm, I., Riccio, M. L., Amicosante, G., Frere, J. M. & Rossolini, G. M. (1999). Structure of In31, a blaIMP-containing Pseudomonas aeruginosa integron phylogenically related to In5, which carries an unusual array of gene cassettes. *Antimicrob Agents Chemother* **43**, 890-901.

Lawrence, E. L. & Turner, I. G. (2005). Materials for urinary catheters: a review of their history and development in the UK. *Med Eng Phys* **27**, 443-453.

Lee, A. R. C., Leem, H., Lee, J. & Park, K. C. (2005). Reversal of silver sulfadiazine-impaired wound healing by epidermal growth factor. *Biomaterials* **26**, 4670-4676.

Lee, D. C., Cottrill, M. A., Forsberg, C. W. & Jia, Z. C. (2003). Functional insights revealed by the crystal structures of Escherichia coli glucose-1-phosphatase. *J Biol Chem* **278**, 31412-31418.

Lee, H. H., Molla, M. N., Cantor, C. R. & Collins, J. J. (2010). Bacterial charity work leads to population-wide resistance. *Nature* **467**, 82-U113.

Lee, J., Jayaraman, A. & Wood, T. K. (2007a). Indole is an inter-species biofilm signal mediated by SdiA. *BMC Microbiol* **7**, 42.

- Lee, J., Page, R., Garcia-Contreras, R., Palermino, J. M., Zhang, X. S., Doshi, O., Wood, T. K. & Peti, W. (2007b). Structure and function of the Escherichia coli protein YmgB: a protein critical for biofilm formation and acid-resistance. *J Mol Biol* **373**, 11-26.
- Leid, J. G., Shirliff, M. E., Costerton, J. W. & Stoodley, P. (2002). Human leukocytes adhere to, penetrate, and respond to Staphylococcus aureus biofilms. *Infect Immun* **70**, 6339-6345.
- Lejeune, P. (2003). Biofilm-dependent regulation of gene expression. In *Medical implications of biofilms*, pp. 8-11. Cambridge, UK: Cambridge University Press.
- Lesic, B., Lepine, F., Deziel, E. & other authors (2007). Inhibitors of pathogen intercellular signals as selective anti-infective compounds. *PLoS Pathog* **3**, 1229-1239.
- Lewis, K. (2001). Riddle of biofilm resistance. *Antimicrob Agents Chemother* **45**, 999-1007.
- Li, B. K. & Logan, B. E. (2004). Bacterial adhesion to glass and metal-oxide surfaces. *Colloid Surface B* **36**, 81-90.
- Li, J., Attila, C., Wang, L., Wood, T. K., Valdes, J. J. & Bentley, W. E. (2007). Quorum sensing in Escherichia coli is signaled by AI-2/LsrR: effects on small RNA and biofilm architecture. *J Bacteriol* **189**, 6011-6020.
- Li, X. Z., Nikaido, H. & Williams, K. E. (1997). Silver-resistant mutants of Escherichia coli display active efflux of Ag⁺ and are deficient in porins. *J Bacteriol* **179**, 6127-6132.
- Liu, H., Yu, C., Feng, D. X., Cheng, T., Meng, X., Liu, W., Zou, H. B. & Xian, M. (2012). Production of extracellular fatty acid using engineered Escherichia coli. *Microb Cell Fact* **11**, 41.
- Lopez-Casado, G., Covey, P. A., Bedinger, P. A., Mueller, L. A., Thannhauser, T. W., Zhang, S., Fei, Z., Giovannoni, J. J. & Rose, J. K. (2012). Enabling proteomic studies with RNA-Seq: The proteome of tomato pollen as a test case. *Proteomics* **12**, 761-774.
- Lopezlopez, G., Pascual, A. & Perea, E. J. (1991). Effect of Plastic Catheter Material on Bacterial Adherence and Viability. *J Med Microbiol* **34**, 349-353.
- Lubec, G., Nonaka, M., Krapfenbauer, K., Gratzer, M., Cairns, N. & Fountoulakis, M. (1999). Expression of the dihydropyrimidinase related protein 2 (DRP-2) in Down Syndrome and Alzheimer's disease brain is downregulated at the mRNA and dysregulated at the protein level. *J Neural Transm Suppl* 161-177.
- Lundberg, E., Fagerberg, L., Klevebring, D. & other authors (2010). Defining the transcriptome and proteome in three functionally different human cell lines. *Mol Syst Biol* **6**, 450.

- MacFarlane, S. & Macfarlane, G. T. (2003).** Bacterial growth on mucosal surfaces and biofilms in the large bowel. In *Medical implications of biofilms*, pp. 262: Cambridge, UK ; New York : Cambridge University Press.
- Macfarlane, S. & Macfarlane, G. T. (2006).** Composition and metabolic activities of bacterial biofilms colonizing food residues in the human gut. *Appl Environ Microbiol* **72**, 6204-6211.
- Macfarlane, S. & Dillon, J. F. (2007).** Microbial biofilms in the human gastrointestinal tract. *J Appl Microbiol* **102**, 1187-1196.
- Madsen, J. S., Burmolle, M., Hansen, L. H. & Sorensen, S. J. (2012).** The interconnection between biofilm formation and horizontal gene transfer. *FEMS Immun Med Microbiol* **65**, 183-195.
- Mah, T. F. & O'Toole, G. A. (2001).** Mechanisms of biofilm resistance to antimicrobial agents. *Trends Microbiol* **9**, 34-39.
- Maki, D. G. & Tambyah, P. A. (2001).** Engineering out the risk for infection with urinary catheters. *Emerging Infect Dis* **7**, 342-347.
- Mangalappalli-Illathu, A. K. & Korber, D. R. (2006).** Adaptive resistance and differential protein expression of *Salmonella enterica* serovar Enteritidis biofilms exposed to benzalkonium chloride. *Antimicrob Agents Chemother* **50**, 3588-3596.
- Marioni, J. C., Mason, C. E., Mane, S. M., Stephens, M. & Gilad, Y. (2008).** RNA-seq: an assessment of technical reproducibility and comparison with gene expression arrays. *Genome Res* **18**, 1509-1517.
- Marouga, R., David, S. & Hawkins, E. (2005).** The development of the DIGE system: 2D fluorescence difference gel analysis technology. *Anal Bioanal Chem* **382**, 669-678.
- Mauzy, C. A. & Hermodson, M. A. (1992).** Structural and functional analyses of the repressor, RbsR, of the ribose operon of *Escherichia coli*. *Protein Sci* **1**, 831-842.
- May, C., Brosseron, F., Chartowski, P., Meyer, H. E. & Marcus, K. (2012).** Differential proteome analysis using 2D-DIGE. *Methods Mol Biol* **893**, 75-82.
- Mayer, C., Moritz, R., Kirschner, C., Borchard, W., Maibaum, R., Wingender, J. & Flemming, H. C. (1999).** The role of intermolecular interactions: studies on model systems for bacterial biofilms. *Int J Biol Macromol* **26**, 3-16.
- McDonnell, G. & Russell, A. D. (1999).** Antiseptics and disinfectants: Activity, action, and resistance. *Clin Microbiol Rev* **12**, 147-179.
- McKenzie, G. J., Harris, R. S., Lee, P. L. & Rosenberg, S. M. (2000).** The SOS response regulates adaptive mutation. *Proc Natl Acad Sci U S A* **97**, 6646-6651.
- Meares, E. M. (1991).** Current Patterns in Nosocomial Urinary-Tract Infections. *Urology* **37**, 9-12.

- Meddings, J. & Saint, S. (2011).** Disrupting the Life Cycle of the Urinary Catheter. *Clin Infect Dis* **52**, 1291-1293.
- Meddows, T. R., Savory, A. P., Grove, J. I., Moore, T. & Lloyd, R. G. (2005).** RecN protein and transcription factor DksA combine to promote faithful recombinational repair of DNA double-strand breaks. *Mol Microbiol* **57**, 97-110.
- Meleady, P. (2011).** 2D gel electrophoresis and mass spectrometry identification and analysis of proteins. *Methods Mol Biol* **784**, 123-137.
- Mendez, J., Reimundo, P., Perez-Pascual, D., Navais, R., Gomez, E. & Guijarro, J. A. (2011).** A novel *cdsAB* operon is involved in the uptake of L-cysteine and participates in the pathogenesis of *Yersinia ruckeri*. *J Bacteriol* **193**, 944-951.
- Menno L. W., Knetsch, & Leo H. Koole. (2011).** New strategies in the development of antimicrobial coatings: the example of increasing usage of silver and silver nanoparticles. *Polymers* **3**, 340-366.
- Merino, S., Camprubi, S., Alberti, S., Benedi, V. J. & Tomas, J. M. (1992).** Mechanisms of *Klebsiella-Pneumoniae* Resistance to Complement-Mediated Killing. *Infect Immun* **60**, 2529-2535.
- Mermel, L. A., Farr, B. M., Sherertz, R. J., Raad, I. I., O'Grady, N., Harris, J. S. & Craven, D. E. (2001).** Guidelines for the management of intravascular catheter-related infections. *Clin Infect Dis* **32**, 1249-1272.
- Miles, A. A., Misra, S. S. & Irwin, J. O. (1938).** The estimation of the bactericidal power of the blood. *J Hyg (Lond)* **38**, 732-749.
- Modak, S. M. & Fox, C. L. (1981).** Sulfadiazine Silver-Resistant *Pseudomonas* in Burns - New Topical Agents. *Arch Surg* **116**, 854-857.
- Monroe, D. (2007).** Looking for chinks in the armor of bacterial biofilms. *PLoS Biol* **5**, e307.
- Moore, G. F., Dunsmore, B. C., Jones, S. M. & other authors (2000).** Microbial detachment from biofilms. In *Community structure and co-operation in biofilms: fifty-ninth symposium of the Society for General Microbiology, held at the University of Exeter, September 2000*, pp. 107-112. Cambridge: Cambridge University Press for the Society for General Microbiology.
- Mortazavi, A., Williams, B. A., McCue, K., Schaeffer, L. & Wold, B. (2008).** Mapping and quantifying mammalian transcriptomes by RNA-Seq. *Nat Methods* **5**, 621-628.
- Mulla, S. A. & Revdiwala, S. (2011).** Assessment of biofilm formation in device-associated clinical bacterial isolates in a tertiary level hospital. *Indian J Pathol Microbiol* **54**, 561-564.
- Munoz-Price, L. S., Hayden, M. K., Lolans, K., Won, S., Calvert, K., Lin, M., Stemer, A. & Weinstein, R. A. (2010).** Successful Control of an Outbreak of

- Klebsiella pneumoniae* Carbapenemase-Producing *K. pneumoniae* at a Long-Term Acute Care Hospital. *Infect Control Hosp Epidemiol* **31**, 341-347.
- Nalca, Y., Jansch, L., Bredenbruch, F., Geffers, R., Buer, J. & Hussler, S. (2006).** Quorum-sensing antagonistic activities of azithromycin in *Pseudomonas aeruginosa* PAO1: a global approach. *Antimicrob Agents Chemother* **50**, 1680-1688.
- Ni, N., Li, M., Wang, J. & Wang, B. (2009).** Inhibitors and antagonists of bacterial quorum sensing. *Med Res Rev* **29**, 65-124.
- Nishino, K. & Yamaguchi, A. (2001).** Analysis of a complete library of putative drug transporter genes in *Escherichia coli*. *J Bacteriol* **183**, 5803-5812.
- Nizet, V. (2006).** Antimicrobial peptide resistance mechanisms of human bacterial pathogens. *Curr Issues Mol Biol* **8**, 11-26.
- Nohr, R. S. & Macdonald, J. G. (1994).** New Biomaterials through Surface Segregation Phenomenon - New Quaternary Ammonium-Compounds as Antibacterial Agents. *J Biomater Sci, Polym Ed* **5**, 607-619.
- O'Hara, C. M., Brenner, F. W. & Miller, J. M. (2000).** Classification, identification, and clinical significance of *Proteus*, *Providencia*, and *Morganella*. *Clin Microbiol Rev* **13**, 534-546.
- O'Toole, G. A. & Kolter, R. (1998).** Flagellar and twitching motility are necessary for *Pseudomonas aeruginosa* biofilm development. *Mol Microbiol* **30**, 295-304.
- Ohta, T., Sutton, M. D., Guzzo, A., Cole, S., Ferentz, A. E. & Walker, G. C. (1999).** Mutations affecting the ability of the *Escherichia coli* UmuD' protein to participate in SOS mutagenesis. *J Bacteriol* **181**, 177-185.
- Orme, R., Douglas, C. W., Rimmer, S. & Webb, M. (2006).** Proteomic analysis of *Escherichia coli* biofilms reveals the overexpression of the outer membrane protein OmpA. *Proteomics* **6**, 4269-4277.
- Orme, R. P. (2006).** Proteomic analysis of *Escherichia coli* biofilm formation on hydrogels. University of Manchester (Thesis).
- Ouyang, Z. & Isaacson, R. (2006).** Identification and characterization of a novel ABC iron transport system, fit, in *Escherichia coli*. *Infect Immun* **74**, 6949-6956.
- Pallett, A. & Hand, K. (2010).** Complicated urinary tract infections: practical solutions for the treatment of multiresistant Gram-negative bacteria. *J Antimicrob Chemother* **65**, iii25-iii33.
- Park, J. H., Cho, Y. W., Cho, Y. H., Choi, J. M., Shin, H. J., Bae, Y. H., Chung, H., Jeong, S. Y. & Kwon, I. C. (2003).** Norfloxacin-releasing urethral catheter for long-term catheterization. *J Biomater Sci Polym Ed* **14**, 951-962.
- Perdivara, I., Deterding, L. J., Przybylski, M. & Tomer, K. B. (2010).** Mass Spectrometric Identification of Oxidative Modifications of Tryptophan Residues in

Proteins: Chemical Artifact or Post-Translational Modification? *J Am Soc Mass Spectrom* **21**, 1114-1117.

Pesci, E. C., Pearson, J. P., Seed, P. C. & Iglewski, B. H. (1997). Regulation of las and rhl quorum sensing in *Pseudomonas aeruginosa*. *J Bacteriol* **179**, 3127-3132.

Piddock, L. J. V. & Walters, R. N. (1992). Bactericidal Activities of 5 Quinolones for *Escherichia-Coli* Strains with Mutations in Genes Encoding the Sos Response or Cell-Division. *Antimicrob Agents Chemother* **36**, 819-825.

Pitt, T. L. (2007). Pseudomonads factsheet: Health Protection Agency.

Podschun, R. & Ullmann, U. (1998). *Klebsiella* spp. as nosocomial pathogens: Epidemiology, taxonomy, typing methods, and pathogenicity factors. *Clin Microbiol Rev* **11**, 589-603.

Polonio, R. E., Mermel, L. A., Paquette, G. E. & Sperry, J. F. (2001). Eradication of biofilm-forming *Staphylococcus epidermidis* (RP62A) by a combination of sodium salicylate and vancomycin. *Antimicrob Agents Chemother* **45**, 3262-3266.

Poole, K. (2005a). Efflux-mediated antimicrobial resistance. *J Antimicrob Chemother* **56**, 20-51.

Poole, R. K. (2005b). Nitric oxide and nitrosative stress tolerance in bacteria. *Biochem Soc Trans* **33**, 176-180.

Price, M. N., Arkin, A. P. & Alm, E. J. (2006). OpWise: operons aid the identification of differentially expressed genes in bacterial microarray experiments. *BMC Bioinformatics* **7**, 19.

Prigent-Combaret, C., Vidal, O., Dorel, C. & Lejeune, P. (1999). Abiotic surface sensing and biofilm-dependent regulation of gene expression in *Escherichia coli*. *J Bacteriol* **181**, 5993-6002.

Privett, B. J., Nutz, S. T. & Schoenfisch, M. H. (2010). Efficacy of surface-generated nitric oxide against *Candida albicans* adhesion and biofilm formation. *Biofouling* **26**, 973-983.

Purevdorj, B., Costerton, J. W. & Stoodley, P. (2002). Influence of hydrodynamics and cell signaling on the structure and behavior of *Pseudomonas aeruginosa* biofilms. *Appl Environ Microbiol* **68**, 4457-4464.

Qiagen (2005). *RNAprotect Bacteria Reagent Handbook*, Second edn.

Raad, II, Darouiche, R. O., Hachem, R., Abi-Said, D., Safar, H., Darnule, T., Mansouri, M. & Morck, D. (1998). Antimicrobial durability and rare ultrastructural colonization of indwelling central catheters coated with minocycline and rifampin. *Crit Care Med* **26**, 219-224.

Rabilloud, T. (1996). Solubilization of proteins for electrophoretic analyses. *Electrophoresis* **17**, 813-829.

- Ramakrishnan, K. & Mold, J. W. (2005).** Urinary catheters: a review. *The Internet J Fam Pract* **3**, 2.
- Rasmussen, T. B., Bjarnsholt, T., Skindersoe, M. E., Hentzer, M., Kristoffersen, P., Kote, M., Nielsen, J., Eberl, L. & Givskov, M. (2005).** Screening for quorum-sensing inhibitors (QSI) by use of a novel genetic system, the QSI selector. *J Bacteriol* **187**, 1799-1814.
- Rawling, E. G., Martin, N. L. & Hancock, R. E. (1995).** Epitope mapping of the *Pseudomonas aeruginosa* major outer membrane porin protein OprF. *Infect Immun* **63**, 38-42.
- Rawlinson, M. & Clark, J. (2004).** Alternative approaches to managing a non-draining urinary catheter. *Br J Community Nurs* **9**, 141-148.
- Raymond, K. N., Dertz, E. A. & Kim, S. S. (2003).** Enterobactin: an archetype for microbial iron transport. *Proc Natl Acad Sci U S A* **100**, 3584-3588.
- Regev-Shoshani, G., Ko, M., Miller, C. & Av-Gay, Y. (2010).** Slow Release of Nitric Oxide from Charged Catheters and Its Effect on Biofilm Formation by *Escherichia coli*. *Antimicrob Agents Chemother* **54**, 273-279.
- Regev-Shoshani, G., Ko, M., Crowe, A. & Av-Gay, Y. (2011).** Comparative Efficacy of Commercially Available and Emerging Antimicrobial Urinary Catheters Against Bacteriuria Caused by *E-coli* In Vitro. *Urology* **78**, 334-339.
- Reisner, A., Kroghelt, K. A., Klein, B. M., Zechner, E. L. & Molin, S. (2006).** In vitro biofilm formation of commensal and pathogenic *Escherichia coli* strains: impact of environmental and genetic factors. *J Bacteriol* **188**, 3572-3581.
- Ren, D., Bedzyk, L. A., Ye, R. W., Thomas, S. M. & Wood, T. K. (2004a).** Stationary-phase quorum-sensing signals affect autoinducer-2 and gene expression in *Escherichia coli*. *Appl Environ Microbiol* **70**, 2038-2043.
- Ren, D. C., Bedzyk, L. A., Setlow, P., England, D. F., Kjelleberg, S., Thomas, S. M., Ye, R. W. & Wood, T. K. (2004b).** Differential gene expression to investigate the effect of (5Z)-4-bromo-5-(bromomethylene)-3-butyl-2(5H)-furanone on *Bacillus subtilis*. *Appl Environ Microbiol* **70**, 4941-4949.
- Revdiwala, S., Rajdev, B. M. & Mulla, S. (2011).** Characterization of bacterial etiologic agents of biofilm formation in medical devices in critical care setup. *Crit Care Res Pract* **2012**, 945805.
- Ribeiro, H. M., Morais, J. A. & Eccleston, G. M. (2004).** Structure and rheology of semisolid o/w creams containing cetyl alcohol/non-ionic surfactant mixed emulsifier and different polymers. *Int J Cosmet Sci* **26**, 47-59.
- Rolando, M., Crider, J. Y. & Kahook, M. Y. (2011).** Ophthalmic preservatives: focus on polyquaternium-1. *Expert Opin Drug Deliv* **8**, 1425-1438.

- Royce, T. E., Rozowsky, J. S. & Gerstein, M. B. (2007).** Toward a universal microarray: prediction of gene expression through nearest-neighbor probe sequence identification. *Nucleic Acids Res* **35**, e99.
- Ryder, M. A. (2005).** Catheter-Related Infections: It's All About Biofilm. *Topics Adv Pract Nurs eJournal* **5** (3).
- Sadovskaya, I., Vinogradov, E., Flahaut, S., Kogan, G. & Jabbouri, S. (2005).** Extracellular carbohydrate-containing polymers of a model biofilm-producing strain, *Staphylococcus epidermidis* RP62A. *Infect Immun* **73**, 3007-3017.
- Saenz, Y., Brinas, L., Dominguez, E., Ruiz, J., Zarazaga, M., Vila, J. & Torres, C. (2004).** Mechanisms of resistance in multiple-antibiotic-resistant *Escherichia coli* strains of human, animal, and food origins. *Antimicrob Agents Chemother* **48**, 3996-4001.
- Saint, S., Elmore, J. G., Sullivan, S. D., Emerson, S. S. & Koepsell, T. D. (1998).** The efficacy of silver alloy-coated urinary catheters in preventing urinary tract infection: a meta-analysis. *Am J Med* **105**, 236-241.
- Saint, S. (2000).** Clinical and economic consequences of nosocomial catheter-related bacteriuria. *Am J Infect Control* **28**, 68-75.
- Saint, S., Wiese, J., Amory, J. K., Bernstein, M. L., Patel, U. D., Zemencuk, J. K., Bernstein, S. J., Lipsky, B. A. & Hofer, T. P. (2000).** Are physicians aware of which of their patients have indwelling urinary catheters? *Am J Med* **109**, 476-480.
- Samartzidou, H. & Delcour, A. H. (1999).** Excretion of endogenous cadaverine leads to a decrease in porin-mediated outer membrane permeability. *J Bacteriol* **181**, 791-798.
- Sandiford, S. K. (2010).** Towards the development of prosthetic joints that inhibit bacterial adhesion and biofilm formation. University of Manchester (Thesis).
- Sauer, K. (2003).** The genomics and proteomics of biofilm formation. *Genome Biol* **4**, 219.
- Sawasdidoln, C., Taweekhaisupapong, S., Sermswan, R. W., Tattawasart, U., Tungpradabkul, S. & Wongratanacheewin, S. (2010).** Growing *Burkholderia pseudomallei* in Biofilm Stimulating Conditions Significantly Induces Antimicrobial Resistance. *PLoS One* **5**, e9196.
- Schairer, D. O., Chouake, J. S., Nosanchuk, J. D. & Friedman, A. J. (2012).** The potential of nitric oxide releasing therapies as antimicrobial agents. *Virulence* **3**, 271-279.
- Schauder, S., Shokat, K., Surette, M. G. & Bassler, B. L. (2001).** The LuxS family of bacterial autoinducers: biosynthesis of a novel quorum-sensing signal molecule. *Mol Microbiol* **41**, 463-476.
- Schmidtchen, A., Frick, I. M. & Bjorck, L. (2001).** Dermatan sulphate is released by proteinases of common pathogenic bacteria and inactivates antibacterial alpha-defensin. *Mol Microbiol* **39**, 708-713.

- Schneider, R. P. (1996).** Conditioning Film-Induced Modification of Substratum Physicochemistry--Analysis by Contact Angles. *J Colloid Interface Sci* **182**, 204-213.
- Schuber, F. (1989).** Influence of polyamines on membrane functions. *Biochem J* **260**, 1-10.
- Shah, D., Zhang, Z., Khodursky, A., Kaldalu, N., Kurg, K. & Lewis, K. (2006).** Persisters: a distinct physiological state of *E. coli*. *BMC Microbiol* **6**, 53.
- Shemesh, M., Kolter, R. & Losick, R. (2010).** The biocide chlorine dioxide stimulates biofilm formation in *Bacillus subtilis* by activation of the histidine kinase KinC. *J Bacteriol* **192**, 6352-6356.
- Shimada, T., Kori, A. & Ishihama, A. (2013).** Involvement of the Ribose Operon Repressor RbsR in Regulation of Purine Nucleotide Synthesis in *Escherichia coli*. *FEMS Microbiol Lett.*
- Silver, S., Phung, L. T. & Silver, G. (2006).** Silver as biocides in burn and wound dressings and bacterial resistance to silver compounds. *J Indust Microbiol Biotech* **33**, 627-634.
- Skindersoe, M. E., Alhede, M., Phipps, R. & other authors (2008).** Effects of antibiotics on quorum sensing in *Pseudomonas aeruginosa*. *Antimicrob Agents Chemother* **52**, 3648-3663.
- Smyth, A. R., Cifelli, P. M., Ortori, C. A. & other authors (2010).** Garlic as an Inhibitor of *Pseudomonas aeruginosa* Quorum Sensing in Cystic Fibrosis-A Pilot Randomized Controlled Trial. *Ped Pulmonol* **45**, 356-362.
- Song, J. A., Lee, D. S., Park, J. S., Han, K. Y. & Lee, J. (2012).** The N-domain of *Escherichia coli* phosphoglycerate kinase is a novel fusion partner to express aggregation-prone heterologous proteins. *Biotech Bioeng* **109**, 325-335.
- Sorensen, S. J., Bailey, M., Hansen, L. H., Kroer, N. & Wuertz, S. (2005).** Studying plasmid horizontal transfer in situ: A critical review. *Nat Rev Microbiol* **3**, 700-710.
- Srinivasan, A., Karchmer, T., Richards, A., Song, X. & Perl, T. M. (2006).** A prospective trial of a novel, silicone-based, silver-coated Foley catheter for the prevention of nosocomial urinary tract infections. *Infect Control Hosp Epidemiol* **27**, 38-43.
- Sriramulu, D. D., Lunsdorf, H., Lam, J. S. & Romling, U. (2005).** Microcolony formation: a novel biofilm model of *Pseudomonas aeruginosa* for the cystic fibrosis lung. *J Med Microbiol* **54**, 667-676.
- Stamm, W. E. & Hooton, T. M. (1993).** Management of urinary tract infections in adults. *N Engl J Med* **329**, 1328-1334.
- Stenudd, C., Nordlund, A., Ryberg, M., Johansson, I., Kallestal, C. & Stromberg, N. (2001).** The association of bacterial adhesion with dental caries. *J Dent Res* **80**, 2005-2010.

- Stickler, D. J. (1996).** Bacterial biofilms and the encrustation of urethral catheters. *Biofouling* **9**, 293-305.
- Stickler, D. J. (2000).** Biomaterials to prevent nosocomial infections: is silver the gold standard? *Curr Opin Infect Dis* **13**, 389-393.
- Stincone, A., Daudi, N., Rahman, A. S., Antczak, P., Henderson, I., Cole, J., Johnson, M. D., Lund, P. & Falciani, F. (2011).** A systems biology approach sheds new light on Escherichia coli acid resistance. *Nucleic Acids Res* **39**, 7512-7528.
- Stone, G., Wood, P., Dixon, L., Keyhan, M. & Matin, A. (2002).** Tetracycline rapidly reaches all the constituent cells of uropathogenic Escherichia coli biofilms. *Antimicrob Agents Chemother* **46**, 2458-2461.
- Stoodley, P., Dodds, I., Boyle, J. D. & Lappin-Scott, H. M. (1999).** Influence of hydrodynamics and nutrients on biofilm structure. *J Appl Microbiol* **85**, 19s-28s.
- Stoodley, P., Hall-Stoodley, L., Boyle, J. D., Jorgensen, F., Lappin-Scott, H. M., Allison, D. G., Gilbert, P. & Wilson, M. (2000).** Environmental and genetic factors influencing biofilm structure. In *Community structure and co-operation in biofilms: fifty-ninth symposium of the Society for General Microbiology, held at the University of Exeter, September 2000*, pp. 59. Cambridge: Cambridge University Press for the Society for General Microbiology.
- Strong, M. J., Xu, G., Coco, J. & other authors (2013).** Differences in Gastric Carcinoma Microenvironment Stratify According to EBV Infection Intensity: Implications for Possible Immune Adjuvant Therapy. *PLoS Pathog* **9**, e1003341.
- Su, Z. Q., Li, Z. G., Chen, T. & other authors (2011).** Comparing Next-Generation Sequencing and Microarray Technologies in a Toxicological Study of the Effects of Aristolochic Acid on Rat Kidneys. *Chem Res Toxicol* **24**, 1486-1493.
- Suh, M. J., Alami, H., Clark, D. J., Parmar, P. P., Robinson, J. M., Huang, S. T., Fleischmann, R. D., Peterson, S. N. & Pieper, R. (2008).** Widespread Occurrence of Non-Enzymatic Deamidations of Asparagine Residues in Yersinia pestis Proteins Resulting from Alkaline pH Membrane Extraction Conditions. *Open Proteomics J* **1**, 106-115.
- Sutherland, I. (2001).** Biofilm exopolysaccharides: a strong and sticky framework. *Microbiology* **147**, 3-9.
- Tambyah, P. A., Knasinski, V. & Maki, D. G. (2002).** The direct costs of nosocomial catheter-associated urinary tract infection in the era of managed care. *Infect Control Hosp Epidemiol* **23**, 27-31.
- Tambyah, P. A. (2004).** Catheter-associated urinary tract infections: diagnosis and prophylaxis. *Int J Antimicrob Agents* **24 Suppl 1**, S44-48.
- Tart, A. H., Blanks, M. J. & Wozniak, D. J. (2006).** The AlgT-dependent transcriptional regulator AmrZ (AlgZ) inhibits flagellum biosynthesis in mucoid, nonmotile Pseudomonas aeruginosa cystic fibrosis isolates. *J Bacteriol* **188**, 6483-6489.

- Tavender, T. J., Halliday, N. M., Hardie, K. R. & Winzer, K. (2008).** LuxS-independent formation of Al-2 from ribulose-5-phosphate. *Bmc Microbiology* **8**.
- Thibon, P., Le Coutour, X., Leroyer, R. & Fabry, J. (2000).** Randomized multi-centre trial of the effects of a catheter coated with hydrogel and silver salts on the incidence of hospital-acquired urinary tract infections. *J Hosp Infect* **45**, 117-124.
- Thornton, G. F. & Andriole, V. T. (1970).** Bacteriuria during indwelling catheter drainage. II. Effect of a closed sterile drainage system. *JAMA* **214**, 339-342.
- Topal, J., Conklin, S., Camp, K., Morris, V., Balcezak, T. & Herbert, P. (2005).** Prevention of nosocomial catheter-associated urinary tract infections through computerized feedback to physicians and a nurse-directed protocol. *Am J Med Qual* **20**, 121-126.
- Torres, A. G., Redford, P., Welch, R. A. & Payne, S. M. (2001).** TonB-dependent systems of uropathogenic *Escherichia coli*: aerobactin and heme transport and TonB are required for virulence in the mouse. *Infect Immun* **69**, 6179-6185.
- Toutain, C. M., Caiazza, N. C., O'Toole, G. A. & Ghannoum, M. A. (2004).** Molecular basis of biofilm development by *Pseudomonads*. In *Microbial biofilms*, pp. 47-51. Washington, D.C.: ASM Press.
- Trabulsi, L. R., Campos, L. C., Whittam, T. S., Gomes, T. A. T., Rodrigues, J. & Goncalves, A. G. (1996).** Traditional and non-traditional enteropathogenic *Escherichia coli* serogroups. *Rev Microbiol* **27**, 1-6.
- Trachoo, N. (2003).** Biofilms and the food industry. *Songklanakarin J Sci Technol* **25**, 9.
- Trautner, B. W. & Darouiche, R. O. (2004).** Role of biofilm in catheter-associated urinary tract infection. *Am J Infect Control* **32**, 177-183.
- Tucker, D. L., Tucker, N. & Conway, T. (2002).** Gene expression profiling of the pH response in *Escherichia coli*. *J Bacteriol* **184**, 6551-6558.
- Tyers, M. & Mann, M. (2003).** From genomics to proteomics. *Nature* **422**, 193-197.
- Vaara, M. (1992).** Agents that increase the permeability of the outer membrane. *Microbiol Rev* **56**, 395-411.
- Vagrati, M. A. (2009).** Siderophore production by uropathogenic *Escherichia coli*. *Indian J Pathol Microbiol* **52**, 126-127.
- Valcu, C. M. & Schlink, K. (2006).** Reduction of proteins during sample preparation and two-dimensional gel electrophoresis of woody plant samples. *Proteomics* **6**, 1599-1605.
- van 't Hof, W., Veerman, E. C. I., Helmerhorst, E. J. & Amerongen, A. V. N. (2001).** Antimicrobial peptides: Properties and applicability. *Biol Chem* **382**, 597-619.

van den Broek, P. J., Wille, J. C., van Benthem, B. H., Perenboom, R. J., van den Akker-van Marle, M. E. & Niel-Weise, B. S. (2011). Urethral catheters: can we reduce use? *BMC Urol* **11**, 10.

Van Gennip, M., Christensen, L. D., Alhede, M. & other authors (2009). Inactivation of the rhlA gene in *Pseudomonas aeruginosa* prevents rhamnolipid production, disabling the protection against polymorphonuclear leukocytes. *APMIS* **117**, 537-546.

Van, H. R. & Michiels, C. W. (2005). Role of bacterial cell surface structures in *Escherichia coli* biofilm formation. *Res Microbiol* **156**, 626-633.

Veinger, L., Diamant, S., Buchner, J. & Goloubinoff, P. (1998). The small heat-shock protein IbpB from *Escherichia coli* stabilizes stress-denatured proteins for subsequent refolding by a multichaperone network. *J Biol Chem* **273**, 11032-11037.

Velraeds, M. M. C., vanderMei, H. C., Reid, G. & Busscher, H. J. (1996). Inhibition of initial adhesion of uropathogenic *Enterococcus faecalis* by biosurfactants from *Lactobacillus* isolates. *Appl Environ Microbiol* **62**, 1958-1963.

Velraeds, M. M. C., vanderMei, H. C., Reid, G. & Busscher, H. J. (1997). Inhibition of initial adhesion of uropathogenic *Enterococcus faecalis* to solid substrata by an adsorbed biosurfactant layer from *Lactobacillus acidophilus*. *Urology* **49**, 790-794.

Verleyen, P., De, R. D., Van, P. H. & Baert, L. (1999). Clinical application of the Bardex IC Foley catheter. *Eur Urol* **36**, 240-246.

Vladimirov, N., Lebedz, D. & Sourjik, V. (2010). Predicted auxiliary navigation mechanism of peritrichously flagellated chemotactic bacteria. *PLoS Comput Biol* **6**, e1000717.

Vrany, J. D., Stewart, P. S. & Suci, P. A. (1997). Comparison of recalcitrance to ciprofloxacin and levofloxacin exhibited by *Pseudomonas aeruginosa* biofilms displaying rapid-transport characteristics. *Antimicrob Agents Chemother* **41**, 1352-1358.

Vu, B., Chen, M., Crawford, R. J. & Ivanova, E. P. (2009). Bacterial extracellular polysaccharides involved in biofilm formation. *Molecules* **14**, 2535-2554.

Waldron, K. J. & Robinson, N. J. (2009). How do bacterial cells ensure that metalloproteins get the correct metal? *Nat Rev Microbiol* **7**, 25-35.

Wang, D. D., Ding, X. D. & Rather, P. N. (2001). Indole can act as an extracellular signal in *Escherichia coli*. *J Bacteriol* **183**, 4210-4216.

Wang, G., Li, X. & Wang, Z. (2009a). APD2: the updated antimicrobial peptide database and its application in peptide design. *Nucleic Acids Res* **37**, D933-937.

Wang, Y. (2002). The function of OmpA in *Escherichia coli*. *Biochem Biophys Res Commun* **292**, 396-401.

Wang, Z., Gerstein, M. & Snyder, M. (2009b). RNA-Seq: a revolutionary tool for transcriptomics. *Nat Rev Genet* **10**, 57-63.

- Weber, H., Polen, T., Heuveling, J., Wendisch, V. F. & Hengge, R. (2005).** Genome-wide analysis of the general stress response network in *Escherichia coli*: sigmaS-dependent genes, promoters, and sigma factor selectivity. *J Bacteriol* **187**, 1591-1603.
- Wellens, A., Garofalo, C., Nguyen, H. & other authors (2008).** Intervening with Urinary Tract Infections Using Anti-Adhesives Based on the Crystal Structure of the FimH-Oligomannose-3 Complex. *PLoS One* **3**, e3040.
- Whitchurch, C. B., Tolker-Nielsen, T., Ragas, P. C. & Mattick, J. S. (2002).** Extracellular DNA required for bacterial biofilm formation. *Science* **295**, 1487-1487.
- Wiles, T. J., Kulesus, R. R. & Mulvey, M. A. (2008).** Origins and virulence mechanisms of uropathogenic *Escherichia coli*. *Exp Mol Pathol* **85**, 11-19.
- Wilhelm, B. T., Marguerat, S., Goodhead, I. & Bahler, J. (2010).** Defining transcribed regions using RNA-seq. *Nat Protoc* **5**, 255-266.
- Wilkinson, D. E. & Gilbert, P. (1987).** Permeation of the Gram-Negative Cell-Envelope by Some Polymeric Biguanides. *J Appl Bacteriol* **63**, 25.
- Willcox, M. D. P., Hume, E. B. H., Aliwarga, Y., Kumar, N. & Cole, N. (2008).** A novel cationic-peptide coating for the prevention of microbial colonization on contact lenses. *J Appl Microbiol* **105**, 1817-1825.
- Williams, P. (2007).** Quorum sensing, communication and cross-kingdom signalling in the bacterial world. *Microbiol-SGM* **153**, 3923-3938.
- Williams, P. & Camara, M. (2009).** Quorum sensing and environmental adaptation in *Pseudomonas aeruginosa*: a tale of regulatory networks and multifunctional signal molecules. *Curr Opin Microbiol* **12**, 182-191.
- Wills, P. (2013).** Novel Biocidal Formulations. University of Manchester (Thesis).
- Wimpenny, J., Allison, D. G., Gilbert, P., Lappin-Scott, H. M. & Wilson, M. (2000).** An overview of biofilms as functional communities. In *Community structure and co-operation in biofilms: fifty-ninth symposium of the Society for General Microbiology, held at the University of Exeter, September 2000*, pp. 9-10. Cambridge: Cambridge University Press for the Society for General Microbiology.
- Wood, T. K. (2009).** Insights on *Escherichia coli* biofilm formation and inhibition from whole-transcriptome profiling. *Environ Microbiol* **11**, 1-15.
- Woods, E. J., Cochrane, C. A. & Percival, S. L. (2009).** Prevalence of silver resistance genes in bacteria isolated from human and horse wounds. *Vet Microbiol* **138**, 325-329.
- Wortham, B. W., Patel, C. N. & Oliveira, M. A. (2007).** Polyamines in bacteria: pleiotropic effects yet specific mechanisms. *Adv Exp Med Biol* **603**, 106-115.
- Xavier, K. B. & Bassler, B. L. (2005).** Regulation of uptake and processing of the quorum-sensing autoinducer AI-2 in *Escherichia coli*. *J Bacteriol* **187**, 238-248.

- Xiao, G. P., Deziel, E., He, J. X. & other authors (2006).** MvfR, a key *Pseudomonas aeruginosa* pathogenicity LTTR-class regulatory protein, has dual ligands. *Mol Microbiol* **62**, 1689-1699.
- Yan, F. & Polk, D. B. (2004).** Commensal bacteria in the gut: learning who our friends are. *Curr Opin Gastroenterol* **20**, 565-571.
- Yi, H., Cho, Y. J., Won, S., Lee, J. E., Jin Yu, H., Kim, S., Schroth, G. P., Luo, S. & Chun, J. (2011).** Duplex-specific nuclease efficiently removes rRNA for prokaryotic RNA-seq. *Nucleic Acids Res* **39**, e140.
- Ymele-Leki, P. & Ross, J. M. (2007).** Erosion from *Staphylococcus aureus* biofilms grown under physiologically relevant fluid shear forces yields bacterial cells with reduced avidity to collagen. *Appl Environ Microbiol* **73**, 1834-1841.
- Young, T. A., Skordalakes, E. & Marqusee, S. (2007).** Comparison of proteolytic susceptibility in phosphoglycerate kinases from yeast and E-coli: Modulation of conformational ensembles without altering structure or stability. *J Mol Biol* **368**, 1438-1447.
- Yu, J., Fedorova, N. D., Montalbano, B. G., Bhatnagar, D., Cleveland, T. E., Bennett, J. W. & Nierman, W. C. (2011).** Tight control of mycotoxin biosynthesis gene expression in *Aspergillus flavus* by temperature as revealed by RNA-Seq. *FEMS Microbiol Lett* **322**, 145-149.
- Zavascki, A. P., Goldani, L. Z., Li, J. & Nation, R. L. (2007).** Polymyxin B for the treatment of multidrug-resistant pathogens: a critical review. *J Antimicrob Chemother* **60**, 1206-1215.
- Zelenitsky, S. A., Harding, G. K., Sun, S., Ubhi, K. & Ariano, R. E. (2003).** Treatment and outcome of *Pseudomonas aeruginosa* bacteraemia: an antibiotic pharmacodynamic analysis. *J Antimicrob Chemother* **52**, 668-674.
- Zhang, L., Hinz, A. J., Nadeau, J. P. & Mah, T. F. (2011).** *Pseudomonas aeruginosa* tssC1 links type VI secretion and biofilm-specific antibiotic resistance. *J Bacteriol* **193**, 5510-5513.
- Zhang, W., Li, F. & Nie, L. (2010a).** Integrating multiple 'omics' analysis for microbial biology: application and methodologies. *Microbiology* **156**, 287-301.
- Zhang, X., Fang, A., Riley, C. P., Wang, M., Regnier, F. E. & Buck, C. (2010b).** Multi-dimensional liquid chromatography in proteomics--a review. *Anal Chim Acta* **664**, 101-113.
- Zhang, X. S., Garcia-Contreras, R. & Wood, T. K. (2007).** YcfR (BhsA) influences *Escherichia coli* biofilm formation through stress response and surface hydrophobicity. *J Bacteriol* **189**, 3051-3062.
- Zhang, Y. M. & Rock, C. O. (2009).** Transcriptional regulation in bacterial membrane lipid synthesis. *J Lip Res* **50**, S115-S119.

Zhao, K., Liu, M. & Burgess, R. R. (2007). Adaptation in bacterial flagellar and motility systems: from regulon members to 'foraging'-like behavior in *E. coli*. *Nucleic Acids Res* **35**, 4441-4452.

Zhu, J. & Marchant, R. E. (2011). Design properties of hydrogel tissue-engineering scaffolds. *Expert Rev Med Devices* **8**, 607-626.

Zhu, M., Takenaka, S., Sato, M. & Hoshino, E. (2001). Extracellular polysaccharides do not inhibit the reaction between *Streptococcus mutans* and its specific immunoglobulin G (IgG) or penetration of the IgG through *S. mutans* biofilm. *Oral Microbiol Immunol* **16**, 54-56.

Zobell, C. E. & Anderson, D. Q. (1936). Observations on the multiplication of bacteria in different volumes of stored sea water and the influence of oxygen tension and solid surfaces. *The Biological Bulletin. Biol Bull* **71 (2)** 324-342.

Zobell, C. E. (1943). The Effect of Solid Surfaces upon Bacterial Activity. *J Bacteriol* **46**, 39-56.